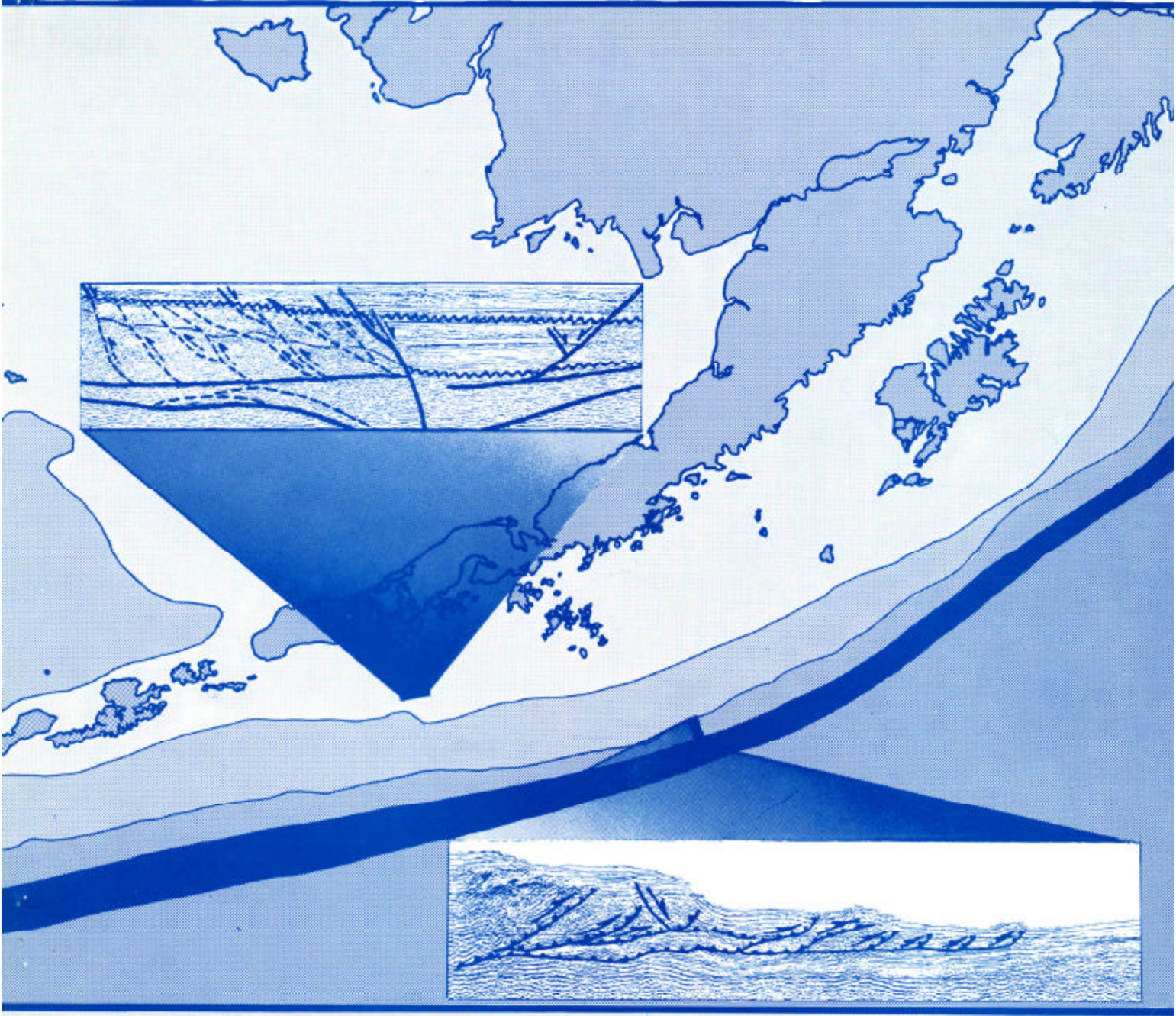


Geologic Report for the Shumagin Planning Area, Western Gulf of Alaska

OCS Report
MMS 89-0097



U.S. Department of the Interior
Minerals Management Service
Alaska OCS Region



Front cover:

Top seismic panel illustrates the uplifted subduction complex of the Sanak Island Transverse High and the West Sanak basin. The panel is shown in more detail on plate 4.

Bottom seismic panel illustrates an active subduction complex along the Aleutian Trench. The panel is also shown in figure 10. Interpretation from Bruns, von Huene, and others, 1987.

Geologic Report for the Shumagin Planning Area, Western Gulf of Alaska

OCS Report
MMS 89-0097

by
Warren L. Horowitz
David A. Steffy
Peter J. Hoose †

edited by
Ronald F. Turner

U. S. Department of the Interior
Minerals Management Service
Alaska OCS Region

Anchorage, Alaska
1989

† *Valued friend, colleague, and researcher, deceased December 1989.*

Library of Congress Cataloging-in-Publication Data

Horowitz, Warren L., 1953-

Geologic report for the Shumagin planning area, western Gulf of Alaska / by Warren L. Horowitz,
David A. Steffy, Peter J. Hoose ; edited by Ronald F. Turner.

p. cm. — (OCS report)

"MMS-89-0097."

Includes bibliographical references.

1. Geology—Alaska—Alaska, Gulf of, Region. 2. Petroleum—Geology—Alaska—Alaska, Gulf of, Region.
I. Steffy, David A. II. Hoose, Peter J. III. Turner, Ronald F. IV. Title. V. Series.

QE84.A33H67 1989

551.46'634—dc20

89-600377
CIP

Available from the National Technical Information Service, 5285 Port Royal Road, Springfield, VA 22161, Order
Number PB 90-146317

*Any use of trade names is for descriptive purposes only and does not constitute endorsement of these products by the
Minerals Management Service.*

Table of Contents

	<u>Page</u>
Abstract	1
Introduction	3
PART 1: REGIONAL GEOLOGY	
1. Geologic Framework	9
2. Geology of Deep-Water Areas	15
Aleutian Abyssal Plain Geology	15
Aleutian Trench Geology	15
Slope Geology	18
3. Onshore Geology	29
Alaska Peninsula Stratigraphy	29
Kodiak Islands	30
Border Ranges Fault	32
Chugach and Prince William Terranes	32
Early Cretaceous Accretion	32
Summary	34
4. Continental Shelf Geology	37
Kodiak DST Wells	37
Miocene Unconformity	39
Shumagin Shelf Geology	39
Seismic Stratigraphy	40
Sequence A (Cretaceous and Paleocene)	40
Sequence B (Eocene)	42
Sequence C (Oligocene to Pleistocene)	43
Summary	46
Structural Geology	46
Basin Boundary Features	46
Border Ranges Fault	46
Shumagin Ridge	47
Sanak Island Wrench Zone	47
Central Sanak High	47

	<u>Page</u>
Sanak Island Transverse High	47
Boundary Fault	48
Unimak Ridge	48
East Sanak Slope Ridge	48
Basin Structure	49
Tugidak Basin	49
Shumagin Basin	49
East Sanak Basin	51
East Sanak Slope Basin	51
West Sanak Basin	51
Unimak Basin	55
Summary and Discussion	55
5. Time-Depth Curves	59
6. Fault Mechanisms, Seismicity, and Transverse Tectonic Features	65
7. Geologic History	71
 PART 2: PETROLEUM GEOLOGY	
8. Exploration History	81
9. Geothermal Gradient	83
10. Source Rock	87
Kodiak Stratigraphic Test Wells and Onshore Geology	87
Shumagin Planning Area	88
Shumagin Continental Slope	88
Shumagin Shelf Basins	89
Summary	90
11. Reservoir Rocks	91
Seismic Sequence C	92
Shumagin Planning Area	92
Alaska Peninsula (Oligocene and Miocene)	92
Onshore Kodiak	92
Kodiak Shelf Stratigraphic Test Wells	94
Seismic Sequence B	94
Seismic Sequence A	94
Summary	95

	<u>Page</u>
12. Play Concepts	97
Source Rocks	97
Reservoir Rocks	97
Migration	97
Seals	97
Shumagin Shelf Plays and Trap Configurations	97
Simple, Faulted Fold Traps in the Shumagin Basin	97
Fold Traps in the West Sanak and Unimak Basins	97
Extensional Fault Traps in the East Sanak, West Sanak, and Unimak Basins	98
Stacked and Imbricate Thrust Traps in the West Sanak and Unimak Basins	101
Stratigraphic-Onlap and Facies Traps	101
Sanak Island Transverse High Play	101
Deep-Water Plays	101
Summary	104

PART 3: SHALLOW GEOLOGY, GEOLOGIC HAZARDS, and ENVIRONMENTAL CONDITIONS

13. Shallow Geology	107
Physiography and Bathymetry	107
Surficial Sediment and Bedrock Outcrops	110
14. Potential Geologic Hazards	117
Seismicity	117
Ground Shaking	117
Fault Displacement	117
Tectonic Uplift or Subsidence	118
Ground Failure	118
Tsunamis	118
Earthquake Potential	118
Shallow Gas	121
Volcanic Activity	121
Sediment Erosion and Deposition	123
Summary	123
15. Climate and Meteorology	125
Summary	129
References	131

FIGURES

1. Location of the Shumagin Planning Area	2
2. Shumagin Planning Area	3
3. CDP seismic-reflection data coverage in the Shumagin Planning Area	4
4. General geologic framework of the Kodiak and Shumagin continental margins and the adjacent Alaska Peninsula	11
5. Regional onshore geology of the Shumagin continental margin and the adjacent Alaska Peninsula	13
6. Locations of DSDP Leg 18 holes 178 through 183 and USGS dredge sites 2, 3, and 4	16
7. Zodiac fan outline and channels over the Gulf of Alaska magnetic anomaly pattern	17
8. Schematic profile from the Giacomini seamount to the eastern Aleutian Trench through DSDP Leg 18 holes 178, 179, and 180	19
9. Longitudinal profile of the Aleutian Trench	20
10. Migrated seismic section and interpreted line drawing of the Shumagin lower trench slope	22
11. Migrated seismic section and interpreted line drawing of the Barbados Ridge accretionary complex along ODP Leg 110	23
12. Fault pattern of the Shumagin continental slope	24
13. USGS Seismic-reflection profile of the Shumagin slope, Unimak ridge, and the Aleutian Trench	25
14. Stratigraphic column for the exposed onshore geology of the Alaska Peninsula, Kodiak, Shumagin, and Sanak Islands	31
15. Location of CDP seismic-reflection profiles	38
16. Shumagin shelf seismic sequence correlation chart	41
17. Structure-contour map of a regional Miocene unconformity	44
18. Structure map contoured in time (seconds) on top of sequence A for the East and West Shumagin subbasins	50
19. Isochron of sequence B for the East and West Shumagin subbasins	52
20. Structure map contoured in time (seconds) on top of the Miocene unconformity for the East and West Shumagin subbasins	53
21. Isochron of the lower seismic facies of sequence C for the East and West Shumagin subbasins	54
22. Time-depth curves, interval velocities, and stratigraphic columns for the three deepest Kodiak DST wells	60
23. Time-depth curve based on seismic-refraction data	61
24. USGS sonobuoy locations along the Shumagin margin	62
25. Time-depth curves generated from refraction and reflection data for the Shumagin margin	63
26. Seismic velocity, density, sediment type, and age of DSDP Leg 18 hole 183	63
27. Rupture zones in southern Alaska and the Aleutian Arc	66

	<u>Page</u>
28. Three seismic events of the Shumagin forearc margin	67
29. Epicenters, hypocenters, and a subset of composite fault plane solutions of microearthquakes along the Shumagin margin	68
30. Chart of geologic history	73
31. Early Cretaceous positions of the North American and Pacific plates and convergence vectors	75
32. Late Cretaceous positions of the North American and Pacific plates and convergence vectors	75
33. Positions of the Kula, Pacific, and North American plates and their relative directions of motion in the Shumagin area since Late Cretaceous time	76
34. Early Oligocene positions of the North American and Pacific plates and convergence vectors	77
35. Provenance of potential reservoir rocks of the Tertiary Shumagin shelf and slope basins	93
36. Traps associated with simple folds along a wrench fault system in the Shumagin basin	98
37. Traps associated with folds in West Sanak and Unimak basins	99
38. Traps associated with extensional faults in East Sanak, West Sanak, and Unimak basins	100
39. Traps associated with thrust faulting in West Sanak and Unimak basins	102
40. Traps associated with lithologic and stratigraphic changes within sequence C	103
41. Index map of the Shumagin continental margin showing bathymetry and high-resolution seismic- data tracklines	108
42. Quaternary geology of the Shumagin Planning Area showing the distribution of drift of the Brooks Lake and Mak Hill glaciations	109
43. Schematic representation of the circulation in the Gulf of Alaska	111
44. Map showing shallow faults, scour zones, and submarine slumps and slides	112
45. 3.5-kHz seismic profile and line interpretation across the shelf break showing bedrock outcrops	113
46. Line drawings of 3.5-kHz seismic profiles across seafloor depressions showing the typical seismic character of seafloor-sediment deposits	114
47. Tectonic map of the eastern Aleutian-Alaska Peninsula region	120
48. Theoretical tectonic cross section of the Shumagin region showing locations of the locked main thrust zone and the reverse-slip event	121

TABLES

1. Source rock analysis for Kodiak Island and the Shumagin continental slope	88
2. Location and description of dredge samples along the Shumagin continental slope, Alaska	91
3. Active volcanoes near the Shumagin Planning Area	122
4. Mean daily maximum and minimum temperature in degrees Fahrenheit	125
5. Mean maximum and minimum monthly precipitation in inches	125

PLATES

1. Tectonic elements of the Shumagin margin and adjacent areas.
2. Seismic-reflection profile showing the Central Sanak high and three major seismic sequences of the East Sanak basin.
3. Seismic-reflection profile of the East Shumagin subbasin showing the margin-oblique master fault and its splays, Neogene basement-involved thrusting, and decollement D1.
4. Seismic-reflection profile showing the internal structure of the Sanak Island Transverse High and West Sanak basin.
5. Seismic-reflection profile showing the three seismic stratigraphic sequences of the East Shumagin subbasin.
6. Seismic-reflection profile showing decollement D2 and extensional faulting and uplift along the outer shelf margin of the East Sanak basin.
7. Seismic-reflection profile showing a possible Pliocene thrust complex that originates in the Sanak Island Transverse High and extends into the Unimak basin.
8. USGS seismic-reflection profile showing the asymmetric graben of West Sanak basin and the thickening of seismic sequence C against the Boundary fault.
9. USGS seismic-reflection profile across the inverted West Sanak basin.
10. Seismic-reflection profile showing imbricate thrusts and growth faults in the Unimak basin.

Abstract

The 130,000-square-mile Shumagin Planning Area encompasses portions of the continental shelf and slope, the Aleutian Trench, and the Aleutian Abyssal Plain. The planning area lies southeast of the Alaska Peninsula and extends 375 miles from Chirikof Island to Unimak Pass. Water depths range from less than 165 feet nearshore to over 21,300 feet in the Aleutian Trench. The Shumagin Oil and Gas Lease Sale 129 was scheduled for January 1992 on the Minerals Management Service 5-year lease sale schedule announced in 1987; at this writing, the sale has been deferred.

The Shumagin continental shelf contains five structurally distinct sedimentary basins that formed on an evolving forearc accretionary prism. These basins are, from northeast to southwest, the Shumagin basin, the East and West Sanak basins, the East Sanak slope basin, and the Unimak basin. Geophysical and geological interpretations suggest the presence of a Neogene and Oligocene sedimentary section (sequence C), an Eocene section (sequence B), and a basement of Cretaceous and early Paleocene age (sequence A).

This study establishes the presence of two major transverse tectonic features, the Sanak Island Transverse High and the Sanak Island Wrench Zone, along the Shumagin margin in the area of the much-studied Shumagin seismic gap. The Sanak Island Transverse High (SITH) is an uplifted portion of the accretionary prism lying between the West Sanak basin and the Unimak basin. Underplating by overpressured slabs of pelagic clays uplifted the SITH. Subsequent erosion has exposed strata as old as the Late Cretaceous Shumagin Formation.

The Sanak Island Wrench Zone (SIWZ) is a zone of accretion and convergent wrenching that incorporates the Sanak Island Transverse High. Neogene strike-slip motion along the SIWZ has overprinted the extensional tectonic framework of the East and West Sanak basins, the Unimak basin, and the East Sanak slope basin with margin-oblique folds and thrust faults. This wrench motion has also offset the accretionary ridges (Unimak

and East Sanak slope ridges) that are the seaward boundaries for these growing basins.

Most of the source rock data for the Shumagin margin has been extrapolated from wells on the nearby Kodiak shelf, where the most prospective source rocks encountered were in the Eocene section of the KSSD No. 3 well. However, these rocks were thermally immature, contained less than 0.5 percent total organic carbon, and the kerogen was the herbaceous-woody type. Although better source rocks cannot be demonstrated in the Shumagin forearc basins, the paleogeothermal gradients may have been elevated because of increased heat flow associated with the subduction of the Kula-Pacific spreading ridge in the Oligocene, the emplacement of granitic plutons in the Paleocene, and the migration of warm, overpressured fluids generated by dewatering in decollement zones.

The best reservoir rocks on Kodiak Island are the transgressive, coarse-grained, quartz-rich sandstones of the Narrow Cape Formation. These sediments were presumably derived from the Kodiak-Shumagin Batholith which is exposed on the Semidi, Outer Shumagin, and Sanak Islands. Similar clastic sediments are thought to be present in sequence C in the Shumagin shelf basins.

There are numerous structures in the Shumagin basins that could potentially trap hydrocarbons. Structures in the SITH formed early during the Cretaceous and Paleocene. Most of these structures are part of a highly faulted subduction complex that may contain reservoir rocks of sequence B. Wrench motion along the Shumagin margin has resulted in a wide range of structures that involve sequence C reservoirs. Potential traps include anticlines, faulted anticlines, stacked thrusts, normal faults, and stratigraphic traps. Unfortunately, the area of closure of these structures is often small.

Potential geologic hazards to oil and gas exploration and development in the Shumagin Planning Area include seismicity and volcanic activity as well as processes associated with sediment erosion and deposition.

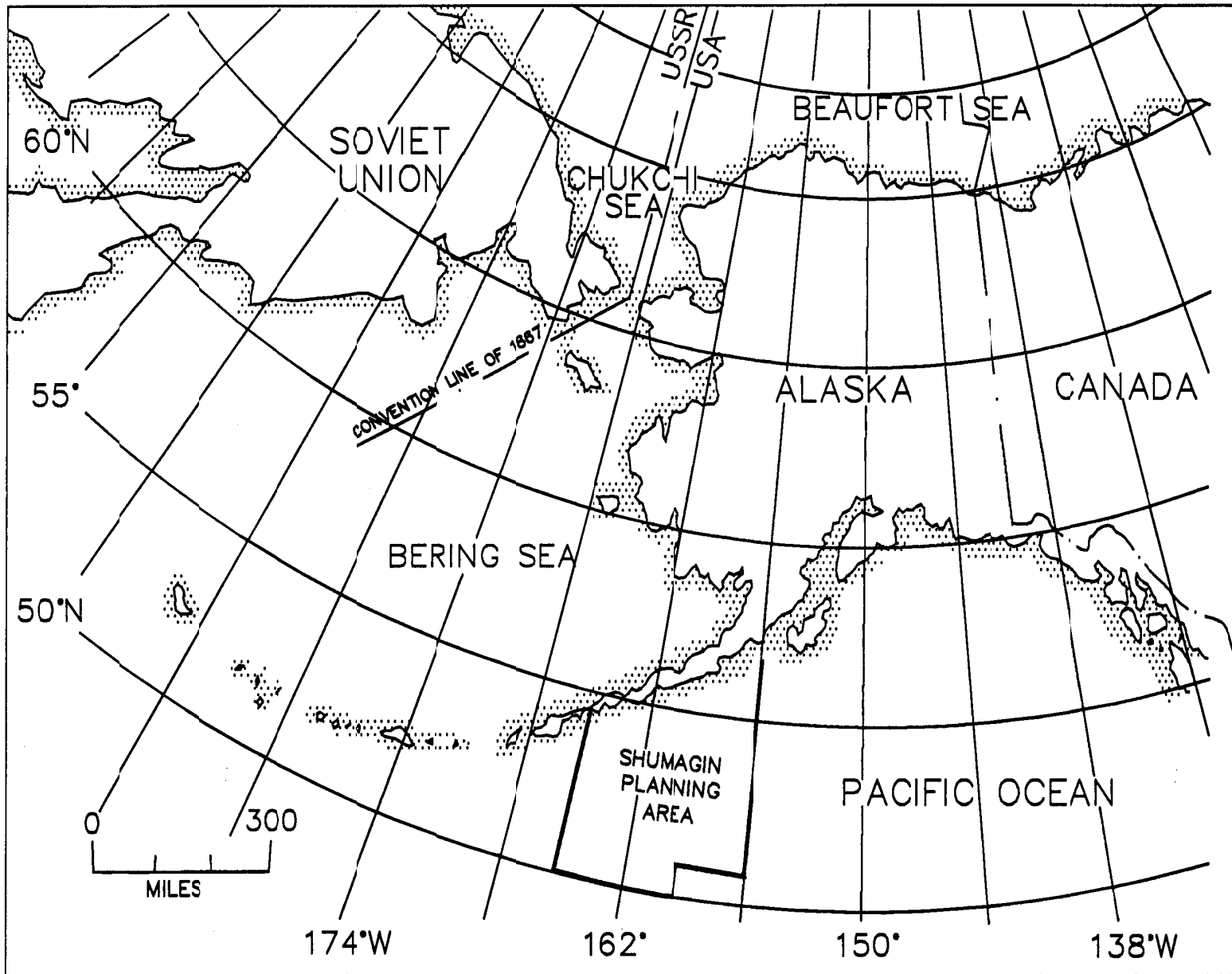


FIGURE 1. Location of the Shumagin Planning Area.

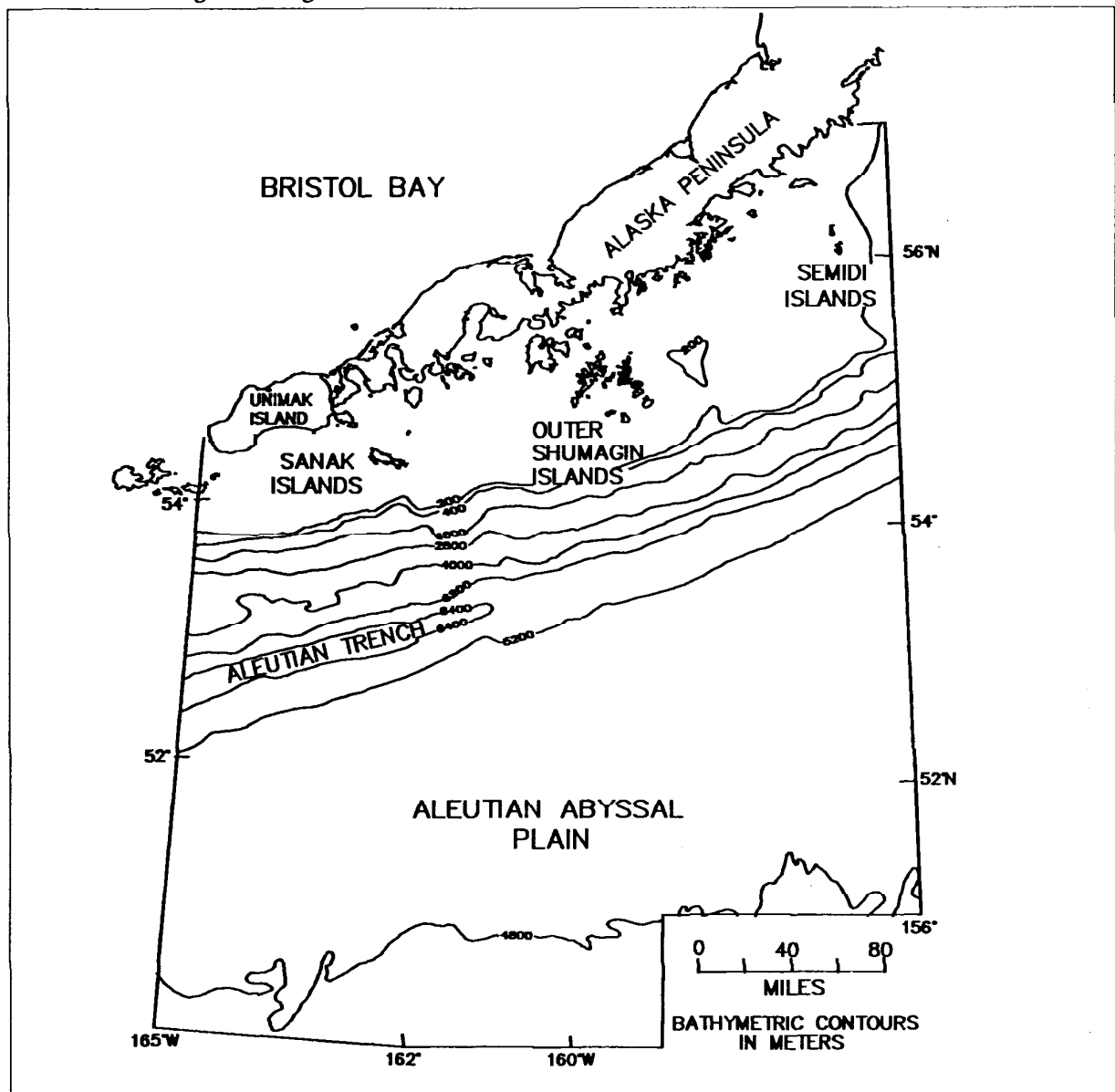
Introduction

This report is a summary of the regional geology, petroleum potential, shallow geology, and geologic hazards of the Shumagin Planning Area (fig. 1). The planning area lies southeast of the Alaska Peninsula and extends for 250 miles from the southwest end of Unimak Island northeastward to the Semidi Islands and seaward for over 300 miles (figs. 1 and 2). The planning

area encompasses portions of the continental shelf and slope, the Aleutian Trench, and the Aleutian Abyssal Plain. Water depths range from less than 165 feet (50 meters) nearshore to over 21,300 feet (6,500 meters) in the Aleutian Trench.

The Shumagin Planning Area is bounded by the 156° W. longitude line on the east and 165° W. longitude line on the west (fig. 2). The planning

FIGURE 2. Shumagin Planning Area.

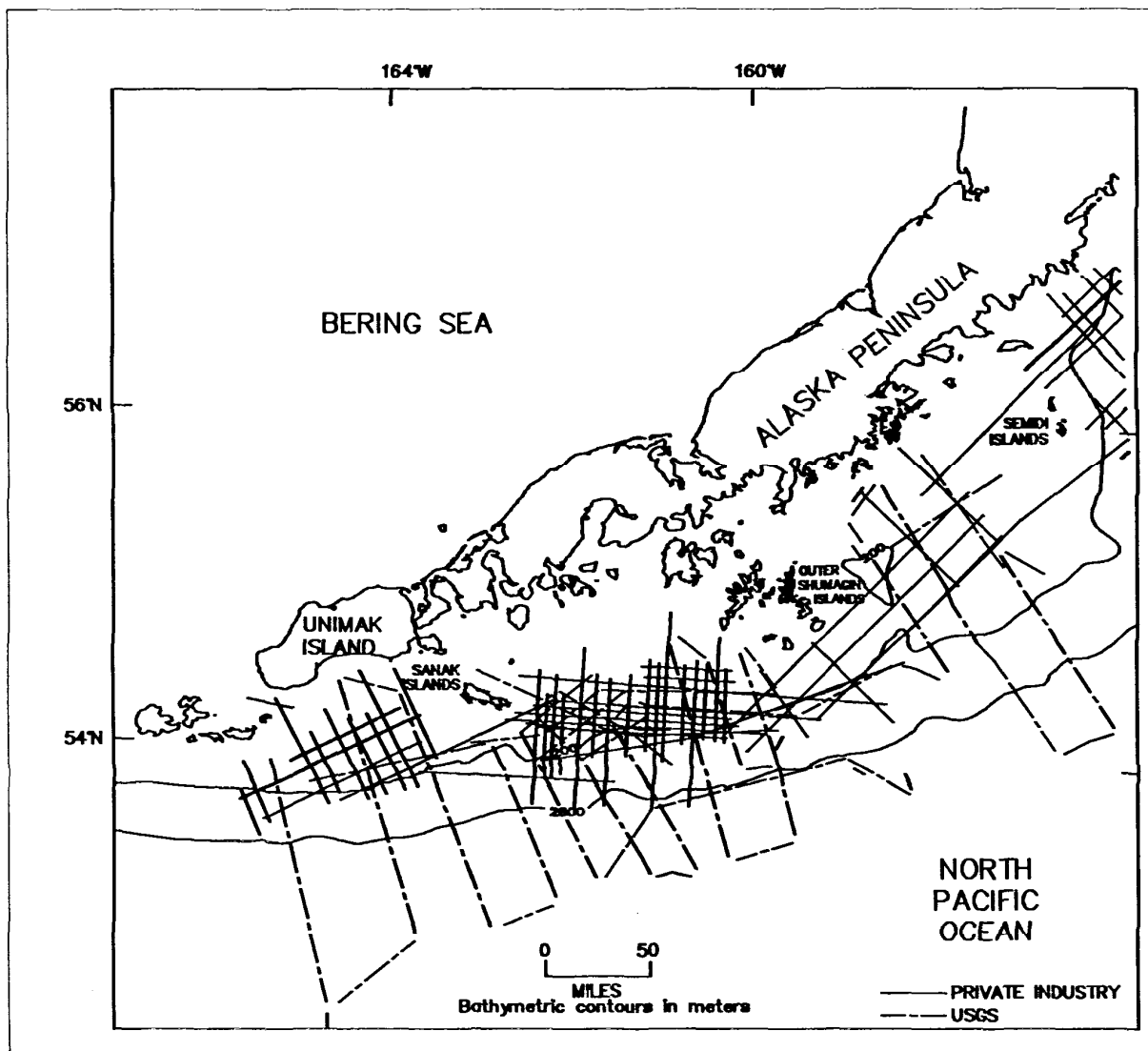


area extends as far south as 50° N. latitude and is bounded on the north by the 3-geographical-mile line of the Alaskan coast. The area contains 83 million acres divided into approximately 15,000 lease blocks. No lease sales or exploratory drilling have been conducted in the planning area. The Shumagin Oil and Gas Lease Sale 129 was scheduled for January 1992 on the Minerals Management Service (MMS) 5-year lease sale schedule announced in 1987; at this writing, the sale has been deferred.

This report is based, in great part, on MMS interpretations of a regional grid of high-quality, common-depth-point (CDP) seismic-reflection data (fig. 3). Conditional permission to use these lines was

granted by a private geophysical company. For illustrative purposes, lines that show multiple features were reproduced here. A number of U.S. Geological Survey (USGS) seismic lines collected in 1977 (Bruns and Bayer, 1977) and 1981 and 1982 (Bruns and others, 1985) were also analyzed, as were magnetic and gravity data collected at the same time. The interpretation presented in the Shallow Geology and Potential Geologic Hazards chapters was based on interpretation of 1,861 miles of single-channel airgun, 3.5-kHz subbottom profiler, and 12-kHz bathymetry data, and of 1,099 line miles of uniboom data collected by the USGS in 1981 and 1982. Although the seismic data base provided adequate coverage for regional interpretation of the continental shelf and portions of

FIGURE 3. CDP seismic-reflection-data coverage in the Shumagin Planning Area.



the upper slope, it provided only limited coverage of deep-water areas.

Geologic data examined for this report include descriptions of dredge samples collected by the USGS from the Shumagin continental slope in 1979 (Bruns and others, 1985; Bruns, Vallier, and others, 1987). Information recently released from six deep stratigraphic test wells drilled on the Kodiak shelf, which lies approximately 250 miles northeast of the eastern border of the Shumagin Planning Area and

occupies a similar tectonic setting (Turner and others, 1987), was also integrated into this report.

The Deep Sea Drilling Project (DSDP) Leg 18, conducted by the Joint Oceanographic Institutions for Deep Earth Sampling (JOIDES), provided the only deep-water samples from the Aleutian Abyssal Plain, Aleutian Trench, and lower slope (Kulm and others, 1973). DSDP analyses were incorporated in this report.

**PART 1:
REGIONAL
GEOLOGY**

1. Geologic Framework

Southwest Alaska has had a complex history of plate convergence since the Cretaceous, and an older and more complex history of convergence that extends back to the Jurassic, with the oceanic plates that floor the Pacific Ocean being continuously subducted beneath the Alaska Peninsula. The Alaska Peninsula lies in a magmatic arc and arc-trench gap setting adjacent to the Shumagin forearc margin (fig. 4, p. 11). The Shumagin margin has grown by tectonic accretion of deep-water sediments and igneous oceanic crust, by sediment deposition in subsiding forearc basins, and by the emplacement of granitic intrusives (Seely and Dickinson, 1977).

The Shumagin forearc exhibits a variety of structural styles, from a simple, sloped forearc in the extreme southwest portion of the planning area, where the shelf is 55 miles wide and the arc-trench gap is 120 miles wide, to a back-tilted, sloped forearc in the northeast portion of the planning area, with a shelf width of 90 miles and an arc-trench gap of 160 miles. The Shumagin margin widens toward the emergent forearc ridge that forms the Kodiak Islands and the Kenai Peninsula, with a shelf width of 150 miles and an arc-trench gap of 240 miles. This emergent ridge (composed of Chugach terrane lithologies) separates an outer "constructed forearc basin," the Albatross basin system, from the Cook Inlet basin (fig. 4) (Pavlis and Bruhn, 1983).

The Mesozoic sedimentary sequence on the Alaska Peninsula consists of volcanoclastic siltstones and sandstones, arkosic sandstones, and conglomerates derived from middle Mesozoic plutons, shallow-water calcarenites, and coal-bearing units (Wilson, Case, and Detterman, 1985). Tertiary sedimentary sequences on the Alaska Peninsula and the inner Shumagin Islands contain mostly continental volcanoclastics derived from andesites and basalts. Plutonic events occurred in the Middle Jurassic, Late Cretaceous, and early to middle Paleogene (Wallace and Engebretson, 1984). Intrusive rocks exposed on the Alaska Peninsula adjacent to the Shumagin Planning Area are Miocene or Pliocene in age (Burk, 1965). Localized late Paleogene and early Neogene volcanic flows, agglomerates, and breccias are present. Pliocene to Recent strato-volcanoes and associated features are abundant.

As the Kula oceanic plate, and then the Pacific oceanic plate, subducted beneath the North American continental plate, a Late Cretaceous to early Tertiary accretionary complex of deep-water sediments amalgamated with the Alaska Peninsula to form the Shumagin-Kodiak shelf and slope. This wedge of melange and flysch deposits includes the Late Cretaceous rocks that form the Outer Shumagin Islands and Sanak Islands and is inferred to be the basement on which the early Tertiary forearc basins formed. These deformed Late Cretaceous rocks were intruded by Paleocene and early Eocene granodiorites of the Gulf of Alaska magmatic belt (Wallace and Engebretson, 1984).

Five sedimentary forearc basins are identified within the Shumagin shelf and trench upper slope: the Shumagin, East Sanak, East Sanak slope, West Sanak, and Unimak basins. The extreme western flank of the Tugidak basin is also present in the eastern planning area. Each of these basins exhibits a different structural style that reflects a distinct geologic evolution. The Sanak Island Transverse High (SITH) separates the Unimak and West Sanak basins and is coincident with the southeast extension of what is thought to be the "old" Beringian transform margin (Steffy and Horowitz, 1987), the site of oblique convergence between the Kula and North American plates from the Jurassic until the Late Cretaceous (Marlow and Cooper, 1980) (plate 1). The southeast extent of the "old" Beringian margin is unknown. For this study, the position of the "old" transform margin was established by projecting the trend of the present 200-meter isobath (north of the Aleutian Ridge) southeastward across the Shumagin shelf. This margin agrees with one proposed by Marlow and Cooper (1980). This projection of the present-day margin may reflect oroclinal bending of the margin in the Late Cretaceous and early Tertiary (Marlow and Cooper, 1980). Bruns, von Huene, and others (1987) suggested that margin-oblique features such as the central Sanak subbasin (the West Sanak basin of this report) divide the margin and indicate that the "old" Beringian margin is a transform margin.

The Central Sanak high separates the West and East Sanak basins (plate 1) and is expressed as a normal-fault-bounded ridge that trends oblique to the shelf break. The East Sanak slope basin is bounded by

the East Sanak slope ridge to the southeast, and is separated from the Shumagin basin by the Shumagin ridge (plate 1).

The 20-mile-wide Shumagin-Kodiak slope, bounded by the continental shelf to the northwest and the Aleutian Trench to the southeast (plate 1), lies in water depths of 600 to 9,200 feet (200 to 2,800 meters). Bruns, von Huene, and others (1987) invoke an accretionary mechanism for the origin of this portion of the Shumagin slope similar to that postulated for the adjacent Kodiak and Aleutian slopes by von Huene (1984), McCarthy and Scholl (1985), and Byrne (1986). The accretionary slope is composed of thrust-faulted deep-sea sediments that have been "scraped off" of the subducting Pacific plate since the Late Cretaceous (Bruns, von Huene, and others, 1987). As accretion continued along the Shumagin margin, the slope and shelf built seaward and were uplifted. A mid-slope structural high present since the Paleogene, the Unimak ridge, provided a barrier behind which the northeastern portion of the Unimak and West Sanak sedimentary basins formed (Bruns, von Huene, and others, 1987). Similarly, a Paleogene compressional ridge, the East Sanak slope ridge, formed a barrier behind which the East Sanak slope basin developed. The East Sanak basin formed landward of the outer shelf Shumagin ridge, which has been present since the late Paleogene or early Neogene.

The sedimentary section in the Aleutian Trench consists of a thick, landward-dipping hemiterrigenous early Miocene sequence (Scholl, 1974) that is overlain by an equally thick (3,300-foot) wedge of Miocene and younger turbidites. Scholl (1974) defines hemiterrigenous as terrigenous deposits that include a volumetrically large (but less than 50 percent) component of pelagic material. The Aleutian Abyssal Plain south of the Aleutian Trench is underlain by the Zodiac fan, a feature composed of channelized Eocene to Oligocene turbidite deposits (Scholl and Creager, 1973). The source of these sediments is uncertain because the original position of the Zodiac fan has not been established (several evolutionary models for the Zodiac fan are briefly discussed in the next chapter).

The tectonostratigraphic terranes of the Alaska Peninsula and the adjacent Shumagin-Kodiak shelf and

slope have different evolutionary histories and lithologies. The Border Ranges fault (BRF) separates the Paleozoic and Mesozoic terrigenous rocks of the Alaska Peninsula from the Late Cretaceous deep-water sediments of the Shumagin-Kodiak shelf and slope (fig. 5, p. 13) (Fisher, 1981; Jones and others, 1981; Fisher and von Huene, 1984; Bruns, von Huene, and others, 1987). In the Shumagin area, the exact position of the BRF is in some dispute. This report places the BRF in approximately the same position given by Bruns, von Huene, and others (1987), although F. H. Wilson (personal commun., 1989) stated that recent field mapping suggests a position about 30 miles northwest.

Rocks of Alaska Peninsula and southcentral Alaska compose the Peninsular terrane of Jones and others (1981), which was redefined and renamed the Alaska Peninsula terrane by Wilson, Casc, and Detterman (1985). In this report, the older name of Peninsular terrane is used.

According to Bruns, von Huene, and others (1987), the Chugach and Prince William terranes are indistinguishable in the Shumagin margin area, where they consist of the Cretaceous deep-water sediments of the Shumagin and Kodiak Formations (fig. 5), Paleocene deep-water sediments and volcanics, and Eocene and Oligocene submarine fan complexes or their shallower water equivalents. The Chugach and Prince William terranes are distinguishable northeast of the Shumagin margin on Kodiak Island, where they are separated by the Contact fault (fig. 5). There, the Chugach terrane is represented by a mid-Late Cretaceous melange on the west side of Kodiak Island and a Maastrichtian trench-turbidite sequence in the central part of the island (Moore and others, 1983). The Prince William terrane consists of a Paleocene melange, turbidite, and volcanic sequence that crops out southeast of the Maastrichtian turbidite unit, and an Eocene to early Oligocene(?) submarine fan complex on the east side of Kodiak Island (Moore and others, 1983). Offshore, southwest of Kodiak Island, the boundary between the Chugach and Prince William terranes has not been delineated. Although definite Chugach terrane rocks crop out on the Outer Shumagin and Sanak Islands, rocks of the Prince William terrane have not been reported.

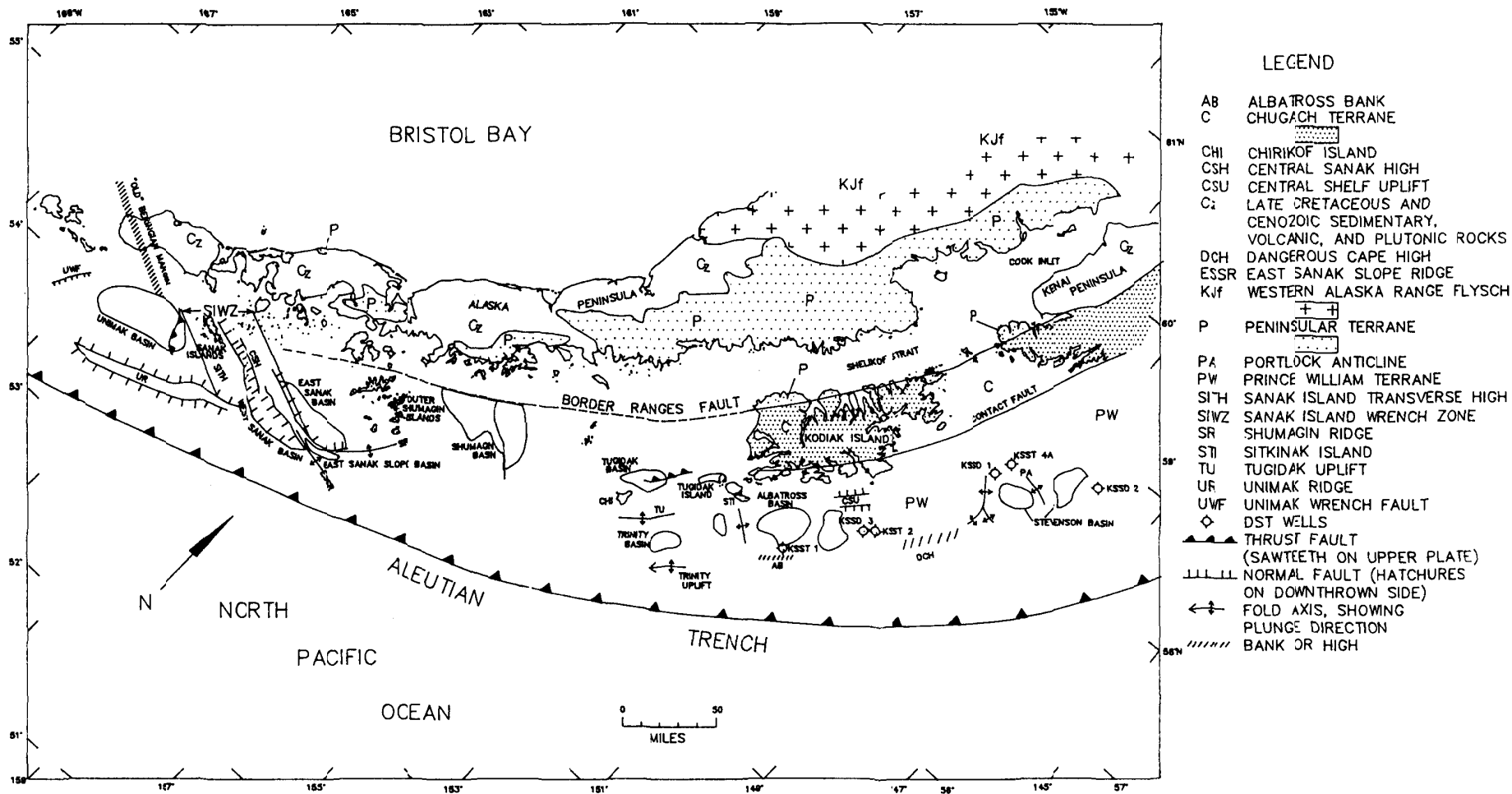


FIGURE 4. General geologic framework of the Kodiak and Shumagin continental margins and the adjacent Alaska Peninsula.

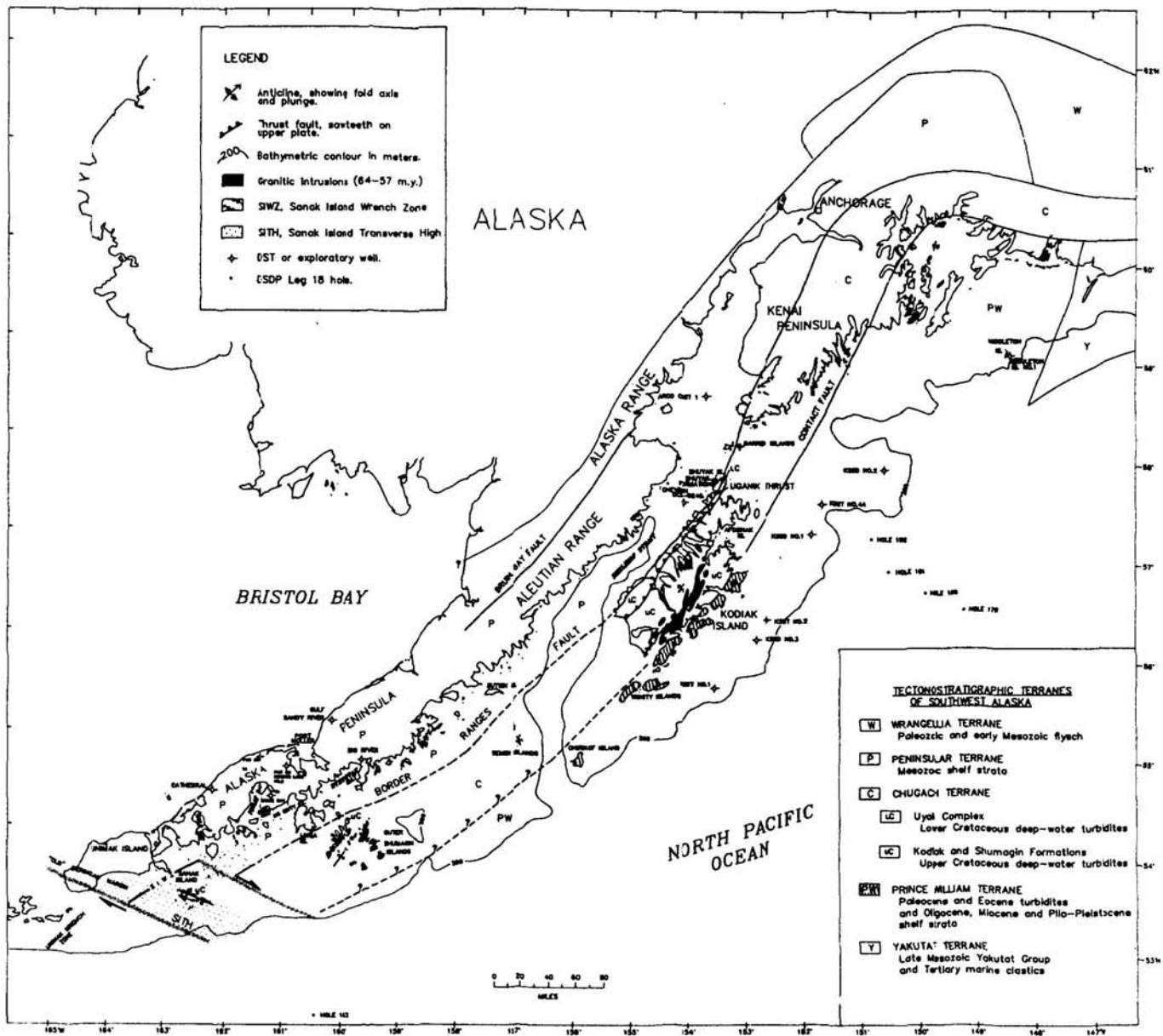


FIGURE 5. Regional onshore geology of the Shumagin continental margin and the adjacent Alaska Peninsula.

2. Geology of Deep-Water Areas

In the Shumagin Planning Area, the Aleutian Trench and the Aleutian Abyssal Plain (fig. 2, p. 3) are at water depths greater than 9,200 feet (2,800 meters). These deep-water features are underlain by the Pacific plate, which has been converging with the North American plate at the Shumagin forearc margin since at least the Cretaceous (Bruns, von Huene, and others, 1987). A third deep-water feature, the trench lower slope, parallels the Aleutian Trench in water depths between 600 and 9,200 feet. The geophysical data used in this report are from the shelf area and do not bear directly on the geology of these deep-water areas, although a better understanding of the shelf may provide some insight into the evolution of the deep-water areas. The following framework discussion is based, in part, on studies by Hamilton (1973), Scholl (1974), Stewart (1976), Stevenson and others (1983), and Kvenvolden and von Huene (1985).

Aleutian Abyssal Plain Geology

The Aleutian Abyssal Plain is the westernmost of three deep-ocean plains in the Gulf of Alaska. The Alaskan and Tufts Abyssal Plains occupy the central and eastern portions of the Gulf, respectively. The Aleutian Abyssal Plain is a fan-shaped sedimentary apron with an area of more than 380,000 square miles that extends southward from the Aleutian Trench for more than 1,200 miles in water depths averaging 13,000 feet (fig. 2). This sedimentary fan ranges in thickness from 1,300 to 2,600 feet near the trench to 650 feet near its southern terminus at the Surveyor fracture zone (Stevenson and others, 1983).

In 1971, DSDP Leg 18 hole 183 (fig. 6, p. 16) penetrated an 810-foot-thick section of pelagic clay containing diatoms and hemipelagic detritus, an 830-foot-thick turbidite section, and a 30-foot-thick layer of pelagic clay. The hole bottomed in oceanic alkaline olivine basalt (Scholl and Creager, 1973). The turbidite deposits are part of the relict Zodiac fan of latest middle Eocene to early Oligocene age (Scholl and Creager, 1973)(fig. 7, p. 17). The source terrane for the Zodiac fan is uncertain and the data discussed in this report do not constrain the formation of the fan.

There are several significantly different models proposed to explain the origin of the fan. Hamilton (1973) described the Zodiac fan as a series of coalescing and overlapping leveed channels (from west to east, the Seemap, Sagittarius, Aquarius, and Taurus systems) that he believed drained southward from Alaska (fig. 7). Stevenson and others (1983) accounted for the relative motion between the North American and Pacific plates by proposing that a large, northward-drifting landmass moved with the Zodiac fan. Reconstructed plate movements place this source terrane beneath the Alaska Peninsula and other parts of southern Alaska. Harbert (1987), however, envisioned the Zodiac source terrane to be rocks presently in British Columbia and the Pacific Northwest. In his model, sediments were transported into the Pacific and channeled and directed by the Cobb and Bowie seamount chains, fracture zones, and the Farallon-Pacific spreading ridge. Stewart (1976) also discussed plutonic terranes in British Columbia as the possible provenance of the fan deposits.

Aleutian Trench Geology

The north Pacific trenches, including the Aleutian Trench, contain thick, axial trench deposits unlike those of other circum-Pacific trenches (Scholl, 1974). The Shumagin Planning Area contains a unique part of the Aleutian Trench, a transition zone between the central and eastern portions that lacks these thick axial deposits because of an apparent structural inversion.

Figure 8 (p. 19) is a line drawing of a cross-section of the lower slope off Kodiak Island through Leg 18 holes 180 and 178 to the Giacomini Seamount and hole 179. At the trench, there is a wedge up to 25 miles wide and 3,200 feet thick composed of reworked slump masses (Scholl, 1974) and channelized turbiditic sediments that were supplied through sea valleys that incise the continental slope (Bruns, von Huene, and others, 1987). Reworking of slump deposits by turbidity currents has redistributed this material as part of the trench fill. The wedge deposits overlie a landward-dipping sequence of pelagic clay and terrigenous to hemiterigenous(?) turbidite that is concordant with the basement topography and extends seaward beneath the Aleutian Abyssal Plain. These deposits were sampled by Leg 18 hole 180 near the Aleutian Trench axis and hole 178, 43 miles southeast of the trench axis (figs. 6 and 8)

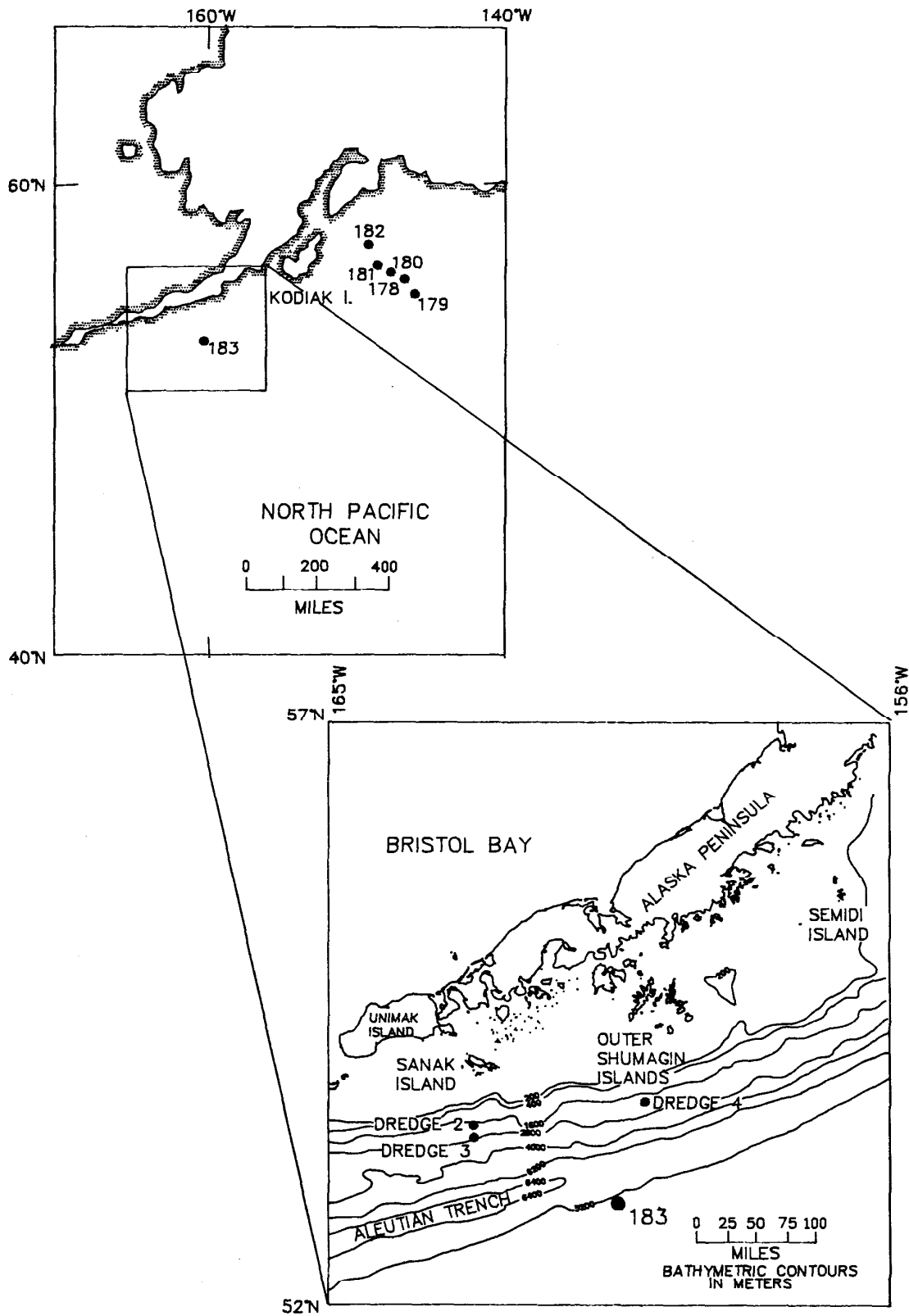


FIGURE 6. Locations of DSDP Leg 18 holes 178 through 183 and USGS dredge sites 2, 3, and 4.

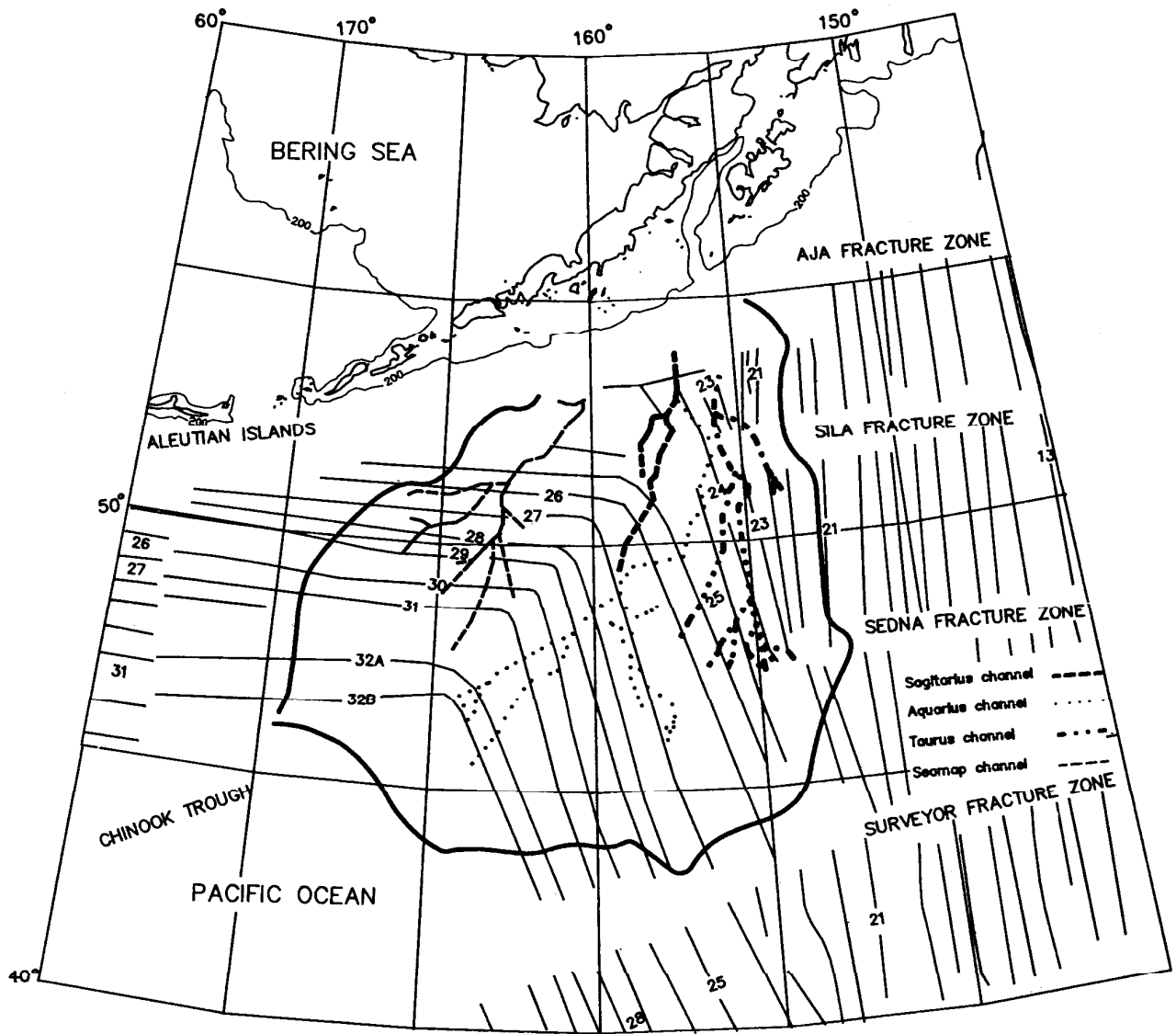


FIGURE 7. Zodiac fan outline and channels over the Gulf of Alaska magnetic anomaly pattern. Adapted from Stevenson, Scholl, and Vallier (1983).

(Kulm and others, 1973). Hole 180, located in 16,150 feet of water in the trench basin northeast of the Kodiak seamount, penetrated 1,544 feet of late Pleistocene mud, silty mud, graded silts, and ash beds (Kulm and others, 1973). Granule-pebble erratics, a displaced detrital shelf fauna, and diatomaceous beds were encountered. Kulm and others (1973) interpreted these sediments as overbank deposits from a turbidity channel. Hole 178 penetrated 2,530 feet of sediment and 56 feet of oceanic basalt. The upper 886 feet of sediment consisted of gray mud and ice-rafted erratics interpreted as glacial-marine sediments that may be as old as middle Pliocene (Kulm and others, 1973). The next 1,549 feet of underlying sediment consisted of interbedded muds, diatomaceous sediments, thin, poorly sorted silts, and turbidite sands of middle Miocene to early Pliocene age. The bottom 95 feet of sediment is a pelagic shale of earliest Miocene age (Kulm and others, 1973) or older (Scholl, 1974). The age of the basaltic basement is about 45 million years (middle Eocene) based on the age of magnetic anomaly 20 (fig. 7) (Pitman and Hayes, 1968).

The wedge deposits along the longitudinal axis of the Aleutian Trench range in thickness from 8,200 feet thick in the western Aleutian Trench to a complete absence in the Shumagin transition zone (fig. 9, p. 20). Scholl (1974) explains the absence or depletion of a middle Miocene to Pleistocene terrigenous turbidite wedge in the Shumagin transition portion of the trench by the greater bathymetric gradient of the trench floor. The gradient, estimated at 0.1° , may be sufficiently steep to have caused sedimentary bypassing rather than deposition (Scholl, 1974).

The central segment of the Aleutian Trench lies west of the Shumagin transition zone and 162° W. longitude (fig. 9). A middle Miocene to Pleistocene turbidite wedge (that is absent or depleted in the transition zone) thickens to over 6,500 feet along the inner wall of the Central Aleutian Trench and overlies a landward-dipping pelagic sequence of Late Cretaceous to Neogene age (Scholl, 1974).

Slope Geology

The juncture between the lower slope and the inner wall of the Aleutian Trench is the seaward limit of a 20-mile-wide belt of active thrusts and folds in which accreted trench and Aleutian Abyssal Plain deposits are being deformed (fig. 10, p. 22). Commonly, the

landward limit of this deformation is the trench-slope break, a discontinuity that separates the rising frontal arc from a subsiding zone landward of the slope ridges (for example, the Unimak ridge along the Unimak and West Sanak basins; plate 1). Early interpretations of this upper-slope discontinuity in the eastern Aleutian Arc system (Kodiak-Shumagin margin) described it as a fault zone (von Huene, 1972). However, recent MMS mapping along the Shumagin margin indicates that the discontinuity is composed of forearc outer ridges that have acted as baffles for Tertiary sediment accumulation on the shelf and upper slope (plate 1). The sediment accumulation commonly laps over the ridges and extends into the trench lower slope.

Accretion along the Central Aleutian Trench has been described by McCarthy and Scholl (1985) and Harbert and others (1986), and along the Shumagin-Kodiak trench by Moore (1978), Moore and Allwardt (1980), Byrne (1986), Sample and Fisher (1986), Bruns, von Huene, and others (1987), and von Huene and others (in press). Along the forearc margin in the Shumagin Planning Area, the upper portion of the subducted sedimentary layer is being accreted to the frontal arc as underthrusting progresses (fig. 10). This accretionary process uplifts the slope and builds the slope seaward (von Huene, 1972; Seely and Dickinson, 1977). The accretionary process includes the offscraping of deep-sea sediments that are bounded by landward-dipping thrust faults. As the accretionary prism grows and a critical overburden pressure is reached, a decollement surface is formed within undeformed pelagic clays present above the subducting oceanic crust. Slabs of sediment are then detached at the decollement and underplated beneath the accretionary prism (fig. 10).

Similar accretionary and underplating configurations in subduction complexes have been identified on seismic data from areas such as the Nankai Trough (Aoki and others, 1982), and the Makran accretionary prism (Platt and others, 1985). More recently, accretionary and underplating features of the Barbados Ridge complex, Lesser Antilles (fig. 11, p. 23), were identified utilizing both seismic data and conventional cores from the ODP Leg 110 (Masche and others, 1988). The drilling results elucidated the structural dynamics associated with the accretionary prism and underthrust segments of the subduction complex. At hole 671, the decollement consists of 131 feet of sheared mudstone that separates 1,641 feet of imbricately thrust, offscraped mudstone from relatively undeformed,

NW

SE

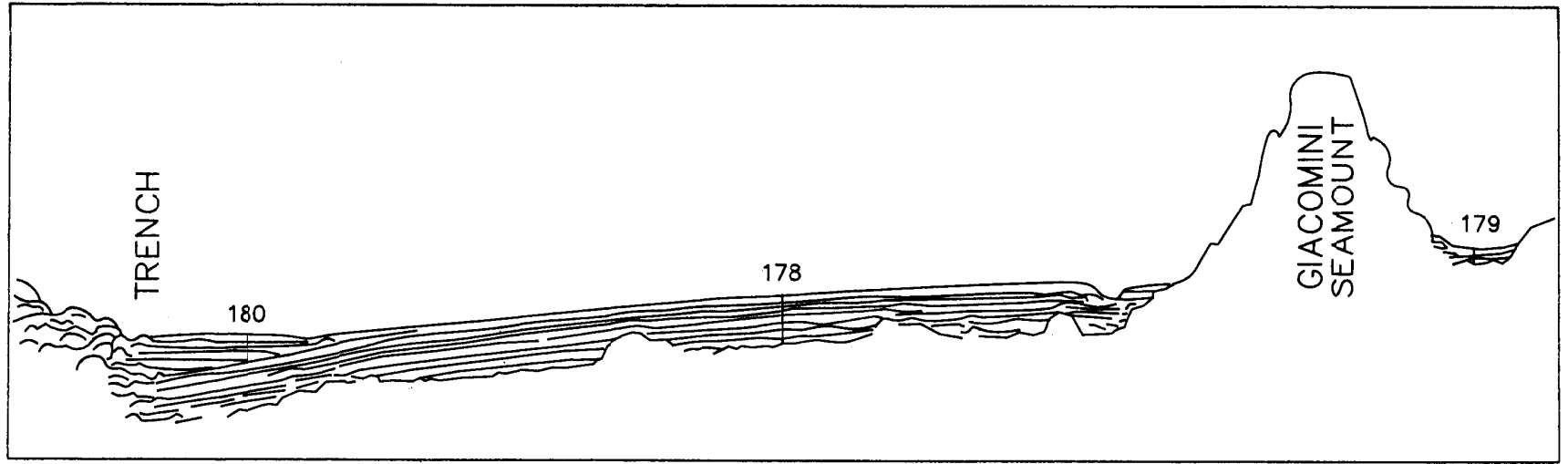


FIGURE 8. Schematic profile from the Giacomini seamount to the eastern Aleutian Trench through DSDP Leg 18 holes 178, 179, and 180. Adapted from Kulm and others (1973).

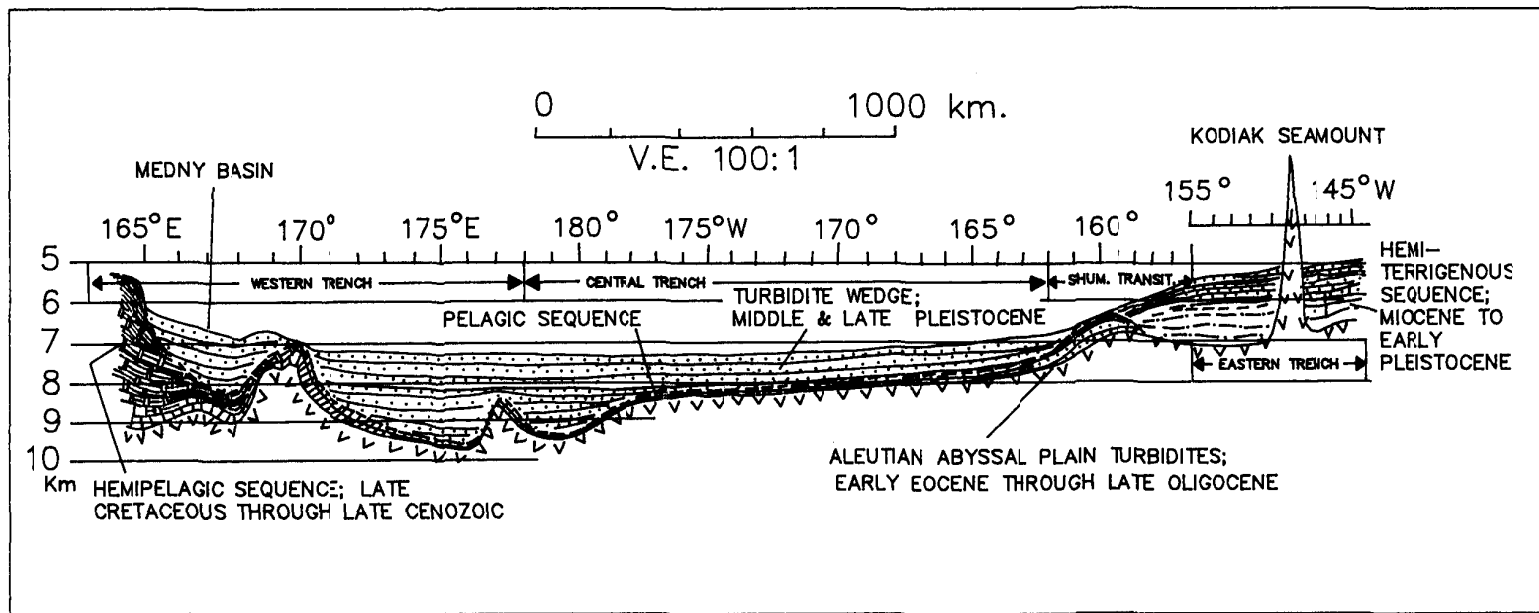


FIGURE 9. Longitudinal profile of the Aleutian Trench. Adapted from Scholl (1974).

underthrust mudstone and siltstone (fig. 11, p. 23). Pore-water chemistry at the various Leg 110 drill sites indicated that the decollement acts as a hydrologic barrier, separating the methane-rich fluids associated with the underthrust strata from the methane-free fluids of the offscraped strata (Masle and others, 1988).

Accreted sediment sequences are commonly bounded by seismically mappable, landward-dipping thrust faults (fig. 10, p. 22). Some of these faults may be fracture pathways by which large volumes of water move during dewatering and compaction of the accreted sediments (Karig and Sharman, 1975; Cloos, 1984). Lewis and others (1986) mapped thrust faults on the surface of the lower slope along the Shumagin margin (fig. 12, p. 24). These thrust faults, which strike subparallel to the trench axis and extend up to 37 miles, are commonly found within 12 to 18 miles of the trench-slope break. The faults are often replaced along strike by anticlinal compressional folds up to 6 miles in length that also parallel the trench. The thrust faults can be traced upslope into apparent strike-slip faults that are oblique to the trench axis and offset the base of the trench slope. Two sets of oblique strike-slip faults exist: one set, west of 161° W. longitude, strikes west-northwest with a right lateral sense of displacement; the other set, east of 161° W. longitude, strikes north-northeast with a left lateral sense of displacement (Lewis and others, 1988). Figure 12 shows that the oblique, right-lateral strike-slip faults are on trend with the Sanak Island Wrench Zone of Steffy and Horowitz (1987) and the projected "old" Beringian transform margin.

The slope subduction complex contains structural ridges (that may also be bathymetric highs) that trend oblique to the trench axis (von Huene, 1972; Bruns and others, 1985; Bruns, von Huene, and others, 1987). Figure 13 (p. 25) and plate 9 depict structural ridges in the Shumagin slope area. The structure of these features suggests that they were formed by uplift. Uplift, expressed by the tilt of the Plio-Pleistocene(?) section towards the trench, was also documented in the adjacent slope area off Kodiak Island by von Huene (1972).

A structural ridge, the mid-slope Unimak ridge (fig. 13), extends from southwest of Sanak Island, where it is a bathymetric high and a depositional boundary for the Unimak shelf basin, to east of Sanak Island, where it becomes a subsurface boundary of the West Sanak basin (plate 1). Dredge samples were collected by the

USGS in 1979 from the northwest and southeast sides of the Unimak ridge (fig. 6, sites 2 and 3) (Bruns and others, 1985). Lithologies identified include a late Eocene calcareous mudstone (interpreted by Bruns, Vallier, and others, 1987, as a probable erratic); an early to middle Miocene sequence of siltstone, mudstone, and sandstone containing abundant pumice, glass shards, and granitic debris; a basalt of early Miocene age; and late Pliocene to Quaternary mudstone cobbles (Bruns, Vallier, and others, 1987). The geochemistry of the basalt, which appears to occur stratigraphically beneath the other dredged lithologies, suggests an arc-related origin (Bruns, von Huene, and others, 1987).

A similar forearc outer ridge northeast of the Unimak ridge, the East Sanak slope ridge, formed as a compressional high parallel to the shelf break during Paleogene time and has functioned as a baffle for sediment accumulation since its inception (plate 1). This ridge is in great part responsible for the existence of the East Sanak slope basin. It is possible that the East Sanak slope ridge may have originally formed parallel to the margin and the Unimak ridge but has been rotated to its present position by late Paleogene strike-slip motion.

Dredge site 4 sampled the trench upper slope approximately 105 miles northeast of sites 2 and 3 (fig. 6). The sample, taken in 7,900 feet of water, recovered late Pliocene and early Pleistocene nodular limestone, calcareous siltstone, and a dacite with calc-alkaline affinities typical of an island-arc setting (Bruns, Vallier, and others, 1987).

The trench lower slope has been sampled by Leg 18 hole 181, which is located seaward of Kodiak Island in 10,120 feet of water (fig. 6). At hole 181, about 1,000 feet of Pleistocene mud interbedded with laminae of well-sorted silt, poorly sorted sand, and pebble erratics were collected (Kulm and others, 1973). The lower 650 feet of section was interpreted as tectonically deformed trench sediments. Such highly deformed sediments are common on the lower Shumagin slope, based on interpretations of CDP seismic profiles (figs. 10 and 13). Horizontal Plio-Pleistocene(?) deposits fill structurally lower areas between uplifted highs and spill over onto the surrounding seafloor.

Slump deposits are present at the base of the slope and in smaller, scattered areas upslope. Uplift of the frontal arc over-steepened the slope and initiated mass

OFFSCRAPING AND UNDERTHRUSTING ASSOCIATED WITH A SUBDUCTION COMPLEX ALONG THE ALEUTIAN TRENCH.

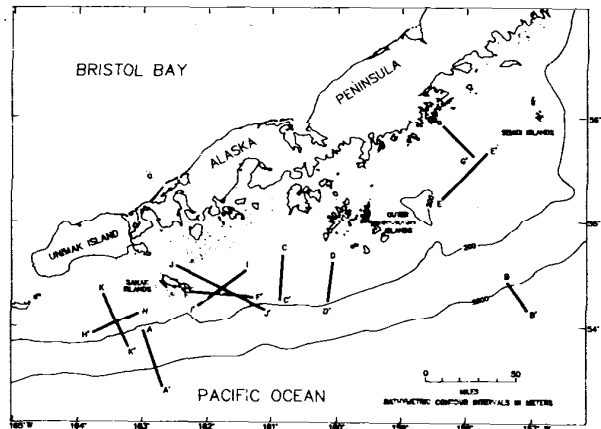
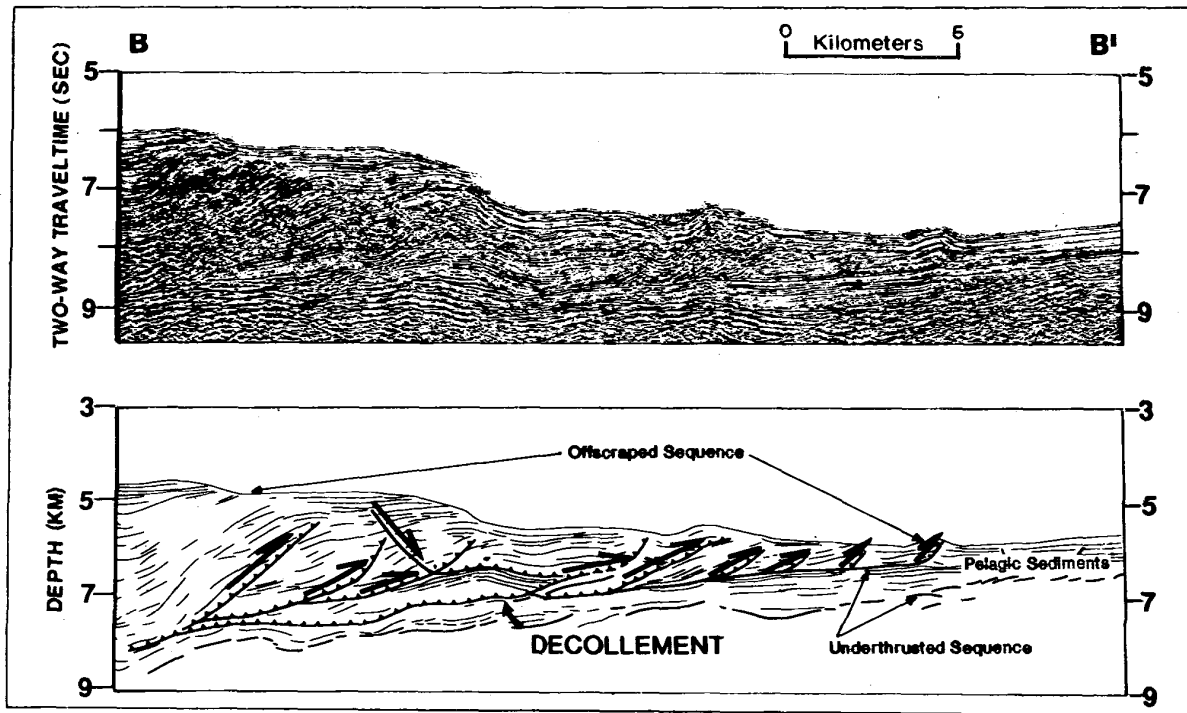


FIGURE 10. Migrated seismic section and interpreted line drawing of the Shumagin lower trench slope (USGS profile 104). Shi (1986) indicates that tectonic overloading of an offscraped sequence coincident with tectonic compression can generate a zone of high pore pressure in impermeable pelagic sediments, thus forming a low-strength decollement. The decollement permits sediment to be continually underthrust beneath it. Location of seismic profile B-B' is indicated. Adapted from Bruns, von Huene, and others (1987).

**OFFSCRAPING AND UNDERTHRUSTING ASSOCIATED WITH THE
BARBADOS RIDGE SUBDUCTION COMPLEX, BARBADOS**

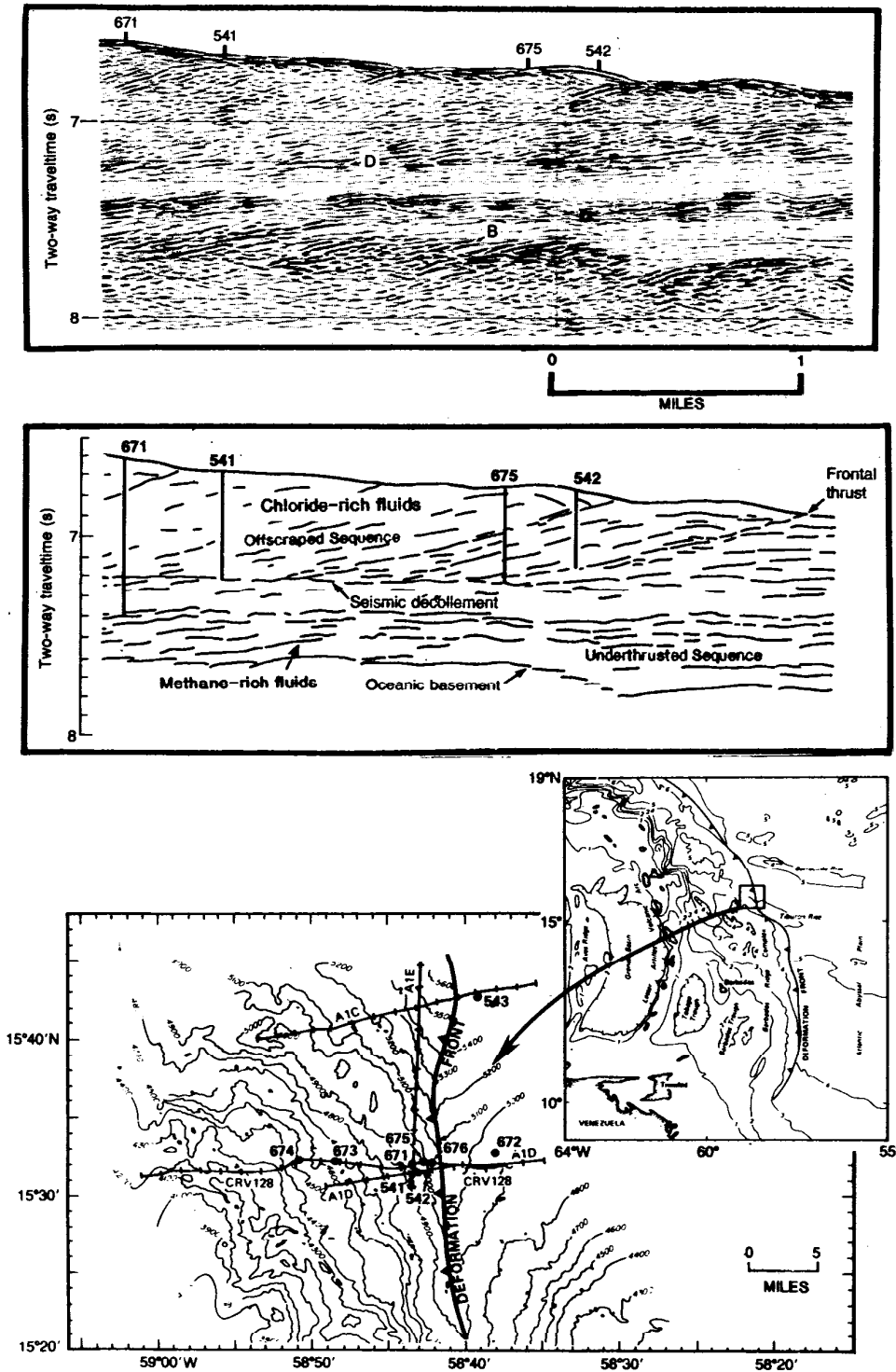


FIGURE 11. Migrated seismic section and interpreted line drawing of the Barbados Ridge accretionary complex along ODP Leg 110. The top illustration is a portion of the migrated seismic section CRV 128 from drill site 671 to drill site 542. Reflector "D" is interpreted to be a decollement and reflector "B" is top of oceanic basement. Adapted from Mascle and others (1988).

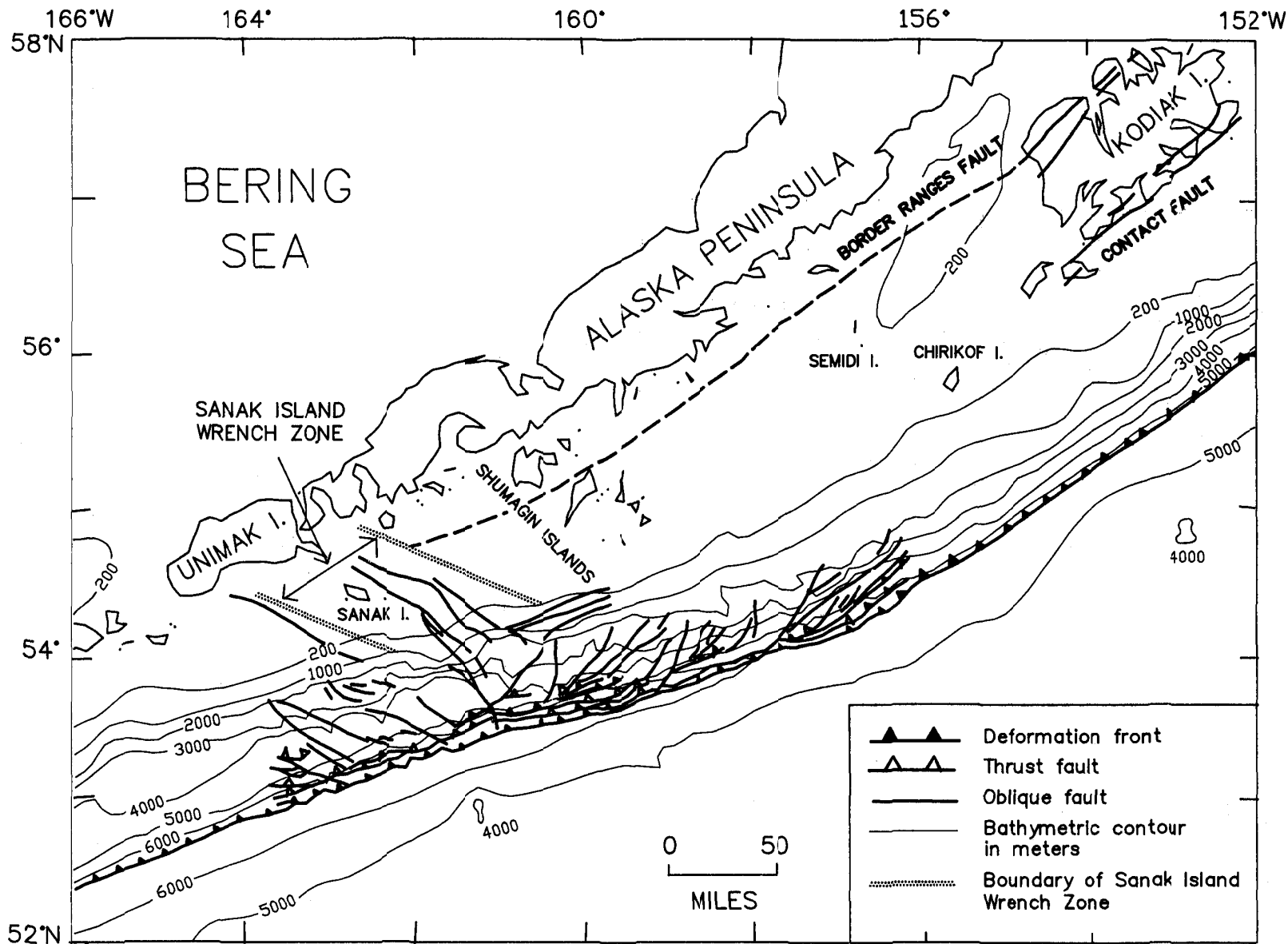


FIGURE 12. Fault pattern of the Shumagin continental slope. Adapted from Lewis and others (1986) and a figure courtesy of T. Bruns (personal commun., 1987).

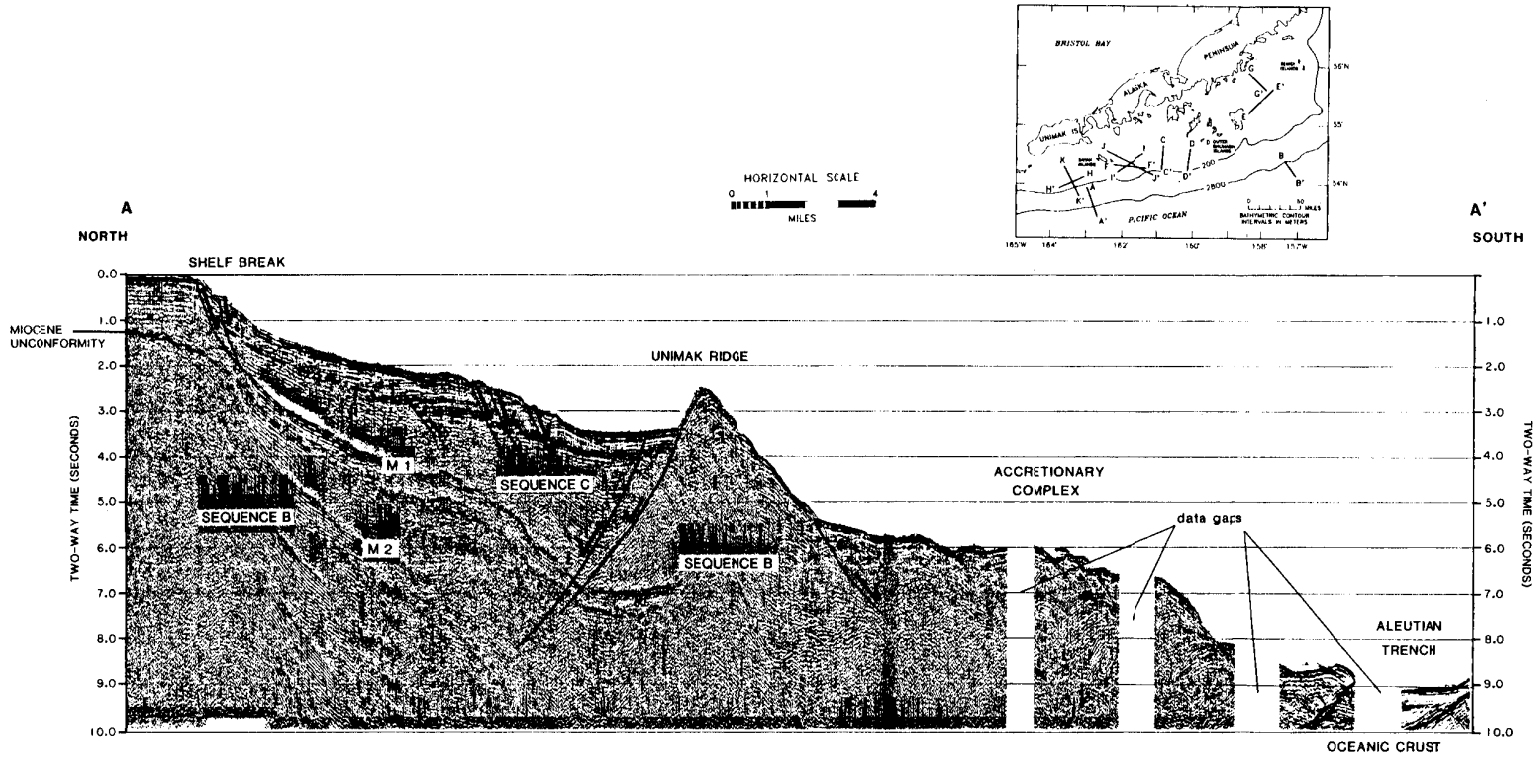


FIGURE 13. USGS seismic-reflection profile of the Shumagin slope, the Unimak ridge, and the Aleutian Trench.

slumping. The slump deposits are usually detached along listric normal faults on the upslope side of the slump, then sole into horizontal slippage planes over

which most of the downslope movement occurs. These mounded seafloor deposits are seismically characterized by disrupted reflections.

3. Onshore Geology

Beginning in the Mesozoic, the Peninsular, Chugach, and Prince William tectonostratigraphic terranes of southwestern Alaska were accreted to the margin of southwestern Alaska (fig. 5, p. 13). The Peninsular terrane consists of Permian through Cretaceous rocks north of the Border Ranges fault on the Alaska Peninsula and in offshore basins. The Border Ranges fault is a major tectonic boundary that separates the Peninsular terrane from the Cretaceous rocks of the Chugach terrane. To the south, the Contact fault separates Chugach terrane rocks from the Paleocene and younger rocks of the Prince William terrane (fig. 5)(Nilsen and Moore, 1979; Detterman and others, 1981, in press; Jones and others, 1981; Moore and others, 1983).

The relationship between the strata north and south of the Border Ranges fault is unclear. It appears that the Peninsular, Chugach, and Prince William terranes were juxtaposed during the Tertiary. Rocks north of the Border Ranges fault are, at least in part, the provenance of sediments deposited on the Kodiak and Shumagin shelf. Cretaceous and younger strata on the Alaska Peninsula may be nearshore facies of Chugach and Prince William terrane strata in the offshore basins of the Shumagin Planning Area (Detterman and others, in press).

Alaska Peninsula Stratigraphy

The surface and subsurface geology of the Alaska Peninsula has been extensively investigated. The combined section includes metamorphic, volcanic, plutonic, and sedimentary rocks as old as Permian. The stratigraphy, structure, and lithology of this area have been discussed by Burk (1965), McLean (1977), Detterman and others (1981, 1987, in press), and Moore and others (1983)(fig. 14, p. 31).

The oldest Peninsular terrane rock that borders the Shumagin Planning Area is the Middle Jurassic Shelikof Formation. This formation consists of nonmarine to deep-water marine sediments, including volcanoclastic sandstones, siltstones, conglomerates, and ash deposits, that were deposited in a rapidly subsiding basin bordering a volcanic island-arc system (Burk, 1965; Brockway and others, 1975; and McLean,

1979). This island-arc system was underlain by plutonic rocks of Jurassic age of the northeast-southwest-trending Alaska-Aleutian Range batholith (fig. 5)(Reed and Lanphere, 1973). The Shelikof Formation is disconformably overlain by the Late Jurassic Naknek Formation, which consists of arkosic sandstones, siltstones, and conglomerates (Detterman and others, in press)(fig. 14). The Naknek Formation was deposited in fluvial to outer shelf environments, and its arkosic sediments record the unroofing of the volcanic island-arc system and exposure of granitic plutons (McLean, 1979). This uplift and erosion is inferred to have begun in the Middle Jurassic and continued into the Early Cretaceous. According to Detterman and others (in press), much of the "middle" Cretaceous (Aptian to Santonian) section is missing from the Alaska Peninsula.

During the Late Cretaceous, a volcanic-plutonic arc terrane north of the present-day Bruin Bay fault provided a heterogeneous influx of volcanic, granitic, and sedimentary detritus that accumulated in a forearc basin associated with a narrow continental shelf (Mancini and others, 1978). The Late Cretaceous Chignik Formation, a cyclic sequence of nonmarine and marine strata which locally unconformably overlies the Naknek Formation, is composed of sandstone, pebble-cobble conglomerates, siltstone, shale, and coal (Detterman and others, 1981, in press)(fig. 14). The Hoodoo Formation overlies and laterally intertongues with the Chignik Formation and is composed of deep-water marine flysch of black shale, siltstone, and sandstone (Burk, 1965). The Kaguyak Formation, a Late Cretaceous flysch deposit, was described by Detterman and Miller (1985).

A regional unconformity separates Mesozoic and Cenozoic strata beneath the Shelikof Strait and on the Alaska Peninsula (Burk, 1965). This unconformity truncates strata ranging in age from Late Jurassic (Naknek Formation) to Late Cretaceous (Hoodoo Formation) and is present at the base of the Paleogene Tolstoi Formation (Detterman and others, 1981).

The Tolstoi Formation of late Paleocene to middle Eocene age consists of nonmarine to shallow-water marine clastics that disconformably overlie the Late Cretaceous Hoodoo Formation. The Tolstoi Formation includes massive- to thin-bedded volcanoclastic

conglomerate, tuff, sandstone, siltstone, shale, and coal deposited primarily in fluvial environments. The upper section is conformable with the lower, but contains numerous distinctive conglomerate clasts and abundant volcanic debris. According to Detterman and others (in press), the highly weathered volcanic and granitic detritus of the Tolstoi Formation was derived from an older Mesozoic terrane.

During the late Eocene and Oligocene, the central Alaska Peninsula was occupied by the Meshik magmatic arc (Wilson, 1985). The Meshik volcanics unconformably overlie the Tolstoi Formation and contain interbedded conglomeratic volcanoclastics, pyroclastic flows, rubble flows, and lahars (Detterman and others, in press). The flows have been radiometrically dated at between 42.4 and 21.2 million years, suggesting that volcanism was active from Eocene to early Miocene time. The Stepovak Formation in the Port Moller area (fig. 14) is stratigraphically equivalent to the Meshik volcanics and consists of tuffaceous, fine-grained sandstone and mudstone (Burk, 1965). Marine fossils from the Coal Bay and McGinty Point sections indicate deposition in neritic to upper bathyal depths.

The Belkofski Formation is probably early and middle Miocene and late Oligocene in age (fig. 14) and consists of a lower marine sequence and an upper nonmarine sequence (Burk, 1965; Detterman and others, in press). The formation consists of volcanoclastic sandstone, carbonaceous mudstone, tuffaceous sandstone, and siltstone. Andesitic dikes and sills and quartz-dioritic stocks intrude the formation. Locally, the Belkofski Formation contains a mixed fossil floral assemblage of evergreen needles and broad-leaf deciduous leaves. These plant fossils, taken in conjunction with bimodal, trough cross-stratification, suggest deposition that was influenced by marine tidal currents. Overall, the Belkofski Formation appears to represent a delta plain in communication with an open marine system to the south (Detterman and others, in press).

The type section of the Unga Formation, located on Unga Island (fig. 5, p. 13), is a nonmarine sedimentary sequence of late Oligocene to early middle Miocene age (Detterman and others, in press). The formation is composed of volcanoclastic conglomerates, sandstones, siltstones, and coal beds that are interbedded with massive welded tuffs, lahars, and debris flows containing logs and carbonized wood. The Oligocene macrofauna and macroflora of the Unga Formation

suggest that it may be in part correlative with the Belkofski Formation (Detterman and others, in press). The Unga Formation is disconformable with the underlying Stepovak Formation and is disconformably overlain by Miocene volcanic rocks (Wilson and others, 1989).

The Bear Lake Formation, primarily exposed along the northern shore of the Alaska Peninsula (fig. 5), contains fossils that range in age between middle and late Miocene (Marincovich, 1988), and consists of nonmarine to marginal-marine sediments deposited in fluvial-deltaic and tidally influenced environments. Sandstones of the Bear Lake Formation contain abundant granitic detritus. Sedimentary structures and mineralogical constituents indicate that the Bear Lake Formation was derived from an emergent volcanic and batholithic terrane to the south, presumably the Kodiak-Shumagin batholith (Lyle and others, 1978). Alternatively, Detterman and others (in press) maintain that the sediment source was the older sedimentary and plutonic rocks of the more proximate Alaska-Aleutian Range batholith. The lower contact of the Bear Lake Formation with the Meshik, Stepovak, and Tolstoi Formations varies from a disconformity to an angular unconformity (Wilson and others, 1989).

The Tachilni Formation is exposed on a cape between Cold Bay and Morzhovoi Bay on the Alaska Peninsula. The Tachilni Formation contains volcanic-rich sandstones, mudstones, and conglomerates deposited in nonmarine and marine environments. The molluscan fauna is similar to that of the Miocene Bear Lake Formation (Marincovich, 1983), although the Tachilni Formation contains far more volcanic clasts (Detterman and others, in press).

The Pliocene Milky River Formation unconformably overlies the Bear Lake and Tachilni Formations (Detterman and others, 1981, in press). The erosional event separating the formations seems to have been regional in extent. The Milky River Formation consists of up to 5,000 feet of nonmarine sedimentary rocks with interlayered volcanic flows and sills. Andesitic flows, lahars, and tuff beds are numerous in the upper part of the formation (Detterman and others, in press).

Kodiak Islands

Exposed Peninsular, Chugach, and Prince William terrane rocks on Kodiak and adjacent islands illustrate a prolonged period of subduction and accretion that

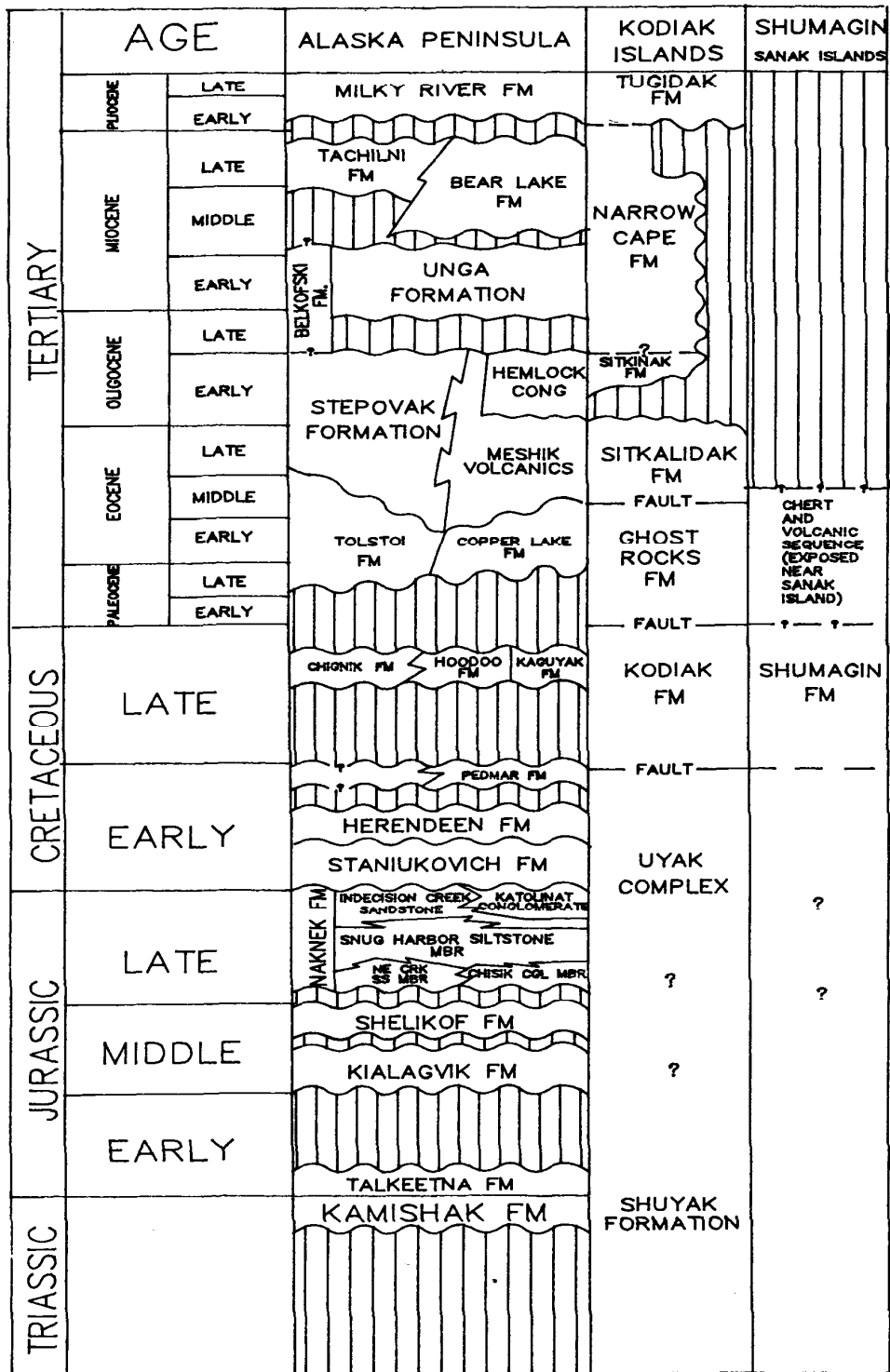


FIGURE 14. Stratigraphic column for the exposed onshore geology of the Alaska Peninsula, Kodiak, Shumagin, and Sanak Islands. Adapted from Moore and others (1983) and Detterman and others (in press).

began in the early Mesozoic (Connelly, 1978). The Kodiak Islands are constructed of parallel accreted tectonostratigraphic terranes that are successively younger to the southeast (Connelly, 1976; Moore and Allwardt, 1980)(fig. 5, p. 13). Rocks of the Chugach and Prince William terranes on Kodiak Island presumably extend southwest along strike and are present beneath the Shumagin Planning Area.

A belt of Peninsular terrane is exposed along the northern border of Kodiak Island and on Afognak and Shuyak Islands (fig. 5). The oldest formation exposed on the islands is the Late Triassic Shuyak Formation (Connelly, 1976), which consists of pillowed greenstone and volcanoclastic turbidites. The Late Triassic or Early Jurassic Kodiak Schist structurally underlies the Late Triassic Shuyak Formation along the Shuyak fault (Forbes and Lanphere, 1973). The structural setting, metamorphic grade, and potassium-argon age dates of the Kodiak Schist are very similar to those of the Seldovia Schist of the Kenai Peninsula. Both formations were metamorphosed under similar high pressure and temperature conditions (Carden and others, 1977). Peninsular terrane rocks on the Barren Islands and on the Kenai and Alaska Peninsulas collectively delineate the southwestern extent of a Mesozoic forearc basin.

Border Ranges Fault

The Border Ranges fault is a major tectonic boundary that separates the much older and more highly metamorphosed Jurassic-Triassic accretionary complex of the Peninsular terrane from the Cretaceous accretionary complex of the Chugach terrane to the south (fig. 5). The Border Ranges fault extends from Chichagof Island in southeastern Alaska to near Sanak Island at the southwestern end of the Alaska Peninsula (MacKevett and Plafker, 1974; Decker and Johnson, 1981; Burns, 1982). Fisher (1981) and Fisher and von Huene (1984) traced the Border Ranges fault 600 miles from the south side of the Copper River Basin, along the southeast side of Cook Inlet and the northwest side of Kodiak Island, to south of Sutwik Island, where it is recognized by parallel positive magnetic anomalies and a gravimetric contrast. The Border Ranges fault on the north side of Kodiak Island is a northeast-striking fault that thrust Triassic and Jurassic volcanic, sedimentary, and ultramafic rocks over Cretaceous sedimentary rocks in the southeast. Wilson, Case, and others (1985) have identified structurally disrupted Oligocene and Miocene strata 30 miles northwest of our projected

location of the Border Ranges fault between the Inner and Outer Shumagin Islands.

Chugach and Prince William Terranes

The Chugach terrane extends from Sanak Island northeast for over 1,200 miles along the southwestern margin of the Gulf of Alaska (fig. 5). Southeast of the Border Ranges fault on Kodiak Island, Cretaceous deep-water melange and flysch deposits of the Uyak Complex and Kodiak Formation were sequentially accreted to the continental margin to form the Chugach terrane. The Valdez Group and McHugh Complex are an expression of this turbidite system in the Gulf of Alaska (Plafker and others, 1977). On the southeast side of Kodiak Island, the Contact fault separates the deep-sea turbidites of the Late Cretaceous Kodiak Formation (Chugach terrane) from the Paleocene and Eocene turbidites of the Ghost Rocks Formation and younger Paleogene and Neogene shelf strata of the Prince William terrane. The Chugach and Prince William terranes are "stitched together" by early Tertiary plutons. Although Mesozoic and Cenozoic sedimentary rocks are exposed on Kodiak and adjacent islands, only the Late Cretaceous Shumagin Formation and the Paleocene plutonic rocks that intrude it are exposed within the Shumagin Planning Area. These rocks crop out on Sanak Island and the Outer Shumagin and Semidi Islands (fig. 5).

Early Cretaceous Accretion

The Uyak Complex on Kodiak Island, a Cretaceous subduction complex that can be traced for 300 miles over much of southwestern Alaska (fig. 5), is structurally and lithologically similar to the McHugh Complex exposed on the Barren Islands, the Kenai Peninsula, and near Anchorage (Connelly, 1978). The Uyak Complex is the oldest in a series of Cretaceous deep-water melange units that were emplaced south of the Border Ranges fault. The Uyak Complex consists of radiolarian chert and fine-grained pelagic sediments that were deposited on oceanic crust between a mid-ocean rise and an oceanic trench. As these sediments were transported into the trench, they were highly deformed and faulted into a tectonic melange (Connelly, 1978). On Kodiak Island, the Uyak Complex is a highly deformed argillite containing gray chert and large blocks of basalt.

A major fault, the Uganik thrust, separates the Uyak Complex from the younger accreted turbidites of the Late Cretaceous Kodiak Formation (fig. 5, p. 13). The Uganik thrust extends for almost 300 miles northeast along the continental margin. Cowan and Boss (1978) correlated this thrust with the Chugach Bay fault of the Kenai Peninsula and the Eagle River fault near Anchorage. The Kodiak Formation is the second in a series of Cretaceous trench-fill deposits that was accreted to the Alaskan continental margin.

The Shumagin Formation, exposed on the Outer Shumagin and Sanak Islands, is lithologically and structurally similar to the Kodiak Formation (Burk, 1965) and the Valdez Group on the Kenai Peninsula (fig. 14). A Late Cretaceous age for the Shumagin-Kodiak-Valdez belt is suggested by the presence of the molluscan macrofossil *Inoceramus kusiroensis* (Jones and Clark, 1973), which has also been found in the Hoodoo and Kaguyak Formations. Sedimentary structures in the arkosic wackes and shales of the Shumagin-Kodiak-Valdez belt suggest deposition in a deep-water environment.

The Shumagin Formation contains interbedded mudstone and sandstone, minor conglomerate, and ash beds (Moore, 1974a). The depositional features and lithologic characteristics present on the Outer Shumagin Islands suggest that the formation represents a transition between a proximal and distal turbidite system. The proximal massive sandstones range between 3 and 60 feet in thickness and are characterized by high sand-shale ratios. A more distal facies contains thinner, graded and massive beds. The most seaward facies is characterized by graded beds less than 1 foot thick that have sand-shale ratios of less than one. Paleocurrent analysis indicates flow parallel to the regional strike of the ancestral Aleutian Trench, predominately southwesterly on the Shumagin Islands and northwesterly on the Sanak Islands (Moore, 1973). Secondary paleocurrent trends from the Outer Shumagin Islands are from the north (Moore, 1973). Compositionally, a large percentage of the Shumagin Formation consists of unweathered angular volcanic rock fragments, which indicates a nearby volcanic source terrane (Moore, 1971).

The Shumagin Formation on the Outer Shumagin Islands is deformed into tight northeast-trending folds and thrust faults, whereas on the Sanak Islands the folds and thrust faults trend northwest (Moore, 1971) (fig. 5). These folded structures delineate the area of initial subduction and accretion of the Shumagin and

Kodiak Formations at the Cretaceous Aleutian Trench. Sample and Moore (1987) propose that these turbidites were accreted to the Cretaceous Kodiak margin by the processes of offscraping and underthrusting; offscraping resulted in the seaward growth of the accretionary wedge, and underplating thickened and vertically uplifted the accretionary prism (Byrne, 1986). The accretionary complex on Kodiak Island appears to be similar in origin to a younger accretionary complex still growing at the present Aleutian Trench (fig. 10, p. 22).

The Ghost Rocks Formation, the next youngest in a series of accreted trench-fill deposits, is exposed on the southeast side of the Kodiak Islands in a belt 100 miles long and 9 miles wide (Byrne, 1984). The Contact fault on Kodiak Island separates the Kodiak Formation from the Ghost Rocks Formation (fig. 5). The Contact fault has been considered a tectonic boundary between the Chugach and Prince William terranes, although recent petrographic evidence by Dumoulin (1988) suggests that the Chugach and Prince William terranes may be a single terrane.

The Ghost Rocks Formation consists of mildly deformed slope deposits and a highly disrupted melange sequence that was deposited in a tectonically active trench setting (Byrne, 1984). The main structures of the Ghost Rocks Formation strike northeast, parallel to older and younger structures on Kodiak Island. The flysch and melange sequences include interbedded massive sandstone, shale, pebbly mudstone, and conglomerate. The low percentage of quartz, the high ratio of plagioclase to total feldspar, and the abundance of volcanic lithic detritus indicates a predominately volcanic source terrane (Magoon and Egbert, 1986).

Both extrusive and intrusive igneous rocks are present in the Ghost Rocks Formation. Extrusive elements include pillow lava, pillow breccia, tuff, and near-trench cogenetic basalts similar to mid-oceanic ridge basalts (Moore and others, 1983). Intrusive rocks include andesitic and basaltic dikes and sills (Hill, 1978; Reid and Gill, 1980; Byrne, 1982; Moore and others, 1983) and quartz dioritic and tonalitic plutons with radiometric ages of 60 to 63 million years (Byrne, 1982). Granitic plutons associated with the Kodiak-Shumagin batholith intruded the Kodiak and Ghost Rocks Formations by the early Paleocene. These granitic rocks are part of a chain of batholiths and stocks that rims the Gulf of Alaska. Locally, west of Prince William

Sound, these dominantly granodioritic rocks have been dated at 62 to 57 million years.

Overall, the metamorphic grade of the Ghost Rocks Formation falls within the prehnite-pumpellyite facies (Moore and others, 1983). Late Cretaceous fossils are incorporated in the highly folded tectonic melange, and Paleocene interpillow pelagic limestones occur in some of the less-deformed units (Moore and others, 1983).

A sequence of bedded chert, pillow lava, sandstone, and mudstone is exposed on Long Island, a small island at the southwestern tip of Sanak Island (Moore, 1974b). This sequence may be correlative with the Ghost Rocks Formation on Kodiak Island.

The Eocene to early Oligocene Sitkalidak Formation, the youngest deep-water turbidite sequence that crops out on the Kodiak Islands, is in fault contact to the southeast with the Ghost Rocks Formation. The Sitkalidak Formation consists of massive sandstone, shale, siltstone, and conglomerate and seldom exhibits a metamorphic grade higher than zeolite facies (Moore and Allwardt, 1980). Nilsen and Moore (1979) maintain that the Sitkalidak Formation was deposited as a submarine fan system. Melange sequences exhibiting boudinage structures are present in outcrop. A mildly deformed sequence with stratal continuity is interpreted as a slope apron deposit; a more highly deformed sequence is considered to represent offscraped trench-fill (Moore and Allwardt, 1980). The Orca Group, a deep-water accretionary sequence of flysch and tholeiitic basalt in the Prince William Sound area (Plafker and others, 1985), is believed to be in part equivalent to the Sitkalidak Formation.

A significant period of uplift and erosion followed the accretion of the Sitkalidak Formation. This was followed by deposition of the early Oligocene Sitkinak Formation (J. A. Wolf, cited in Fisher, von Huene, and Hampton, 1984). In contrast to the exclusively deep-marine sediments of the Sitkalidak Formation, the Sitkinak Formation contains nonmarine and deep-water marine sequences including volcanoclastic siltstone, sandstone, conglomerate, and coaly sediments. On Sitkinak Island, the conglomerates and nonmarine coal-bearing sediments of the Sitkinak Formation rest with sharp discordance on the highly folded Sitkalidak Formation (Magoon and Egbert, 1986) (fig. 14). Granitic clasts, graywacke cobbles, and chert derived from the Late Cretaceous Kodiak Formation are commonly found within the Sitkinak Formation and suggest the timing of uplift and erosion

of the Kodiak accretionary complex and associated batholith (Clendenen and others, 1987).

The Narrow Cape Formation overlies the Sitkalidak Formation with pronounced angular unconformity at its type locality on the southeastern border of Kodiak Island (Nilsen and Moore, 1979). Molluscs from the type locality are late early and early middle Miocene in age (Allison and Marinovich, 1981). The Narrow Cape Formation on Kodiak Island exhibits a fining-upwards sequence of sandstones and siltstones that includes a basal deposit of shell debris. According to Allison (1978), this transgressive sequence represents a progressive shift in depositional facies from inner to outer neritic. On Sitkinak Island, a shallow-marine sequence of siltstone disconformably overlies the Sitkinak Formation and contains molluscs that are late Oligocene to early Miocene in age (Allison and Marinovich, 1981). There is disagreement as to whether this older stratigraphic section is part of the Narrow Cape Formation (Moore, 1969; and Allison and Marinovich, 1981) or should be designated a new formation (the Trinity Island siltstone of Armentrout, cited in Moore and Allwardt, 1980). In this report, this siltstone unit is provisionally considered part of the Narrow Cape Formation. The quartzo-feldspathic sandstones of the Narrow Cape Formation contain significantly greater percentages of quartz than older Tertiary and Cretaceous formations south of the Border Ranges fault on Kodiak Island and probably reflect the continued uplift and stripping of the Kodiak accretionary complex and associated plutonic rocks.

The Tugidak Formation is exposed on Tugidak and Chirikof Islands, where it consists of glacio-marine sandstones, siltstones, and mudstones of late Pliocene and early Pleistocene age (Allison, 1978). The Tugidak Formation is disconformable with the underlying Narrow Cape Formation on Kodiak Island, although it unconformably overlies the Sitkalidak Formation on Chirikof Island (Fisher, von Huene, and Hampton, 1984).

Summary

The Cretaceous and Tertiary stratigraphic section on the Alaska Peninsula may be, in part, correlative with rocks south of the Border Ranges fault on Kodiak, Shumagin, and the Sanak Islands. The Late Cretaceous Hoodoo Formation may be, in part, correlative with the Kodiak and Shumagin Formations. Tertiary rocks on the Alaska Peninsula predominately reflect nonmarine

to marginal-marine sedimentary facies. Tertiary formations south of the Border Ranges fault consist of strata that were deposited predominately on the outer shelf, slope, and abyssal plain. Therefore, some Tertiary strata on the Alaska Peninsula may be nearshore facies equivalents of the basement and basin fill strata beneath the Kodiak and Shumagin outer continental shelf.

South of the Border Ranges fault, the shelf is made up of Cretaceous, Paleocene, and Eocene turbidites and late Paleogene, Neogene, and younger shelf deposits. The Cretaceous Uyak, Kodiak, and Shumagin Formations and the early Paleogene Ghost Rocks and Sitkalidak Formations were accreted to the margin by a

complicated process of offscraping and underthrusting. During the late Paleogene, the Cretaceous and Paleogene accretionary complex was uplifted and truncated. This unconformity was overlain by shelf deposits of the early Oligocene Sitkinak Formation, and the late Oligocene and younger strata of the Narrow Cape and Tugidak Formations. These sediments were derived from the uplifted accretionary complex on Kodiak Island and from reworked older Mesozoic sediments on the Alaska Peninsula. Differential uplift through the late Neogene on Kodiak Island is indicated by the fact that both Miocene and Pliocene strata unconformably overlie the Eocene Sitkalidak Formation.

4. Continental Shelf Geology

Previously published studies on the forearc region in the Shumagin Planning Area were based on wide-spaced, single-channel and multichannel CDP seismic-reflection data, potential field data, and seismic-refraction data integrated with data derived from dredge samples (Bruns and Bayer, 1977; Bruns and von Huene, 1977; Bruns and others, 1985, 1986; Bruns, Vallier, and others, 1987; Bruns, von Huene, and others, 1987). This report utilizes those studies and newly available CDP seismic-reflection data (figs. 3 and 15, p. 4 and 38) that are tied to the Kodiak shelf stratigraphic test wells (fig. 5, p. 13).

Kodiak Island stratigraphy was projected offshore to the Kodiak wells by Turner and others (1987) and tied to the studies of Fisher (1979, 1980), Fisher and von Huene (1980), and Fisher and others (1984). A regional diachronous Miocene unconformity established by these previous studies was tied into the Shumagin Planning Area in this report. Our interpretations of seismic data below the Miocene unconformity, *although somewhat speculative*, are based on recent structural evolutionary models and processes (offscraping, accretion, underthrusting, underplating, and duplexing) proposed for other forearc margins (Karig and Sharman, 1975; Aoki and others, 1982; Byrne, 1986; Lewis and others, 1986, 1988; Sample and Fisher, 1986; Fisher and Byrne, 1987; Sample and Moore, 1987; Mascle and others, 1988; Westbrook and others, 1988). Basin geometry, geologic history, and petroleum potential are based, to a great extent, on extrapolated stratigraphic data. This approach assumes that southern Alaska consists of a series of accreted tectonostratigraphic terranes and that geologic trends within these terranes can be extrapolated along strike.

Kodiak DST Wells

The Kodiak shelf stratigraphic test wells are discussed because the Kodiak shelf is believed to be geologically similar to the Shumagin margin. Kodiak shelf geology is discussed in detail by Fisher (1979), Fisher and Holmes (1980), Fisher and von Huene (1984), Fisher

and others (1984), Moore and others (1983), and Turner and others (1987).

Six stratigraphic test wells were drilled on the shelf southeast of Kodiak Island (fig. 4, p. 11). Data from these wells and an interpretation of the structure, stratigraphy, and evolution of the Kodiak shelf were released by the MMS (Turner and others, 1987).

The KSSD No. 1 well was drilled to a total depth (TD) of 8,517 feet (logger's depths measured from the Kelly bushing) on the west side of the southern subbasin of the Stevenson basin (Turner and others, 1987). The Quaternary and Neogene section (1,670 to 6,142 feet) consists of mudstones, siltstones, sandstones, and conglomerates deposited in neritic to bathyal environments. Beneath the angular unconformity at 6,142 feet, the well encountered 2,370 feet of structurally deformed, probably bathyal, marine clastic sediments of Eocene age.

The KSSD No. 2 well, located 138 miles northeast of Kodiak Island, was drilled to a TD of 10,460 feet on the northern flank of the northern subbasin of the Stevenson Basin (fig. 4). The Quaternary and Neogene section (1,470 to 8,774 feet) consists of mudstones, siltstones, and shales deposited in neritic to bathyal environments. Beneath the angular unconformity at 8,774 feet, the well encountered 1,686 feet of moderately dipping (15° to 25°), probably bathyal, marine clastic sediments of middle to late Eocene age.

The KSSD No. 3 well, located 60 miles southeast of Kodiak Island, was drilled to a TD of 9,357 feet. The well was sited on a broad, flat saddle between two structural highs that are part of the Dangerous Cape High (fig. 4). The Quaternary to Neogene section (1,370 to 7,805 feet) consists of mudstones, siltstones, and sandstones deposited in neritic to bathyal environments. Beneath the unconformity at 7,805 feet, the well encountered 1,547 feet of structurally deformed, probably bathyal, marine clastic sediments of middle(?) to late Eocene age.

The KSST Nos. 1, 2, and 4a wells were also located on the Kodiak shelf (fig. 4) and drilled through thicknesses of up to 4,000 feet of Plio-Pleistocene glaciomarine diamictites.

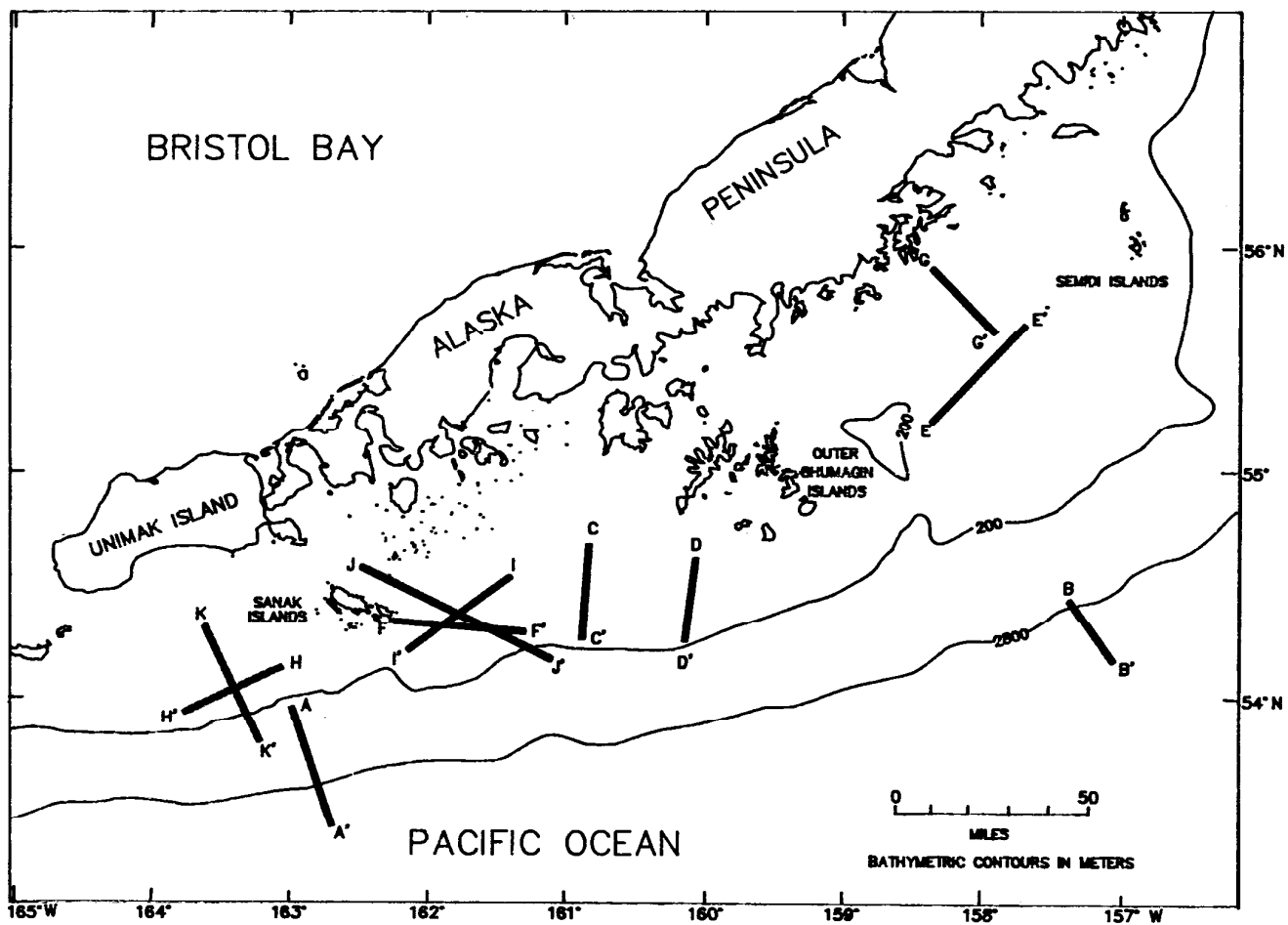


FIGURE 15. Location of CDP seismic-reflection profiles.

Turner and others (1987) believe that the Quaternary and Neogene sections in all six of the DST wells are correlative with the Tugidak (Pliocene) and Narrow Cape (Miocene) Formations on Kodiak Island (fig. 14, p. 31). Similarly, the Eocene sections encountered in the wells are correlative with the Sitkalidak Formation. No Sitkinak Formation (Oligocene) or age equivalents were identified in the wells.

The Tenneco Middleton Island No. 1 well was drilled in 1969, approximately 150 miles northeast of the KSSD No. 2 well, but seaward of the Contact fault and within the Prince William terrane (fig. 5, p. 13). About 12,000 feet of Tertiary sediments were encountered in the well. An unconformity separates a late Miocene to Pleistocene section above from a late Miocene section below (Keller and others, 1984). Rau and others (1983) place this unconformity at 2,050 feet and believe that the lower section is early to middle Miocene in age. The oldest sediments in the well are middle to late Eocene according to Rau and others (1983) and Keller and others (1984), although Larson (personal commun., 1987) suggests an early to middle Eocene age. Baxendale and Hemler (1984) proposed the presence of Paleocene sediments as shallow as 10,880 feet in the well. Although they found no evidence for a major unconformity, they interpreted a late Eocene weathered zone at 9,300 feet as a possible brief nonmarine erosional episode. Keller and others (1984) noted an unconformity between the middle and late Eocene, whereas Rau and others (1983) indicate no Paleogene unconformities.

Miocene Unconformity

A diachronous angular unconformity was recognized between Neogene and Eocene strata on Kodiak Island and in offshore wells (Fisher and others, 1984; Turner and others, 1987) (fig. 16, p. 41). For this report, this horizon is termed the Miocene unconformity and is an important marker horizon on interpreted seismic-reflection panels.

Late Oligocene rocks are not present in the three deeper Kodiak shelf wells (fig. 22, p. 60) (Turner and others, 1987). Paleobathymetric data from the Kodiak shelf wells suggest a gradual shoaling from the Eocene to the Miocene (Turner and others, 1987). In the KSSD wells, the regional unconformity was recognized on the basis of microfossil data, dip changes, increases in resistivity, and a sudden velocity increase on the sonic log. Moore and others (1983) place the

nonmarine Sitkinak Formation (early Oligocene) above this regional unconformity on Kodiak Island (fig. 14).

Sonic-log data from two of the three deeper Kodiak wells show a velocity increase across the Miocene unconformity. In the KSSD No. 1 well, interval velocities for the early(?) to late Miocene section above the unconformity (at 6,142 feet) range from 8,000 to 10,500 feet per second (ft/sec), whereas the velocity for the early to late(?) Eocene section below the unconformity ranges from 11,100 to 15,400 ft/sec. In the KSSD No. 2 well, the acoustic characteristics of the strata above and below the unconformity are masked by overpressuring, which begins at a depth of approximately 6,500 feet and continues to the bottom of the well (Sherwood, personal commun., 1987). The middle to late Miocene section just above the overpressured zone exhibits an interval velocity range of 9,100 to 10,000 ft/sec. In the KSSD No. 3 well, interval velocities for the middle to late Miocene section above the unconformity (at 7,450 feet) range from 8,300 to 10,000 ft/sec, whereas the velocity for the middle(?) to late Eocene section below the unconformity ranges from 10,600 to 13,300 ft/sec. These general velocity characteristics were assumed to remain relatively consistent along strike between the Kodiak and Shumagin margins.

Shumagin Shelf Geology

Seismic studies of the Shumagin shelf revealed a number of local and regional unconformities in addition to the widely recognized Miocene unconformity. Seismic sequence analysis was used to define and interpret regional depositional systems. Previous mapping efforts by Bruns and von Huene (1977), Bruns and others (1985), and Bruns, von Huene, and others (1987) delineated five Tertiary sedimentary basins on the Shumagin shelf and slope (the Shumagin, East Sanak, Central Sanak, "west" Sanak, and Unimak basins). In this report the "west" and Central Sanak basins are combined as the West Sanak basin, and a basin parallel and adjacent to the East Sanak basin in the outer shelf and trench upper slope was identified as the East Sanak slope basin (plate 1). In addition, a relatively small area between the Semidi Islands and the eastern boundary of the Shumagin Planning Area (the 156° W. longitude line) is underlain by the western flank of the Tugidak basin.

Over 20,000 feet of Quaternary and Neogene marine clastics have accumulated in the Shumagin margin shelf basins. The basement consists of accreted Cretaceous and Paleocene deep-water clastics and Paleocene intrusives. These rocks are probably found everywhere beneath the Shumagin margin except under the Unimak basin, where an Eocene basement complex is thought to be present.

The Shumagin basin is an asymmetric graben bounded on the north by an extension of the Border Ranges fault, on the east and west by the Semidi and Outer Shumagin Islands, and on the south by a broad, shelf-edge high. The East Sanak basin occupies the continental shelf landward of the northeast-trending Shumagin ridge and the northwest-trending Central Sanak high. The East Sanak slope basin is a narrow extensional rift situated on the outer shelf and upper slope between the Shumagin ridge and the East Sanak slope ridge. The West Sanak basin, situated east of Sanak Island, trends northwest-southeast. Most of the West Sanak basin is on the continental shelf although a portion is on the upper slope. The West Sanak basin is an asymmetric graben bounded by the Central Sanak high on the northeast, the Sanak Island Transverse High to the southwest, the Unimak ridge on the south, and the East Sanak slope ridge on the southeast. Southwest of Sanak Island, the Unimak basin is filled with a progradational sedimentary sequence that was probably deposited on an accretionary basement.

Seismic Stratigraphy

The Shumagin shelf section is divided into three major seismic sequences, A, B, and C, and the distribution, reflection characteristics, stratigraphy, and depositional setting are described for each. Seismic-reflection profiles (plates 2 through 10) are presented to illustrate these general characteristics and to support interpretations of each sequence.

Sequence A (Cretaceous and Paleocene)

Seismic sequence A is a basement complex that floors the Shumagin margin. Seismic-reflection data indicate that sequence A consists of a thick, highly faulted, sedimentary section that is buried to depths greater than 40,000 feet. A portion of sequence A rises to form the Outer Shumagin, Sanak, and Semidi Islands, which consist predominately of Late Cretaceous Shumagin Formation, and Paleocene granodiorite intrusives, but may also include the Early Cretaceous Uyak Complex (fig. 16). Sequence A is also assumed to include rocks

coeval with the Paleocene Ghost Rocks Formation (fig. 16), although this formation does not crop out within the Shumagin Planning Area. This assumption is based on the fact that Paleocene intrusives cut both the Kodiak and Ghost Rocks Formations on Kodiak Island (Moore and Allwardt, 1980).

Sequence A is bounded at the top by an unconformity that is recognizable in the Shumagin and East Sanak basins (plates 2 and 3). The unconformity displays dips greater than 45° in the East Shumagin subbasin and the northern end of the East Sanak basin. These steep dips may indicate that there was topographic relief of the erosional surface as it formed. Where this upper boundary is not apparent, sequence A is undifferentiated from the overlying sequence B.

Seismic sequence A is considered to be the acoustic basement throughout most of the Shumagin margin, although some internal reflections are present (for example, plate 2 shows sequence A in the East Sanak basin characterized by relatively high-amplitude, tilted, parallel, and discontinuous reflections). Adjacent to the East Sanak basin, the Central Sanak high contains undifferentiated sequence A and B strata and is characterized by the absence of internal seismic-reflection continuity. To the northeast, in the East Shumagin subbasin, a southwest-northeast seismic profile depicts sequence A as consisting of sharp, relatively high-amplitude reflections that display moderate continuity within large fold structures (plate 3). To the southwest in the West Sanak basin (plate 4), an east-west seismic profile depicts the basin and an adjacent uplifted basement complex termed the Sanak Island Transverse High (SITH). Because the SITH rises to the northwest to form the Sanak Islands, it is assumed to consist predominately of sequence A, although it may also include younger sequence B strata.

The Late Cretaceous Shumagin Formation (part of sequence A) was deposited in a trench setting and was later uplifted, deformed, and accreted to the Shumagin margin (Bruns and von Huene, 1977). Modern analogs of such accretionary complexes are present south of the Shumagin shelf (fig. 10, p. 22), and in the Barbados Ridge complex, Lesser Antilles (fig. 11, p. 23). Accretion along a forearc margin may include the formation of a decollement, a zone of sheared clays that separates offscraped from underthrust material and is necessary for the underplating process (figs. 10 and 11). The deepest resolvable seismic features beneath

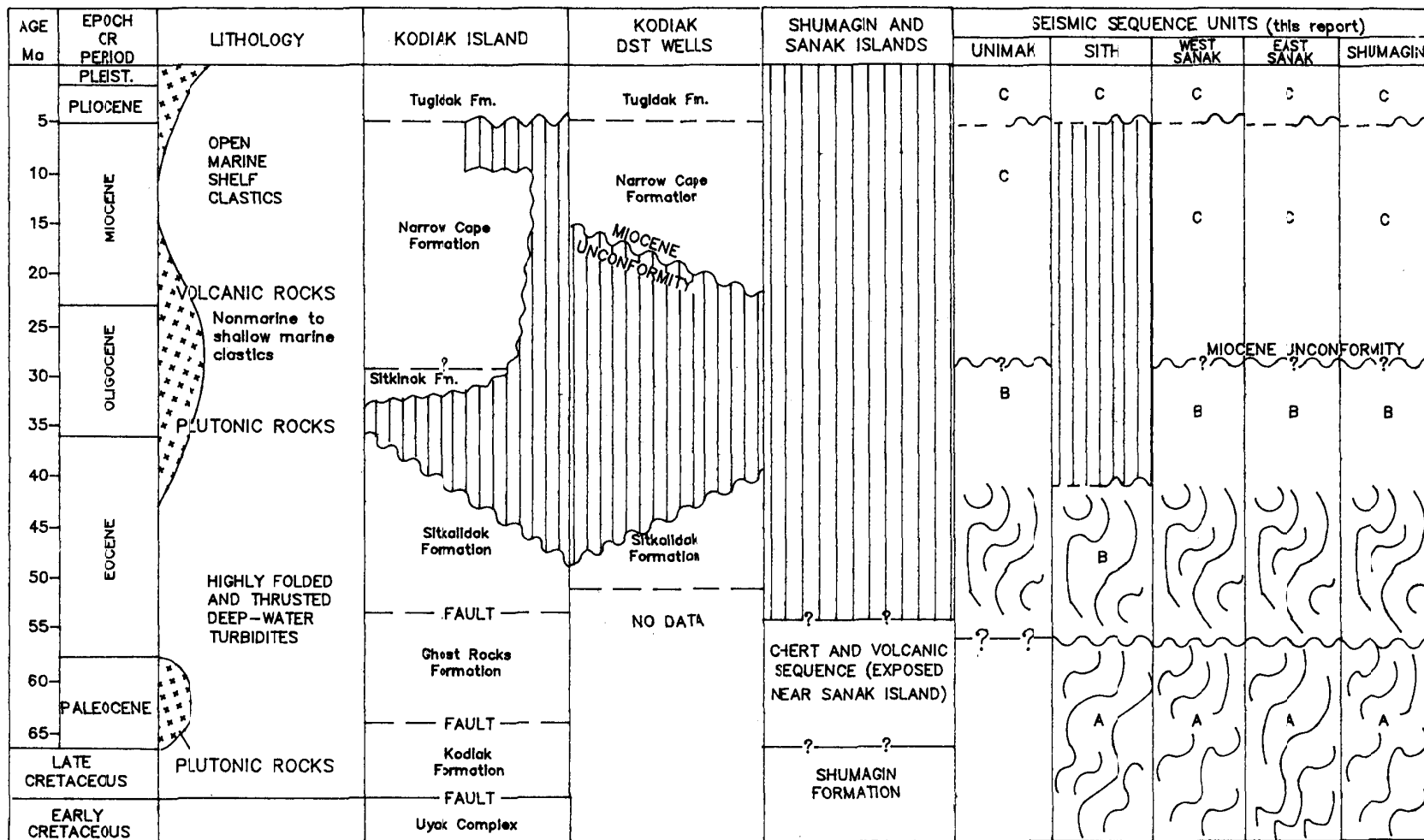


FIGURE 16. Shumagin shelf seismic sequence correlation chart. Adapted from Bruns, von Huene, and others (1987), Moore and others (1983), and Turner and others (1987).

the Shumagin margin are a series of relatively high-amplitude, continuous reflections that are interpreted to be elevated decollements that originate in sequence A. Seismic reflections that probably represent decollements are found beneath the Shumagin basin (D1 on plate 3), East Sanak basin (D2 on plate 6), and West Sanak basin (D3 on plate 4), as well as within the Sanak Island Transverse High (D4 and D5 on plate 4).

Beneath the Shumagin basin at a depth of 4 to 6 seconds (24,000 to 40,000 feet), decollement D1 appears as a continuous, subhorizontal reflection within sequence A that is offset by a basement-controlled strike-slip fault (plate 3). Several northeast-dipping thrust faults originate at the decollement and offset overlying sequence A strata. Similar northeast-dipping thrust faults that emanate from an area northeast of the seismic section appear to offset sequence C. The seismic-reflection characteristics of sequence A appear consistent above and below decollement D1.

Beneath the East Sanak basin and the Shumagin ridge (plate 6), decollement D2 appears as a continuous, relatively high-amplitude reflection that occurs at a depth of 3 seconds (16,000 feet). The decollement is offset by north-dipping normal faults that formed in response to Neogene extension. Because the boundary between sequences B and A is not apparent beneath the East Sanak basin and the Shumagin ridge, an undifferentiated sequence B/A is identified between decollement D2 and the Miocene unconformity even though sequence A must be present directly above the decollement.

Decollement D3 is believed to be present within sequence A along the southwestern margin of the West Sanak basin, although that part of sequence A above the decollement cannot be differentiated from sequence B (plate 4). Decollement D3 rises to the east where it is overlain by seismic sequence C (plate 4). Beneath the SIH (plate 4), decollement D4 is overlain by an undifferentiated section of sequence B/A characterized by relatively low-amplitude, discontinuous, steeply dipping reflections that are offset by numerous high-angle faults. The exact position and offset of individual faults is difficult to ascertain, but the trend can be determined with some degree of reliability. Decollement D4 overlies a section of sequence A characterized by gently dipping, relatively high-amplitude reflections that contain decollement D5 (plate 4). The section above

decollement D4 is thought to be an offscraped sequence, whereas the section below decollement D4 is probably an underplated sequence.

Dix interval velocities (Dix, 1955), derived from industry-supplied CDP stacking velocity data, characteristically exhibit an increase across the upper boundary of sequence A. The velocity increases from 11,000 to 15,900 ft/sec for seismic sequence B, to 15,000 to 18,000 ft/sec for seismic sequence A.

In summary, sequence A represents basement rocks thought to have formed in a Cretaceous to Paleocene subduction complex. The southwestern extent of the subduction complex is recognized by outcrops of the Late Cretaceous Shumagin Formation on the Sanak Islands (fig. 5, p. 13). Equivalent rocks are not expected to be present southwest of the Sanak Islands beneath the Unimak basin.

Sequence B (Eocene)

Seismic sequence B was deposited on basement rocks of sequence A. The lower boundary of sequence B, where it can be recognized, is an unconformity. For example, in the East Sanak basin, the lower boundary of sequence B is defined by an angular discordance with sequence A reflections (plate 2). In the East Shumagin subbasin, the lower boundary of sequence B is an unconformity identified by discordance between continuous to discontinuous reflections (plate 5). Also in the East Shumagin subbasin but adjacent to a major basement-controlled fault system, sequences B and A are in fault contact due to Neogene tectonic motion (plate 3). Where the lower boundary of sequence B cannot be distinguished, an undifferentiated sequence B/A is indicated on seismic profiles (for example, plates 4 and 6).

The upper boundary of sequence B is a mappable seismic horizon present throughout the Shumagin margin. This marker horizon has been seismically tied to the Kodiak shelf wells (fig. 5). At the wells, this horizon correlates to a late Oligocene to Miocene unconformity (the "Miocene unconformity") recognized by Turner and others (1987). Figure 17 (p. 44) is a structure-contour map of the Miocene unconformity on the Shumagin shelf. In the Kodiak shelf wells, the Miocene unconformity separates overlying Neogene strata from underlying Eocene strata (fig. 16). According to Turner and others (1987), the Eocene section is correlative with the Sitkalidak

Formation on Kodiak Island. On this basis, sequence B in the Shumagin margin is also considered to be at least in part equivalent to the Sitkalidak Formation and is here assigned an Eocene age.

Sequence B is present in the Shumagin basin (plate 5) and the northwestern margin of the East Sanak basin (plate 2), where it fills structural depressions in the Cretaceous-Paleocene basement. An isochron map of sequence B in the Shumagin basin shows that the thickest accumulations occur along the northern margin (fig. 19, p. 52). The northeast-trending East Shumagin subbasin contains up to 6,000 feet of sequence B strata, with a thinner accumulation in a smaller depression to the south (plates 3 and 5). The west-trending West Shumagin subbasin contains sequence B accumulations less than 4,000 feet thick.

Plate 5, a north-south seismic profile of the East Shumagin subbasin, shows closely spaced, concordant, variable-amplitude reflections that represent relatively undeformed sequence B strata. On the northern basin margin, steeply dipping sequence B strata are truncated by the Miocene unconformity or another Neogene unconformity. The parallel to subparallel reflections of sequence B display strong reflection continuity at the northern subbasin margin, but weaker continuity and relatively high amplitudes along the southern flank. The discordant, discontinuous reflections at the southern basin margin are similar to the "chaotic reflection configuration" described by Vail and others (1977) and probably represent either a structurally disrupted section or strata deposited in a variable, high-energy setting.

Beneath the northwestern margin of the East Sanak basin, a highly deformed sequence B section is unconformably overlain by concordant reflections of sequence C (plate 2). The internal reflection characteristics of sequence B are similar to those described from the East Shumagin subbasin (plate 5).

Sequence B cannot be differentiated from underlying sequence A at the southern margins of the East Sanak basin, Shumagin ridge, East Sanak slope ridge, West Sanak basin, and the Sanak Island Transverse High (plates 4 and 6). When a decollement is present or sequence B is poorly defined, undifferentiated sequence B/A is identified above the decollement even though it is understood that the decollement is within sequence A (plate 6). Plate 4, an east-west profile of

the West Sanak basin and the adjacent Sanak Island Transverse High, shows that the West Sanak basin is underlain by undifferentiated sequence B/A bounded by the Miocene unconformity and decollement D3. Plate 9 shows the basement of the West Sanak basin and its southeastern border, the East Sanak slope ridge, to be made up of undifferentiated sequence B/A.

In the Unimak basin, sequence B represents basement. Plate 7, a southwest-northeast seismic profile of the eastern half of Unimak basin, shows the upper part of sequence B characterized by high-amplitude, concordant reflections. This part of sequence B ranges from 1,500 to 4,500 feet in thickness, and is thickest near Sanak Island and toward the Alaska Peninsula. The lower part of sequence B grades into the "noise" of the basement complex. At the shelf break, sequence B reflections are concordant with those of sequence C, suggesting a stable prograding shelf environment. Near Sanak Island, sequences B and C exhibit a discordant relationship, suggesting that some uplift occurred along the margin before the deposition of sequence C. Sequence B also composes the Unimak ridge, a bathymetric ridge that acted as a baffle for sediments in the Unimak basin. USGS dredge samples of the Unimak ridge included late Eocene calcareous mudstones, early to middle Miocene siltstones, mudstones, and sandstones, early Miocene basalt, and late Pliocene to Quaternary mudstones (Bruns, Vallier, and others, 1987).

Seismic-reflection-derived interval velocities for this sequence range from 11,000 to 15,900 ft/sec. These velocities are similar (10,600 to 15,400 ft/sec) to those of the Eocene section in the KSSD wells (fig. 22, p. 60).

In summary, sequence B is an undeformed to highly deformed section considered to be correlative with the Eocene Sitkalidak Formation on Kodiak Island (Moore and Allwardt, 1980) and the Eocene turbidites encountered in the Kodiak test wells (Turner and others, 1987). Because sequence B is present along the same convergent margin as the Sitkalidak Formation, it is also assumed to consist of volcanic-rich sediments derived from a volcanic-arc system and deposited in a trench-slope setting.

Sequence C (Oligocene to Pleistocene)

Over 20,000 feet of sequence C strata are present in some of the Shumagin margin basins. Seismic sequence C represents deposits that filled the evolving shelf

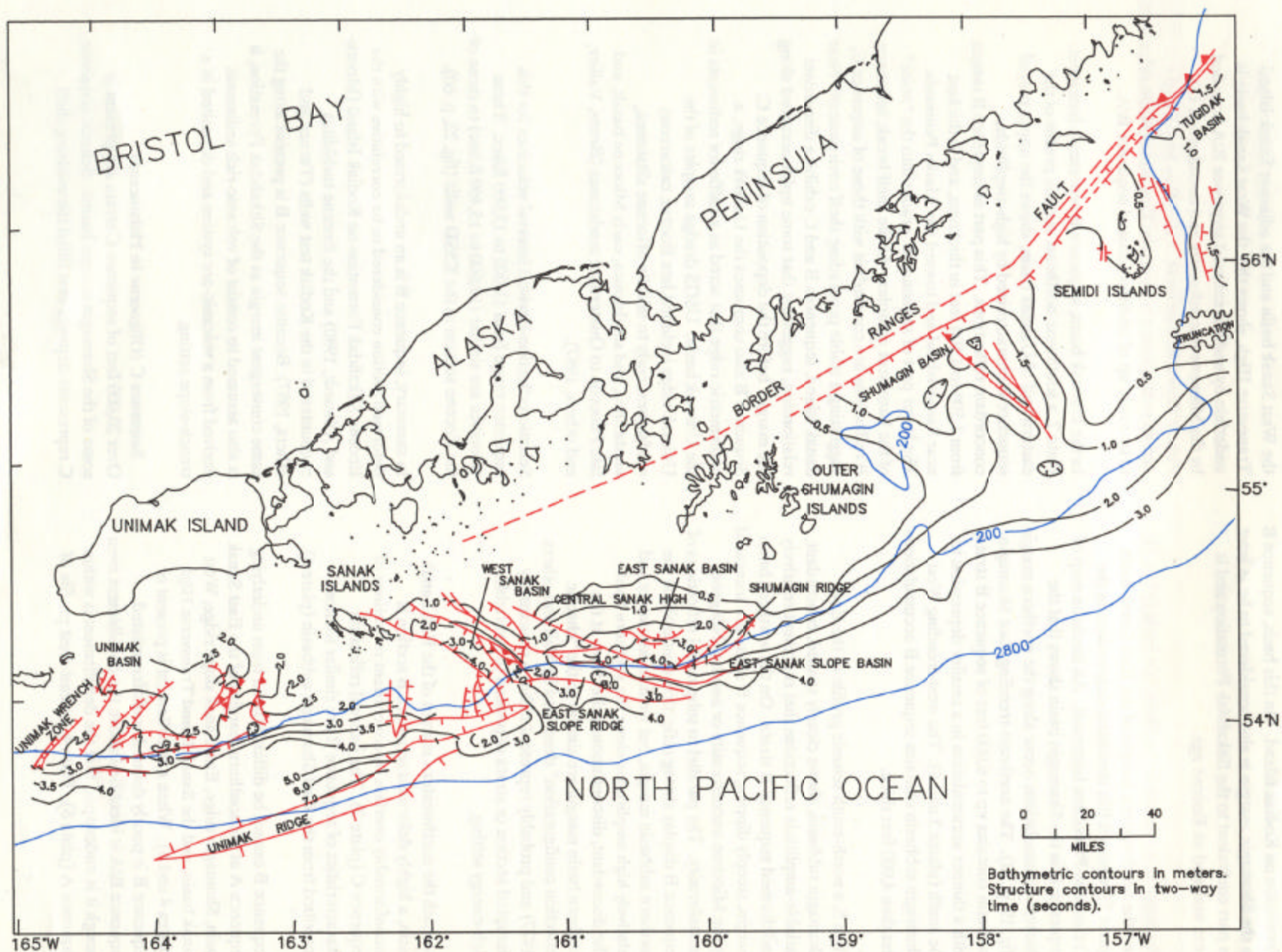


FIGURE 17. Structure-contour map of a regional Miocene unconformity.

basins then extended onto the trench upper slope. The lower boundary of seismic sequence C is the regional Miocene unconformity that is present throughout the Shumagin margin and the adjacent Kodiak shelf area. In the Kodiak wells, the section above the unconformity is correlative with the Miocene Narrow Cape Formation and the late Pliocene and early Pleistocene Tugidak Formation on the Kodiak Islands. Therefore, a portion of sequence C may resemble the glacio-marine sediments that compose the Tugidak Formation and reflect the glacioeustatic events that characterize most other areas of the Gulf of Alaska. Equivalents of the Oligocene Sitkinak Formation were not identified in the Kodiak wells (Turner and others, 1987). The diachronous Miocene unconformity appears to be the same unconformity described on Sitkinak Island by Magoon and Egbert (1986) that separates the Sitkinak Formation from the underlying Eocene Sitkalidak Formation. For this report, we assume that strata coeval with the Sitkinak Formation, if present, would lie above the diachronous Miocene unconformity that originated during the Oligocene (fig. 17).

On the Shumagin shelf, the Miocene unconformity separates the variable-amplitude, steeply dipping reflections of sequence B and the relatively low-amplitude, flat to gently dipping, continuous reflections of sequence C. Several unnamed Pliocene unconformities are present within sequence C. These local unconformities truncate structural highs that delimit the individual basins. Within the basins, these unconformities become disconformities. Unlike the Miocene unconformity, which probably represents a major period of erosion, these younger unconformities appear to denote glacioeustatic events and relatively minor changes in the depositional dynamics for individual basins.

Within the Shumagin basin, sequence C exhibits three seismic facies that are separated by unconformities (plate 5). In the East Shumagin subbasin, the lower facies is characterized by concordant, discontinuous reflections; the middle facies by concordant to diverging, continuous to discontinuous reflections; and the upper facies by continuous, horizontal reflections. In the East Shumagin subbasin, the lower facies is disconformable with underlying sequence B. Lower facies strata are truncated along the northern margin by an unconformity. Where the lower facies has been truncated, the middle facies unconformably overlies sequence B. To the south, the middle facies is

paraconformable or disconformable with the lower facies. The base of the upper facies is in angular contact with the middle facies at the northern margin of the basin, but becomes paraconformable or disconformable to the south. An isochron map of the lower facies shows two northwest-trending subbasins with accumulations of over 2,000 feet of section occurring along the subbasin axes (fig. 21, p. 54). An additional 4,000 feet of middle and upper facies are present within the subbasins (plate 5).

Up to 20,000 feet of sequence C was deposited in the East Sanak basin (plate 6) as a southward-thickening wedge characterized by parallel and coherent reflections that downlap against the Miocene unconformity. The thickest accumulation of sequence C in the East Sanak basin occurs north of the Shumagin ridge and east of the Central Sanak high (fig. 17).

As sequence C accumulated, deposition eventually extended beyond the Shumagin ridge and into the adjoining East Sanak slope basin (plate 1). The elongate East Sanak slope basin, situated on the outer shelf and upper slope between two parallel basement ridges, the Shumagin and East Sanak slope ridges, contains over 15,000 feet of sequence C strata. The seismic-reflection characteristics of sequence C in the East Sanak slope basin are similar to those in the East Sanak basin.

The northwest-trending West Sanak basin contains over 20,000 feet of sequence C strata that can be subdivided into an upper and lower facies separated by a paraconformity or disconformity that becomes an angular unconformity in other portions of the basin (fig. 17 and plate 4). Along the northeast side of the basin, the lower facies is discordant with the upper facies, whereas in the western portion of the basin these facies are concordant.

In the West Sanak basin, the lower facies of sequence C is characterized by parallel, continuous reflections that exhibit baselap against the Miocene unconformity (plate 8). Plate 9, a northwest-southeast seismic profile of the West Sanak basin, shows the lower facies thickening to the southeast where it appears to onlap the East Sanak slope ridge, a northwest extension of the East Sanak slope basin and the southeastern boundary of the West Sanak basin. The upper facies of sequence C is characterized by continuous to discontinuous concordant reflections. To the southeast, this facies

onlaps and progrades over the East Sanak slope ridge (plate 9). To the west, the upper facies onlaps the unconformity that cuts the Sanak Island Transverse High (plates 4 and 8). Here, the lower facies is missing, and the upper facies unconformably overlies undifferentiated sequence B/A.

The unconformity between the upper and lower seismic facies of sequence C can be carried across the West Sanak basin and the Sanak Island Transverse High and into the Unimak basin. In the Unimak basin, several Plio-Pleistocene unconformities can be recognized within sequence C (plate 7). These unconformities are seismically characterized by relatively high-amplitude single or doublet reflections that show angularity with the discontinuous to continuous reflections of sequence C. Plate 10 is a northwest-southeast seismic profile of Unimak basin that illustrates these Plio-Pleistocene unconformities and shows that they commonly grade into paraconformable or disconformable relationships beyond the shelf break.

The number of unconformities may represent multiple glacioeustatic events and/or frequent uplift and erosion of the shelf followed by progradation. Some terrigenous sediments accumulated behind the Unimak ridge (fig. 13, p. 25), a northeast-trending bathymetric high (plate 1) that is composed of sequence B strata. Where this bathymetric ridge is absent, sequence C deposition extended into slope and trench areas. A structure-contour map of the Miocene unconformity illustrates the general distribution of sequence C in the Unimak basin (fig. 17).

Seismic-reflection-derived interval velocities for the possible Pleistocene section range from 5,100 to 6,000 ft/sec. Interval velocities for the Neogene section are as high as 15,000 ft/sec, but most are 8,000 to 12,300 ft/sec. These interval velocities fall within the range of Neogene sonic-log velocities measured in the KSSD wells (fig. 22, p. 60).

Summary

The Shumagin shelf contains six structurally distinct sedimentary basins that formed on an evolving forearc accretionary prism. The Shumagin shelf sedimentary section is divided into three major seismic stratigraphic sequences (A, B, and C) that are believed to be correlative with the Cretaceous and Tertiary section south of the Border Ranges fault on Kodiak Island (fig. 16). These seismic sequences are present

throughout the Shumagin shelf except in the area that underlies the younger Unimak basin, where sequence A is missing. Seismic sequence A represents the oldest and most deeply buried strata and is the economic and seismic basement. Sequence A is correlative with Cretaceous and Paleocene folded strata of the Uyak, Shumagin, and Ghost Rocks Formations and Paleocene granodiorite intrusives. Seismic sequence B is believed to be correlative with the Eocene Sitkalidak Formation on Kodiak Island and with the Eocene section in the KSSD wells. Seismic sequence C is believed to be correlative with the Narrow Cape (Miocene) and Tugidak (Pliocene and Pleistocene) Formations exposed on Kodiak Island, the Neogene section above the diachronous Miocene unconformity offshore in the KSST and KSSD wells, and, perhaps, the Sitkinak Formation on Kodiak Island.

Structural Geology

The structural geology of the Shumagin margin is discussed in terms of features that delimit the basin boundaries, the structure of individual basins, and the overall evolution of the Shumagin margin. The present-day orientations of tectonic features in the Shumagin Planning Area, both margin-parallel and margin-oblique (plate 1 and fig. 17), are discussed in terms of age, lithology, and structure. Margin-parallel structures include the Tugidak and Unimak basins, the Shumagin ridge, and the Border Ranges fault. Margin-oblique structures include the Shumagin basin, the East Sanak basin, and the Sanak Island Wrench Zone, which includes the West Sanak basin, the Central Sanak high, the East Sanak slope ridge, the Boundary fault, and the Sanak Island Transverse High (plate 1). For purposes of convenience, the Shumagin margin tectonic elements are divided into basins and basin boundary features.

Basin Boundary Features

Border Ranges Fault. The regional significance of the Border Ranges fault was discussed in the *Geologic Framework* chapter. Within the Shumagin Planning Area northeast of the Sanak Island Wrench Zone, the Border Ranges fault defines a northern tectonic boundary (plate 1). The Border Ranges fault (as located by Fisher and von Huene, 1984) appears to correspond to a zone of thrusts and normal faults that truncate the northern margin of the Tugidak, Shumagin, and East Sanak basins (plate 1 and fig. 17).

Shumagin Ridge. The Shumagin ridge, one of five structural highs that delimit the Shumagin shelf basins, is made up of an en echelon series of northeast-trending fault blocks consisting of undifferentiated sequence B/A strata. The Shumagin ridge is the southern margin of the East Sanak basin and the northern margin of the East Sanak slope basin. A major northwest-trending basement-involved fault that corresponds with the northeastern extent of the Sanak Island Wrench Zone (plate 2) truncates the southwestern end of the Shumagin ridge (plate 1). Faults associated with the Shumagin ridge appear to offset decollement D2, the Miocene unconformity, and Neogene and younger strata in the East Sanak basin. Uplift of undifferentiated sequences B/A and A has occurred along these faults.

Sanak Island Wrench Zone. The Sanak Island Wrench Zone (SIWZ) is a 60-mile-wide zone containing margin-oblique extensional and compressional structures. The SIWZ, located between the northeastern boundary of the Central Sanak high and the southwestern margin of the Sanak Island Transverse High, parallels the "old" Beringian margin and is oblique to the present Shumagin continental shelf (plate 1). The northeastern margin of the Sanak Island Wrench Zone is a major northwest-trending, margin-oblique, basement-involved fault that truncates structures of the Shumagin ridge (plate 1) and represents the western boundary of the East Sanak basin (plate 2). Numerous other margin-oblique structures that are evident within the SIWZ include the Central Sanak high, the East Sanak slope ridge, the Boundary fault, and the Sanak Island Transverse High (plate 1). Movement within the SIWZ may have produced margin-oblique structures such as the Boundary fault and reactivated older structures such as the Central Sanak high, the East Sanak slope ridge, and the Sanak Island Transverse High. Movement within the SIWZ generated Neogene compressive features, such as positive flower structures (plate 9) and the duplexes that inverted the West Sanak basin (plate 4). The southwestern boundary of the SIWZ (plate 1) corresponds to a plate boundary and the westernmost extent of the Chugach terrane (fig. 5, p. 13). The structural elements of the SIWZ are discussed in the following text.

Central Sanak High. The Central Sanak high is a northwest-trending, margin-oblique feature (plate 1) consisting of an uplifted fault block of undifferentiated

sequence B/A (plate 2). This basement high separates the northwestern segment of the East Sanak basin from the West Sanak basin. The northeast boundary of the Central Sanak high is a steeply dipping, basement-involved fault (plate 2). The southeast boundary of the high is truncated by a margin-parallel, cross-cutting fault that also forms the northwestern boundary of the East Sanak slope basin (plate 1). The high extends northwest for approximately 30 miles where it broadens and rises to within 2,000 feet of the seafloor. Uplift along the faults that bound the Central Sanak high offset the Miocene unconformity and continued through the Neogene (plate 2).

Sanak Island Transverse High. The Sanak Island Transverse High (SITH), an uplifted section of sequences B/A and A, occupies over 1,000 square miles on the Shumagin continental shelf and upper slope (plates 1 and 4). The SITH is a margin-oblique structural high that separates the West Sanak basin from the Unimak basin. The SITH appears to be coincident with a southeastward projection of the "old" Beringian margin (plate 1) and the southwestern extent of the Chugach terrane (fig. 5). The SITH and other transverse features are discussed in the *Summary and Discussion* section at the end of this chapter.

The SITH contains a prominent reflection, decollement D4, that separates steeply dipping, highly faulted strata above from an underlying, less deformed section (plate 4). The upper section is considered to represent offscraped material; the lower, underplated material. The offscraped section is truncated by an unconformity of probable Pliocene age and can be subdivided into two units separated by a prominent but discontinuous group of reflections at a depth of 2.7 seconds near the west end of seismic profile F-F' (plate 4). Highly disrupted and discontinuous reflections between decollement D4 and this prominent structural horizon midway up the section are replaced by more continuous reflections above it (plate 4). Numerous closely spaced faults that offset undifferentiated sequence B/A strata strike northwest, dip northeast, and terminate at decollement D4.

The relatively undeformed section below decollement D4, the presumably underplated unit, consists of sequence A strata that display gentle dips relative to those of the overlying section and appear to have been deformed as duplex structures (plate 4).

Boundary Fault. The Boundary fault is a margin-oblique, basement-controlled transtensional fault system that forms the southwest margin of the West Sanak basin and lies within the Sanak Island Wrench Zone (plates 1 and 4). The Boundary fault separates the uplifted Cretaceous and Paleogene accretionary complex of the Sanak Island Transverse High from the downdropped younger basin-fill of sequence C in the West Sanak basin.

From the shelf break to a latitude of about 54° N., the Boundary fault system trends northwest and dips to the east (fig. 17). North of latitude 54° N., the Boundary fault bends westward and dips to the northeast. North of this bend, the Boundary fault curves west-northwest parallel to the Sanak Islands. Plate 8, seismic profile I-I', depicts a northeast-southwest-trending seismic profile north of the major bend of the Boundary fault. This profile crosses the basement-controlled Boundary fault, the eastern portion of the SITH, and the northern portion of the West Sanak basin and shows the Boundary fault to be nearly vertical and to have a normal sense of displacement. The fault separates the lower seismic facies of sequence C in the basin from the uplifted strata of undifferentiated sequence B/A in the SITH and offsets the seafloor. Plate 4 shows normal displacement with reverse drag on the east side of this fault.

The Boundary fault appears to be dominantly a strike-slip feature. Strike-slip motion is indicated by the nearly vertical, basement-involved nature of the faults, which have great linear extent, and the geometry of the West Sanak basin. The West Sanak basin has experienced concurrent extension in one area (plate 8) and compression in another area (plate 9).

Unimak Ridge. The Unimak ridge is a margin-parallel basement ridge located seaward of the Unimak basin and the Sanak Island Transverse High (plate 1). South of the Unimak basin, it is a bathymetric high overlapped by sequence C (fig. 13, p. 25) that forms a barrier that prevents recent sediments from entering the Aleutian Trench. A major bend or offset in the ridge occurs at the southwestern boundary of the Sanak Island Wrench Zone (plate 1 and fig. 17). This major bend is accompanied by a corresponding change in the continental shelf break as defined by the 200-meter isobath. Further northeast, the Unimak ridge is overlapped by sequence C strata and truncated by the Boundary fault. Here, the axis of the Boundary fault

corresponds to a second landward offset of the continental shelf break (plate 1). A prominent reflection "caps" the Unimak ridge and may represent a fault plane between sequence C and the highly disrupted and faulted rocks of sequence B (fig. 13). The seismic signature of the Unimak ridge contains numerous internal diffractions. Rock samples dredged from the ridge include early to middle Miocene feldspathic sandstone, Eocene(?) calcareous mudstones, and early Miocene basaltic rock (Bruns, Vallier, and others, 1987)(tables 1 and 2, p. 88 and 91).

The basalt resembles volcanic-arc basalt and was dated as early Miocene by the potassium-argon method, although it is probably older (Bruns, Vallier, and others, 1987). The basalts recovered from the Unimak ridge have no mineralogical affinity with either the Eocene through Oligocene rocks of the Meshik Arc described by Wilson (1985) or the Miocene through Holocene volcanic rocks of the Aleutian Arc (Bruns, Vallier, and others, 1987). The location of the Unimak ridge is also anomalous with respect to the "normal" distribution of eruptive sites landward of the Aleutian Trench (plate 1). The Miocene sandstones dredged from the ridge exhibit no thermal alteration that might associate them with the origin of the Unimak ridge (Bruns, Vallier, and others, 1987). All available evidence thus suggests that the Unimak ridge is older than the early Miocene strata in the basin.

East Sanak Slope Ridge. The East Sanak slope ridge extends from the southeastern boundary of the West Sanak basin and plunges southeast beneath the outer continental slope, south of the East Sanak slope basin (fig. 17 and plate 1). Bruns, von Huene, and others (1987) identified the East Sanak slope ridge as consisting of acoustic basement material made up of highly magnetic rock types. Their data over the ridge showed a residual magnetic value of 170 gammas (plate 9). The morphology and seismic character of the East Sanak slope ridge is similar to that of the Unimak ridge, located 20 miles to the southwest. The magnetic anomaly over the East Sanak slope ridge indicates that the structural core consists of highly magnetic material. This material may be basalt similar to that dredged from the adjacent Unimak ridge. Geophysical data show that the East Sanak slope ridge is "capped" by a prominent reflection, most likely a fault plane, that separates concordant sequence C reflections from the discontinuous reflections within the structure (plate 9). This reflection, which appears to correspond with the

D3 horizon (plate 4), dips to the southwest beneath the Neogene basin fill of West Sanak basin and appears to be rooted in sequence A.

Basin Structure

Tugidak Basin. The western flank of the Tugidak basin is present in the Shumagin Planning Area east of the Semidi Islands (plate 1 and fig. 17). The northwest flank of the Tugidak basin is bounded by a set of northeast-trending, northwest-dipping thrusts that trend parallel with the axis of the Border Ranges fault (fig. 17). A second set of northeast-trending, steeply dipping normal faults, present seaward of these thrusts (fig. 17), offsets sequence C, which thickens towards the basin axis to the northeast, and bounds the ridges that parallel the Border Ranges fault.

Shumagin Basin. The Shumagin basin is an elongate, northwest-trending basin that is oblique to the present Shumagin margin. It is bounded on the southwest by the Outer Shumagin Islands, on the northeast by the Semidi Islands, on the northwest by the Border Ranges fault, and on the south by a broad, shelf-edge high (fig. 17).

Figure 18 (p. 50), a structure map contoured on top of sequence A, shows the predominately northeast-trending East Shumagin subbasin and the west-trending West Shumagin subbasin divided by a margin-oblique fault system. The structure of the margin-parallel East Shumagin subbasin is parallel to folds of the Shumagin Formation on the adjacent Outer Shumagin Islands. The folding took place during northwest-directed subduction and accretion in the Late Cretaceous. Structures in sequence A in the West Shumagin subbasin are oblique to those found on the Outer Shumagin Islands. Plate 3, a southwest-northeast profile of the East Shumagin subbasin, shows the margin-oblique fault that separates uplifted sequence A in the southwest from Neogene basin-fill to the northeast. The margin-oblique, basement-controlled fault offsets decollement D1 and extends 50 miles from the Border Ranges fault southeast towards the shelf edge. The basement-controlled nature of the fault, the presence of splays, and the different orientation of adjacent subbasins are best explained by strike-slip motion along this margin-oblique fault system during sequence A time.

Figure 19 (p. 52) is an isochron map of sequence B in the Shumagin basin. Sequence B was probably

deposited in synclines formed after the Late Cretaceous and early Paleogene deformation of sequence A. The isochron map roughly represents the strata between the top of sequence A and the Miocene unconformity structure map. Sequence B is generally less than 2,000 feet thick, although it is greater than 6,000 feet thick in the northern portion of the East Shumagin subbasin and adjacent to the margin-oblique fault system. In the West Shumagin subbasin, sequence B is cut by a steep margin-parallel fault (fig. 19), whereas in the East Shumagin subbasin, sequence B was truncated as a result of uplift and erosion (fig. 19 and plate 5).

The structure map of the Miocene unconformity (fig. 20, p. 53) shows that the segmented, northwest-trending margin-oblique Shumagin basins are bounded along their southwest, northeast, and southeast flanks by the Cretaceous structures that form the Outer Shumagin and Semidi Islands. Sequence C strata onlap these structures. Along the northwest basin margin, the Miocene unconformity is offset by faulting and truncated by uplift (fig. 20). In the West Shumagin subbasin, strata above the Miocene unconformity have been truncated by a margin-parallel, basement-involved fault that trends parallel to the Border Ranges fault (fig. 20). In the East Shumagin subbasin, uplift along the northwestern basin margin has resulted in the truncation of the Miocene unconformity by an unconformity that is probably Pliocene in age (plate 5). The lower seismic facies of sequence C was deposited in northwest-trending basins (fig. 21, p. 54). The isochron map of sequence C reflects the top of the Miocene structure (fig. 20). The reorientation of the basin axis from northeast in the Paleogene to northwest in the Neogene may be the result of movement along the margin-oblique, strike-slip fault system (fig. 19 and plate 3).

Structures along the axis of the margin-oblique master fault display both extensional and compressional features, which suggests strike-slip motion (figs. 17 and 20 and plate 3). Extensional features are predominant along the southern segment of the master fault, and compressional structures are more numerous to the north. These structures formed after sedimentation began in the Neogene basins. Plate 3, a profile across a northern segment of the East Shumagin subbasin and the margin-oblique fault, illustrates reverse faults that appear to emanate from sequence A and involve strata as young as the middle facies of sequence C. To the

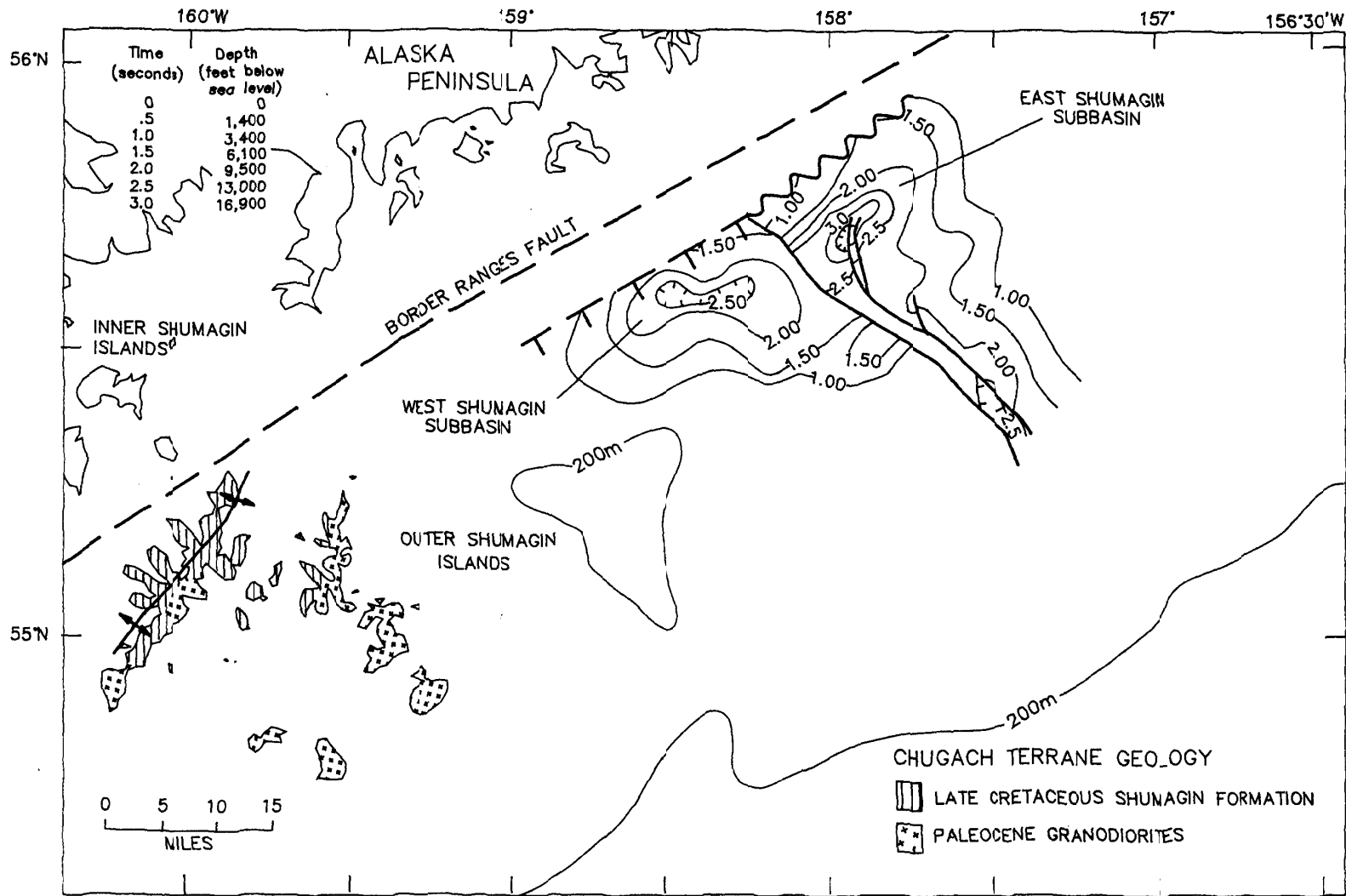


FIGURE 18. Structure map contoured in time (seconds) on top of sequence A for the East and West Shumagin subbasins.

south, equivalent strata within asymmetrical basins are displaced along extensional faults and show only minor deformation. Compression associated with uplift in the East Shumagin subbasin (plate 3) appears to have ceased sometime between lower and middle facies time, as evidenced by the onlap of Pliocene strata on the large, folded structure and the flat-lying, relatively undeformed strata of upper facies sequence C (plate 5). Uplift along the northern basin margin ceased before the upper facies was deposited.

East Sanak Basin. The East Sanak basin is a west-trending, margin-oblique, asymmetrical graben bounded on the southeast by the extension of the Shumagin ridge and on the west by the Sanak Island Wrench Zone (fig. 17). Plate 6 illustrates a southward-thickening wedge of sequence C and a decollement (D2) that rises along the shelf break. The deepest part of the East Sanak basin is adjacent to a basement-involved fault that bounds the northern, uplifted margin of the Shumagin ridge. The main fault strand on the northern flank of the Shumagin ridge bifurcates and bounds both upthrown and downthrown blocks (plate 1). Differential movement caused extensional faults in the thick Neogene section that was downdropped to the north (plate 6). Movement on the main fault produced rollover and antithetic faults on the downthrown side. The steep, basement-involved faults offset the Miocene unconformity and decollement D2. Decollement D2 steepens and plunges beneath the northern margin of the Shumagin shelf.

The western flank of the East Sanak basin is a northwest-trending margin-oblique fault system that bounds the eastern extent of the Sanak Island Wrench Zone (plate 1). Plate 2 shows the Central Sanak high and the asymmetry of the East Sanak basin. The bounding fault appears to be basement controlled and extends from the Border Ranges fault over 60 miles southeast, where it appears to truncate the Shumagin ridge.

Uplift of the Central Sanak high probably began in the late Paleogene and resulted in the erosion or nondeposition of the lower facies of sequence C; the upper facies lies unconformably on sequence B/A in the Central Sanak high. The upper facies of sequence C onlaps the Central Sanak high to the west, where it is offset by faults believed to be associated with strike-slip motion of the SIWZ (plate 2). Uplift along the Central

Sanak high and the northern Shumagin basin margin appears to have ceased at the same time.

East Sanak Slope Basin. The East Sanak slope basin occupies the outer shelf and upper slope between the East Sanak slope ridge and the Shumagin ridge (fig. 17 and plate 1). Its western margin is the junction of a northwest-trending fault system associated with the Central Sanak high and the eastern extent of the SIWZ. The northern perimeter of the basin is delimited by the fault system that forms the southern flank of the Shumagin ridge. The East Sanak slope basin was initially the slope portion of the East Sanak basin. It probably originated during the late Paleogene and Neogene strike-slip motion that uplifted the Shumagin ridge.

West Sanak Basin. The West Sanak basin is part of the northwest-trending, margin-oblique Sanak Island Wrench Zone (plate 1). The basin is bounded on the northeast by the Central Sanak high, on the southeast by the East Sanak slope ridge, and on the west by the Boundary fault and the Sanak Island Transverse High. The West Sanak basin contains a braided system of northwest-trending faults that display both normal and reverse dip displacement (fig. 17). In the northern sector of the basin, normal displacement seems to predominate, whereas reverse faults predominate in the southern sector, where structural inversion of the West Sanak basin occurs. Plate 8 depicts an asymmetrical graben that deepens toward the Boundary fault. Numerous northwest-trending, basement-controlled extensional faults offset the seafloor and strata as young as the upper facies of sequence C. Normal displacement along these faults appears to correspond with similar movement along the basement-controlled Boundary fault.

Plate 9 depicts the structural inversion of sequence C by a margin-oblique fault system that consists of a steeply dipping, basement-controlled master fault with upward and outward spreading branches (described as a "positive flower structure" by Harding and others, 1984). The inverted portion of this basin is located between the East Sanak slope ridge and the major bend in the Boundary fault (fig. 17). Plate 4, an oblique profile across the West Sanak basin and the major bend of the Boundary fault, shows deep-seated thrust faults that emanate from the basement (sequence B/A). Plate 4 also shows decollement D3 plunging southwest toward the Sanak Island Transverse High. Between

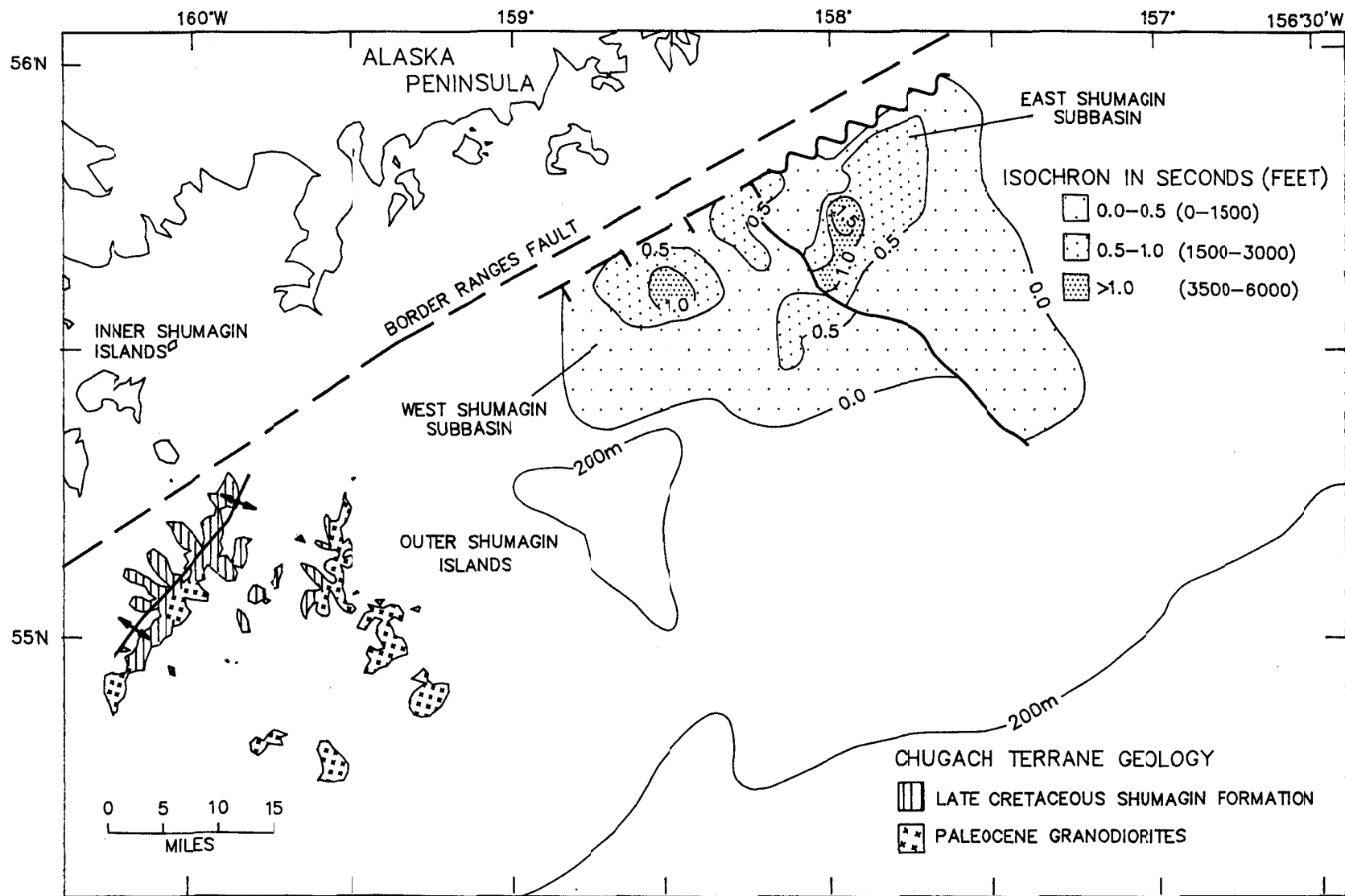


FIGURE 19. Isochron of sequence B for the East and West Shumagin subbasins.

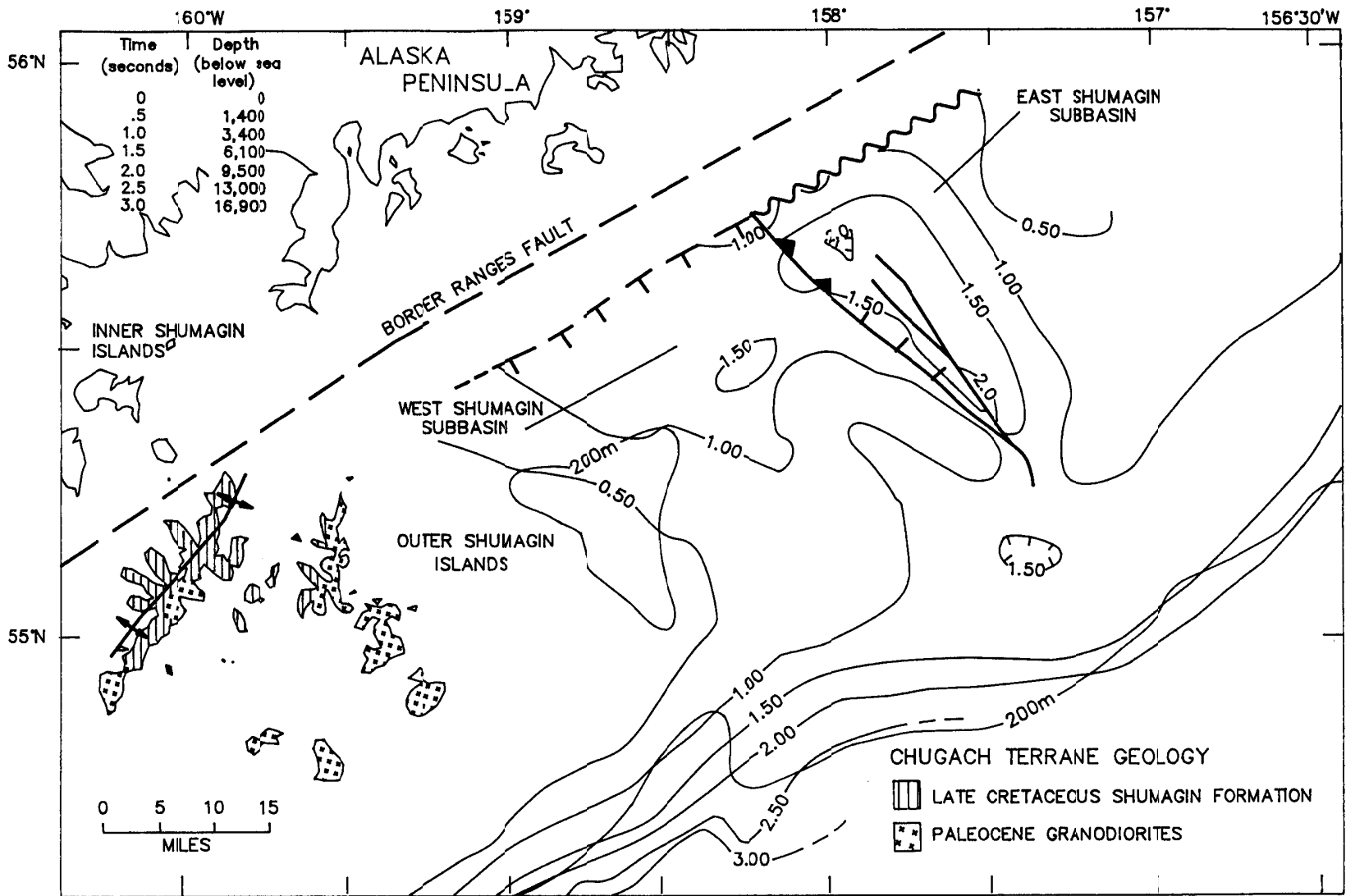


FIGURE 20. Structure map contoured in time (seconds) on top of the Miocene unconformity for the East and West Shumagin subbasins.

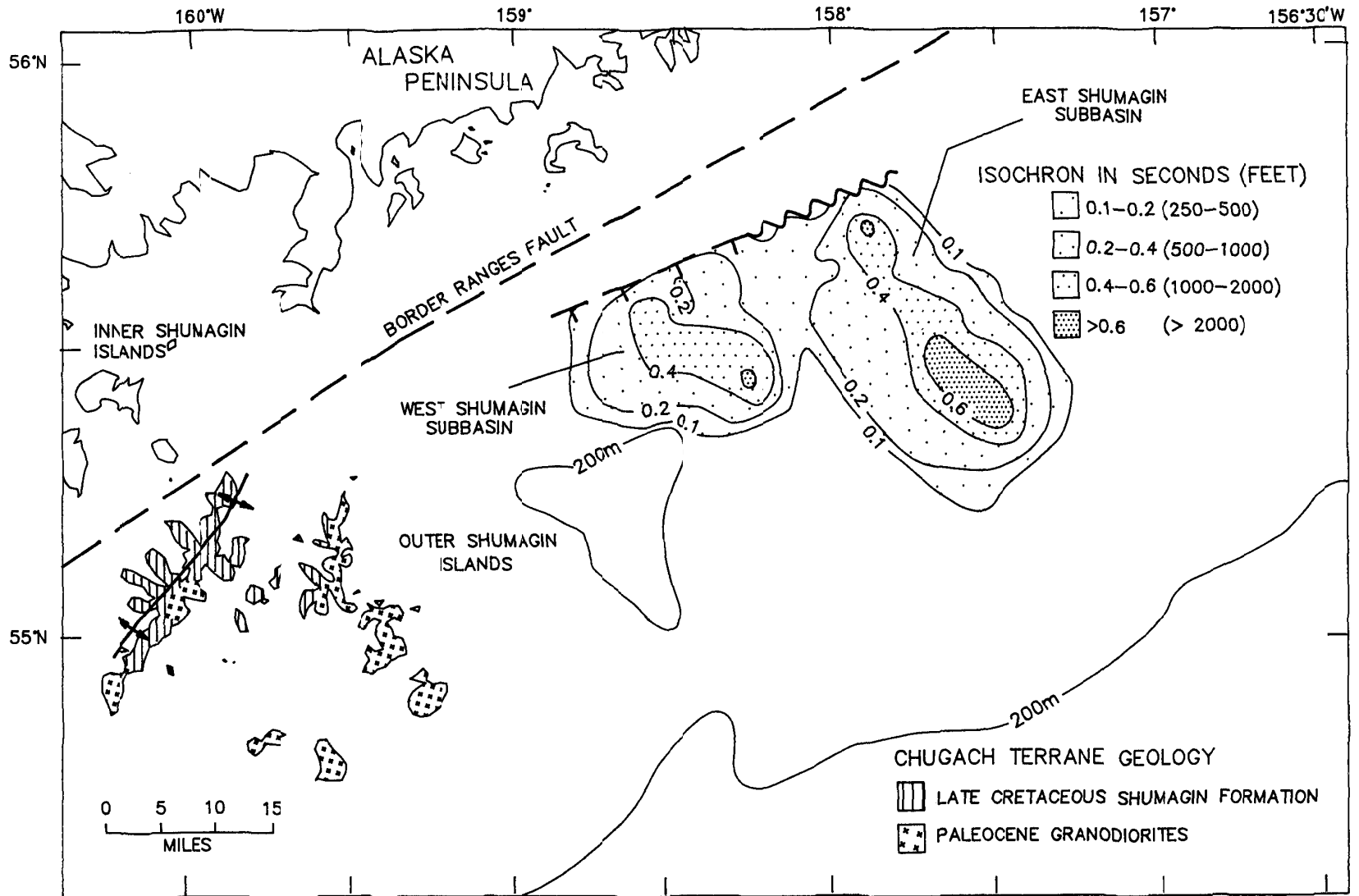


FIGURE 21. Isochron of the lower seismic facies of sequence C for the East and West Shumagin subbasins.

decollements D3 and D4, basement-involved thrusts that deform the lower facies of sequence C exhibit tectonic transport to the northeast. These thrusts progressively stack to the northwest along this major bend and deform strata as young as the upper facies of sequence C. The fold axes strike northwest and the faults dip southwest (fig. 17). This stacking resulted in the uplift and structural inversion of the West Sanak basin (plates 4 and 9) and precipitated block faulting of sequence C. Extensional faults above the thrusts trend northwest and appear to emanate from basement-controlled faulting (plate 4).

Unimak Basin. The Unimak basin is situated on the shelf and upper slope southwest of the Sanak Island Transverse High, southeast of the Aleutian Ridge (fig. 17 and plate 1). Plate 10 depicts a progradational wedge of sequence C over a basement of sequence B. Over 20,000 feet of sequence C sediments accumulated on a generally southeast-sloping surface.

A zone of stacked thrusts trends subparallel to the SIWZ (plate 1). The leading edge of the thrust zone offsets the Miocene unconformity (plate 7). The transport direction is to the west and northwest. The thrusts originated in sequence B and uplifted and deformed strata of sequence C. The oblique trend and transport direction of these thrusts are consistent with right-lateral strike-slip movement along the adjacent southwest border of the Sanak Island Wrench Zone.

Plate 1 and figure 17 depict north-northeast-trending folds and reverse and normal faults west of the Sanak Island Transverse High. Plate 10 shows some reverse faults that occur as individual thrusts or as part of an imbricate thrust system. The dominant direction of transport was to the west or northwest, although east-southeast transport is also indicated. The oblique trend of these faults suggests that they are associated with strike-slip motion along the Sanak Island Wrench Zone, rather than with the subduction-related thrusting that has been mapped by Lewis and others (1986, 1988) on the Shumagin lower trench slope. The upper part of sequence C is commonly undisturbed by the thrusting.

Plate 1 depicts a number of antiforms generated in response to episodes of Neogene thrust faulting. These structures include anticlines, a broad regional high, and "horses" (thrust-fault-bounded anticlines that are uncut by syntectonic erosional surfaces [Boyer and Elliott, 1982]). These "horses" are commonly part of a larger

structural high that was segmented as thrusting progressed. Closures on the "horses" are typically less than 20 square miles. Also present are fault-bounded anticlines that were generated syntectonically with the thrusting. These antiforms parallel the major structural trend reflected by the thrust faults. Their closures are also typically less than 20 square miles. A broad, regional, north-trending high occupies the center of the Unimak margin.

In the Unimak basin (south of Unimak Pass) is a major north-northeast-trending strike-slip fault, here termed the Unimak wrench fault (plate 1). The trend of the fault zone is oblique to the continental shelf, the Aleutian Trench axis and Aleutian Arc, and the Sanak Island Wrench Zone. Major indications of strike-slip motion in a compressive regime are the presence of "positive flower structures" and changes in stratigraphic sequence thicknesses across faults (Christie-Blick and Biddle, 1985).

A series of listric growth faults that dip seaward and strike roughly parallel to the Shumagin margin are present at the shelf break (plate 10). These faults formed in response to gravity-induced mass movement along the upper slope. The faults cut sequence C strata and extend down to, and usually sole at or beneath, the Miocene unconformity between sequences B and C.

Summary and Discussion

New geophysical evidence better delimits and defines the Sanak Island Transverse High, several decollements, the Shumagin ridge, the Central Sanak high, and the Sanak Island Wrench Zone. Our interpretations of these features are based on extrapolations from the adjacent Kodiak shelf as well as on established evolutionary models of ancient and recent forearc margins.

Late Cretaceous structures beneath the Shumagin basin (fig. 18) and in the Sanak Island Transverse High (plate 1), as well as those exposed on the Outer Shumagin and the Sanak Islands (fig. 5, p. 13), reflect the orientation of the Late Cretaceous Shumagin margin. The Sanak Island Transverse High may have initially formed as a northwest-trending subduction complex. High sedimentation rates, tectonic loading, and compression at the site of the Late Cretaceous and Paleogene subduction complex resulted in the formation of a decollement. Offscraping of landward-dipping thrust packages above the decollement was

contemporaneous with the underthrusting of relatively undeformed strata. Uplift of the SITH by underplating in the late Paleogene and early Neogene culminated in the formation of the Unimak and West Sanak basins. Uplift occurred along the Boundary fault and juxtaposed the Cretaceous and Paleogene strata of the Sanak Island Transverse High with the predominately Neogene fill of the Unimak and West Sanak basins (plates 4 and 7).

The nature of the decollement beneath the Shumagin margin is unknown, although it may be similar to a decollement of the Barbados accretionary complex (fig. 11, p. 23). Recent drilling of the Barbados Ridge accretionary complex in Leg 110 by the drilling vessel *JOIDES Resolution* penetrated a 131-foot-thick decollement consisting of sheared clays and a lower, relatively undeformed, underthrust section that contained high concentrations of methane-rich fluids (Masle and others, 1988)(fig. 11). That decollement appears to represent a permeability barrier that separates methane-rich fluids of the underthrust sequence from chloride-rich fluids of the overlying, offscraped sequence. Thermogenic methane was probably derived from organic-rich pelagic sediment that was underthrust beneath the margin. The methane-rich fluids apparently migrated laterally through and beneath the decollement seaward of the accretionary prism, whereas the chloride-rich fluids were transmitted along faults within the offscraped sequence (fig. 11).

The offscraped sequence A section along the Shumagin margin may be analogous to the inner-trench slope accretionary complex of the Nankai trough in Japan. This complex rides on the Philippine plate, which is being subducted beneath the Eurasian plate. Aoki and others (1982) describe thrusts that originate above a decollement at the front of the inner trench slope of this accretionary prism and note that considerable compressional stress initiated by the subducting slab is taken up by folding and thrusting within the offscraped section above the decollement.

The offscraped sequence overlying decollement D4 of the Sanak Island Transverse High (plate 4) is represented by a section of highly faulted and disrupted reflections. A structural horizon midway up from the base of the section separates a lower section of highly discontinuous reflections from an upper section of more continuous, coherent reflections. Typically, in

modern accretionary prisms, strata above decollements are highly fractured because they become more rigid after dewatering, whereas folding is the dominant mode of deformation in the shallower parts of an accretionary complex where significantly less dewatering has taken place. This mode of deformation may have been preserved as the SITH was vertically uplifted.

Investigations by Platt and others (1985) of the Makran accretionary prism of southwest Pakistan and by Fisher and Byrne (1987) of the Kodiak accretionary complex indicate that sediments are being underthrust beneath the fronts of these accretionary complexes along decollement surfaces. Westbrook and Smith (1983) reinterpreted seismic sections by Chase and Bunce to show undeformed sedimentary strata extending several kilometers below the deformed accretionary complex of the Barbados Ridge. Seismic profiles across the front of the Barbados accretionary complex (Westbrook and others, 1982), the Nankai trough (Aoki and others, 1982), the Makran accretionary complex (Platt and others, 1985), and the accretionary complex south of the Shumagin shelf (Bruns, von Huene, and others, 1987)(fig. 10, p. 22) show relatively undeformed sediment beneath decollement surfaces many kilometers landward of the deformation front.

Westbrook and Smith (1983) suggest that as a consequence of the loss of overpressured pore-fluids into the overlying offscraped sequence, a decollement will move to a deeper level along ramps, thereby producing duplex structures. Possible duplex structures present along the Shumagin margin between decollements D4 and D5 (plate 4) may be explained similarly. This process may be responsible for the late Paleogene and Neogene underplating and uplift of the Sanak Island Transverse High.

Strike-slip motion may have begun as early as the Late Cretaceous in the Shumagin Planning Area, as reflected by the segmentation of the Shumagin basin (plate 3). Later Neogene strike-slip movement along this same fault (plate 3) reconfigured Cretaceous and Paleogene basins and formed Neogene basins oblique to the continental shelf (figs. 19 and 21). Compressive structures formed along restraining bends of the fault and extensional faults formed along the releasing bends. Contemporaneous uplift along the northern basin margin resulted in the truncation of Miocene and younger strata (plate 5).

Along the outer shelf margin of the East Sanak basin, uplift of the Shumagin ridge was accommodated by normal faults (plate 6). Uplift probably commenced in the late Paleogene and continued throughout the deposition of sequence C. The origin of these landward-dipping faults and the Shumagin ridge is problematic. Loading of the Neogene section could have precipitated contemporaneous movement on the principal faults and led to differential uplift of the outer margin ridges. Sediment loading also could have initiated the bending of the basal detachment surface and the formation of planar normal faults farther updip. Alternatively, uplift along the outer shelf margin (Shumagin ridge) could have occurred as a result of underplating. This might have been followed by the deposition of sequence C and the formation of landward-dipping extensional faults. Differential uplift between the East Sanak slope and Shumagin ridges resulted in the formation of the East Sanak slope basin.

Neogene wrench motion has been identified within the Sanak Island Wrench Zone, which is characterized by margin-oblique faulting and folding that appears to be basement controlled. Seismic-reflection data (this report) and geologic and geophysical data from Bruns, von Huene, and others (1987) suggest that the Unimak and East Sanak slope ridges are probably similar in composition, although they appear to have originated at different times. The margin-parallel Unimak ridge appears to be composed of sequence B, the East Sanak slope ridge of sequence A. Our interpretation of recent data suggests that the Unimak ridge may have been segmented and the East Sanak slope ridge translated clockwise during Neogene strike-slip motion within the Sanak Island Wrench Zone. Subsequent Neogene strike-slip motion created an opening between the translated ridges and allowed large volumes of sediment to be carried out beyond the shelf edge. Similar motion may have translated the Central Sanak high into its present position, forming the western flank of the East Sanak basin.

The West Sanak basin initially formed above an accretionary prism that was contiguous with the Sanak Island Transverse High. The Sanak Island Transverse High was uplifted as the West Sanak basin was

down-dropped along the Boundary fault. Neogene translational faulting within the Sanak Island Wrench Zone is responsible for the asymmetry and structural segmentation of West Sanak basin. It appears that margin-oblique wrench faulting was, and continues to be, a major factor in the formation of the West Sanak basin. Divergent wrench motion predominates north of a major bend of the Boundary fault at approximately 54° N. latitude (plate 8), whereas transpressional wrench motion is more evident to the south (plates 1, 4, and 9). Convergent wrench motion is evident where there are large, basement-controlled, positive flower structures that are associated with thrusts that uplifted and deformed segments of the basin (plates 4 and 9).

The structural inversion of the West Sanak basin occurred contemporaneously with the uplift of the Sanak Island Transverse High. Underplating may have played a significant role in the origin of the SITH. The underplated sequence beneath decollement D4 may have contained over-pressured sediments which subsequently released fluids into the West Sanak basin during the uplift of the SITH (plate 4). This in turn may have facilitated the development of northeast-directed thrusts during convergent wrench motion. These thrusts deformed and uplifted segments of the basin, exposing portions of sequence C to subaerial erosion (plate 4). Movement along these faults above the highly disrupted zone continued well into the Quaternary, as evidenced by offsets of the upper part of sequence C and the presence of seafloor scarps (plate 8).

The geologic evolution of the Unimak basin is unlike that of the rest of the Shumagin forearc margin. The basement complex is probably composed of accreted Eocene turbidites that formed landward of the Unimak ridge and south of the Eocene Shumagin margin. The Eocene accretionary complex is covered by a thick progradational wedge of late Oligocene(?) and Neogene marine clastics that accumulated shoreward of the mid-slope Unimak ridge. Compressional stress imposed on the region by plate convergence was partially released through strike-slip motion along the Sanak Island Wrench Zone and the Unimak wrench zone. Margin-oblique faults and folds within the basin developed as a response to Neogene wrench motion.

5. Time-Depth Curves

Time-depth curves were calculated using stacking velocity spectra displays generated from seismic-reflection velocity data and USGS seismic-refraction velocity data collected along the Shumagin shelf. Time-depth curves were also calculated from sonic well logs from the three deeper Kodiak DST wells. Sonic log information from DSDP hole 183 is also included. Most of the seismic-reflection data were provided by a private company. Data from the Kodiak DST wells, 250 miles northeast of the Shumagin Planning Area (fig. 5, p. 13), represent the only available information about the subsurface Kodiak-Shumagin shelf geology (Turner and others, 1987). The time-depth curves presented here are useful only in areas of the basins characterized by relatively undisturbed flat-lying strata.

Interval velocities and time-depth curves were calculated for the three deeper Kodiak shelf wells (KSSD No. 1, KSSD No. 2, KSSD No. 3) by using the borehole compensated (BHC) sonic logs (fig. 22, p. 60). Interval velocities are plotted against time-stratigraphic sequences recognized by Turner and others (1987). All depths given in this section were measured from the Kelly bushings of those wells unless otherwise specified. These correlations aided in the identification of similar features in the adjacent Shumagin continental margin.

An increase in interval velocity across the Miocene unconformity is apparent in the KSSD No. 1 well at 6,142 feet. Velocities for the Neogene section above the unconformity increased gradually with depth, ranging from 6,500 to 10,500 feet per second (ft/sec), with no distinct breaks or reversals. Velocities for the Eocene section below the unconformity range from 12,500 to 14,500 ft/sec. At about 7,800 feet, a noticeable interval velocity increase to 15,263 ft/sec occurs. However, no petrophysical cause for this velocity kick could be determined from other wire-line logs and it is therefore likely to be spurious. Although present on Kodiak Island, Oligocene rocks were not identified in the KSSD No. 1 well. Paleocene and older sedimentary rocks were not encountered but are presumably present below the bottom of the well.

No increase in interval velocity across the Miocene unconformity was detected in the KSSD No. 2 well. Paleontological data indicate that this unconformity

occurs at a depth of 8,774 feet. Overpressuring of the Tertiary section begins at 6,500 feet and continues to the bottom of the well. Such overpressuring may have masked any velocity jump that might be associated with an unconformity. The Neogene section above 6,500 feet has an interval velocity range of 8,100 to 10,000 ft/sec that increases with depth. There were no distinct breaks or velocity reversals.

The KSSD No. 3 well encountered the Miocene unconformity at 7,805 feet. Interval velocities for the Neogene section above the unconformity range from 7,000 to 11,000 ft/sec and increase with depth. Within the Neogene section there is a distinct velocity break near the Pliocene-Miocene boundary. Interval velocities for the Eocene section below the Miocene unconformity range from 11,500 to 13,500 ft/sec.

Time-depth pairs were computed from seismic-refraction data collected in 1981 and 1982 by the USGS (fig. 23, p. 61). The areal distribution of the data is shown in figure 24 (p. 62). Time-depth calculations were limited to those data collected in the region of the continental shelf away from the Sanak Island Transverse High and the Outer Shumagin Islands in order to avoid highly faulted sequence A strata. The plot of time-depth pairs shows increasing dispersion of data points with depth.

A separate time-depth curve was generated from seismic-reflection data from the East and West Sanak basins, Unimak basin, and the Shumagin basin. The seismic-reflection-derived curve has a smaller velocity gradient than the refraction-derived curve and a larger gradient than that found in the DST wells (fig. 25, p. 63).

DSDP Leg 18 hole 183 was drilled in the northern edge of the Aleutian Abyssal Plain within the Shumagin Planning Area (fig. 6, p. 16). Figure 26 illustrates the velocity profile of the strata penetrated in hole 183 and the corresponding density, sediment type, and age. Velocities from core samples ranged from 4,900 to 5,300 ft/sec for Neogene clay and diatomaceous ooze, from 5,300 to 5,600 ft/sec for Oligocene silty and sandy clay, and from 5,600 to 6,000 ft/sec for Eocene silty and sandy clay. The underlying oceanic basalt had a reported velocity of 20,500 ft/sec (Creager and others, 1973).

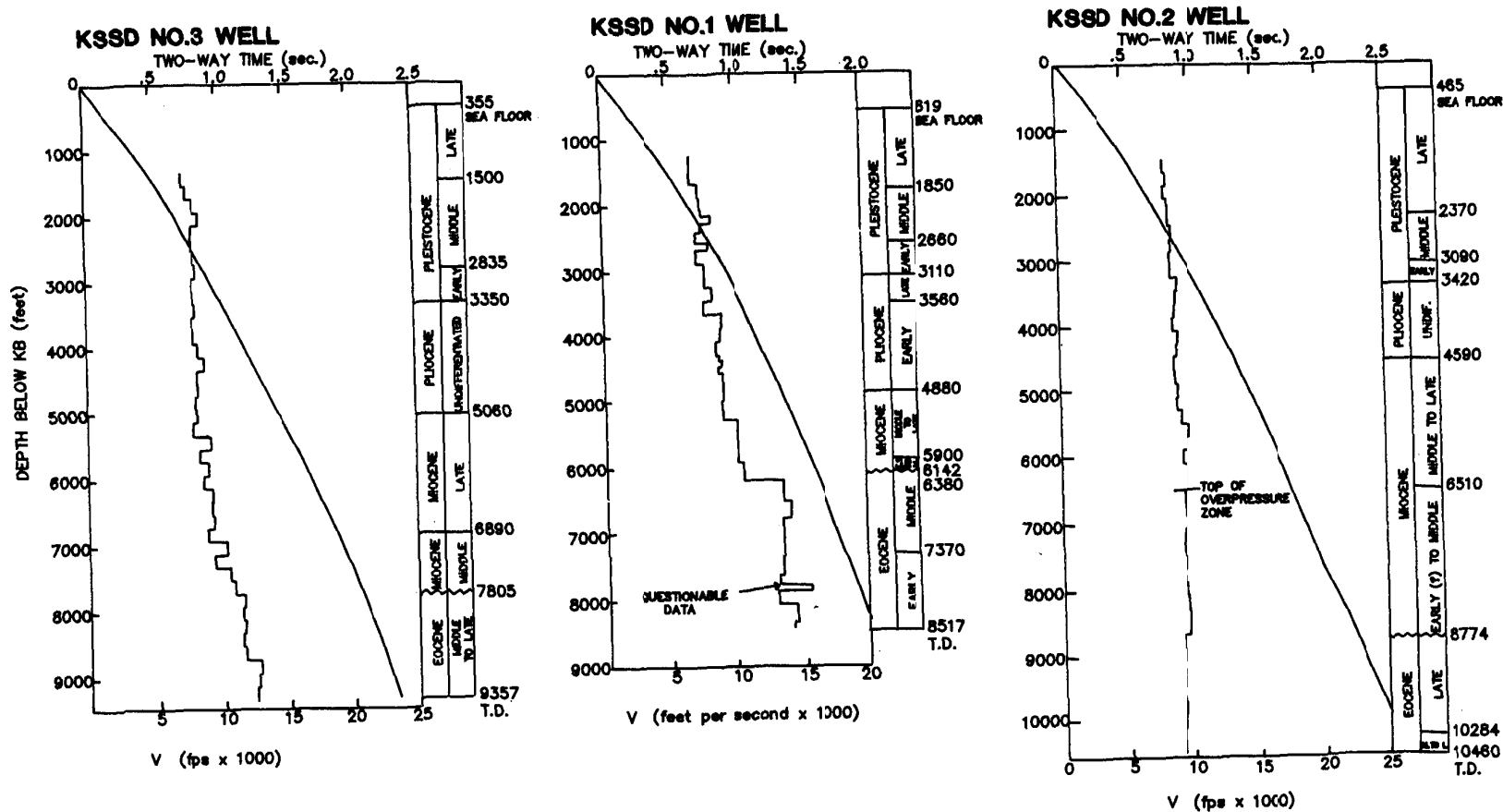


FIGURE 22. Time-depth curves, interval velocities, and stratigraphic columns for the three deepest Kodiak DST wells. Adapted from Turner and others (1987).

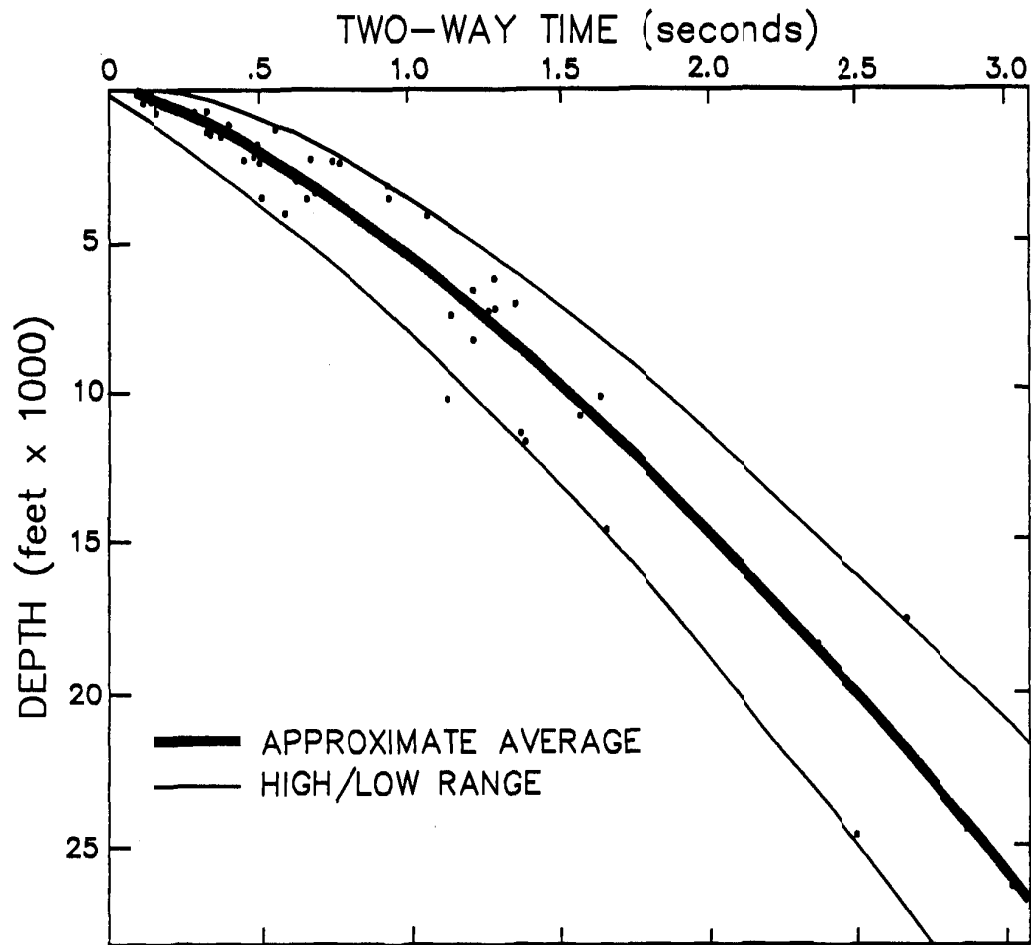


FIGURE 23. Time-depth curve based on seismic-refraction data.

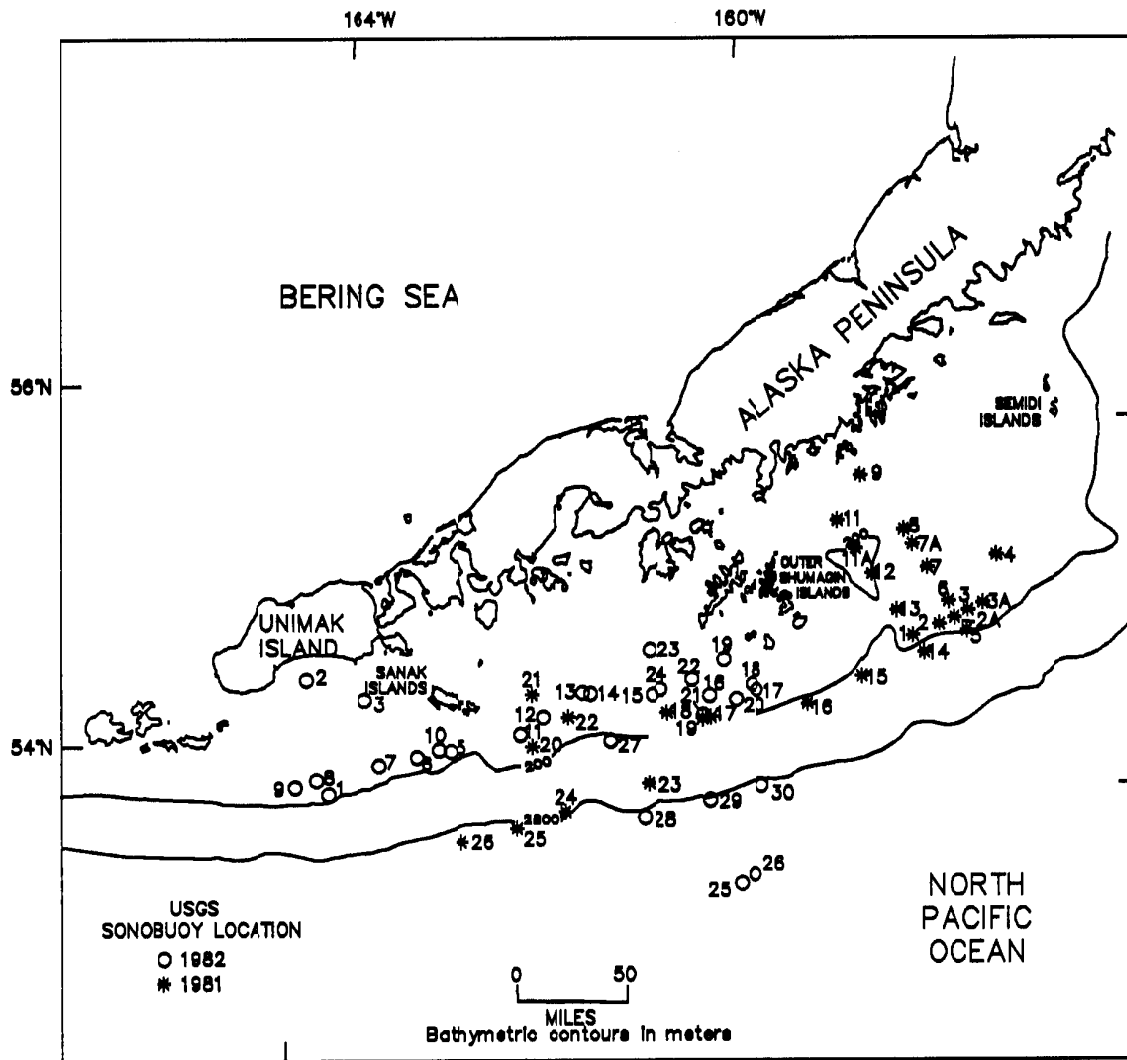


FIGURE 24. USGS sonobuoy locations along the Shumagin margin.

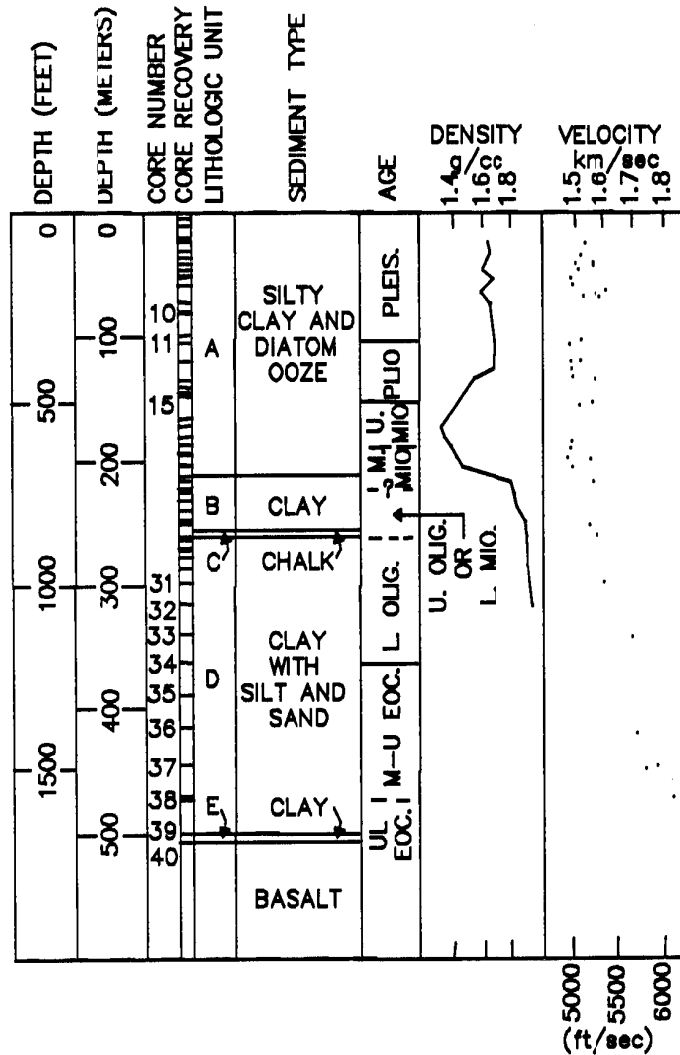
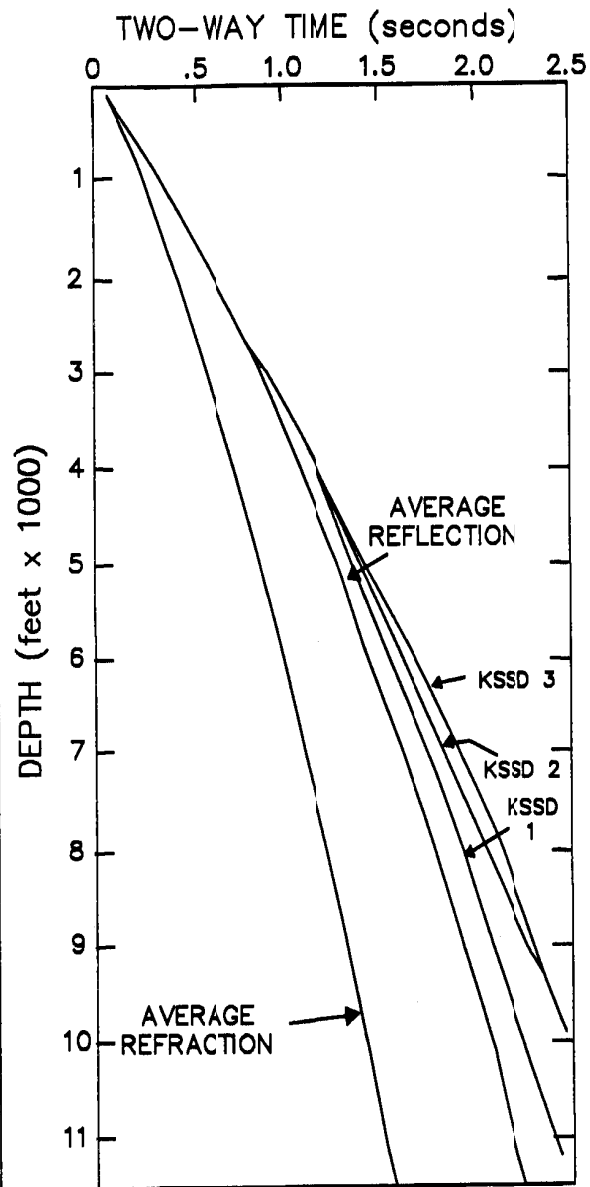


FIGURE 25 (left). Time-depth curves generated from refraction and reflection data for the Shumagin margin and from sonic log data from the three deepest Kodiak DST wells. FIGURE 26 (right). Seismic velocity, density, sediment type, and age of DSDP Leg 18 hole 183. Adapted from Creager and others (1973).

6. Fault Mechanisms, Seismicity, and Transverse Tectonic Features

This section briefly discusses the Shumagin seismic gap and a double Wadati-Benioff zone (fig. 27, p. 66). Minerals Management Service interpretations of newly available seismic-reflection data from the Shumagin margin delineate two major, arc-normal tectonic features coincident with the Shumagin seismic gap. These features, the Sanak Island Wrench Zone and the Sanak Island Transverse High (plate 1), were described in chapter 4. Unfortunately, the new CDP seismic-reflection data neither provide insight into why the Shumagin seismic gap exists nor why these transverse features are coincident with the gap. Fault plane solution studies, however, confirm the presence of strike-slip faults along the Shumagin margin and within the Sanak Island Wrench Zone.

The Sanak Island Transverse High is a positive structural element that trends northwestward and terminates at a seaward deflection of the continental shelf break (plate 1). It was originally recognized by Bruns and others (1985) as a near-surface crustal feature involving faults that bound the West Sanak basin. Bruns, von Huene, and others (1987) identified margin-oblique structures that could have been caused by subsidence or minor transform motion along a pre-Aleutian Ridge (Beringian) margin. Steffy and Horowitz (1987) described these structures and other features as part of the Sanak Island Transverse High and as coincident with the margin-oblique faults that bound the West Sanak basin on the east and the eastern flank of the Unimak basin on the west.

The western boundary of the Sanak Island Transverse High is coincident with the western border of the Shumagin seismic gap as defined by Sykes (1971), Sykes and others (1981), and Davies and others (1981). Similarly, the western limit of the postulated Unimak seismic gap, as defined by Sykes and others (1981) and Davies and others (1981), corresponds with the eastern limit of the Unimak basin. Figure 28 (p. 67) depicts the locations of the Sanak Island Transverse High and the Sanak Island Wrench Zone with respect to the Shumagin seismic gap as defined by Boyd and others (1988). Although the orientation of the seismic gap is not exactly the same as that of the two transverse

features, all are margin-oblique and in the same area of the Shumagin margin.

The Shumagin seismic gap (figs. 27 and 28), an area that has not been ruptured by a large earthquake for at least 40 years (Kanamori, 1977; Boyd and others, 1988), is delimited by the location of a 1938 great earthquake ($M_w = 8.2$) and its associated aftershocks, and by the location of a 1946 large earthquake ($M_s = 7.4$) and its aftershocks. Within the Shumagin seismic gap, the last large earthquake ($M_s = 7.5$), in 1948, was focused along the main thrust zone at a depth greater than 18.5 miles (30 km). Taber and others (1987) and Boyd and others (1988) speculate that the Shumagin seismic gap is divided into two or three arc-normal segments that might be seismically independent. They also believe that the main thrust zone is seismically segmented downdip.

A well-developed Wadati-Benioff zone (a dipping plane usually near the top of a subducting oceanic plate along which earthquake foci occur) and a prominent oceanic trench with an associated outer bulge are present along the Alaska Peninsula. A plot of hypocenters of microearthquakes delineates the zone and shows its depth relationship in the arc and trench along the Shumagin margin (fig. 29, p. 68).

Reyners and Coles (1982) recognized a double-planed Wadati-Benioff zone below 28 miles (45 km) within the Shumagin seismic gap (figs. 29a and 29b). Figure 29b, adapted from the study of Reyners and Coles (1982), illustrates the presence of two distinct planes of seismicity that dip away from the trench. The upper plane dips arcward at 32° between the depths of 28 and 62 miles (45 and 100 km). Below 62 miles (100 km), an abrupt steepening of the dip to about 60° occurs. The lower plane begins at a depth of 40 miles (65 km) and merges with the upper plane at a depth of 75 miles (120 km). A more recent study based on more seismic events (Hudnut and Taber, 1987) indicates that the lower plane begins at 43 miles (70 km) and merges with the upper plane at a depth of 87 miles (140 km). The vertical boundary between the single and double Wadati-Benioff zones is perpendicular to the arc and bisects the gap just southwest of the Shumagin Islands (fig. 27) (Hudnut and Taber, 1987). This transitional boundary marks the location where the lower plane

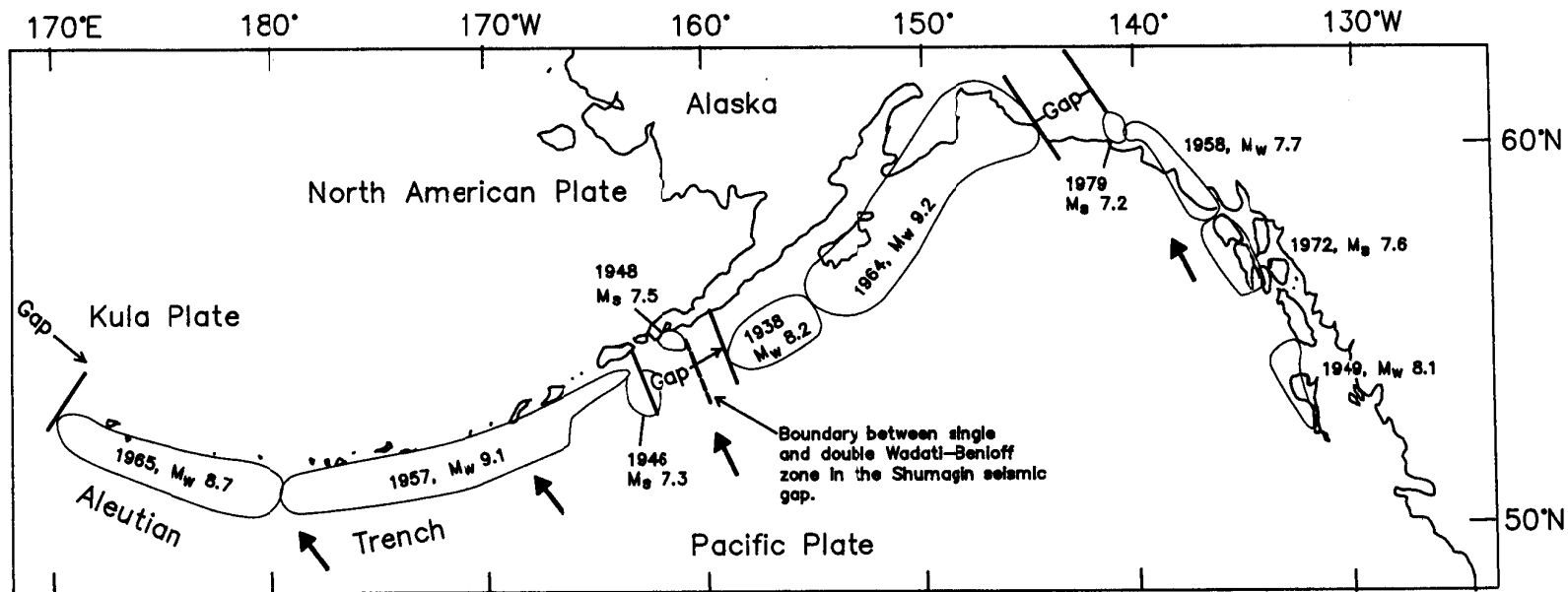


FIGURE 27. Rupture zones in southern Alaska and the Aleutian Arc. Seismic gaps and year and size of the most recent large earthquakes are indicated. Solid arrows indicate direction of relative plate movements. Adapted from Beavan and others (1984) and Hudnut and Taber (1987).

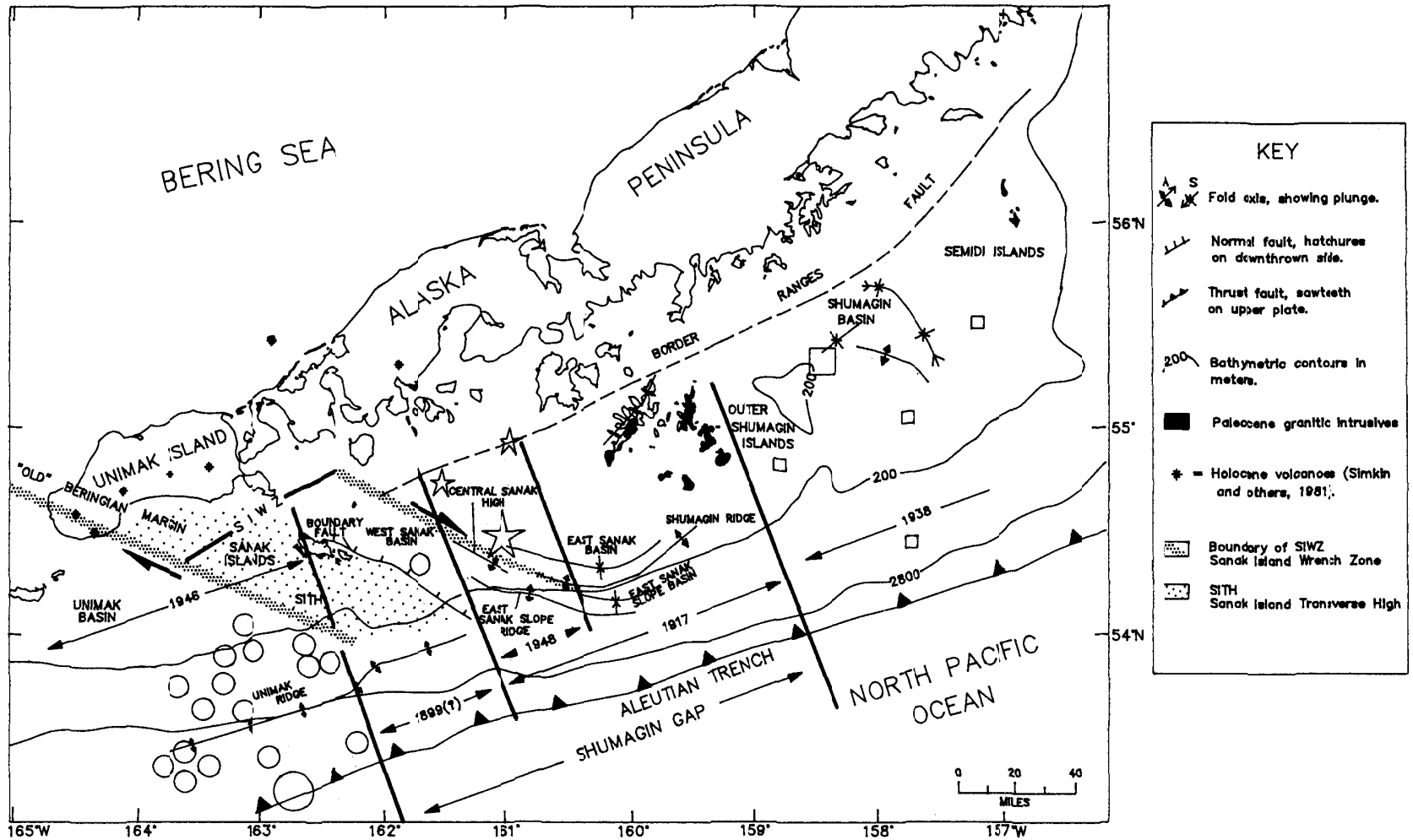
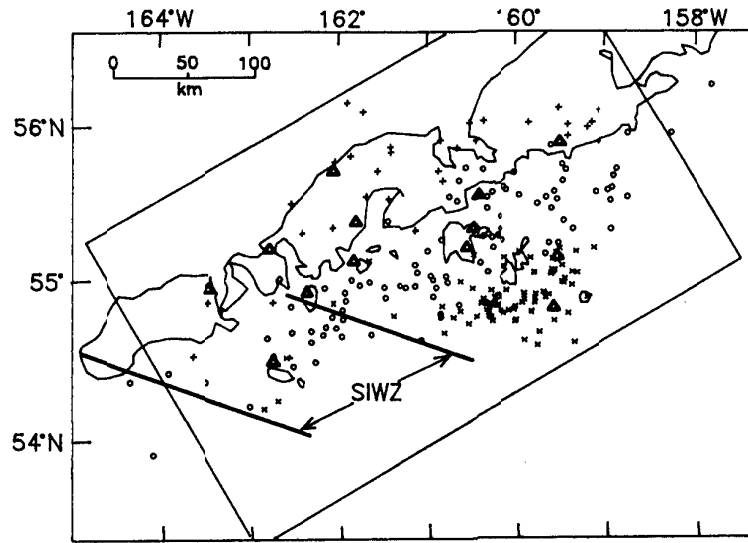


FIGURE 28. Three seismic events are indicated by three symbols (circle, 1946; star, 1948; square, 1938). Mainshock epicenters are indicated by largest symbols and aftershocks are indicated by smaller symbols. Seismic events are taken from Boyd and others (1988).

A.



B.

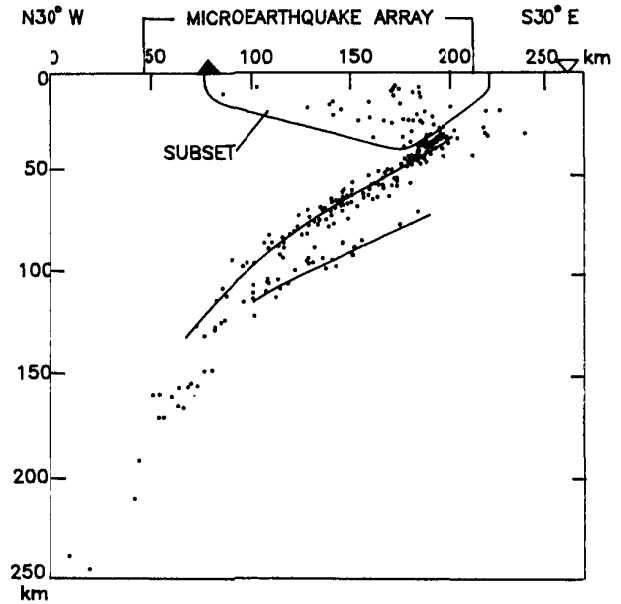
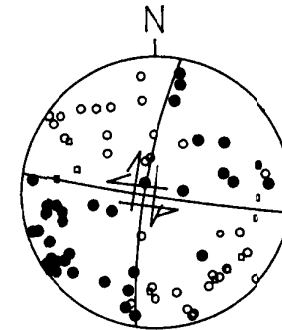


FIGURE 29. Epicenters, hypocenters, and a subset of composite fault plane solutions of microearthquakes along the Shumagin margin. (a) Location of study area, epicenters of microearthquakes, and position of the Sanak Island Wrench Zone. The "x" symbols denote hypocenters occurring between 0-50 km, open circles denote hypocenters occurring between 50-100 km, and pluses denote hypocenters occurring deeper than 100 km. (b) Cross section of all microearthquakes within the study area, and the location of a shallow subset of hypocenters. (c) Composite fault plane solution of the shallow subset located in figure 29b indicates a strike-slip mechanism, where open symbols represent dilational, and solid symbols compressional, P-wave first motion. Circles represent arrivals leaving focus in an upward direction; squares are critically refracted arrivals projected from lower hemisphere. Small symbols represent less reliable readings. Adapted from Reyners and Coles (1982).

C.



starts to appear as much as 16 miles (25 km) below the upper plane in the southwest portion of the seismic gap. The upper zone is continuous across the boundary, whereas the lower zone is present only to the southwest. Hudnut and Taber (1987) do not consider the presence of "shallow" transverse structural features in the overlying continental plate and accretionary prism, such as the Sanak Island Transverse High and Wrench Zone, to be responsible for the double-to-single Wadati-Benioff transition.

Seismicity studies of the Shumagin seismic gap area have provided insight into inter- and intraplate tectonics and the fault characteristics of the Shumagin subduction complex. According to Kawakatsu (1986), stress produced by downdip compression is released by earthquakes that define the upper Wadati-Benioff zone. These earthquakes are associated with movement along the main thrust zone, which defines the upper boundary, or detachment surface, of the subducting plate and is a region of major interplate deformation. In areas such as the Shumagin seismic gap, the main thrust zone is well coupled to the overlying plate and appears to be locked (Davies and others, 1981). Compressional stress that is built up in the subducting plate may be transferred upward and released through shallow seismicity localized arcward of the subducting plate (as illustrated by the fault pattern in figure 10, p. 22). Alternatively, Beavan and others (1983) interpret shallow seismicity and stress to reflect temporal changes in the aseismic slip that occurs in an unlocked main thrust zone. In either case, composite fault-plane solutions of these shallow earthquakes indicate consistent strike-slip mechanisms behind the trench-slope break with a strike of their composite solutions being 10° or 280° (fig. 29c) (Reyners and Coles, 1982). The majority of shallow seismic events studied by Reyners and Coles (1982) occurred northeast of the Sanak Island Wrench Zone near the Outer Shumagin Islands (fig. 29a); none occurred in the area where Lewis and others (1986) mapped margin-oblique strike-slip faults in the Shumagin trench lower slope. Nothing in Reyners and Coles' (1982) study refutes or supports the contention of this report that the Sanak Island Wrench Zone is a major margin-oblique right-lateral feature.

The margin-oblique faults that bound the Sanak Island Wrench Zone parallel the projection of the "old"

Beringian transform margin into the Shumagin region (Steffy and Horowitz, 1987). The "old" Beringian transform margin is thought to have existed between the northwestwardly moving Kula plate and the North American plate (fig. 33, p. 76). Motion along this transform margin in the Bering Sea may have included a component of oblique subduction (Scholl and others, 1975; Cooper and others, 1976; Marlow and others, 1976). Steffy and Horowitz (1988) proposed that this Late Cretaceous subduction created an accretionary basin oblique to the current trend of the Shumagin margin and that continued growth of this complex caused the basin to encroach upon the Shumagin continental shelf and become what is now the West Sanak basin.

The Sanak Island Wrench Zone is a structural consequence of strike-slip motion in the Pliocene, as evidenced by thrust faults that cut strata above the Miocene unconformity (plates 4 and 9). A number of other features, among them the presence of the Unimak wrench zone in the southwestern portion of the Unimak basin, the inversion (uplift and broad anticlinal folding of the basin fill) of the West Sanak basin, the presence of offsets in the Unimak Ridge, the oblique alignment of strike-slip faults that cut the seafloor in the continental slope, and an abrupt change in the continental shelf break, all suggest strike-slip motion normal to the Aleutian Arc and Alaska Peninsula.

Many of the margin-oblique basin features, structural highs, and faults are best explained as related to the Sanak Island Wrench Zone. However, a number of uncertainties and ambiguities remain, such as the absence of an offset of the Quaternary volcanic arc where the Sanak Island Wrench Zone intersects the Aleutian Arc-Alaska Peninsula, the absence of equivalent features in the immediate back-arc area of the Bering Sea, and the absence of an obvious feature on the Shumagin shelf to take up the strike-slip motion.

The Shumagin seismic gap and a double Wadati-Benioff zone are unique features found within the Shumagin Planning Area. Their presence does not appear to be tied to the SITH or SIWZ, other than being coincident, although some relationship might be established by further study.

7. Geologic History

Tectonic plates underlying the Pacific Ocean have been continuously subducted beneath the Alaska Peninsula since the Cretaceous (fig. 30, p. 73), with an older more complex history of convergence as early as the Jurassic. Southwest Alaska consists of a set of amalgamated tectonostratigraphic terranes (Peninsular, Chugach, and Prince William) that were rafted northward by oceanic plates and fused with the North American continental plate during collision. These terranes consist of continental margin deposits and arc-derived turbidite deposits. The accretion of the two southernmost and youngest terranes, the Chugach and Prince William, created the continental shelf and provided the basement complex (Chugach terrane) upon which the Tertiary Shumagin shelf basins developed (fig. 5, p. 13).

Paleomagnetic, geologic, and paleontologic data from southern Alaska lend support to the concept that the Peninsular, Chugach, and Prince William terranes are allochthonous with respect to the North American plate. Inclinations of the ancient geomagnetic field for the Peninsular and Chugach terranes show systematic northward motion, at an average rate of 6 centimeters per year (cm/yr), from the Late Cretaceous to the present (Stone and others, 1982). Recent plate-motion reconstructions have been approached quantitatively using mantle hot-spot locations in the Pacific and Atlantic Oceans as fixed points of reference (Engelbrechtsen and others, 1985; Rea and Duncan, 1986).

Before the Late Cretaceous, the Farallon plate, the dominant plate in the North Pacific region during the Mesozoic (fig. 31, p. 75), was being subducted beneath the North American plate at a rate of 10 cm/yr (Rea and Duncan, 1986). A major strike-slip fault, the predecessor of the present-day Border Ranges fault, existed between southern Alaska and the Farallon plate during the Late Jurassic (Fisher and others, 1984). In the Late Cretaceous, the Kula spreading ridge system divided the Farallon plate into the Kula plate and the smaller Chinook plate (fig. 32, p. 75). Between 85 and 43 million years ago, the Kula plate moved northward and converged with southern Alaska at a rate of 20 cm/yr (Rea and Duncan, 1986)(fig. 33, p. 76). The Kula plate obliquely subducted or "transformed past"

the Beringian margin during the Late Cretaceous and early Tertiary, which initiated the formation of the Navarin, St. George, Pribilof, and North Aleutian basins (figs. 30 and 33)(Scholl and others, 1975; Cooper and others, 1976; Marlow and Cooper, 1980; Fisher and others, 1984; Steffy and others, 1985; Comer and others, 1987).

As the Kula plate was subducted, the allochthonous terranes it carried were amalgamated onto the North American plate. The spatial and temporal constraints on the successive accretion of these terranes are in some dispute, and much evidence is apparently contradictory. Studies of Paleocene lava flows that are interbedded with strata of the Peninsular and the Wrangellia terranes (Talkeetna superterrane)(fig. 5) suggest that the superterrane docked against or was within 8° of the North American plate by Paleocene time (Thrupp and Coe, 1986). Also, by early Paleocene, the Chugach and Prince William terranes, located somewhere south of Alaska, were probably moving northward as an amalgamated unit (Plumley and others, 1983). This movement was facilitated by rotation between the Kula and the North American plates between 56 and 55 million years ago (early Eocene) as the direction of convergence became more northwestwardly (fig. 30)(Lonsdale, 1988).

Estimates on the time of arrival of the Chugach and Prince William terranes and their amalgamation with the Peninsular terrane vary widely. For example, Fisher and others (1984) located the Border Ranges fault where mildly deformed middle or late Paleozoic rocks (Peninsular terrane) are juxtaposed with structurally complex accreted Cretaceous rocks (Chugach terrane). They suggest that this great contrast may mark the arrival of the Chugach terrane in the Late Cretaceous, and at that time, motion along the Border Ranges fault changed from strike-slip to reverse (fig. 30). Because both Peninsular and Chugach terrane rocks exposed on the Kodiak Islands are intruded by late Paleocene granodioritic batholiths, the arrival/amalgamation must have occurred before this time (fig. 30)(Davies and Moore, 1984).

However, the structural evidence of Fisher and others (1984) and the radiometric data of Davies and Moore (1984) are contradicted by paleomagnetic data from the

Ghost Rocks Formation, a Cretaceous to Paleocene subduction complex on the Kodiak Islands and part of the Prince William terrane. These data suggest that these terranes moved north by as much as 25 degrees of latitude during the Tertiary and that the Prince William terrane may not have been juxtaposed with the Talkeetna superterrane until the middle Eocene (Gromme and Hillhouse, 1981; Plumley and others, 1983).

On the basis of magnetic anomaly data, there may have been 45° to 55° counterclockwise rotation of southwest Alaska contemporaneous with the Eurasia-North American plate convergence in the Late Cretaceous (Coe and others, 1985; Thrupp and Coe, 1986). Hillhouse (1987) postulates as much as 50° of rotation about a longitudinal axis of 146° W. between the Late Cretaceous and the Eocene. Rotational movement also occurred between the Kula and North American plates and may have initiated subduction at the Aleutian Arc (Lonsdale, 1988).

Subduction of the Kula plate beneath the Aleutian Trench eventually led to the subduction of the Kula-Pacific spreading ridge at the trench. The arrival time of the ridge has been estimated to be Paleocene (Hayes and Pitman, 1970; Byrne, 1979) or Eocene (Marlow and others, 1973; Engebretsen and others, 1985). The consumption of the spreading ridge resulted in the Pacific plate converging toward the North American plate in a northwestwardly direction at a reduced rate of 5 cm/yr in the late Eocene (Rea and Duncan, 1986)(fig. 34, p. 77). Lonsdale (1988) described a remnant portion of the Kula-Pacific spreading ridge just south of the Central Aleutian Trench (fig. 33, p. 76) and postulated that the Kula-Pacific spreading ridge realigned to a more northeastwardly trend between 56 and 55 million years ago (early Eocene) during the counterclockwise rotation of the Kula and North American plates. He also suggests that the Kula-Pacific spreading ridge became inactive about 43 million years ago (middle Eocene) before its partial subduction at the Aleutian Trench. The rotation of the Kula-Pacific plates resulted in a more perpendicular convergence with the North American plate and may have been associated with a major pulse of magmatism in the late Eocene and Oligocene on the Alaska Peninsula (Meshik Arc) and in the Alaska Range (figs. 30 and 33)(Wilson, 1985).

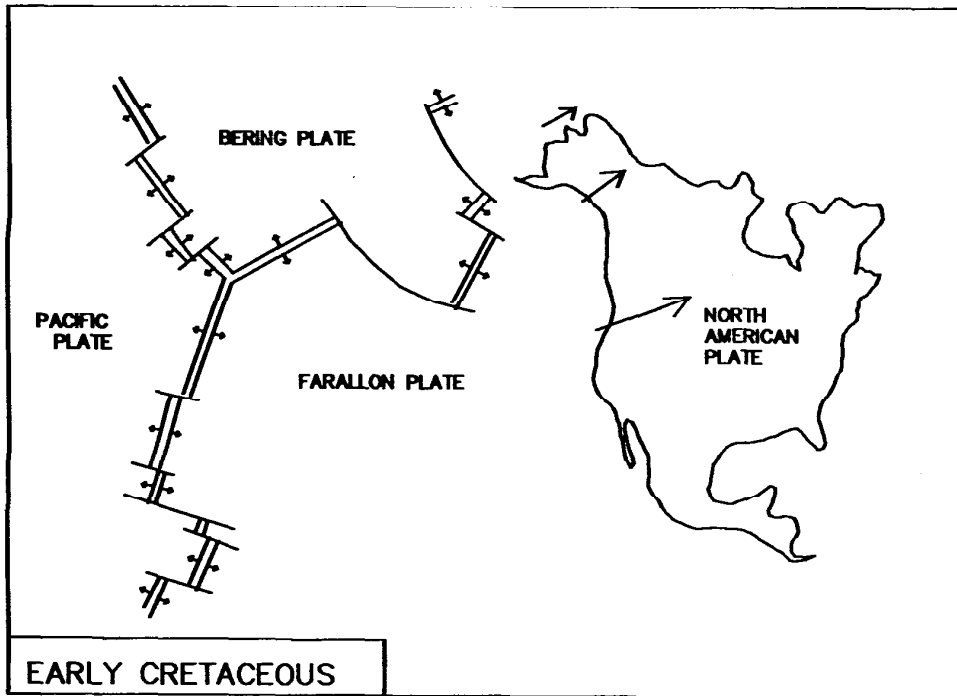
The arrival of the spreading ridge is constrained by the formation of the Aleutian Arc in the early Eocene (Lonsdale, 1988). The formation of the Aleutian Arc isolated the portion of the Kula plate north of the arc from a remnant of the Kula plate that still existed north of the Kula-Pacific spreading ridge (fig. 33). The relative position of the newly formed Aleutian Arc with respect to the Alaska Peninsula and southern Alaska in the Eocene is uncertain. There is evidence, however, that the arc formed south of its present position and moved northwestward during the late Eocene (Whitney and Wallace, 1984; Herman and others, 1987). Paleomagnetic data show no significant poleward motion of the Aleutian Arc since the early Oligocene (Harbert, 1987)(fig. 33). Dextral transform motion along the "old" Beringian margin provides the means by which the arc moved northwestward and subjected the Paleocene strata of the Shumagin shelf to strike-slip tectonics.

The Tertiary evolution of the Shumagin forearc basins is genetically related to the complex pattern of plate convergence that has occurred since the Cretaceous. The Cretaceous and early Tertiary Shumagin margin consisted of a subduction complex where deep-water turbidites of sequence A were emplaced. This complex was built by underthrusting and offscraping, in addition to underplating and accretionary duplexing processes similar to those proposed for the adjacent Kodiak margin (Byrne, 1986; Sample and Fisher, 1986).

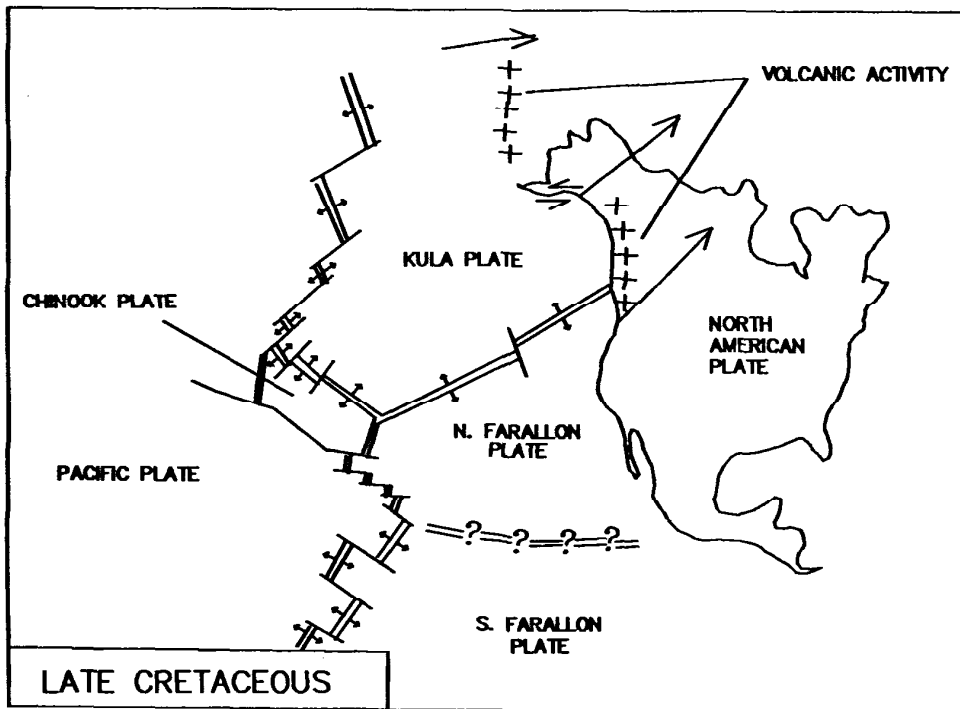
The Shumagin and East Sanak basins formed initially in the Late Cretaceous and early Tertiary as margin-parallel forearc basins in a lower trench slope setting (fig. 30). Northeast-trending folds of the Shumagin Formation (exposed on the adjacent Outer Shumagin Islands) were formed synchronously with the adjacent Shumagin basin. Paleocene granodiorites intruded the folded Shumagin Formation and date the latest possible time of this deformation (fig. 30).

The West Sanak basin formed as a northwest-trending forearc basin parallel to the proposed "old" Beringian transform margin (plate 1 and fig. 30). The basin axis is parallel to the strike of Late Cretaceous rocks exposed on Sanak Island (fig. 5, p. 13) and to possible northeast-dipping imbricate thrusts within the Sanak Island Transverse High (plate 4).

In the early Eocene, after sequence A was accreted, the Shumagin slope basins were uplifted and eroded,



FIGURES 31 and 32. Early and Late Cretaceous positions of the North American and Pacific plates and convergence vectors. Modified from Rea and Duncan (1986).



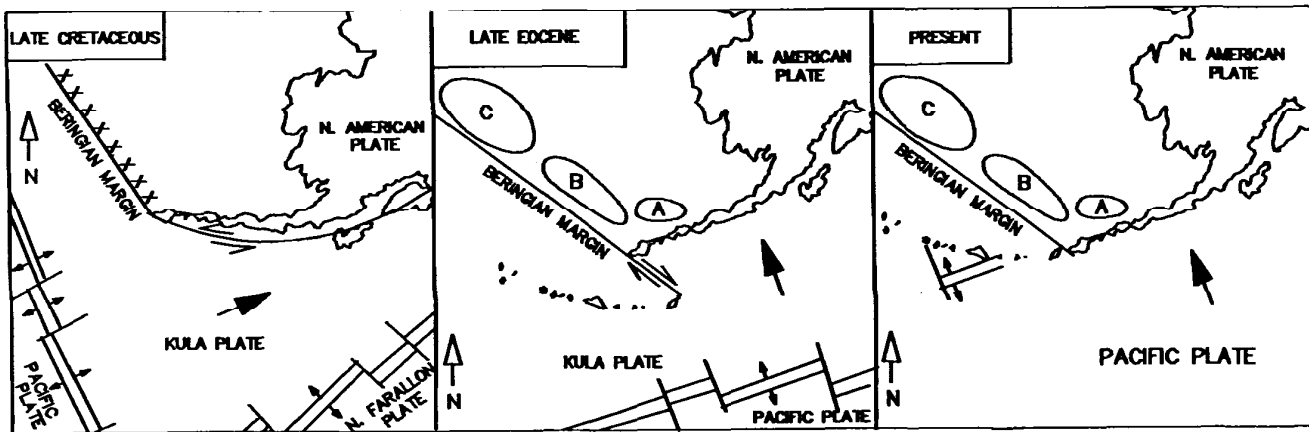


FIGURE 33. Positions of the Kula, Pacific, and North American plates and their relative directions of motion in the Shumagin area since Late Cretaceous time. The locations of the North Alcutian basin (A), St. George basin (B), and the Navarin basin (C) are shown.

resulting in an unconformity between sequence A and the overlying sequence B (plates 2 and 5).

The seaward growth of the Shumagin margin continued through the Paleogene with the deposition of the deep-water turbidites of sequence B in structural depressions in sequence A in the Shumagin, East Sanak, and West Sanak basins (fig. 18, p. 50). The accretionary complex (sequence B) that forms the basement upon which the Unimak basin was built did not develop until the Aleutian Arc formed in the early Eocene (fig. 30).

Ridges composed of accreted material, early predecessors of the Unimak and East Sanak slope ridges, formed along the outer trench–continental slope parallel to the Aleutian Trench (fig. 30). As the accretionary prism grew, these ridges were translated upslope and provided baffles for sediment accumulation and facilitated the formation of forearc basins. The Shumagin margin grew seaward, engulfing the accretionary basins and their bounding slope ridges (plate 1).

Vertical uplift of the continental slope imposed extensional tectonics on the basins by rifting along existing faults that were rooted within the basement complex. Uplift and erosion of the Shumagin-Kodiak continental margin are reflected in the Miocene unconformity (figs. 17 and 30). Regional uplift in the late Oligocene and Miocene resulted in the truncation of sequence A and B strata and the deposition of

sequence C. Differential uplift also occurred along the Shumagin Ridge, forming the East Sanak slope basin (fig. 30).

Docking of the Aleutian Ridge before the early Oligocene (Harbert, 1987) may have been synchronous with the uplift of the Sanak Island Transverse High, a margin-oblique compressional ridge. This uplift exposed strata as old as Late Cretaceous to erosion (fig. 30). Transform motion along the Beringian margin diminished once the Aleutian Ridge docked, and probably ceased by the late Oligocene. Subsequent compressional strain imposed on the Shumagin shelf by convergence was taken up, in part, by strike-slip faults. These faults are expressed in Tertiary sections by master wrench faults and associated splays. The accretionary complex and the Paleogene forearc basins have been overprinted by features generated by convergent wrench motion.

The Shumagin basin was restructured in the late Paleogene by renewed movement along an oblique transcurrent fault system that has been present since the Cretaceous (fig. 30)(Horowitz and Steffy, 1988). The master wrench fault, which extends to the Border Ranges fault, dips northeastward and cuts an existing decollement within sequence A. The basin was reoriented and reconfigured into an elongated half-graben parallel to the northwest-trending master wrench fault.

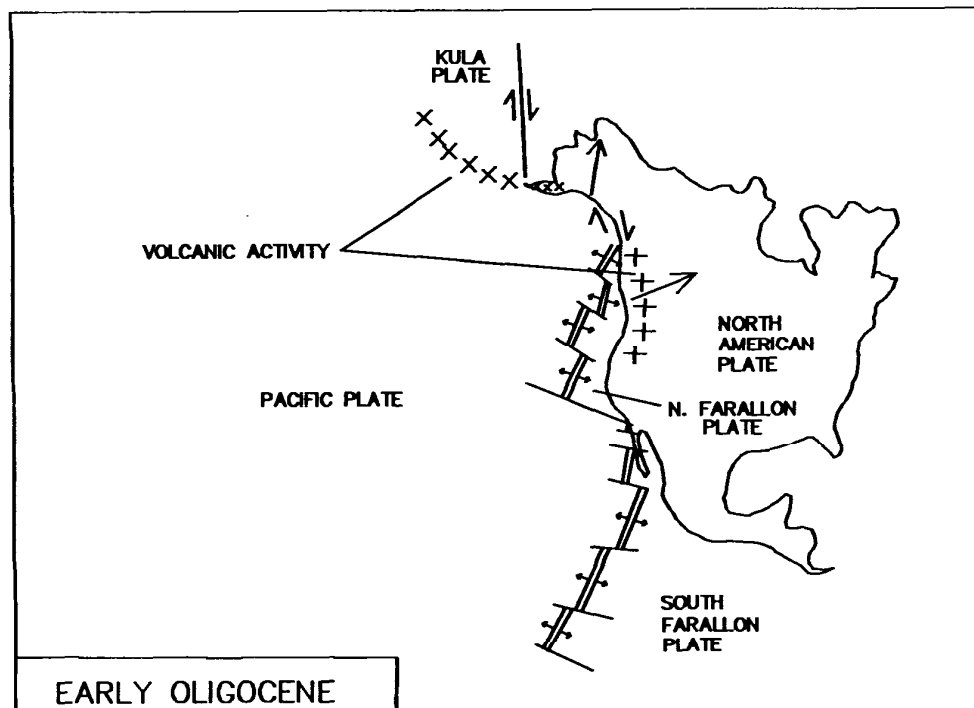
Continued seaward growth of the Shumagin margin led to the upslope migration of accretionary highs (Unimak ridge, East Sanak slope ridge). These highs were subjected to strike-slip motion in the Sanak Island Wrench Zone before being cut by the Miocene unconformity (fig. 30). This episode of wrench tectonics resulted in the offset of the Unimak ridge and the clockwise rotation of the East Sanak slope ridge to its present position, subparallel to the SITH and SIWZ. This wrench motion was also associated with the relative uplift of the Central Sanak high and the East Sanak slope ridge (fig. 30). At the same time, the SITH appears to have been uplifted, and normal faulting occurred along pre-existing thrust planes. The uplift involved both underplating and wrench-faulting mechanisms.

Wrench movement along the Shumagin margin was probably reactivated with Pliocene extensional deformation. In the Shumagin basin, continued movement along the master wrench fault subjected the newly formed Shumagin half-graben to laterally changing stress that produced transpressional features

at restraining bends and transtensional features at releasing bends. Dextral wrench movement occurred in conjunction with normal movement just seaward of the Border Ranges fault and the uplift of an adjacent block of the Peninsular terrane. Motion along this portion of the shelf lasted until the late Pliocene.

Uplift of the Sanak Island Transverse High and subsidence of the West Sanak basin along the northwest-trending Boundary fault continued into Pliocene time. Stacked thrusts occur near a restraining bend of the Boundary fault (plates 4 and 9). The thrusting may have been a response to convergent strike-slip motion of the Sanak Island Wrench Zone that localized at a restraining bend of the Boundary fault (Steffy and Horowitz, 1988). The thrusting, probably facilitated by the movement of overpressured-fluids from beneath the uplifted SITH, generated antiforms and structurally inverted the West Sanak basin. Basin subsidence continued along normal faults that formed in response to post-thrusting extension.

FIGURE 34. Early Oligocene positions of the North American and Pacific plates and convergence vectors. Modified from Rea and Duncan (1986).



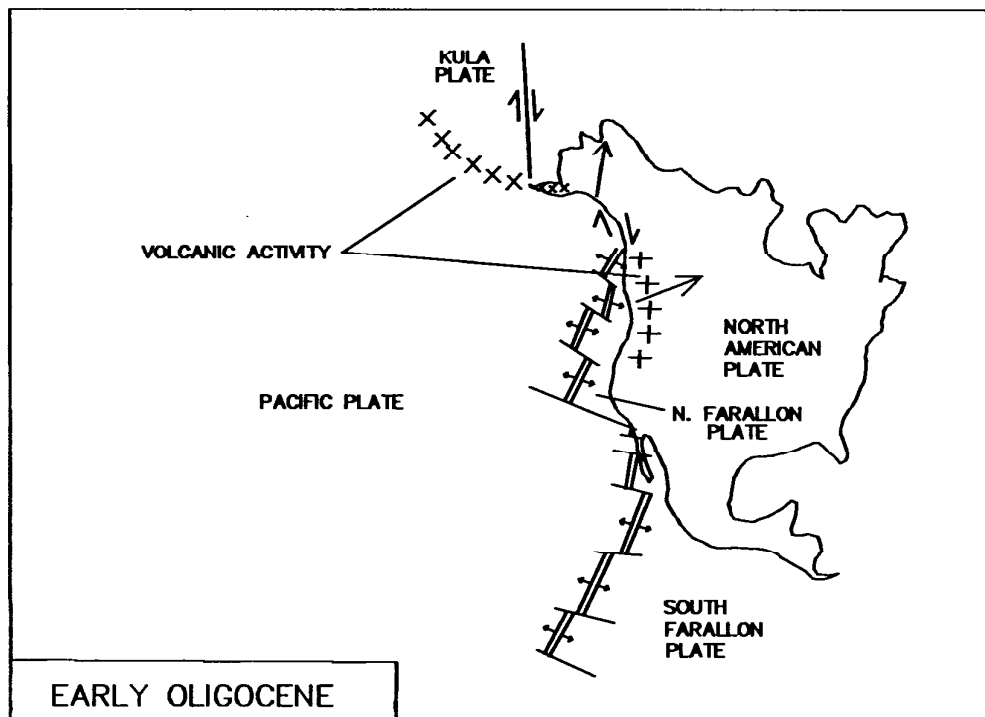
Continued seaward growth of the Shumagin margin led to the upslope migration of accretionary highs (Unimak ridge, East Sanak slope ridge). These highs were subjected to strike-slip motion in the Sanak Island Wrench Zone before being cut by the Miocene unconformity (fig. 30). This episode of wrench tectonics resulted in the offset of the Unimak ridge and the clockwise rotation of the East Sanak slope ridge to its present position, subparallel to the SITH and SIWZ. This wrench motion was also associated with the relative uplift of the Central Sanak high and the East Sanak slope ridge (fig. 30). At the same time, the SITH appears to have been uplifted, and normal faulting occurred along pre-existing thrust planes. The uplift involved both underplating and wrench-faulting mechanisms.

Wrench movement along the Shumagin margin was probably reactivated with Pliocene extensional deformation. In the Shumagin basin, continued movement along the master wrench fault subjected the newly formed Shumagin half-graben to laterally changing stress that produced transpressional features

at restraining bends and transtensional features at releasing bends. Dextral wrench movement occurred in conjunction with normal movement just seaward of the Border Ranges fault and the uplift of an adjacent block of the Peninsular terrane. Motion along this portion of the shelf lasted until the late Pliocene.

Uplift of the Sanak Island Transverse High and subsidence of the West Sanak basin along the northwest-trending Boundary fault continued into Pliocene time. Stacked thrusts occur near a restraining bend of the Boundary fault (plates 4 and 9). The thrusting may have been a response to convergent strike-slip motion of the Sanak Island Wrench Zone that localized at a restraining bend of the Boundary fault (Steffy and Horowitz, 1988). The thrusting, probably facilitated by the movement of overpressured-fluids from beneath the uplifted SITH, generated antiforms and structurally inverted the West Sanak basin. Basin subsidence continued along normal faults that formed in response to post-thrusting extension.

FIGURE 34. Early Oligocene positions of the North American and Pacific plates and convergence vectors. Modified from Rea and Duncan (1986).



The oblique-trending Unimak wrench fault (plate 1) deformed the Neogene section in the Unimak basin by thrusting and compression (fig. 30). On seismic-reflection profiles, this convergent wrench zone is expressed by "positive flower structures." Individual and stacked Pliocene thrust features within the Unimak basin are parallel to and cogenic with imbricate thrusts found within the compressional ridge of the Sanak Island Transverse High (plate 7). Margin-parallel growth faults and extensional normal faults parallel to the thrust trend represent the latest phase of deformation in the Unimak basin.

Along the Shumagin margin, deposition of quartz-rich sequence C sediments extended over the shelf and across the slope to the Aleutian Trench (fig. 13, p. 25). After the Miocene, most turbidite deposition was

restricted to the trench. The Plio-Pleistocene unconformities found throughout the Shumagin shelf are thought to be indicative of both glacioeustatic events and the uplift and growth of the margin by the accretionary processes of underplating and duplexing associated with convergent wrenching. Quaternary and Tertiary glacial episodes recognized onshore, however, were not here correlated with specific offshore unconformities. As a result of these glacial events, a portion of sequence C probably resembles the glacio-marine deposits that compose the late Pliocene and early Pleistocene Tugidak Formation that is exposed on Tugidak and Chirikof Islands to the northeast (Allison, 1978). Glacioeustatic events are also expressed as sea valleys that incise the Shumagin outer shelf and slope.

PART 2:
PETROLEUM
GEOLOGY

8. Exploration History

The remote setting and hostile subarctic marine environment of the Shumagin margin have long deterred petroleum exploration. Not until 1971 did offshore seismic exploration by private industry commence. Since then, a regional grid of 9,700 line miles of common-depth-point (CDP) seismic-reflection data covering most of the Shumagin continental shelf has been collected (fig. 3, p. 4). Surface and near-surface geologic investigations by industry include over 160 miles of high-resolution seismic-reflection data and various samples collected from the sea bottom. Over 23,000 line miles of potential field (magnetic and gravity) data were also collected by industry over the continental shelf. The USGS collected an additional 310 miles of reflection data in 1977 (Bruns and Bayer, 1977) and 2,480 miles of reflection data in 1981 and 1982 (Bruns and others, 1985). In addition, the USGS collected seismic-refraction data at 49 sonobuoy sites on the Shumagin shelf and slope (fig. 23, p. 61) and lithologic and paleontologic data at three dredge sites on the slope (fig. 6, p. 16).

No petroleum exploration wells have been drilled in the Shumagin Planning Area. The nearest wells are located on the geologically similar Kodiak continental shelf, which lies approximately 150 miles to the northeast. Six Deep Stratigraphic Test (DST) wells were drilled on the Kodiak shelf between 1976 and 1977 (figs. 4 and 5, p. 11 and 13) (Turner and others, 1987). In 1976, Exploration Services, Inc., drilled three wells (KSST No. 1, KSST No. 2, KSST No. 4A), which ranged in depth from 1,391 to 4,307 feet. In 1977, Sun

Oil Company drilled three wells (KSSD No. 1, KSSD No. 2, KSSD No. 3), which ranged in depth from 8,517 to 10,460 feet.

Petroleum exploration in the nearby but geologically dissimilar Alaska Peninsula (fig. 4) has been ongoing since the early 1900's. Between 1903 and 1959, 11 wells were drilled onshore in the Kanatak district near Lake Becharof, about 120 miles north of the northeast corner of the Shumagin Planning Area. Since 1959, another 16 wells were drilled west and south of the Kanatak district. None of these wells were reported to have discovered producible hydrocarbons.

In 1971, the Deep Sea Drilling Project (DSDP) of the Joint Oceanographic Institutions for Deep Earth Sampling (JOIDES) drilled Leg 18 hole 183 in the Aleutian Abyssal Plain south of the Shumagin continental shelf (fig. 6). An additional five coreholes were drilled in the adjacent Kodiak continental slope and Aleutian Abyssal Plain. A description and investigation of the Shumagin Leg 18 hole 183 is found in Creager and others (1973), and for Kodiak Leg 18 holes 178 through 182 in Kulm and others (1973). The water depth at the Shumagin site was 15,450 feet, and the core penetrated 1,693 feet of section. Water depths at the Kodiak sites ranged from 4,708 to 16,152 feet and the core holes ranged from 358 to 2,607 feet deep.

No lease sale has been held for the Shumagin Planning Area. The Shumagin Oil and Gas Lease Sale 129 was scheduled for January 1992 on the Minerals Management Service 5-year lease sale schedule announced in 1987; at this writing, the sale has been deferred.

9. Geothermal Gradient

An evaluation of the hydrocarbon potential of the Shumagin Planning Area requires that a general geothermal gradient be estimated. A sufficient geothermal gradient and depth of burial are necessary to ensure that any kerogen present will be mature enough to have generated hydrocarbons. Since there are no wells in the planning area, estimates of the geothermal gradient must be extrapolated from wells drilled in adjacent, geologically similar areas (Middleton Island, Cook Inlet, and the Kodiak continental shelf). However, extrapolated gradients are subject to the constraints of thermal models appropriate to the geologic setting. Another, somewhat exotic, approach involves geothermal gradient calculation and extrapolation based on the pressure-temperature dependency of clathrates occurring on the Shumagin continental slope (Kvenvolden and McMenamin, 1980; Kvenvolden and von Huene, 1985).

Convergent margins, such as the Shumagin, are numerically modeled to have low heat flows due to the subduction of cold lithospheric crust at the trench (Uyeda, 1977; Anderson and others, 1978). Subduction of a cold oceanic plate depresses the isotherms and lowers the heat flow by as much as 60 percent within 62 miles of the trench axis. Therefore, the thermal regime of the forearc basin is partially dependent on its proximity to the subducting lithosphere, which is a function of the distance of the arc-trench gap and the angle of subduction. This is in contrast with the high geothermal gradient associated with the adjacent volcanic arc (Aleutian Arc-Alaska Peninsula).

The analogous region of Cook Inlet is an abandoned forearc basin that was isolated by the emergence of an outer shelf ridge, now the Kenai Peninsula, in the Late Cretaceous (von Huene and others, 1977). Cook Inlet lies nearly 500 miles northeast of the Shumagin area and 125 miles northwest of the modern axis of the Aleutian Trench. The present-day temperature gradient for this region, a mean value of 1.42 degrees Fahrenheit per 100 feet ($^{\circ}\text{F}/100$ feet), a median value of $1.32^{\circ}\text{F}/100$ feet, and a range from 1.04 to $1.97^{\circ}\text{F}/100$ feet, was calculated from 43 wells shown on the American Association of Petroleum Geologists (AAPG) Geothermal Map (1976) of the hydrocarbon producing area of Cook Inlet. This AAPG study was

part of a multiyear geothermal survey of North America (a description of the methodology was given in Kehle, 1973). The temperature data published are believed to represent corrected thermal gradients computed using well log heading bottom hole temperatures (BHT). The correction was based on a statistical study of the deviation between the gradient calculated from a well log heading BHT and the gradient calculated using equilibrium BHT for a large number of west Texas wells. Magoon (1986) calculated a geothermal gradient for the ARCO Lower Cook Inlet COST No. 1 well, which is located in the same area as the AAPG map, of 22.8 degrees Celsius per kilometer ($^{\circ}\text{C}/\text{km}$) ($1.25^{\circ}\text{F}/100$ feet) from the seafloor to total depth using the formation temperature derived from a Horner plot. Magoon (1986) also stated that the COST well gradient compares well with the gradient calculated for the Swanson River Oil Field, which lies nearly 100 miles to the northeast. Here, a gradient of $23.7^{\circ}\text{C}/\text{km}$ ($1.30^{\circ}\text{F}/100$ feet) was reported by Castano and Sparks (1974).

The Tenneco Middleton Island No. 1 well was drilled in 1969, approximately 450 miles northeast of the Shumagin Planning Area, in the western Gulf of Alaska (fig. 5, p. 13). This well is located on the continental shelf only 40 miles northwest of the axis of the modern Aleutian Trench. The geothermal gradient calculated by Fisher (1980) from uncorrected BHT data was $28^{\circ}\text{C}/\text{km}$ ($1.53^{\circ}\text{F}/100$ feet) using data from depths of 8,822 to 12,015 feet and assuming a 7°C (45°F) surface temperature. A corresponding gradient for corrected BHT data is $35^{\circ}\text{C}/\text{km}$ ($1.92^{\circ}\text{F}/100$ feet). These values appear anomalously high when compared to the Cook Inlet wells, which are farther from the Aleutian Trench, and therefore should have higher gradients. The corrected geothermal gradient predicts a BHT of 252°F (122°C), which is 35 percent higher than the measured temperature of 187°F (86°C). The corrected geothermal gradient appears to be unreasonably high.

Sherwood of the MMS (personal commun., 1987) reevaluated the temperature data from the Middleton Island No. 1 well and revised downward the geothermal gradient calculated by Fisher (1980). Maximum BHT data were available at depths of 8,816 feet, 10,426 feet, 11,510 feet, and 12,015 feet. A straight-line extrapolation from an assumed 40°F seafloor

temperature to a depth of 8,816 feet yielded a geothermal gradient of 1.39 °F/100 feet. Below 8,816 feet, Sherwood estimated a geothermal gradient of 0.84 °F/100 feet by a straight-line fit through the recorded uncorrected temperatures. The 0.84 °F/100 feet gradient differs substantially from the corrected and uncorrected values of Fisher (1980). If the 0.84 °F/100 feet is extrapolated to the seafloor, a temperature of 88 °F is predicted. Therefore, somewhere between the seafloor and 8,816 feet, an inflection of this gradient is needed in order to intersect the more reasonable seafloor temperature of 40 °F. The inflection is believed to occur within the upper few thousand feet, where the water content of the section may exceed 70 percent and thermal conductivities are correspondingly lower.

The KSSD No. 1 well, located within 100 miles of the modern Aleutian Trench axis (fig. 4, p. 11), was the only one of the six DST wells drilled on the adjacent Kodiak shelf that collected data useful for evaluating the geothermal gradient (Turner and others, 1987). The well was situated on the Kodiak forearc margin and tested a section analogous to that of the Shumagin margin. The evaluation of temperature data from the well consisted of Horner-plot extrapolations for temperature buildups at infinite time following the stoppage of circulation. This generated static temperatures at depths of 4,651 feet and at the bottom of the well at 8,525 feet. A straight-line fit through the highest static temperatures of the Horner plots yielded a geothermal gradient of 1.03 °F/100 feet. Straight-line extrapolation of this gradient yields a seafloor temperature of 52 °F.

An indirect measurement of the geothermal gradient can be extracted from depths at which gas hydrates have formed. A gas hydrate is a water-methane clathrate that may contain ethane, propane, and other hydrocarbons under suitable pressure (depth of burial) conditions at temperatures well above the freezing point of water (Kvenvolden and McMennamin, 1980). The gas hydrate occurs as chemical inclusions in interstitial pore spaces in sediments. Clathrates in arctic marine environments are commonly found in water depths greater than 1,000 feet, with subsurface depths to the bottom of the solidus-liquidus phase boundary being less than 4,000 feet (Kvenvolden and McMennamin, 1980). Seismically, the solidus-liquidus phase boundary of the clathrate is associated with a significant acoustic impedance contrast in unconsolidated sediment. The boundary, or the base of the solid clathrate, may appear on seismic-reflection

profiles as a bottom simulating reflection (BSR). Using the phase relation of the gas hydrate for the Shumagin continental slope, MacLeod (1982) calculated from the depth of the BSR a geothermal gradient of 30 °C/km (1.64 °F/100 feet). Kvenvolden and von Huene (1985), using a similar technique, calculated a geothermal gradient of 28 to 36 °C/km (1.53 to 1.97 °F/100 feet) for the adjacent Kodiak continental slope. Clathrates appear only in the upper few thousand feet of sediment, and extrapolation to deeper depths is not warranted (Sherwood, personal commun., 1987). Elevated thermal gradients, as indicated by this clathrate method, may be the result of reduced thermal conductivities stemming from the presence of a water-saturated sedimentary section.

The KSSD No. 1 well-data-derived geothermal gradient probably best represents the present-day geothermal gradient on the Shumagin continental shelf. These data are considered more representative of the lithified section than is the indirect temperature estimate extracted from a clathrate phase change on the continental slope. The KSSD No. 1 well gradient is considered more representative of the Shumagin shelf than are the Cook Inlet data because the KSSD well is closer to the modern axis of the Aleutian Trench. Disagreement exists over the interpretation of the Middleton Island No. 1 well temperature data, although Sherwood's reevaluated gradients of 1.39 and 0.84 °F/100 feet are closer to those of the KSSD No. 1 well than are those of Fisher (1980). In the following discussion of heat flow on the Shumagin continental shelf, the geothermal gradient is assumed to be 1.03 °F/100 feet.

If the onset of oil generation begins at about 212 °F, then by using a geothermal gradient of 1.03 °F/100 feet and assuming that the seafloor temperature is 40 °F, the approximate depth to the top of the "oil window" is estimated to be 16,700 feet. The KSSD No. 1 well, with a total depth of 8,517 feet, did not reach the top of the oil window, but did suggest a shallower depth of 11,500 feet to the oil window (Turner and others, 1987). Mature Paleogene rocks are exposed on nearby Kodiak Island, however, and have been exposed since the late Miocene, as evidenced by the onlap of upper Miocene and Pliocene strata offshore (Fisher, 1980). Maturation of these onshore Paleogene rocks, therefore, was accomplished prior to the late Miocene. Fisher (1980) proposed two geologic events that may have expedited the maturation of these Paleogene rocks, one being the emplacement of plutons in the forearc region, the other being the subduction of the Kula spreading ridge.

Paleocene and Eocene plutonic activity is represented by granodiorite outcrops on many of the shelf islands, including Kodiak Island. Heat from these plutonic intrusions may have subjected Paleogene sediments to temperatures high enough to have initiated catagenesis. Alternatively, a high paleogeothermal gradient might have been a consequence of the subduction of an active spreading ridge. The east-west-trending Kula-Pacific ridge was a spreading center that was partially subducted beneath the Shumagin margin, although the age of subduction is in dispute (either Paleocene or Eocene), as is the time the ridge ceased spreading. The thermal effects of consuming a spreading ridge that was abandoned before or just after the onset of subduction would be minimal. DeLong and others (1978) speculate that the spreading ridge continued to exist after subduction commenced. DeLong and others (1979) calculated that an active, subducted spreading ridge would cause a sudden temperature rise in the accretionary prism followed by a slow cooling. Based on the model of DeLong and others (1979), Fisher (1980) estimated that at a depth of 5 km (16,400 feet) within the margin, temperatures would rise 20 to 50 °C (68 to 106 °F) within 1 to 2 million years after the spreading ridge began to be subducted and that it would take another 10 to 20 million years for the

temperature to cool to the present-day level. A paleotemperature rise of 68 to 106 °F at a depth of 16,400 feet could have raised the ancient oil window to depths of 9,000 to 8,000 feet, respectively. Fisher (1980) believes that the model of DeLong and others (1979) may underestimate the amount of temperature rise because the model assumed a subduction angle of 45°, whereas Fisher believes that an angle of 6° to 8° is more realistic. In either case, the Paleogene section would probably have been subjected to significant temperatures for a long enough time to have initiated catagenesis of the kerogen present, a contention that is supported by the presence of thermally mature sedimentary rocks onshore.

Regional mapping of a Miocene unconformity and older horizons indicates that Paleogene and Cretaceous rocks are present in the Shumagin shelf. These rocks, under the conditions of the model proposed by DeLong and others (1978 and 1979), may have been subjected to a higher paleogeothermal gradient during the subduction of an active Kula spreading ridge. Therefore, the assumption that the present-day geothermal gradient is representative of the past may be misleading.

10. Source Rock

A source rock is defined as a sedimentary rock that has generated and released a quantity of hydrocarbon sufficient to form a commercial accumulation of oil and gas (Hunt, 1979). Shales and carbonate rocks are the two dominant types of source rocks. The conversion of organic material to hydrocarbons is generally very efficient in carbonate rocks because the organic material often consists predominately of amorphous algal material, whereas the organic material in shales and other clastic rocks often contains an admixture of woody, coaly, and recycled material that is not readily converted to hydrocarbons. Because of this, shale source rocks generally must contain a higher minimum percentage of organic material than carbonate source rocks. The minimum total organic carbon (TOC) level for shale is 0.5 percent, whereas for many carbonate rocks it can be as low as 0.3 percent (Hunt, 1979).

Forearc basins are generally unfavorable environments for the generation and accumulation of hydrocarbons. Although there may be numerous large structures and potential reservoirs, the absence of good source rocks and the presence of low geothermal gradients are major limiting factors. In those forearc basins that do contain significant amounts of favorable kerogen, low geothermal gradients often inhibit the development of hydrocarbons. The low geothermal gradients are thought to be related to the distance of the basin from the magmatic-arc heat source and proximity to the cold, subducting oceanic plate at the trench.

Typically, continentally derived gas-prone kerogen is deposited on an open marine shelf. Because of the presence of well-oxygenated waters at the shelf edge, much of the kerogen is quickly oxidized or metabolized by aerobic bacteria. This organic material may ultimately be transported down the continental slope into the trench or onto the abyssal plain.

Kodiak Stratigraphic Test Wells and Onshore Geology

The nearest source rock data applicable to the Shumagin Planning Area are from exposed Tertiary rocks on the Kodiak Islands and from the six Kodiak shelf stratigraphic test wells (fig. 5, p. 13). Geochemical

data from outcrops of the Sitkalidak Formation (Fisher and others, 1984) were used as possible analogs to Shumagin source rocks (table 1, p. 88). The Eocene section in the KSSD wells appears to be correlative with the Sitkalidak Formation on Kodiak Island and with sequence B in the Shumagin shelf basins (fig. 16, p. 41). The Sitkalidak Formation consists predominately of volcanic-rich, clastic sediments derived from source terranes to the north. These deep-water turbidites contained approximately 0.5 percent total organic carbon, which makes them poor source rocks. A sedimentary rock must contain at least 800 to 850 parts per million (ppm) of extractable hydrocarbons before it can be considered a good source rock (Tissot and Welte, 1984). The extractable hydrocarbon values of 400 and 412 ppm obtained from the Sitkalidak Formation are, therefore, below the minimum necessary for a good source rock (Bruns, von Huene, and others, 1987)(table 1).

The 9,357-foot-deep KSSD No. 3 well sampled the most prospective potential source rock thus far discovered in the area (Turner and others, 1987). The Eocene shales and siltstones unfortunately contained thermally immature herbaceous-woody kerogen and had TOC values of less than 0.5 percent. In the KSSD No. 3 well, methane was the predominant light hydrocarbon from the surface to the unconformity at 7,805 feet. Below the unconformity, the wetness ratio increased sharply and gasoline-range hydrocarbons were present. Chromatograms of Eocene samples show that the paraffins are skewed towards a high molecular weight range, which is representative of immature C₁₅ + hydrocarbons (Turner and others, 1987).

The only reliable temperature data from the Kodiak shelf is from the KSSD No. 1 well, which had a geothermal gradient of 1.03 °F/100 feet. On the basis of this gradient, the depth to the top of the oil window is estimated to be 16,700 feet. However, considering the dynamic tectonic setting, it seems unlikely that a uniform thermal gradient persisted through geologic time. A comparison of vitrinite reflectance data to the present geothermal gradient from the KSSD wells suggests that heat flow in the Kodiak basin may have been significantly higher than the present geothermal gradient indicates. Vitrinite reflection values extrapolated from the surface suggest that catagenesis of humic kerogen should occur at a depth of about

TABLE 1. Source rock analysis for Kodiak Island and the Shumagin continental slope.

Geochemical Results from Selected Oligocene and Eocene Outcrops from Kodiak Island¹

Formation	Sitkinak	Sitkinak	Sitkinak	Sitkalidak	Sitkalidak	Sitkalidak	Sitkalidak
Age	Oligocene	Oligocene	Oligocene	Oligocene and Eocene	Oligocene and Eocene	Oligocene and Eocene	Oligocene and Eocene
Total Organic Carbon (percent)	0.62	0.44	0.43	0.49	0.47	0.50	0.45
Vitrinite Reflectance	—	—	—	—	—	—	—
Total Extractable Hydrocarbons (mean) (ppm)	380	309	243	264	412	400	335

Geochemical Results of Selected Dredge Samples from the Shumagin Slope²

Sample No.	2-9	2-10	2-12	2-13	2-16	4-3
Age	Early to mid Miocene	Mid to late Miocene	Early to mid Miocene	Eocene	Early to mid Miocene	Pleistocene
Lithology	Mudstone	Dolomite	Clastic Dolomite	Mudstone	Mudstone	Nodular Limestone
Total Organic Carbon (percent)	0.45	0.33	0.24	0.66	0.80	0.30
Vitrinite Reflectance	—	—	—	0.50	0.38	—

¹Fisher and others, 1984.

²Bruns, von Huene, and others, 1987.

11,500 feet. The estimated depth to the top of the oil window of 16,700 feet is probably too great considering that the vitrinite reflection data suggest a much shallower depth of 11,500 feet (Turner and others, 1987). Thermally mature Eocene or older sediments may be present in deeper sections of the basin, although they probably do not contain sufficient amounts of organic material to be prospective source rocks.

Shumagin Planning Area

Shumagin Continental Slope

The only public geologic data from the Shumagin slope are dredge samples taken during a USGS cruise in 1979. Six dredge samples from two sites on the

Shumagin continental slope were analyzed for organic carbon (Bruns, von Huene, and others, 1987)(table 1). Three mudstones, two dolomites, and a limestone were analyzed by the pyrolysis technique. The average total organic carbon content for all samples was near the lower limit for source rock. The amount of "live carbon" in the samples was less than 30 percent, indicating gas-prone rather than oil-prone organic matter (Bruns, von Huene, and others, 1987). Selected sample material indicated gas-prone organic matter when the hydrocarbon index to carbon index was plotted on a Van Krevelen diagram (Bruns, von Huene, and others, 1987). Vitrinite reflectance values (table 1) indicate that the organic matter is thermally immature.

Shumagin Shelf Basins

Seismic sequence A represents economic basement in the Shumagin shelf basins, northeast of the Sanak Island Transverse High. Sequence A is made up of Late Cretaceous through Paleocene deep-water turbidites and associated Paleocene plutons (fig. 16, p. 41). Vitrinite reflectance values from correlative formations on Kodiak Island (the Kodiak and Ghost Rocks Formations) show that the kerogen is overmature (Fisher and others, 1984). The unpromising geochemical data obtained on the Shumagin continental slope do not completely preclude the presence of source beds in the thick sedimentary section underlying the shelf. Most of the dredge samples collected on the continental slope contained fossils of Miocene and younger age and were from the relatively shallow and probably thermally immature strata of sequence C. Thermally mature potential source beds in the Shumagin Planning Area are most likely in the Eocene strata of sequence B and, perhaps, in the more deeply buried section of sequence C.

A 6,000-foot-thick, areally extensive volume of sequence B is present in the Shumagin basin (fig. 18, p. 50). Sequence B may also be present beneath the other Shumagin shelf basins (plate 2) and in the Sanak Island Transverse High, although the thickness and areal extent are difficult to interpret southwest of the Shumagin basin because of Neogene structural complications. Sequence B is buried to depths ranging from 5,000 feet to over 30,000 feet beneath the East Sanak, West Sanak, and Unimak basins. Sequence B strata are economic basement beneath the Unimak basin.

Mechanisms associated with accretionary processes during the Cretaceous and early Paleogene and with the subsequent formation of the Late Paleogene and Neogene shelf basins may have acted to enhance heat flow and thermal maturation in the potential source beds. This includes the possible production and retention of residual amounts of thermogenic methane within the underthrust sequence (Kvenvolden and von Huene, 1985; Mascle and others, 1988) and the expulsion of these fluids into adjoining basins during subsequent uplift (plate 4).

The maturation of disseminated organic matter within potential source rocks is dependent on the total sediment thickness and the thermal regime. The discrepancy between vitrinite reflectance and geothermal gradient data in the Kodiak DST wells

indicates that the geothermal gradient has not been linear through geologic time. Locally, geothermal gradients may have been raised during accretion at subduction complexes of sequences A and B along the Shumagin margin. These deep-water accretionary units were buried to shallow depths in close proximity to the subducting oceanic plate, which suggests a rather low geothermal gradient.

However, according to Davis and Hussong (1984), the migration of warm overpressured fluids is a mechanism for heat transfer within sedimentary basins. These warm fluids could increase the maturation of potential source rock. Subduction complexes from around the world, such as the Barbados Ridge complex, are characterized by the generation and migration of warm fluids that may have influenced the thermal maturation of organic material during accretion. Leg 110 hole 671 of the Ocean Drilling Program penetrated the accretionary prism, decollement, and underthrust section of the Barbados subduction complex. Mascle and others (1988) provide evidence that the decollement is a permeability barrier between flow regimes in the underthrust section and the overlying accretionary prism. Underthrusting of strata at the deformation front (fig. 11, p. 23) presumably sets up a system whereby warm fluids travel updip from depth through permeable zones beneath a decollement. These fluids, which typically contain thermogenic methane, may reach near-surface sedimentary layers where they may facilitate the formation of gas hydrates. In contrast, methane-free fluid flow within the offscraped sequence occurs along vertical faults. Evidence from hole 671, drilled through an offscraped sequence, demonstrated that warm fluids act as a heat source as they migrate updip along steeply dipping faults from higher to lower lithostatic pressures and raise the temperature of adjacent sediments. This process may also contribute to the development of nonlinear temperature profiles.

In the Shumagin area, late Paleogene and Neogene extension related to strike-slip motion generated small, elongate, pull-apart basins such as the West Sanak and Shumagin basins. Subsidence probably outpaced sedimentation at the opening of these shelf basins, when the basal part of sequence C was deposited. Initially, these basins may have been anoxic. If so, significant amounts of organic matter may have been preserved.

After the initial infilling of the Shumagin margin basins, regional uplift and structural deformation had a significant effect on the thermal history and timing of

hydrocarbon generation in the Shumagin shelf basins. Methane preserved from earlier accretionary processes may have been released from the underplated sections of the Sanak Island Transverse High during its uplift and juxtaposition with younger, and possibly more permeable, strata of the West Sanak basin (plate 4). Such fluids could have locally raised the geothermal gradient and transported hydrocarbons in from deeper, more mature portions of the basin.

Summary

Most of the source rock data for the Shumagin basins have been extrapolated from the nearby Kodiak shelf stratigraphic test wells. Eocene rocks from these wells exhibited poor source rock potential; they contained low levels of TOC and immature kerogen. The minor amount of wet gas found in the Eocene section of the KSSD No. 3 well did not form in situ. Limited dredge samples from the Shumagin slope also indicate poor source rock potential. If the low TOC and immature kerogen in samples from the Shumagin and Kodiak Planning areas are representative, then neither area has much potential for hydrocarbon generation.

The hydrocarbon potential of the Shumagin Planning Area may have been enhanced by the retention of organic-rich sediments in underthrust sequences and the subsequent expulsion of hydrocarbon-rich fluids

and gas into adjacent basins (plate 4). Overpressured fluids released from beneath the Sanak Island Transverse High into the overlying formations of the Shumagin shelf basins may have raised the geothermal gradient, thereby increasing thermal maturity and possibly transmitting hydrocarbons from deeper and more mature strata.

The Barbados Ridge complex may be a thermal analog of the Sanak Island Transverse High. Evidence from this complex suggests that the low geothermal gradients associated with forearc basins do not necessarily preclude the presence of mature kerogen. A personal communication from Speed and Claypool (in Larue and others, 1985) indicates that oils from the Woodbourne Oil Field in Barbados were probably generated from type III kerogen with TOC concentrations generally greater than 1 percent, and vitrinite reflectance values of 0.5 to 0.6. Sequence B probably contains mostly type III kerogen with vitrinite reflectance values of 0.5. Estimated geothermal gradients in the Woodbourne Field are 0.82 °F/100 feet of depth. This agrees with geothermal gradients calculated from the Tenneco Middleton Island No. 1 well (0.84 °F/100 feet) and the KSSD No. 1 well (1.03 °F/100 feet). The Woodbourne Oil Field also demonstrates that significant concentrations of oil-prone organic matter can be found in an accretionary complex.

11. Reservoir Rocks

Sediments in the Shumagin Planning Area are dominantly derived from the erosion of rocks of the Peninsular, Chugach, and Prince William tectonostratigraphic terranes. The discussion of

potential reservoirs in the planning area is based on outcrop data from the Alaska Peninsula (figs. 5 and 14, p. 13 and 31) (Burk, 1965; Detterman and others, in press), dredge samples from the Shumagin slope (table 2) (Bruns, Vallier, and others, 1987), data from the Kodiak shelf stratigraphic test wells (Turner and

TABLE 2. Location and description of dredge samples along the Shumagin continental slope, Alaska, USGS cruise S7-79-WG. Location of dredge sites on figure 6. (Except where otherwise noted, this information taken from Bruns, von Huene, and others, 1987.)

DREDGE SITE NO.	LOCATION LAT. (°N) LONG. (°W)	SAMPLE NO.	LITHOLOGY	COMMON MINERALOGY	FOSSIL AGES
2	53°43.04' 53°41.66' Taken from the northern flank of the Unimak ridge approximately 50 miles southwest of Sanak Island. Water depth: 5,905 to 5,413 ft	2-1	Sandstone (Arkosic wacke)	Feldspar, quartz, and hornblende	—
		2-2	Sandstone (Arkosic wacke)	Feldspar, quartz, hornblende, volcanic rock fragments	—
		2-4	Sandstone	Volcanic glass, pumice, feldspar	—
		2-6	Mudstone	—	late early and early middle Miocene
		2-8	Siltstone	Feldspar, glauconite	late early and early middle Miocene
		2-10	Calcareous mudstone	—	middle and/or late Eocene ¹
3	53°40.38' 53°42.07' Taken from the southern flank of the Unimak ridge. Water depth: 5,249 to 4,593 ft	3-1	Basalt	Plagioclase, olivine, clinopyroxene	—
		3-2	Mudstone/siltstone	—	late Pliocene and Quaternary
		3-3	Basalt ²	Plagioclase, olivine, clinopyroxene	early Miocene ³ 19.8 ± 1.0 my.
4	54°10.50' 54°10.42' Taken from the west wall of a submarine canyon approximately 60 miles southwest of the outer Shumagin Islands. Water depth: 7,219 to 6,562 ft	4-1	Limestone	—	late Pliocene
		4-3	Limestone	—	early Pleistocene
		4-6	Carbonate sandstone	Limestone and sedimentary rock clasts with carbonate cement	late Pliocene
		4-4 and 4-11	Hornblende dacite porphyry	—	—
		4-8, 4-9, and 4-12	Basaltic andesite	Plagioclase, clinopyroxene, orthopyroxene	—

¹Possible erratic.

²Arc basalt (Bruns, Vallier, and others, 1987).

³Radiometric age date of plagioclase utilizing the potassium-argon method. Minimum age due to altered plagioclase (Bruns, Vallier, and others, 1987).

others, 1987), onshore exposures on the Kodiak Islands (Moore, 1969; Nilsen and Moore, 1979; Lyle and others, 1978), and interpretations of seismic sequences and erosional events (fig. 16, p. 41).

Paleogene and Neogene clastic rocks are not exposed on the shelf islands of the Shumagin Planning Area, although strata correlative with Paleogene and Neogene formations exposed on the southern part of Kodiak Island were encountered in the Kodiak shelf stratigraphic test wells. These rocks are also assumed to be present beneath the adjacent Shumagin shelf (fig. 16). Of the six wells drilled on the Kodiak shelf, only three sampled the Paleogene section and none penetrated the Cretaceous-Paleocene basement, which geophysical data suggest is present beneath the Kodiak and Shumagin shelf basins.

Most of the potential reservoir rocks in the Shumagin Planning Area are thought to be sandstones. The major factors that determine the potential of a sandstone as a hydrocarbon reservoir are its diagenetic history and mineralogical composition. Forearc basins develop on the flanks of volcanic-plutonic arc systems and typically contain poor reservoir rock. Erosion of such volcanic-plutonic arc systems proceeds by the unroofing of extrusive volcanics followed by exposure of the intrusive granitic core. When exposed to surface temperatures, minerals from basaltic rocks weather faster than those from quartz-rich granitic rocks. Sediments derived from volcanic terranes are especially rich in compositionally unstable suites of minerals that readily degrade into fragments, some of which are chemically altered to clays. With deep burial and increased consolidation, pressure solution occurs along grain boundaries and significantly reduces available pore spaces. Also typical of volcanic-rich sediments is the growth of authigenic minerals, principally zeolites and clays, that further reduce porosity and permeability.

In the Shumagin shelf basins, sequences A and B are probably made up mostly of volcanic detritus shed from the newly emergent volcanic arc system. These seismic sequences consist mostly of deep-water turbidites characterized by poorly sorted sediments. Because of this, these sequences have very poor reservoir potential. Seismic sequence C strata contain better sorted shelf sediments, probably much richer in granitic detritus and recycled older volcanic detritus from the Chugach and Prince William terranes. Sequence C probably

contains the most favorable reservoirs in the Shumagin Planning Area.

Seismic Sequence C

Shumagin Planning Area

Late Paleogene uplift along the Shumagin margin probably subaerially exposed sequences A and B. First-cycle, granitic-rich detritus from the Kodiak-Shumagin batholith and recycled turbiditic volcanoclastics were then shed into flanking basins from adjacent Neogene highs in the Shumagin Planning area and from the Alaska Peninsula (fig. 35). The Unimak basin received additional volcanic-rich sediments from the Eocene Aleutian volcanic arc. Over 20,000 feet of these sequence C marine shelf clastics are present in the Shumagin shelf basins. In 1979, the USGS collected rocks from three dredge sites along the Shumagin slope (table 2). At site 2, early and middle Miocene siltstones and mudstones containing volcanic debris were recovered from the Unimak ridge. These rocks are similar in age and composition to those of the Neogene section in the Kodiak shelf wells.

Alaska Peninsula (Oligocene and Miocene)

On the Alaska Peninsula, the Paleogene and older volcanoclastic section is separated from the dominantly quartzofeldspathic Neogene section by the Miocene unconformity (fig. 14, p. 31). The most prospective reservoirs occur in late Oligocene to Miocene age strata of the Unga and Bear Lake Formations. These formations were also encountered in exploratory wells. The late Oligocene to early Miocene Unga Formation (Detterman and others, in press) is composed of volcanoclastic sedimentary rocks and interbedded volcanic flows that outcrop on Unga Island and along the southern shore of the Alaska Peninsula (fig. 35). The predominately late Miocene Bear Lake Formation consists of quartz-rich nonmarine to marginal marine sediments exposed on the Bristol Bay side of the Alaska Peninsula (Detterman and others, in press). These sediments were derived in part from the older Mesozoic quartz-rich sedimentary rocks of the Alaska Range magmatic belt and the Kodiak-Shumagin batholith (fig. 5, p. 13).

Onshore Kodiak

Age-equivalent strata of sequence C, the Sitkinak and Narrow Cape Formations (fig. 16), crop out on the

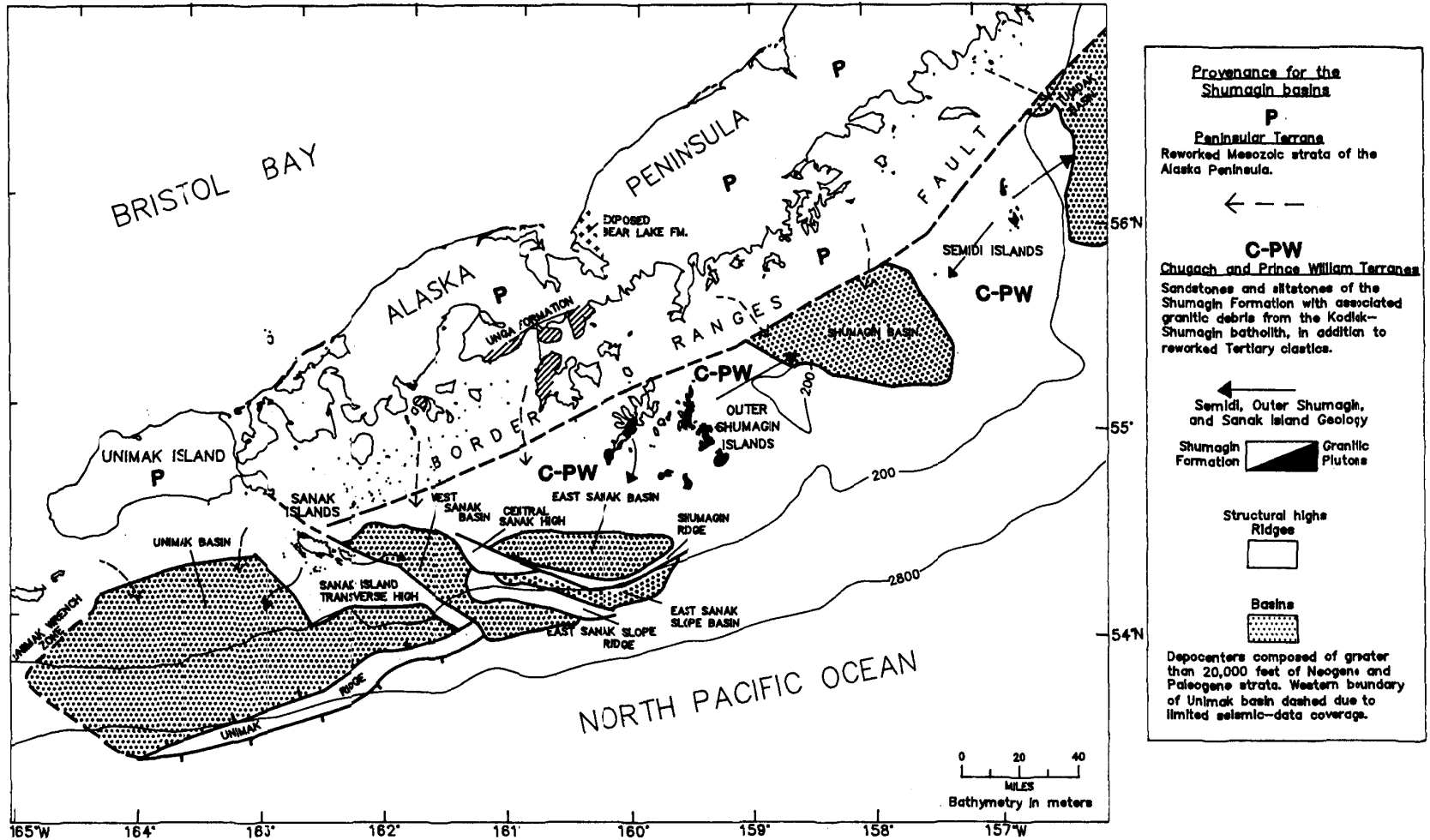


FIGURE 35. Provenance of potential reservoir rocks of the Tertiary Shumagin shelf and slope basins.

southern portion of the Kodiak Islands (fig. 5, p. 13). Clendenen (1987) provides mineralogical evidence that the unroofing of the Kodiak accretionary complex and the granitic plutons that intrude it is recorded in the deposition of the Oligocene Sitkinak Formation. Sediments of the overlying Narrow Cape Formation had a similar provenance, although richer in granitic detritus. Samples collected from the Narrow Cape Formation by Lyle and others (1978) had an average mineralogical composition of 65 percent quartz and chert, 18 percent feldspar, and 17 percent rock fragments. Nilsen and Moore (1979) estimated that the Narrow Cape Formation had a composition of 50 percent quartz, 26 percent feldspar, and 24 percent lithic fragments, although some samples contained as much as 30 percent matrix material, which significantly reduces permeability. First-cycle quartz- and feldspar-rich rock fragments, along with recycled volcanic-lithic fragments, were also shed from the newly exposed Kodiak accretionary complex and deposited in a nearby marginal marine environment. The high concentrations of quartz described by Lyle and others (1978) and Nilsen and Moore (1979) may be a result of reworking of the Narrow Cape sandstones by currents and wave action.

Kodiak Shelf Stratigraphic Test Wells

The Narrow Cape Formation on the Kodiak Islands is at least in part correlative with the Miocene section in the Kodiak wells (fig. 16, p. 41) (Turner and others, 1987). The best potential reservoirs encountered offshore are in a middle Miocene sandstone sequence in the KSSD No. 3 well. These rocks were interpreted as a progradational deep-water fan facies. Southeasterly dip-trends suggest that the direction of progradation was from the northwest, from Kodiak Island, with the Peninsular terrane and older formations of the Chugach and Prince William terranes as probable sediment sources. Logs and cores from the Miocene section of the well show relatively clean, well-cemented sandstones with an aggregate thickness of 462 feet in beds ranging from 20 to 127 feet thick; the net sandstone thickness is 388 feet. The effective porosity indicated by logs and sidewall cores ranges from 13.3 to 27.2 percent. Sidewall core data indicate that some individual beds may have permeabilities in the range of 20 to 55 millidarcies, although log-derived calculations suggest lower permeabilities for the basal middle Miocene sands. These lower permeabilities are a function of siliceous, cherty, and calcitic cementation. The sandstones range in composition from cherty, arkosic arenites to feldspathic graywackes. The

abundant quartz and feldspar indicates that these sands were derived from a granitic pluton, probably the Kodiak-Shumagin batholith on Kodiak Island. The mixture of poorly sorted and well-sorted sandstones and the subrounded nature of the sand grains indicate that the grains were recycled from a high-energy nearshore environment to a low-energy deep-water marine environment (Turner and others, 1987).

Dredge samples of Plio-Pleistocene sandstones in the Shumagin area are generally similar to those of the Miocene, although the younger sediments have been less affected by diagenesis and cementation, probably because of their shallower burial depth. These upper sequence C sandstones are presumably correlative with the Tugidak Formation on the Kodiak Islands and equivalent strata in the Kodiak wells. Log-derived effective porosities and permeabilities from Plio-Pleistocene sandstones in the Kodiak test wells indicate low to moderate reservoir potential, although some reservoir quality sandstones are present (Turner and others, 1987).

Seismic Sequence B

Seismic sequence B is probably correlative with the Eocene section beneath the Miocene unconformity on the Kodiak shelf and the Sitkalidak Formation on Kodiak Island (fig. 16). In the Shumagin basins, sequence B is probably made up of unstable, volcanic-rich sediments derived from the Peninsular terrane. Seismic-reflection data show that these rocks are highly faulted and folded and are buried to depths of over 20,000 feet. Low permeabilities (less than 5 millidarcies) for the equivalent Eocene sandstones in the KSSD wells were indicated on wire-line logs by a low spontaneous potential curve response (Turner and others, 1987). Petrographic examination of thin sections from conventional cores of the KSSD No. 3 well show that the low permeabilities and porosities are due to cementation and pressure solution at grain boundaries (Turner and others, 1987). Eocene sandstones on Kodiak Island are also characterized by low permeabilities. The available data suggest that the reservoir potential of sequence B is probably poor.

Seismic Sequence A

Sequence A consists of volcanic-rich sandstones, siltstones, and shales initially deposited in a deep-water fan contemporaneously with the Kodiak and Shumagin Formations (fig. 16). These rocks were later intruded

by Paleocene granodiorites which may have mobilized mineralizing solutions and reduced the permeability by cementation. Sequence A is not believed to be present southwest of the Sanak Island Transverse High. Rocks equivalent to sequence A are exposed on Kodiak, Shumagin, and Sanak Islands. The Shumagin Formation consists predominately of highly indurated sandstones that are texturally and compositionally immature (Moore, 1971) and would make poor reservoirs.

Summary

The most favorable reservoir rocks on the Alaska Peninsula and Kodiak shelf are late Paleogene and early Neogene sandstones derived from the regional uplift and erosion of quartz-rich sedimentary rocks and granitic batholiths. The best reservoir potential in the Shumagin Planning Area is likely to be found in the

age-equivalents of the Unga and Bear Lake Formations of the Alaska Peninsula, and equivalents of the Narrow Cape Formation of Kodiak Islands. Plio-Pleistocene sandstones equivalent to the Tugidak Formation of the Kodiak Islands also represent potential reservoirs. The sedimentary rocks of the Alaska Peninsula are thought to have better reservoir characteristics than those of the Kodiak and Shumagin Planning Areas because they contain cleaner and more stable constituents. Logs and cores from the Kodiak stratigraphic test wells indicate that sandstones above the Miocene unconformity (sequence C) have better reservoir potential than sandstones below the unconformity. The inner shelf deposits of sequence C probably contain the most quartz-rich sediments, although unstable feldspar and lithic fragments are probably major constituents. Fine-grained, volcanic-rich sequence B sandstones are characterized by lower permeabilities.

12. Play Concepts

The Shumagin margin has been a site of convergent plate interaction since at least the Cretaceous. The margin remains tectonically active, as evidenced by modern seismic events and the presence of faults that cut the seafloor. The structurally complex Shumagin shelf is the product of continuous plate convergence and associated oblique wrench motion. This structural complexity has given rise to a diversity of potential structural and stratigraphic traps. Newly available geophysical data allow the identification of trap configurations in the Neogene section and, locally, in the Paleogene section. Play concepts are addressed in decreasing order of prospectiveness and by reservoir stratigraphy. Play concepts for deep-water areas are discussed because portions of the slope, Aleutian Trench, and Aleutian Abyssal Plain are present within the Shumagin Planning Area.

Source Rocks

Sequence B probably contains the best potential source rock. Equivalent strata encountered in the Kodiak stratigraphic test wells, although organically lean, were deemed the most likely source rocks in the section (Turner and others, 1987). Sequence B along the Shumagin margin probably has the same generally poor source rock potential as the equivalent section of the Kodiak shelf.

Reservoir Rocks

Reservoir rock potential is highest in sequence C, above the Miocene unconformity. On the basis of Kodiak stratigraphic test well data and outcrops on Kodiak Island, the highest potential reservoir sandstones are of middle Miocene and Pliocene age, although they have relatively low permeabilities and would likely make only fair reservoir rocks. Thin turbiditic, volcanic-rich sandstone stringers in sequence B might also have some reservoir potential.

Migration

Hydrocarbons may have migrated along faults that cut permeable sequence B and C strata and that are in hydrodynamic contact with source rocks. Hydrocarbons

may also have migrated laterally along unconformities and by means of fracture permeability associated with fault zones, including decollements.

Seals

Several local unconformities of Pliocene age and shaly horizons within sequence C probably represent barriers to fluid migration. In addition, sequence B may contain shale seals for Paleogene and Neogene reservoirs in some prospects. Highly thrust-faulted areas, such as the Sanak Island Wrench Zone, may have seals consisting of impermeable Paleogene strata that have been thrust above Neogene reservoirs.

Shumagin Shelf Plays and Trap Configurations

Simple, Faulted Fold Traps in the Shumagin Basin

In the Shumagin basin, potential hydrocarbon traps occur in folded sequence B and C strata along a northwest-trending strike-slip fault system (fig. 36, p. 98). Figure 17 (p. 44) shows a large fold, or series of relatively uncomplicated folds, that parallels the western margin of the East Shumagin subbasin. The areal extent of closure on this flexure is unknown because of sparse seismic-reflection data coverage. The top of the flexure is less than 6,000 feet beneath the seafloor. Hydrocarbons could have migrated into the sequence C reservoirs by way of the master fault on the western flank of the structure (fig. 36, map view). The seals would likely be the Pliocene unconformity at the top of the structure and a possible shaly horizon within sequence C.

Fold Traps in the West Sanak and Unimak Basins

Northwest-trending folds that involve potential Pliocene reservoir sands are located at the northeastern margin of the West Sanak basin (fig. 37a). These folds resulted from northeast-directed thrusts that displaced sequence B/A and C strata. The fault planes dip toward the Boundary fault and the deeper part of the West Sanak basin. Permeable strata and nonsealing faults may have provided pathways for hydrocarbon migration.

In the Unimak basin, broad anticlinal folds developed in sequences B and C as a result of early Pliocene

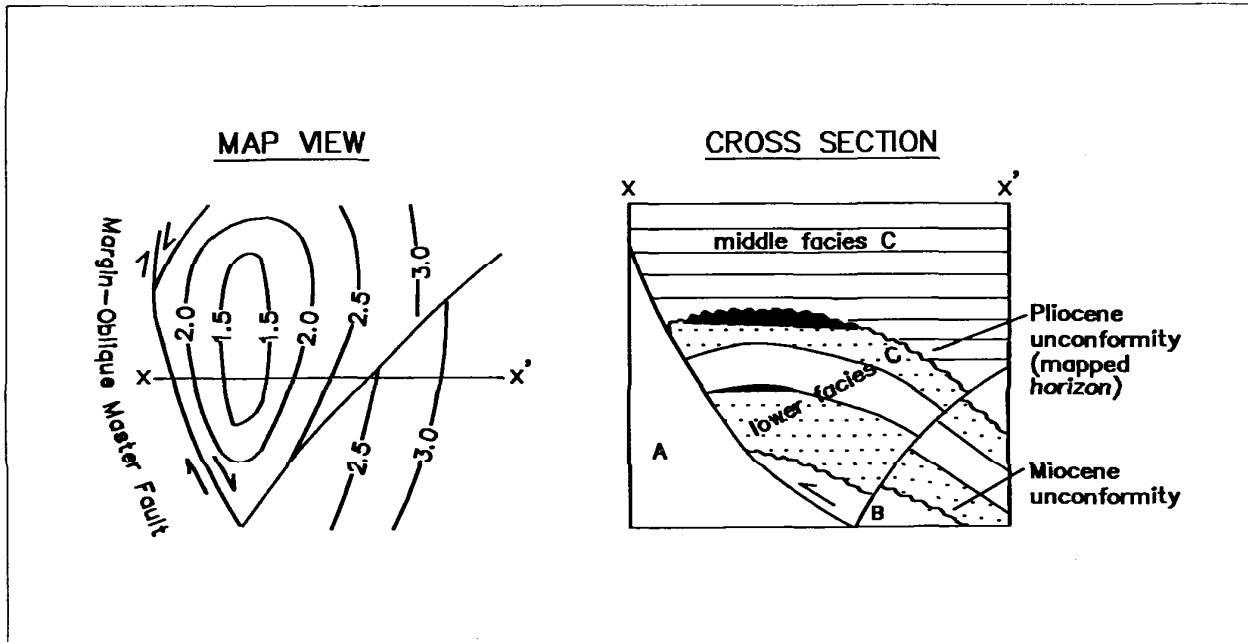


FIGURE 36. Traps associated with simple folds along a wrench fault system in the Shumagin basin. The structure contours are in time (seconds).

compression (fig. 37b). The fold axes parallel contemporaneous thrust fault trends. Both folding and thrusting were generated by strike-slip motion within the Sanak Island Wrench Zone. The intensity of deformation appears to decrease southwestward, and unfaulted anticlinal folds are present farther away from the wrench zone. The primary reservoirs are sequence C sands that are sealed by impermeable shale beds or unconformities. A secondary objective is a permeable sequence B section that is sealed by the Miocene unconformity and an impermeable sequence C section (fig. 37b). Hydrocarbon migration routes to both potential reservoirs are via permeable strata that are in hydrodynamic contact with sequence B source rocks.

Some of the anticlinal folds of sequence B are cut by thrust faults. The folding occurred after the deposition of sequence C reservoirs, but the thrust faults, termed blind thrusts, commonly do not offset overlying sequence C seals (fig. 37c). These anticlinal features appear as highs on a structure-contour map of the Miocene unconformity and can be seen on seismic profiles (plate 10). The fold axes usually parallel thrust-fault trends. Hydrocarbon migration to sequence C reservoirs may be via nonsealing faults and permeable strata that are in hydrodynamic contact with sequence B source rocks.

Extensional Fault Traps in the East Sanak, West Sanak, and Unimak Basins

Rollover anticlines associated with normal faulting are evident landward of the Shumagin ridge in the East Sanak basin (plate 6 and fig. 38a, p. 100). Movement landward of the Shumagin ridge since the late Paleogene probably generated detached fault blocks that contain sequence C and possibly some sequence B. Rollover anticlines formed on the downthrown side of these extensional faults are viable hydrocarbon traps. The tops of these structures are typically 13,000 feet (2.5 seconds) below the seafloor. Hydrocarbon migration was probably along a fault that is rooted in sequence A and cuts sequence B source rocks.

Normal-fault traps are present along the southwestern graben edge of the West Sanak basin (fig. 38b). Sequence C strata were downfaulted into the basin along the Boundary fault as the Sanak Island Transverse High was being uplifted during the Neogene. This uplift led to exposure and truncation of the sedimentary section by a Pliocene unconformity. Coarse-grained alluvial aprons related to this event may have accumulated along the fault-controlled basin edge. Hydrocarbons could migrate from where the Boundary fault cuts the deeper part of the West Sanak basin (plate 4).

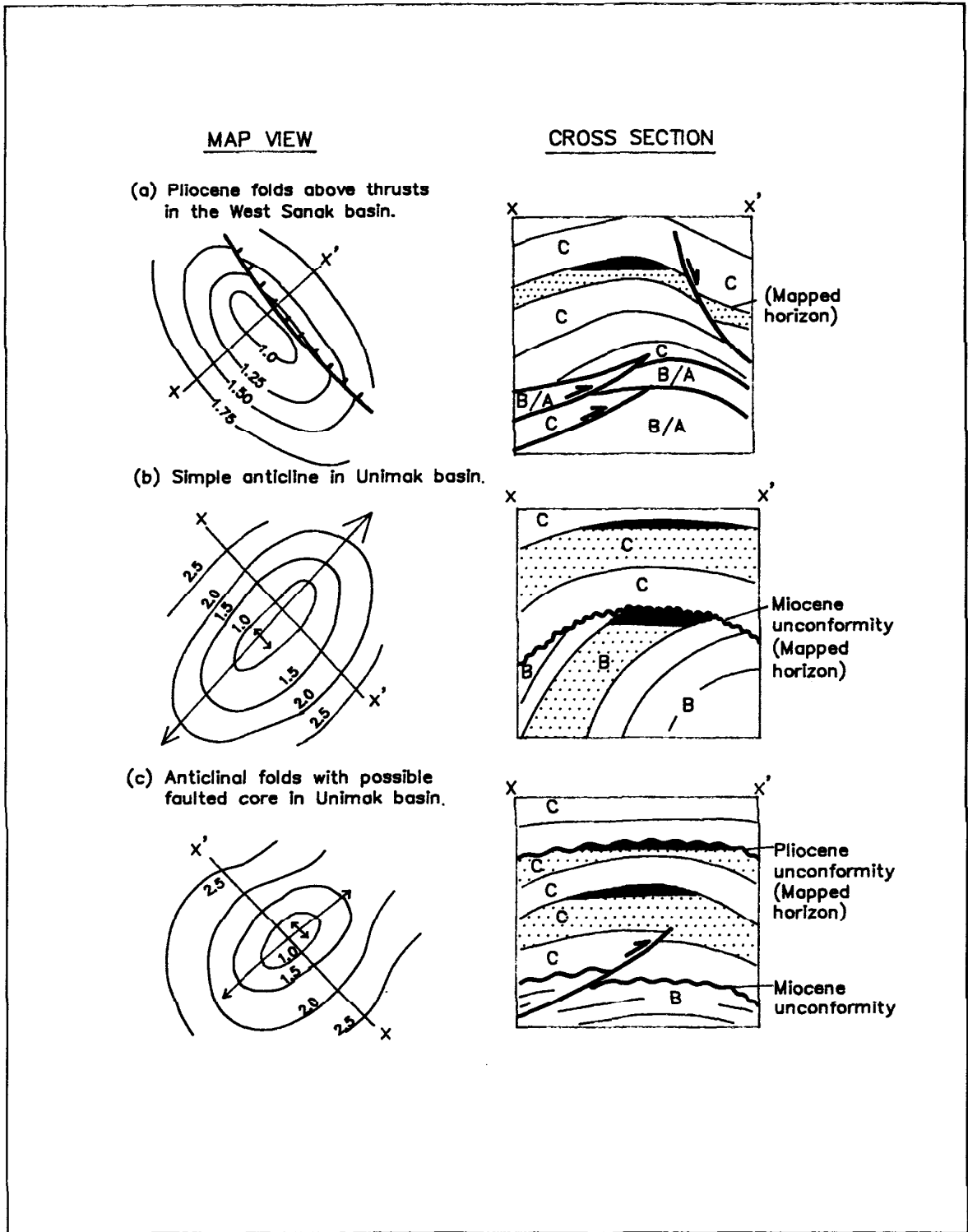


FIGURE 37. Traps associated with folds in West Sanak and Unimak basins. The structure contours are in time (seconds).

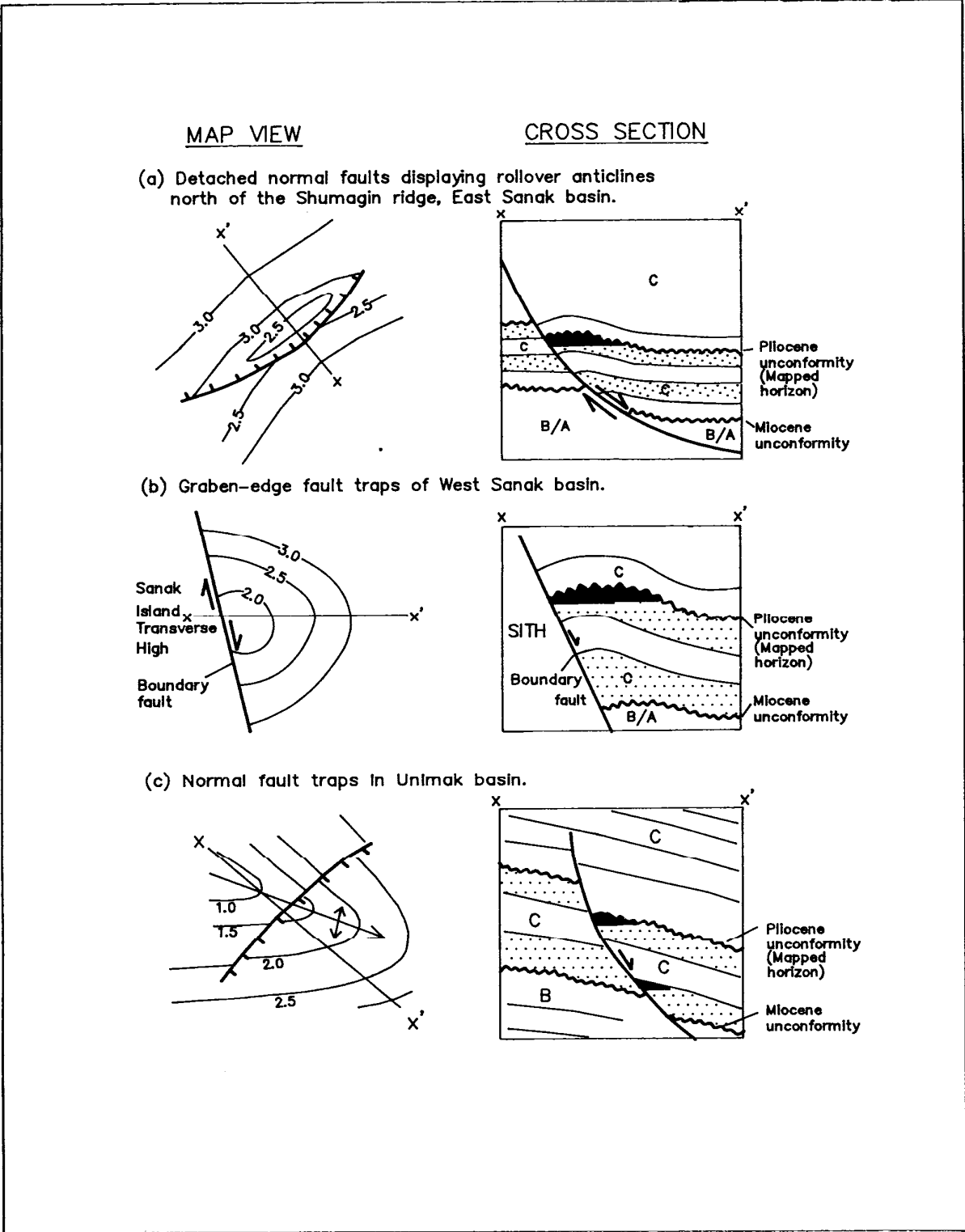


FIGURE 38. Traps associated with extensional faults in East Sanak, West Sanak, and Unimak basins. The structure contours are in time (seconds).

Additional potential fault traps consist of rotated, detached blocks that formed in response to seaward mass movement or gravity sliding along listric growth faults parallel to the shelf break. Continuous movement along such faults, however, may have decreased their effectiveness as traps in sequence C. In the Unimak basin, a second set of normal faults is oriented transverse to the shelf break (fig. 38c). These faults are kinematically related to regional strike-slip movement along the SIWZ. The highly faulted nature of this portion of the Shumagin shelf typically results in small fault trap closures.

Stacked and Imbricate Thrust Traps in the West Sanak and Unimak Basins

The stacked thrusts of the West Sanak basin (fig. 39a, p. 102) are localized east of the uplifted Sanak Island Transverse High (plate 1 and fig. 17, p. 44). Sequence B/A, a possible seal, has been thrust over sequence C, a possible reservoir. The thrust packages dip to the southwest and stack to the north. Seismic-reflection data indicate that they are deeper than 9,400 feet (2.0 seconds) below the seafloor. The thrusts began to form in the late Paleogene; deformation of strata above the thrusts suggests that some structures may be as young as Pleistocene. Migration of hydrocarbons could have occurred along fault planes that dip toward the deepest part of the basin along the axis of the Boundary fault. The stacking could enhance sealing attributes as well as result in multiple pay zones.

In Unimak basin, stacked thrusts along the western edge of the Sanak Island Transverse High generated fault and fold traps in sequence C (fig. 39b). These thrusts trend north and northeast and dip to the east and southeast. Possible seals are interbedded impermeable strata and thrust fault surfaces. Hydrocarbon migration may have occurred along faults or permeable beds that are in hydrodynamic contact with source rocks within sequence B. Thrusting may have resulted in vertical superposition of traps associated with each stacked sequence. Closure is typically less than 20 square miles.

Elsewhere in the Unimak basin, margin-oblique imbricate thrusts that originate in sequence B and cut the Miocene unconformity have formed a series of parallel, thrust-fault traps (fig. 39c). Sequence B reservoirs are sealed by the Miocene unconformity and thrust faults. Possible source rocks are shales in sequence B. These highly segmented traps appear to be

small in areal extent, although accurate assessments of closure are difficult because of sparse seismic coverage.

Stratigraphic-Onlap and Facies Traps

Stratigraphic-onlap traps may be present in sequence C where Neogene sands have been reworked against an unconformity and subsequently onlapped by a sealing shale bed (fig. 40a, p. 103). Facies migration is common in shelf settings sensitive to eustatic and tectonic mechanisms. Figure 40b depicts two such hypothetical facies-dependent stratigraphic traps resulting from updip terminations of sandy facies enclosed by shales.

Sanak Island Transverse High Play

The Sanak Island Transverse High exhibits an unique set of traps in the highly faulted Cretaceous and Paleocene subduction complex (plate 4). This complex was uplifted as a result of underplating. Available data do not permit us to specifically associate reservoirs with any of these fault traps. Closures are small because of segmentation related to faulting. These early formed structures in the SITH may have trapped hydrocarbons generated in sequence B during accretion at the trench. Another type of trap is present beneath the unconformity that truncates the folded strata of the Sanak Island Transverse High.

The Sanak Island Transverse High play may be analogous to the Barbados Ridge accretionary complex located seaward of the Lesser Antilles volcanic arc, the uplifted part of which forms the island of Barbados. Wells in the Woodbourne Oil Field produce oil from an early Eocene basal complex of clastic turbidites, hemipelagic sediments, and melanges (Larue and others, 1985). Source and reservoir rocks occur within the Scotland Formation. The pay zone consists predominately of 10-foot-thick sands in a 3,000- to 4,000-foot sand-shale sequence. In 1981, the Woodbourne Oil Field produced a daily average of 579 barrels of oil and 959,000 cubic feet of gas (Deal, 1982). In 1986, prior to a curtailment of drilling activities, additional wells had increased field production to 1,860 barrels of oil per day. Cumulative oil production was 2,510,000 barrels of oil.

Deep-Water Plays

Deep-water areas of the Shumagin Planning Area appear to contain few petroleum exploration objectives. The area is characterized by an absence of traditional

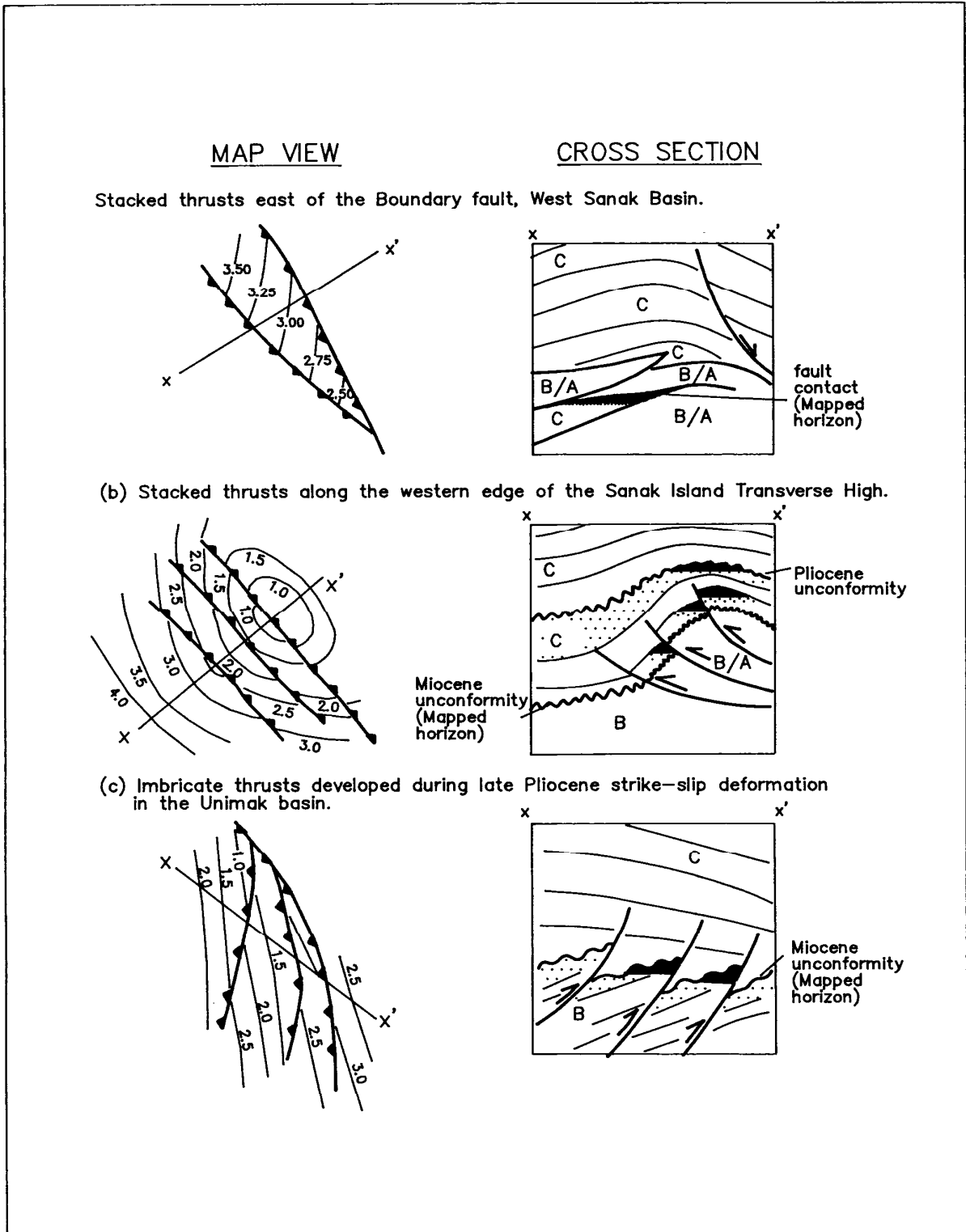


FIGURE 39. Traps associated with thrust faulting in West Sanak and Unimak basins. The structure contours are in time (seconds).

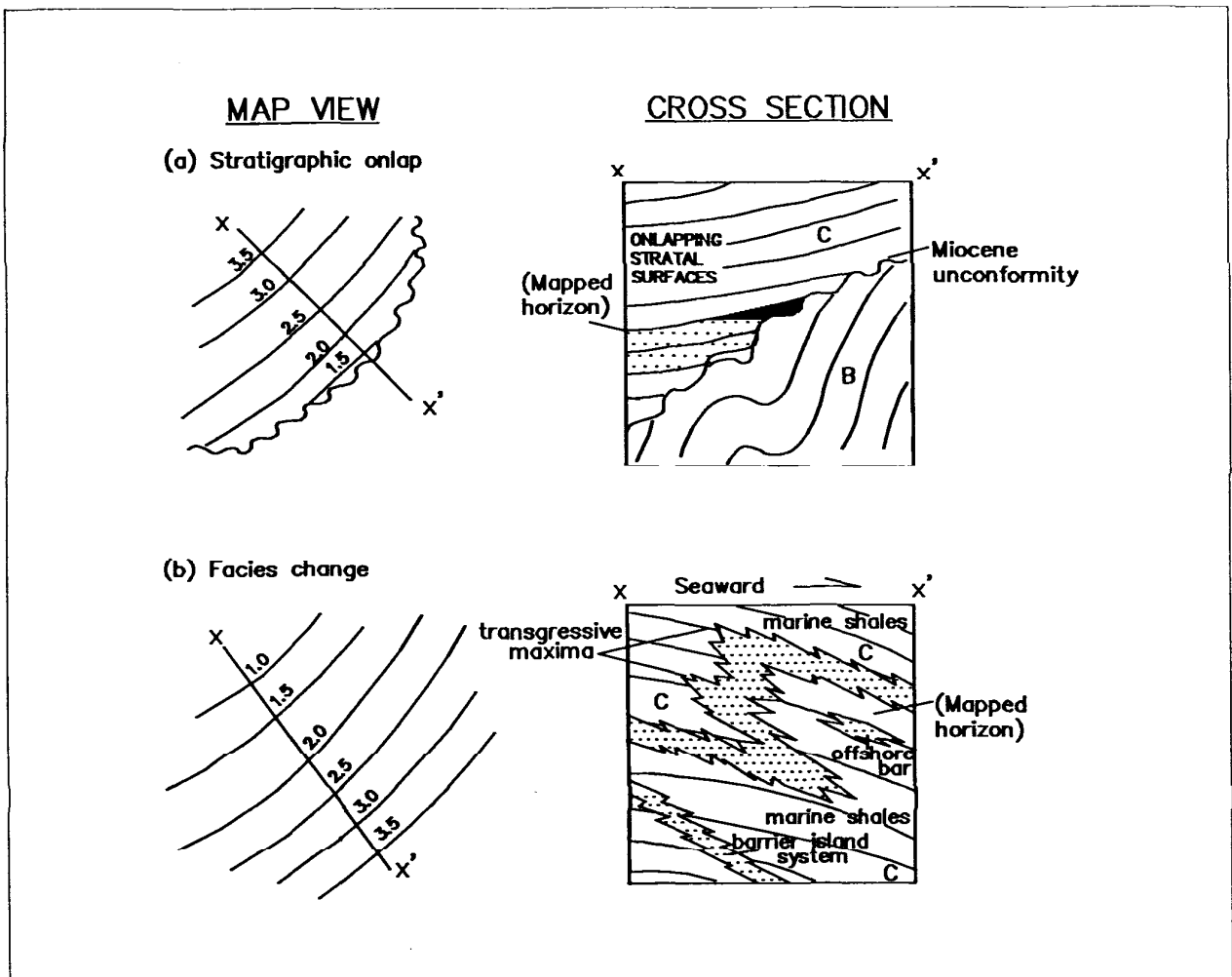
stratigraphic or structural traps. The Aleutian Abyssal Plain consists of a relatively thin, flat-lying veneer of unconsolidated pelagic and distal turbiditic deposits that overlie oceanic crust. DSDP Leg 18 holes encountered a Tertiary section with an average TOC content of 0.4 percent (Kvenvolden and von Huene, 1985), which is too low to be a good source rock. The Aleutian Trench contains thousands of feet of accreted sedimentary rock, but is an active zone where the sediment is continuously deformed. These conditions, and a low geothermal gradient, are not conducive to hydrocarbon generation or entrapment.

The slope is characterized by a thick accumulation of highly deformed sediments. Normal faults, thrust faults, oblique strike-slip faults, and folds are present. Unfortunately, active accretionary processes continuously remold and destroy early formed traps.

The organic carbon content of slope deposits can be quite high because the slope is often an area of high biogenic productivity related to nutrient-rich upwelling currents. However, in the absence of a closed anoxic basin or a stable oxygen-minimum zone that intersects the slope, the concentration of kerogen is low because of ongoing oxidation. The convertibility of the remaining mixture of kerogen (terrestrial, marine, recycled) is assumed to be low (Dow, 1981).

Kvenvolden and von Huene (1985) suggest that large volumes of gas may be present beneath the upper slope of the eastern Aleutian Trench. This gas is thought to have been generated from kerogen contained in accreted abyssal plain and trench sediments. Mascle and others (1988) reported from ODP Leg 110 that the thermogenic methane being produced seaward of the trench within the underthrust sequence is migrating

FIGURE 40. Traps associated with lithologic and stratigraphic changes within sequence C. The structure contours are in time (seconds).



many miles updip. This might also represent a source for the gas hydrates found in this portion of the subduction complex.

Summary

Accretionary processes that have been active along the Shumagin forearc margin since the Cretaceous have generated abundant small, structurally complex traps. Fault traps, which are the most common, include imbricate thrusts, individual thrusts, normal faults, and strike-slip faults. The small anticlinal features present are typically faulted, or "cored," by thrust faults. Only the Shumagin shelf basin appears to have retained broad simple folds. Both the simple folds and the

structurally complex features involve sequence C strata, which probably contain the best reservoirs in the Shumagin margin. Sequence B strata are also involved in these structural traps, but probably have minimal reservoir potential. Faults, unconformities, permeable strata, and decollements provide hydrocarbon migration pathways from potential source rocks. Sequence B is believed to have the highest source rock potential, although if it is not better than the Sitkalidak Formation, with which it is correlated, it probably does not contain sufficient organic carbon to generate mobile oil. Sequence A, a time-stratigraphic equivalent of the Late Cretaceous Shumagin Formation, is considered to be economic basement.

PART 3:
SHALLOW GEOLOGY,
GEOLOGIC HAZARDS,
and
ENVIRONMENTAL
CONDITIONS

13. Shallow Geology

Physiography and Bathymetry

The Shumagin Planning Area extends for approximately 350 miles along the southern continental margin of Alaska and encompasses parts of the continental shelf and slope, the Aleutian Trench, and the Aleutian Abyssal Plain (fig. 2, p. 3). The width of the continental shelf, as defined by the 200-meter isobath, ranges between 40 and 80 miles (fig. 41, p. 108). The shelf is composed of four relatively flat banks separated by troughs 330 to 720 feet (100 to 220 meters) deep (fig. 41). The submerged parts of the banks are generally flat with the exception of four 6- to 50-mile-wide seafloor depressions. The banks are presumed to be underlain by Cretaceous and Tertiary rocks similar to those exposed on Sanak, Shumagin, and the Semidi Islands, and the Lighthouse Rocks.

Glaciation played a significant role in shaping the geomorphology of the southern continental margin of Alaska, as is evidenced by abundant glacial till of both Quaternary and Tertiary age, the presence of modern glaciers, and the prevalence of glacial landforms. On the Shumagin shelf, the troughs that separate the four banks (fig. 41) resemble similar features that incise the continental shelf in the Kodiak Island region, 100 miles northeast of the Shumagin shelf (Turner and others, 1979), and in the northeastern Gulf of Alaska (Molnia and Sangrey, 1979; Thrasher and Turner, 1980). Thrasher (1979) proposed that the Kodiak troughs are glacial sea valleys on the basis of their morphologies and similarities in the seismic characteristics and depositional patterns of the sediments lining the troughs with those of glacial deposits elsewhere along the southern Alaska continental shelf. Carlson and others (1982) also proposed that the troughs in the northeastern Gulf of Alaska are glacial sea valleys on the basis of their U-shaped cross sections, concave longitudinal profiles, the till-like deposits that line the valley floors and walls, and seismic correlations that can be made between the sediment-fill and sediments of known glacial origin deposited elsewhere on the shelf. The Gulf of Alaska sea valleys lie adjacent to major Holocene glaciers still present onshore and correspond to the probable routes of glacier flow during Pleistocene time (Molnia, 1986). Thus, on the basis of their similar morphologies, it is quite likely that the

troughs that incise the Shumagin shelf are also of glacial origin.

Further evidence supporting a glacial origin for the Shumagin troughs comes from onshore geology. Evidence of extensive glaciation on the Alaska Peninsula was described by Muller (1953), Coulter and others (1965), and Detterman and others (1981). During late Wisconsin (late Pleistocene) time, alpine glaciers at the western end of the Alaska Peninsula coalesced to form large piedmont lobes (Detterman, 1986) that extended considerable distances over the now-submerged Aleutian platform (Thorson and Hamilton, 1986). Hamilton and Thorson (1983) proposed that at that time, ice caps, which were part of the Cordilleran ice sheet, probably covered all of the major islands in the Aleutians. In the Shumagin region, Funk (1973) and Weber (1985) mapped moraine and till deposits across the western end of the Alaska Peninsula and determined that glaciers of probable late Wisconsin age once filled Port Moller, Pavlof, Herendeen, Cold, and Morzhovoi Bays (figs. 41 and 42). Detterman (1986) speculated that the glacial lobes that incised those bays were fed by an ice cap centered near the Shumagin Islands. As evidence of that ice cap, he cited the presence of scattered erratics on the higher hills and glacial striations and chattermarks on the bedrock exposed on islands at the mouth of Pavlof Bay and in the Inner Shumagins. On the basis of the orientations of the bays along the Alaska Peninsula and the presumed directions of flow of the ice that filled them, it appears that the source of the glaciers must have been one or more ice fields situated on the shelf somewhere seaward of the mouths of Morzhovoi, Cold, and Pavlof Bays, and along the peninsula south of Herendeen Bay and Port Moller (fig. 42, p. 109). The inferred locations of these ice fields lie offshore and in alignment with the embayments in the peninsula to the north and the troughs discussed above that dissect the shelf to the south. These offshore troughs radiate southward from Unga and Popof Islands in the Inner Shumagin Islands and from the vicinities of Cold Bay and the Kupreanof Peninsula on the Alaska Peninsula. Although no morainal deposits that would confirm a glacial origin have yet been mapped or sampled in the troughs, it is likely that they were also formed by glacial lobes that flowed out of the same ice fields that carved the embayments in the peninsula to the north.

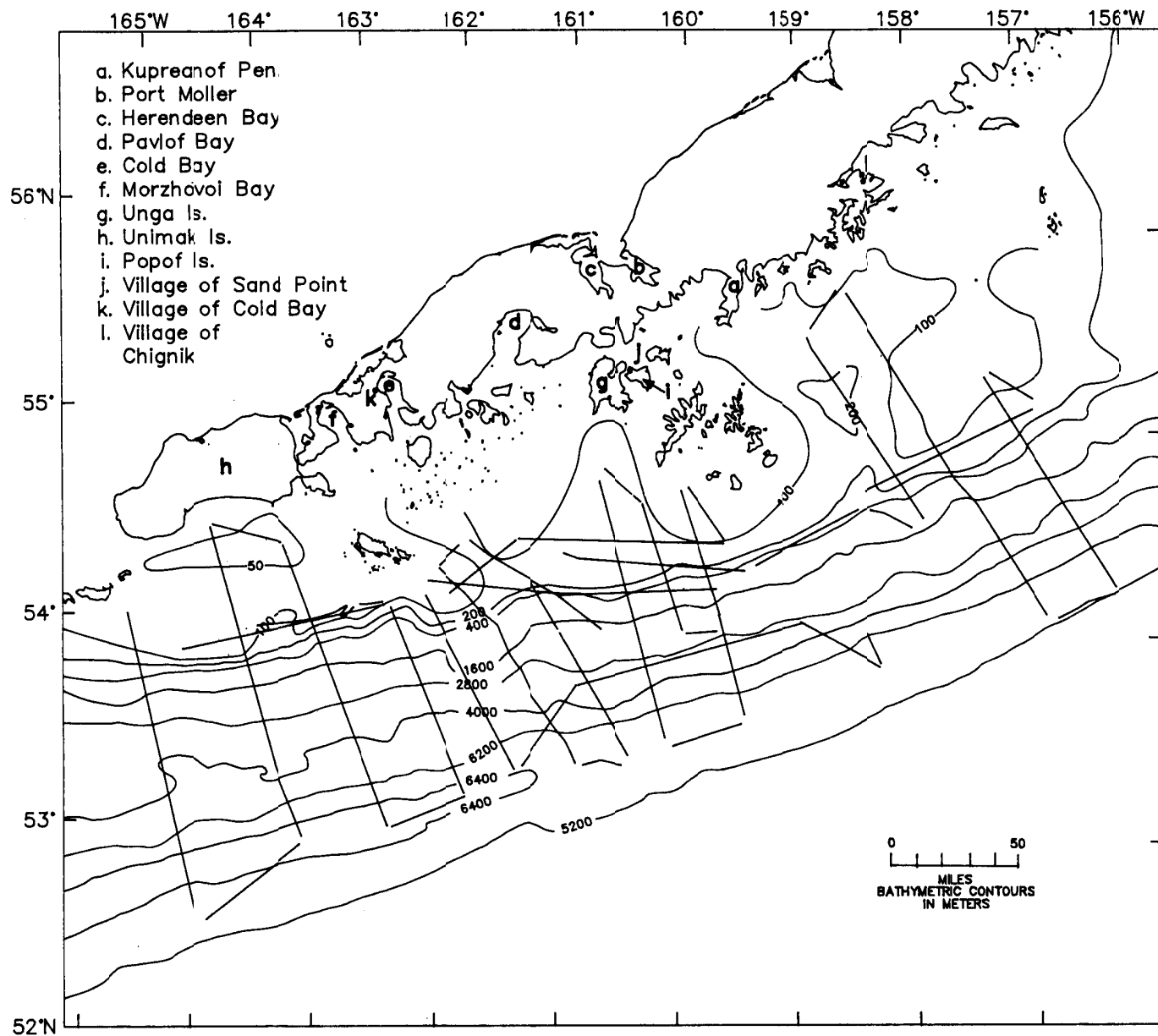


FIGURE 41. Index map of the Shumagin continental margin showing bathymetry, high-resolution seismic-data tracklines, and place names mentioned in this chapter. The bathymetry of the Shumagin continental shelf and slope was contoured from data collected using a hull-mounted 3.5-kHz precision depth recorder. Depth corrections were made using a velocity of sound in water of 1,500 meters per second.

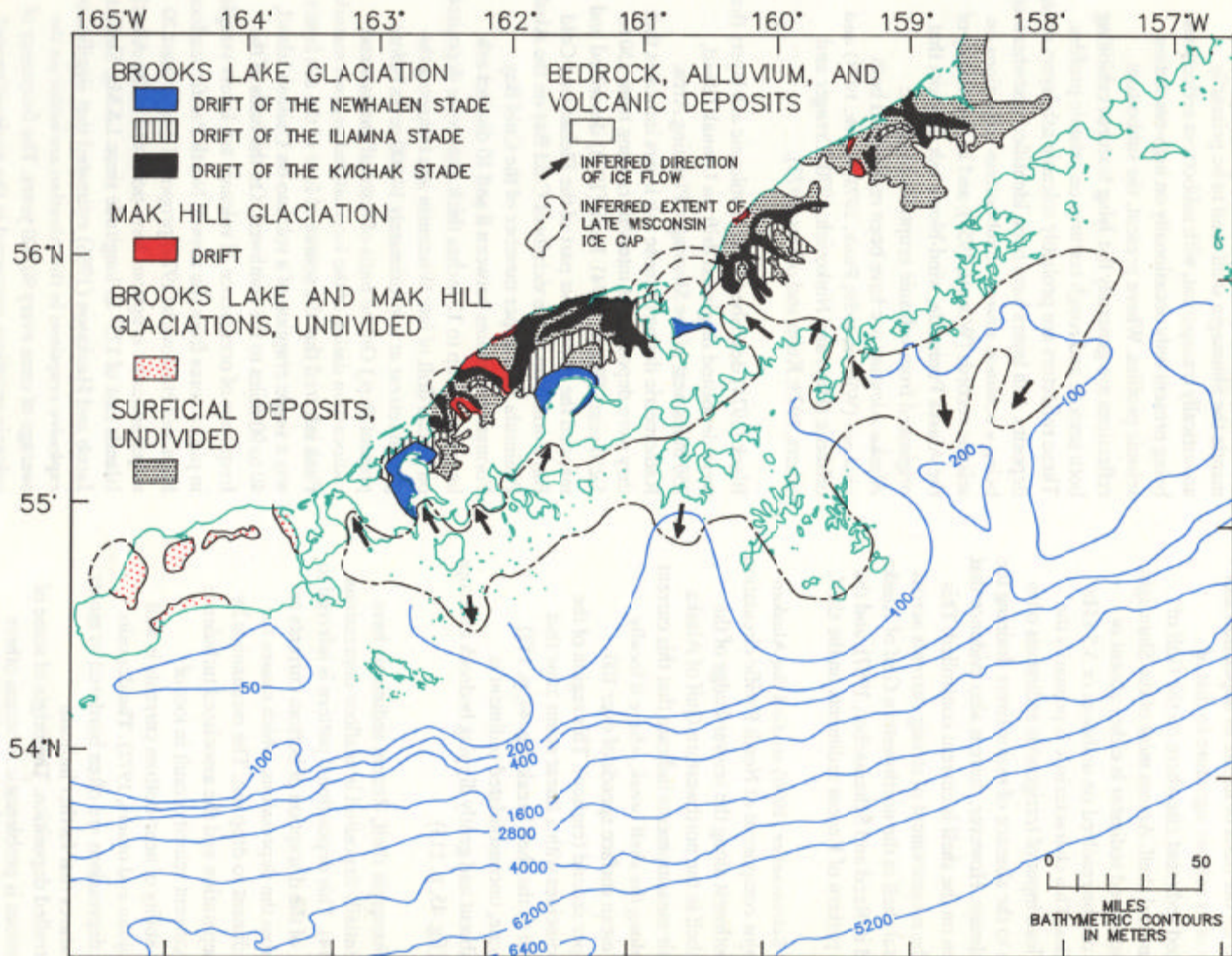


FIGURE 42. Quaternary geology of the Shumagin Planning Area showing the distribution of drift of the Brooks Lake and Mak Hill glaciations (from Karlstrom and others, 1964; Dettnerman and others, 1981; and Weber, 1985) and the inferred extent and direction of ice movement of the late Wisconsin ice cap.

Surficial Sediment and Bedrock Outcrops

In the absence of seafloor sediment samples and core data from the Shumagin shelf, unconsolidated sediment was identified on the basis of its site of deposition and the similarity of its seismic signature to that of unconsolidated sediment elsewhere on the Gulf of Alaska continental shelf. Across most of the Shumagin shelf, unconsolidated sediment is either absent or thinner than can be resolved on uniboom or 3.5-kHz seismic profiles. This characteristic is primarily the result of the lean input of terrigenous sediments onto the shelf due to the absence of major rivers draining the adjacent landmass. However, there is also evidence that sedimentation on the shelf is current controlled. This evidence is the measurement of strong currents across the continental shelf in the northwestern Gulf of Alaska (summarized in Reed and Schumacher, 1987), and the depositional pattern of Recent sediments on the shelf.

Muench and Schumacher (1980) studied the Alaskan Stream, a major component of North Pacific circulation that flows southwest along the seaward edge of the continental shelf in the northwestern Gulf of Alaska (fig. 43). Their measurements indicate that this current is strongest along the shelf break, where it locally attains daily mean surface speeds of over 100 centimeters per second (cm/sec). This region of the outer shelf coincides with a linear scour zone that trends parallel to the shelf break (fig. 44, p. 112). Within this zone, unconsolidated sediment is completely absent and gently dipping bedrock outcrops are present (fig. 45, p. 113).

Across the Shumagin shelf, Recent sediments have been preferentially deposited in seafloor depressions (fig. 46, p. 114). This depositional pattern is inferred to be the result of the disruption of bottom currents as they flow across the depressions, which causes the entrained sediment to drop out. The mechanism by which flow separation and the associated turbulence and drop in current velocity result in loss of entrainment ability of near-bottom currents is well known (Pettijohn and others, 1972). The deposits within these depressions are often bordered by moats (fig. 46b), features that further indicate current-controlled deposition. The origin of some of these depressions is problematic, whereas others coincide with major Cenozoic depocenters on the shelf (fig. 17, p. 44). One particular depression (fig. 46c)

appears to have formed as a seafloor sag created by motion on a near-surface fault (fig. 44).

With the exception of a prominent basal reflector related to the seafloor depressions discussed above (fig. 46), deposits of unconsolidated sediment that mantle the Shumagin shelf tend to be primarily acoustically transparent, with subbottom reflections being present only occasionally on high-resolution seismic profiles. Where present, the subbottom reflections are generally flat-lying features exhibiting both smooth and rough textures on seismic profiles. These reflectors are probably volcanic ash layers or lag deposits. Ash layers have been identified elsewhere as being a common source of subbottom reflections on seismic records (Worzel, 1959), and in the vicinity of the Alaska Peninsula, wind-blown ash deposits that originated from volcanic eruptions along the Alaska-Aleutian arc have been recognized both onshore (Wilcox, 1959; Funk, 1973; Black, 1974) and offshore (Hays and Ninkovich, 1970; Creager and others, 1973; Kulm and others, 1973).

Black (1974) described Recent volcanic ash layers that were deposited on glacial drift on Umnak Island, 250 miles west of the Shumagin Planning Area. Radiometric dating of those ash layers indicates that they were deposited at intervals ranging from 150 to 5,250 years (Black, 1974). Funk (1973) described and mapped the uppermost part of the Pleistocene Cold Bay Formation in the vicinity of Cold Bay on the Alaska Peninsula. The upper member of the Cold Bay Formation contains between 8 and 10 distinct ash layers, some up to 12 inches thick, that were deposited on glacial drift of late Wisconsin age following the glacial retreat at approximately 10,000 years before present (b.p.) On the basis of textural analysis and radiocarbon dating of the intercalated organic material, Funk inferred that the source of four of the ash layers was a single eruption of a volcano on Unimak Island, 40 to 90 miles to the southwest. On the basis of the frequency of occurrence of volcanic ash layers sampled in piston cores from the abyssal North Pacific seafloor, Hays and Ninkovich (1970) proposed that at least 20 major andesitic eruptions have occurred in the Aleutian Islands east of 175° E. longitude since 1.8 Ma. Similarly, Jacob and Hauksson (1986) estimated that significant explosive eruptions in the Aleutian arc occur on the average of once every 90,000 years. The frequency of volcanic eruptions preserved in the geologic record indicates that volcanic ash is abundant in the vicinity of the Aleutian arc and represents a likely source of at

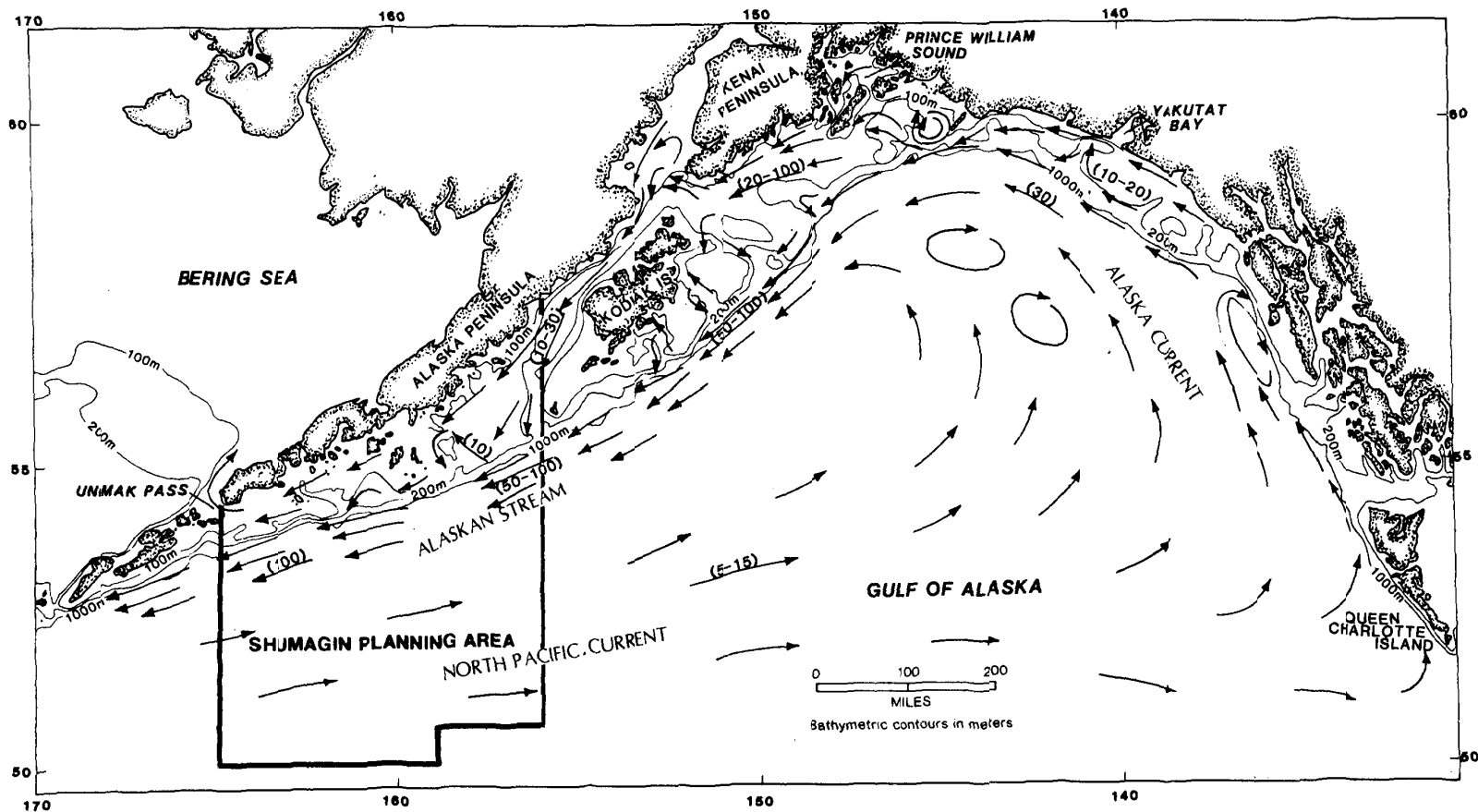


FIGURE 43. Schematic representation of the circulation in the Gulf of Alaska (after Muench and Schumacher, 1980, and Reed and Schumacher, 1987). Arrows indicate the direction of mean surface flow. The numbers in parentheses refer to the approximate range of current speeds in centimeters per second.

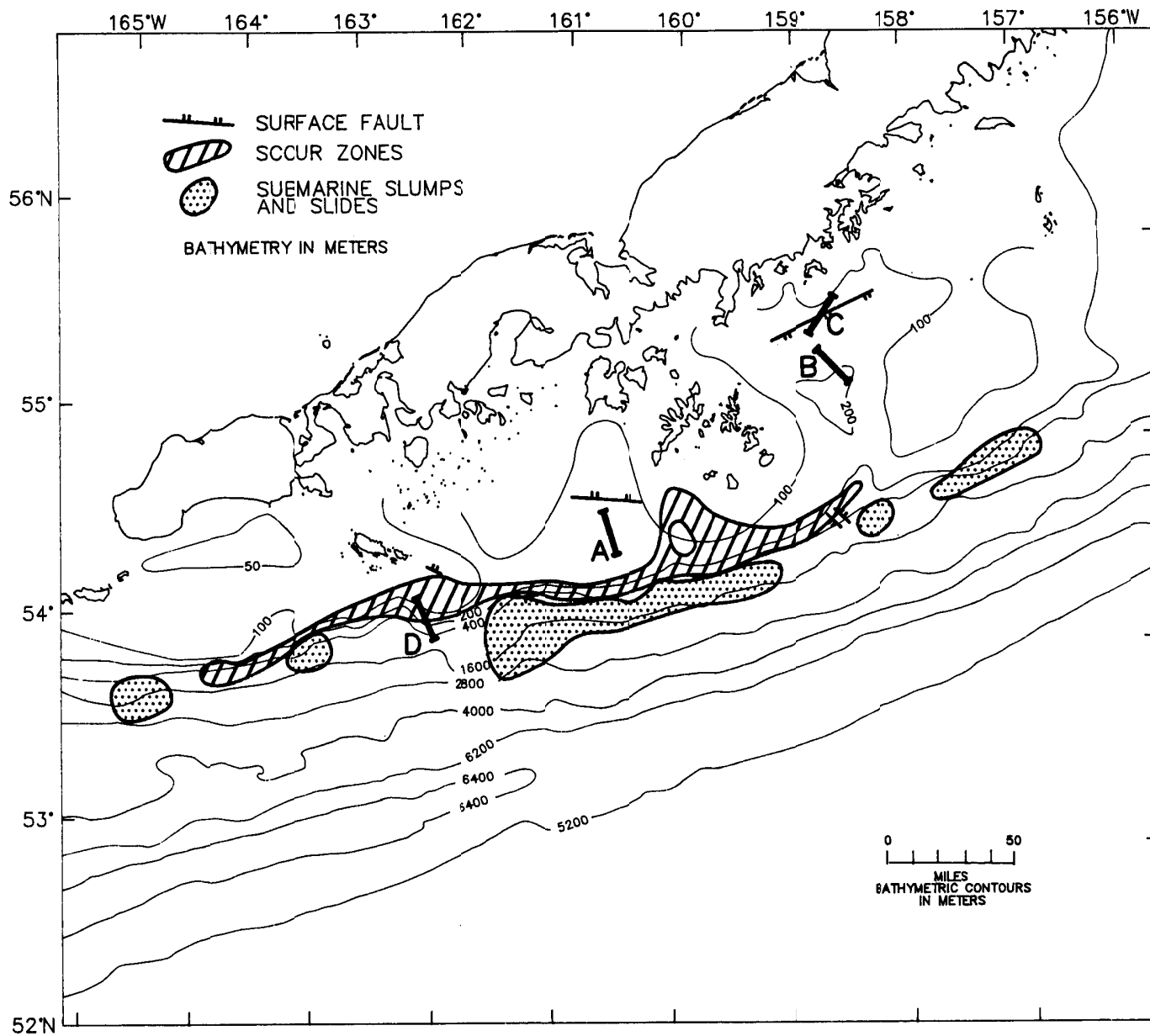


FIGURE 44. Map showing shallow faults, scour zones, and submarine slumps and slides. Tracklines are shown in figure 41. The heavy trackline segments correspond to the seismic profile and line drawings shown in figures 45 and 46.

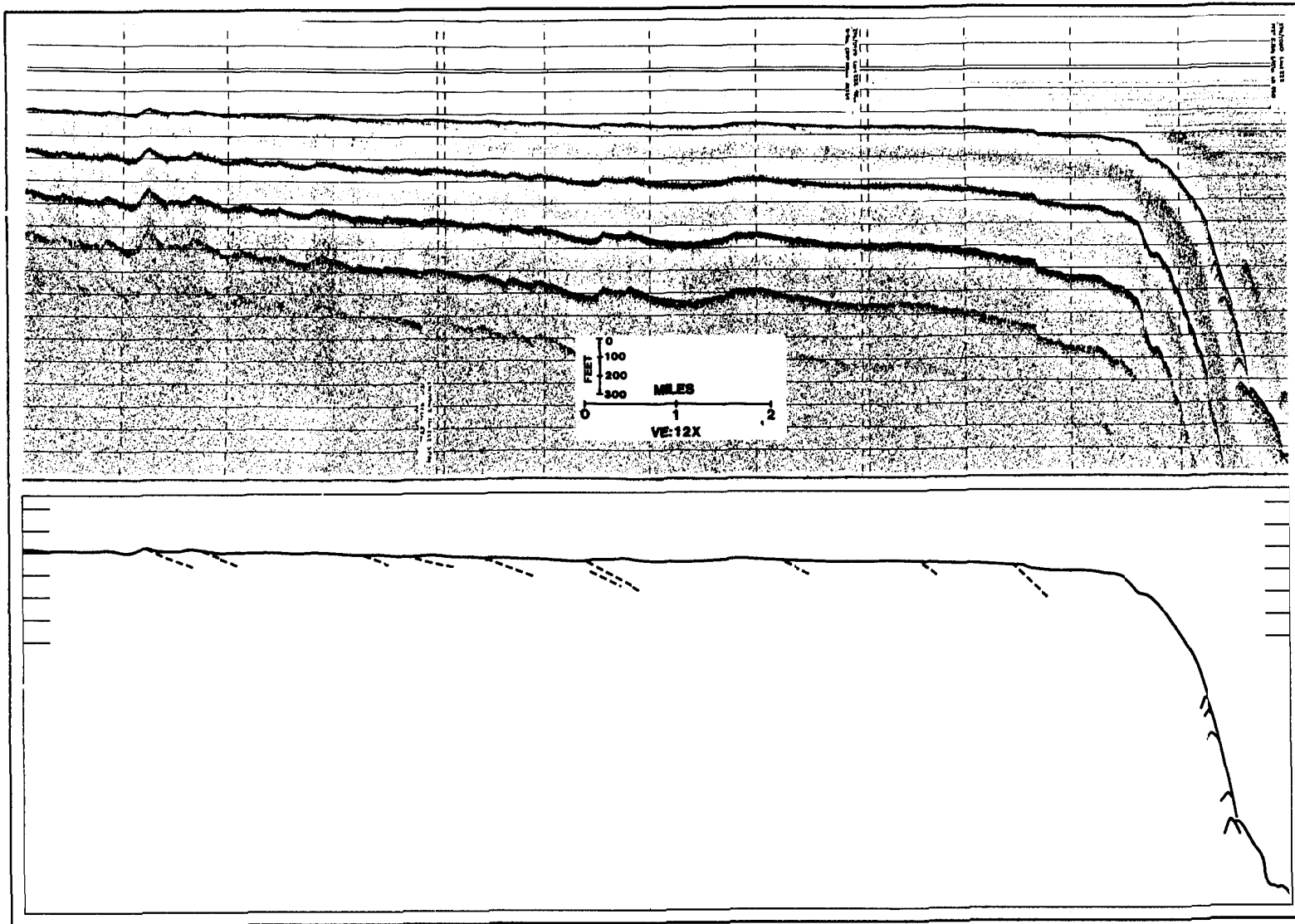


FIGURE 45. 3.5-kHz seismic profile and line interpretation across the shelf break showing bedrock outcrops (trackline segment D, figure 44).

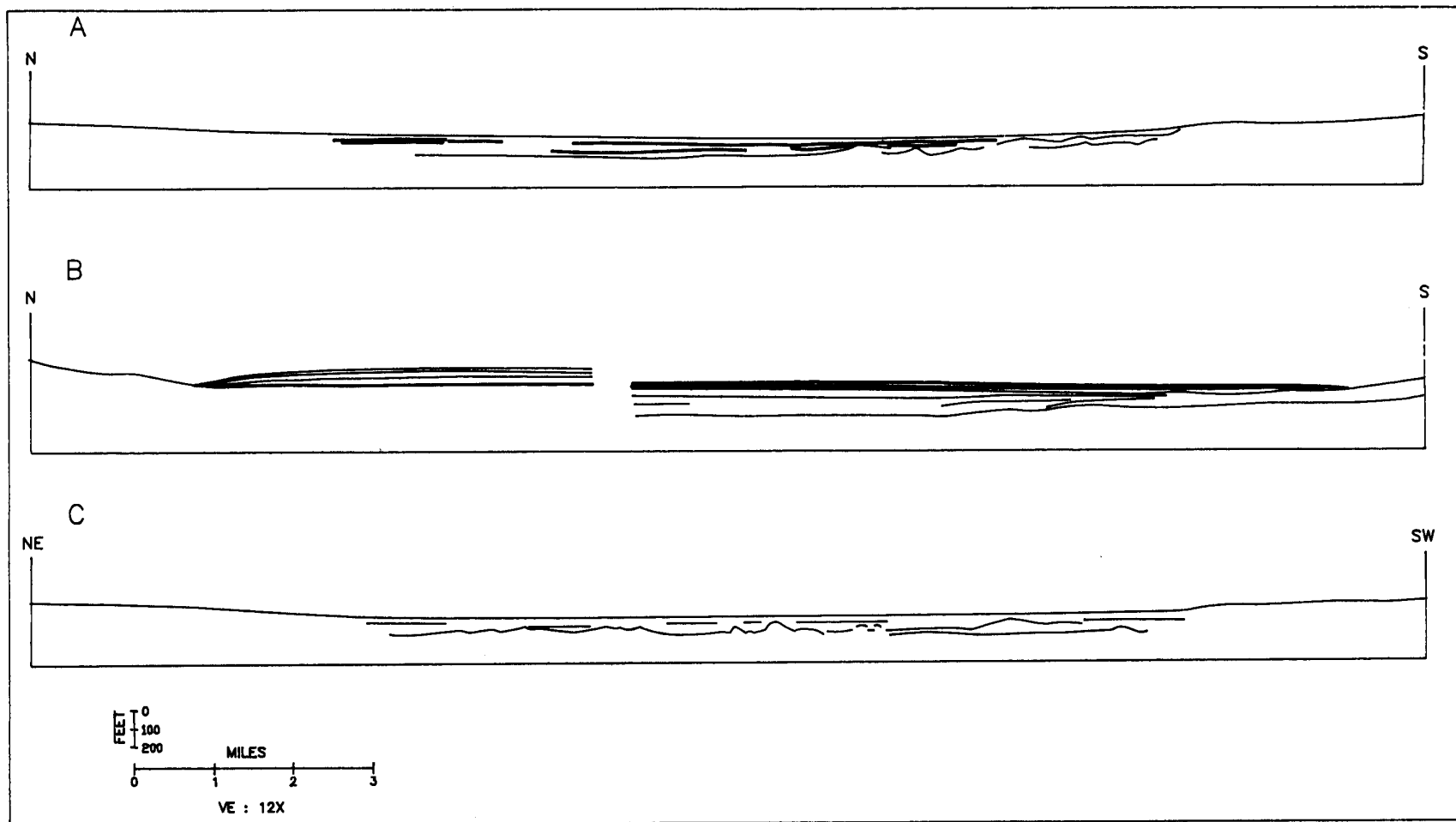


FIGURE 46. Line drawings of 3.5-kHz seismic profiles across seafloor depressions showing the typical seismic character of seafloor-sediment deposits. The locations of the profiles are shown in figure 44. Note the moat at the left end of profile B.

least some of the subbottom reflections recorded on seismic profiles across the Shumagin shelf.

Lag deposits created by the winnowing action of currents flowing across the shelf may also be responsible for some of the subbottom reflections apparent on high-resolution seismic data. Muench and Schumacher (1980) identified a complex circulation pattern on the continental shelf around Kodiak Island (fig. 43) that is driven both directly and indirectly by the southwestward-flowing Alaskan Stream. The Alaskan Stream, discussed above, flows along the edge of the continental shelf, and in the vicinity of Kodiak Island, attains mean surface speeds of 50 to 100 cm/sec (fig. 43). Since the Shumagin Planning Area is situated adjacent to and immediately downstream from the Kodiak shelf region, it is likely that similar currents also rake the Shumagin shelf. Thus, lag deposits resulting from such currents represent an alternate source for some of the subbottom reflections discussed above.

One particularly prominent subbottom reflection is present on most of the high-resolution seismic profiles that traverse the seafloor depressions. This reflection is usually the deepest one apparent on 3.5-kHz subbottom

profiler records. In some depressions, this reflector is smooth and generally horizontal except near the edges of the depression, where it rises and merges with the surrounding seafloor; in other depressions, this reflector is rough and hummocky (fig. 46a). The smooth versus rough characteristic of this reflector may be the result of the contrasting nature of the seafloor prior to the deposition of the overlying sediments. Where the reflector is smooth, it probably represents either a volcanic ash layer or a lag deposit; where it is rough it probably represents a poorly sorted glacial deposit.

Near the shelf break along much of the Shumagin shelf, unconsolidated sediment is absent and gently dipping bedrock outcrops are present (fig. 45). These features appear on seismic records as asymmetrical ridges with up to 60 feet of relief. Bedding planes extending from the outcrop can often be recognized in the subsurface as dipping reflections (fig. 45). Such outcrops are probably present across much of the shelf but are generally indistinguishable from thin sediment veneers because of the limits of resolution of the seismic systems and because the bedding is either horizontal or only slightly dipping.

14. Potential Geologic Hazards

Because of its proximity to the Alaska-Aleutian arc trench system, the Shumagin Planning Area is susceptible to hazards associated with earthquakes, ground failure, and volcanic phenomena. These hazards are a consequence of the subduction of the Pacific lithospheric plate beneath southern Alaska. If a large earthquake occurs along the plate boundary in the Shumagin Planning Area, rapidly oscillating ground motion and substantial regional uplift or subsidence are likely to occur, any of which could have a major impact on permanent facilities located along the Alaska Peninsula and in the offshore parts of the planning area. An additional potential hazard is posed by sediment erosion and deposition caused by currents sweeping the shelf. Such modifications of seafloor morphology could be hazardous to bottom-founded structures because of the possibility of structural undermining.

Seismicity

If a large earthquake occurs along the plate boundary in the Shumagin Planning Area, damage to facilities could be caused either directly by ground shaking, fault displacement, and surface tilt, or indirectly by ground failure, sediment consolidation, sediment liquefaction, or tsunami inundation.

Ground Shaking

The severity of the destruction caused by ground shaking is a function of the amount of displacement, the direction of motion, the duration of ground motion, the frequency content of the seismic waves, the thickness of the underlying unconsolidated sediments, and the geometry of the sedimentary basin. In general, a structure built on unfractured bedrock or on well-consolidated sediment will experience less damage than one that is built on an unconsolidated, fine-grained, water- or gas-saturated deposit. Large or tall structures are particularly vulnerable to ground shaking because their proportions tend to give them low natural frequencies (± 1 Hertz). Such natural frequencies are close to the frequencies typical of surface waves and would tend to cause the structure to resonate if it experienced more than one cycle of motion. Resonance is a particularly destructive phenomenon because it

exposes the structure to more stress and strain than it would normally experience during a single cycle of displacement, and also because the failure mode of a structure occurs after cyclic loading has reduced the strength of a supporting member to the fatigue limit. Tucker and others (1981) pointed out that a structure's susceptibility to damage from ground motion could be mitigated with proper location and orientation. An example given by those investigators is that damage to a long structure, such as a pipeline or bridge, situated in a sediment-filled valley with a high impedance contrast between the sediment and the surrounding bedrock could be reduced by supporting the structure at places of equal sediment thickness.

The damage caused by ground shaking tends to be worse in areas underlain by thick, unconsolidated sediment deposits, particularly where the deposits are water-saturated. Tucker and others (1981) determined experimentally that the earthquake response of sediment-filled valleys was strongly dependent on the frequency content of the seismic wave, the valley dimensions, and the contrast in acoustic impedance between the valley-filling sediments and the underlying bedrock. Those investigators observed that in valleys with small dimensions and high impedance contrasts, the motion measured by an instrument situated on the sediment pile was characteristically ten times greater than the motion measured on the adjacent bedrock for frequencies between 15 and 25 Hz. They also observed that in addition to shock-wave amplification by the sediments (ten-fold), there was a significant amplification produced by topographical effects (five-fold). Because of the limited high-resolution seismic data base, it is not possible to thoroughly map the distribution and thickness of unconsolidated sediments on the Shumagin shelf for the purpose of making recommendations regarding the siting of bottom-founded structures.

Fault Displacement

Fault displacement poses a hazard to permanent structures, particularly large or linear ones such as terminal facilities and pipelines. Davenport and others (1981) pointed out that gas pipelines are particularly vulnerable to damage from even moderate-sized earthquakes because, by nature, they are already highly stressed by internal pressure and temperature and have very little additional resilience available to

accommodate displacement. Faults that have been inactive for long periods, as well as those faults that have experienced recent movement, may be activated during an earthquake. Figure 44 shows near-surface faults mapped on the Shumagin shelf using high-resolution seismic data. This compilation includes faults that are buried and show no recent motion as well as those that displace the seafloor. The areal coverage of the high-resolution seismic data on which this interpretation was based (fig. 41, p. 108) is sparse, however, and more faults are likely to be present.

Tectonic Uplift or Subsidence

Vertical displacement due to tectonic uplift or subsidence associated with an earthquake can be substantial. Regional deformation from the March 27, 1964, Prince William Sound earthquake (magnitude M_w 9.2, Kanamori, 1977) extended for 500 miles along the Aleutian arc-trench system and produced as much as 30 feet of uplift on Montague Island, while parts of the Kenai and Chugach Mountains subsided by as much as 6 feet (Plafker, 1965). Tectonic uplift or subsidence of this magnitude is capable of submerging dock facilities or elevating them beyond the reach of high tide, as occurred in Cordova, Alaska, during the 1964 earthquake.

Ground Failure

The types of ground failure associated with earthquakes include rockfall, slumps, landslides, submarine slides, sediment liquefaction, and sediment consolidation. Localized submarine slides that occurred during and after the March 27, 1964, earthquake severely damaged the harbor facilities in the communities of Homer, Valdez, Seward, and Whittier. Seismic profile data collected across the upper continental slope in the Shumagin Planning Area reveal that submarine slides and slumps have also occurred in that area below a depth of 100 meters (fig. 44, p. 112). Much of the continental slope below those features is covered with slide scars and debris that was released from above. Head scarps associated with those slides and slumps range in height from 40 to 120 feet. Landward of the head scarp of one particular slide, the surface that forms the upper continental slope (and down which the slide material translated) merges with a seismic horizon, possibly representing primary bedding, which is traceable for a short distance under the shelf. This relationship suggests that locally the shear strength across some horizons underlying the Shumagin shelf may be weak. Lewis (1971) described slumps that occurred on the continental slope of North

Island, New Zealand, that took place on surfaces that were dipping as little as 1° . Embley and Jacobi (1977) described large submarine slumps and slides from several different continental margins bordering the North and South Atlantic that also occurred on slopes of 1° or less. If the shear strength across some horizons underlying the Shumagin shelf is weak, then much of the region along the shelf-slope break could be considered a potential site for a future submarine slump or slide.

Tsunamis

Tsunamis are generated when large volumes of sea water are displaced by tectonic deformation of the seafloor or by the movement of voluminous submarine slides. Along the Alaska Peninsula and Aleutian archipelago, tsunami run-up height is dependent on shoreline aspect and coastal geography. In general, tsunami run-up height on north-facing shorelines along the Alaska Peninsula and major islands of the Aleutian archipelago is much smaller, 3 feet or less, than the run-up height on south-facing shorelines, where run-up heights have exceeded 90 feet (Soloviev, 1968, cited in Davies and others, 1981, p. 3829 and 3830; Jacob and Hauksson, 1986). For example, the 1946 earthquake that occurred south of Unimak Island (M_s 7.4) generated one of the most destructive tsunamis in the Pacific and completely destroyed the Scotch Cap lighthouse on Unimak Island, the foundation of which was 45 feet above mean low water (Sykes, 1971).

The size, shape, and orientation of the earthquake source area also strongly influence any resulting tsunami. Kowalik and Murty (1987) used numerical models to study the directional characteristics of tsunamis generated by both circular and elongate source regions. Those investigators demonstrated that a tsunami generated by an earthquake with an elongate source region oriented parallel to the trench axis (the most likely geometry for the source region if the Shumagin seismic gap ruptures in a single great earthquake) would tend to have its energy focused in a direction normal to the trench axis. In contrast, a tsunami generated by an earthquake with a more equidimensional source region (a possible geometry for the source region if the seismic gap ruptures in more than one large earthquake) would tend to have a much less directional character.

Earthquake Potential

The Shumagin region is generally considered to be a likely site for the occurrence of a great earthquake

(M_s 7.8) sometime during the next few decades. This high risk is a consequence of the continuing subduction of the Pacific lithospheric plate beneath the North American plate and the absence of recent earthquakes large enough to relieve the accompanying accumulated elastic strain. In the paradigm of plate tectonics, seafloor spreading at mid-ocean ridges is accommodated on a worldwide basis by an equivalent amount of subduction at arc-trench systems. The process of subduction involves the accumulation of large amounts of elastic strain between the subducting and overriding plates. This strain is relieved periodically by large, thrust-type earthquakes. Recent studies of these earthquakes and the areal extents of their aftershock zones reveal that the accumulated elastic strain is not relieved along the entire length of the subduction zone during a single earthquake. Instead, subduction zones are segmented into discrete blocks that respond individually to subduction-related tectonics (Tobin and Sykes, 1968; Kelleher, 1970; Sykes, 1971; Davies and others, 1981)(figs. 27 and 28, p. 66 and 67).

Minster and Jordan (1978) and Chase (1978) calculated a convergence rate between the Pacific and North American plates in the region of the Shumagin Planning Area of 7.4 to 7.7 centimeters per year. Estimates of the repeat time for earthquakes large enough to relieve the corresponding elastic strain resulting from that rate of convergence range from 30 years (Sykes, 1971) to 800 years (Plafker and Rubin, 1967). More recently, Jacob (1984) and Jacob and Hauksson (1986) estimated that the mean repeat time for great earthquakes (M_w 7.8 or greater) along the Aleutian arc is 70 to 80 years. Sykes (1971) recognized that an arc segment that is relatively aseismic or that has not experienced a large earthquake within a probable repeat time represents a likely site for a future large earthquake and designated it a "seismic gap." The segment of the Aleutian subduction zone that lies within the boundaries of the Shumagin Planning Area (fig. 47, p. 120) has not experienced a large earthquake since sometime between 1899 and 1903, and has therefore, exceeded the mean repeat time (Davies and others, 1981). This segment of the subduction zone, termed the Shumagin seismic gap, is likely to experience a large earthquake sometime during the next few decades (Kelleher, 1970; Kelleher and others, 1973; McCann and others, 1979; Sykes and others, 1980; Davies and others, 1981). Sykes and others (1980) predict that the style of rupture of the Shumagin seismic gap will be through one or more large earthquakes within the next 10 to 20 years. In contrast,

Jacob (1983) proposed that the Shumagin seismic gap will fail during a single great earthquake sometime within the same time frame.

Beavan and others (1983 and 1984) discussed surface tilt measured in the Shumagin Islands using geodetic leveling lines that have been resurveyed periodically since 1972. Those investigators detected a steady tilt downward toward the trench, which they interpreted to represent deformation produced as a consequence of the continuing subduction of the Pacific plate while the shallow part of the plate boundary (the main thrust zone) remained locked to a depth of approximately 37 miles (fig. 48, p. 121). From 1978 through 1980, this steady downward tilt into the trench was interrupted by a rapid episode of tilt in the opposite direction. That event was caused by an episode of aseismic reverse slip downdip of the locked part of the plate boundary (fig. 48). Those investigators postulated that an effect of such an episode of reverse slip would be to increase the state of stress in the overlying, locked main thrust zone. On the basis of their study, they concluded that such reverse slip events are common occurrences in subduction zones, and that because of the long time period since the last major earthquake (1899–1903), it is possible that in the near future such an event could initiate the rupture of the Shumagin seismic gap.

In contrast to the proposed mode of rupture of the Shumagin seismic gap during a future great earthquake or series of large earthquakes as described above, Savage and Lisowski (1986) and Savage and others (1986) postulated that the main thrust zone is not locked but rather is slipping stably. Those investigators proposed that the Shumagin gap represents an anomalously aseismic segment of an otherwise highly seismic subduction zone. They formulated their conclusion on the basis of strain accumulation measurements determined from repeated trilateration surveys in the Shumagin Islands and southern Alaska Peninsula. Their measurements indicated that the rate of shear-strain accumulation during the period 1980 to 1985 was an order of magnitude less than the rate predicted for seismic subduction. This absence of shear-strain accumulation was the primary basis for their conclusion that the main thrust zone is not locked but rather is slipping aseismically.

Another likely site for a large earthquake is the segment of the Aleutian subduction zone that lies to the west of the Shumagin Planning Area (fig. 47). It is not certain whether this region, termed the Unalaska seismic gap, ruptured during the 1957 earthquake

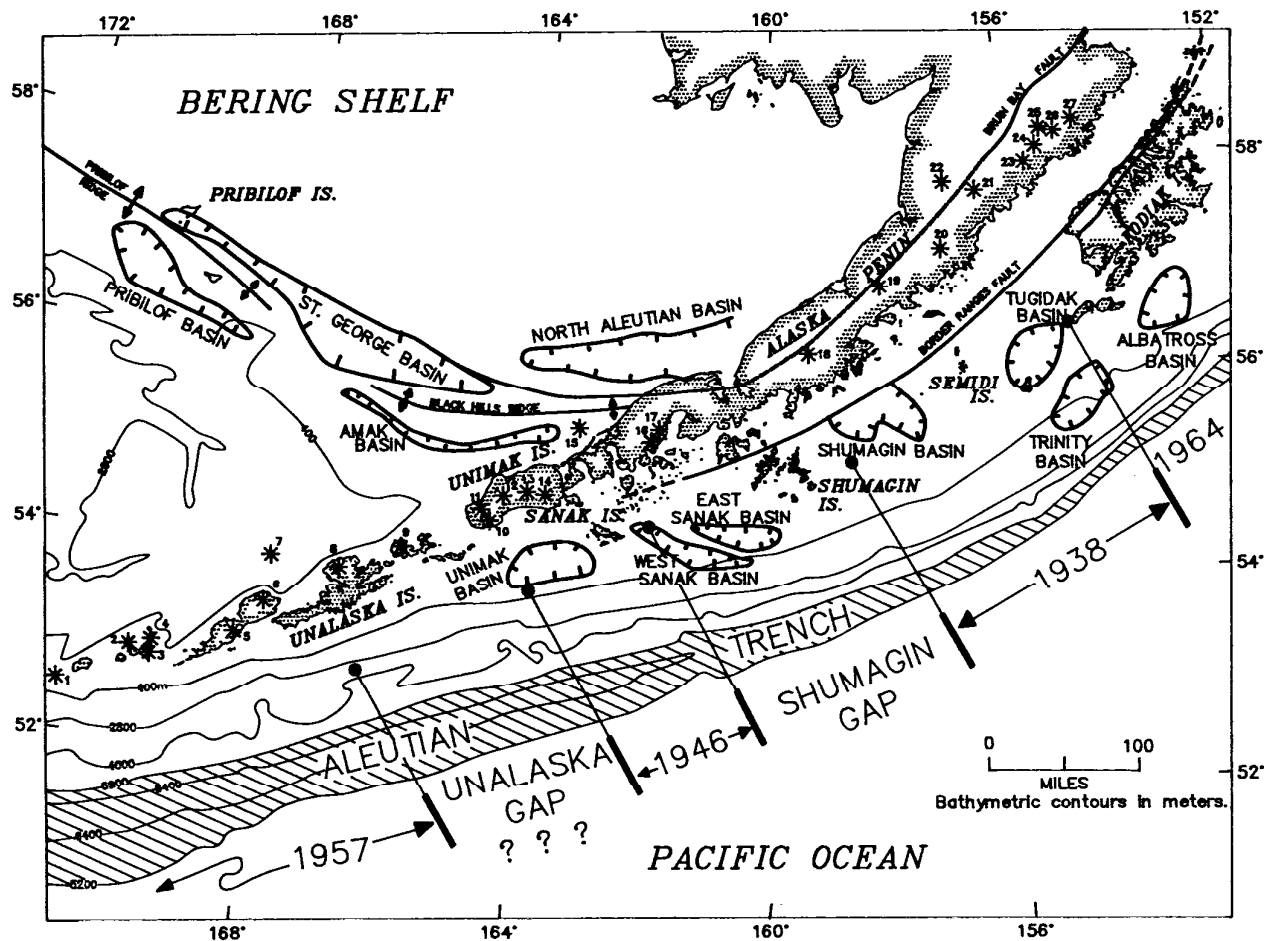


FIGURE 47. Tectonic map of the eastern Aleutian-Alaska Peninsula region (after Davies and others, 1981; Comer and others, 1987; and Hoose, 1987). Outlines of the major offshore sediment basins after Comer and others (1987) and Horowitz (unpublished MMS interpretation). Volcanoes from Simkin and others (1981); numbers correspond to those in table 3.

(M_w 9.1) that involved the subduction zone west of Unalaska Island, or whether it has not ruptured since 1902 (House and others, 1981). If this region was not included in the rupture zone of the 1957 event, then it also represents a seismic gap with a high probability of rupturing in a large earthquake sometime during the next few decades.

Shallow Gas

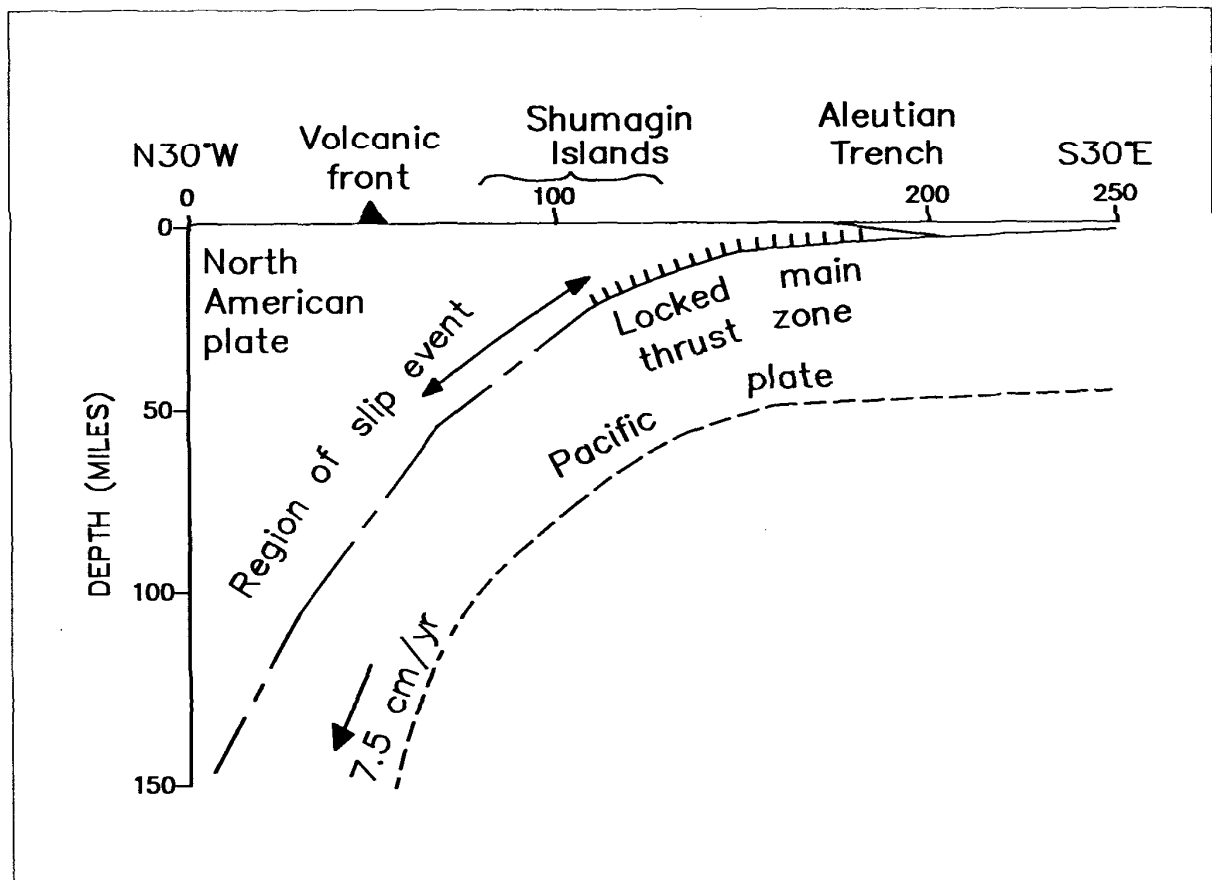
The possible presence of gas-charged sediment is significant because on continental shelves elsewhere it has been associated with seafloor instability, the formation of seafloor craters, sediment overpressuring, and reduced sediment shear strength (Whalen and others, 1976; Nelson and others, 1978). Due to the limited coverage and poor quality of the high-resolution seismic data across the Shumagin shelf, it is not possible to evaluate whether shallow, gas-charged sediments are present. However, similarities may be inferred between the sediment blanket that mantles the

Shumagin shelf and that of nearby Alaskan shelves, where the data coverage is more extensive. It is noteworthy that shallow, gas-charged sediments have been detected beneath the adjacent Kodiak shelf (von Huene and others, 1980; Hampton and Kvenvolden, 1981). Shallow, gas-charged sediments have also been identified on the Bering Sea shelf in Norton Sound (Holmes and others, 1978; Holmes, 1979; Nelson and others, 1979; Steffy and Hoose, 1981), the North Aleutian Basin Planning Area (Hoose and others, 1984), and the St. George Basin Planning Area (Marlow and others, 1979; Marlow and Cooper, 1980; Comer, 1984; Cooper and others, 1984). In those regions, biogenic gas is present in the shallow sediment, and in some areas, seafloor craters and gas seeps have been observed.

Volcanic Activity

Because of its proximity to the Alaska-Aleutian volcanic arc, the Shumagin Planning Area is susceptible

FIGURE 48. Theoretical tectonic cross section of the Shumagin region showing the locations of the locked main thrust zone and the reverse-slip event (after Beavan and others, 1983).



to hazards associated with volcanic activity. Over 74 active volcanoes make up the volcanic arc, and 10 that have been active during the last 200 years are situated along the northern border of the planning area (fig. 47) (table 3). These volcanoes are andesitic and their eruptions tend to be violent and characterized by both ash and lava production. Locally hazardous phenomena related to these eruptions could include lava flows, nuée ardente, mud slides, pyroclastic bombs, floods, ash deposits, noxious fumes, poisonous gases, acid rain, lightning strikes, tsunamis, and earthquake swarms. Volcanic phenomena that could be hazardous over extended distances are ash fall, radio interference, and acid rain.

Andesitic eruptions are capable of producing large volumes of ash that can be transported long distances in highly mobile flows and by winds (Eaton, 1963). Miller and Smith (1977) described ash deposits around Aniakchak and Fisher Calderas on the Alaska Peninsula that were deposited by ash flows that traveled as far as 30 miles and surmounted obstacles as high as 1,600 feet. W.R. Eubank (personal commun., 1979, cited in Heusser, 1983) reported that in 1976, ash from an eruption of Pavlof volcano was deposited 80 miles away on the Shumagin Islands. The 1912 eruption of Mt. Katmai ejected more than 6 cubic miles of material and mantled the village of Kodiak, 100 miles downwind, with 10 inches of ash (Wilcox, 1959). Ash from the Katmai eruption caused considerable damage to the communities downwind of Katmai due to the

TABLE 3. Active volcanoes near the Shumagin Planning Area (Simkin and others, 1981).

Map No.*	Name	Most Recent Eruption	Type of Eruption
1	Amukta	1963	Explosive
2	Carlisle	1838?	
3	Cleveland	1951 (1975?)	Explosive
4	Kagamil	1929	
5	Vsevidof	1957	Explosive/Phreatic
6	Okmok	1945	Explosive
7	Bogoslof	1931 (1951?)	Explosive
8	Makushin	1980	Explosive/Phreatic
9	Akutan	1986	
10	Westdahl	1978	Explosive
11	Pogromni	1830	Explosive
12	Fisher	1827	Explosive
13	Shishaldin	1979	Explosive
14	Isanotski	1845	
15	Amak Island	1710	
16	Pavlof	1987	
17	Pavlof Sister	1786	
18	Veniaminof	1984	
19	Aniakchak	1931 (1942?)	Explosive
20	Chiginagak	1972	
21	Peulik	1814 (1852?)	Explosive
22	Ukinrek Maars	1977	Explosive/Phreatic
23	Martin	1953	
24	Mageik	1936 (1946?)	Explosive
25	Novarupta	1950	Explosive
26	Trident Volcano	1975	Explosive
27	Mt. Katmai	1929 (1931?)	

* Numbers refer to figure 47

abrasive action of the particles and the corrosiveness of the ash-produced acid (Arctic Environmental Information and Data Center and Institute for Social Economic, and Government Research, 1974).

Sediment Erosion and Deposition

Sediment erosion and deposition can pose hazards to bottom-founded structures as a result of modifications of seafloor topography, loading due to burial, and the undermining of structural supports. In the shallow water of the inner shelf, large, storm-generated waves and swift tidal currents that flow through the straits separating the islands are capable of eroding and transporting seafloor sediments. As previously discussed, a linear zone is present along the shelf break within which no post-glacial sediment has accumulated (fig. 44, p. 112). The erosion or nondeposition of modern sediments within this zone is attributed to the Alaska Stream that flows along the shelf edge (fig. 43, p. 111).

Summary

Potential geologic hazards in the Shumagin Planning Area can be grouped into three categories: hazards associated with seismicity, hazards associated with volcanic activity, and hazards associated with sediment

erosion and/or deposition. Because of the low quality and sparse coverage of high-resolution seismic data across the shelf, no reliable assessment can be made regarding the presence of gas-charged sediments. However, because gas-charged sediments have been identified on other continental shelves bordering the Gulf of Alaska and the Bering Sea, the presence of such accumulations on the Shumagin shelf cannot be ruled out.

Because of the likelihood of a major earthquake occurring within the Shumagin Planning Area during the time span when hydrocarbon exploration and production facilities would be present, it would be prudent to design and situate the facilities accordingly. In this regard, structures should be sited on bedrock or on well-consolidated sediments and should be designed to withstand substantial accelerations and multiple cycles of displacement. Harbor facilities should be situated in such a way as to reduce their susceptibility to tsunami inundation. Pipelines should be routed so as to avoid crossing faults and should be supported on bedrock or on sediment deposits of equal thickness. Offshore pipelines and production structures should be designed and situated in such a manner as to prevent their supports from being undermined or loaded due to sediment erosion or deposition.

15. Climate and Meteorology

The climate of the Shumagin Planning Area is dominated by maritime influences. Because the planning area is situated in the Gulf of Alaska and transected by the relatively warm southwestward-flowing Alaska Stream (fig. 43, p. 111), it is characterized by cloudy skies, moderately heavy precipitation, moderate winter temperatures, and cool summer temperatures. The seasonal development of the Honolulu, Arctic, and Siberian high-pressure systems and the Aleutian low-pressure system results in strongly seasonal weather patterns. The location of the planning area also makes it subject to the passage of storm systems along the Aleutian storm track. Because of the passage and dissipation of these storm systems, this region is one of the most meteorologically dynamic places on earth. The presence of high mountains along the western, northern, and eastern margins of the Gulf of Alaska forms a barrier to the passage of storms, typically causing them to stagnate and dissipate. Storm passage is also impeded by the presence of a high-pressure ridge in the eastern North Pacific that is present during much of the year.

The planning area is characterized by relatively cool summers and warm winters compared to temperatures associated with interior continental regions at comparable high latitudes. This temperature pattern is caused by the relatively warm Alaska Stream, an extension of the Kuroshio Current which originates in the western equatorial Pacific. In the winter, this current warms the air, which keeps the temperature fairly mild and also provides moisture for cloud formation. In the summer, this current also provides moisture for cloud formation and precipitation, but at that time of year the water mass tends to be cooler than the air temperature over the adjacent Alaska Peninsula, which results in cooler temperatures. Table 4 shows the mean daily maximum and minimum temperatures recorded at three stations across the planning area (Cold Bay, Sand Point, and Chignik)(fig. 41, p. 108).

TABLE 4. Mean daily maximum and minimum temperature in degrees Fahrenheit (Arctic Environmental Information and Data Center and Institute for Social, Economic, and Government Research, 1974).

Station	Maximum Mean	Minimum Mean	Annual Mean
Cold Bay	55.7 (August)	22.9 (January)	37.9
Sand Point	56.5 (July)	24.2 (March)	39.6
Chignik	60.4 (August)	19.6 (March)	38.5

TABLE 5. Mean maximum and minimum monthly precipitation in inches (Arctic Environmental Information and Data Center and Institute for Social, Economic, and Government Research, 1974).

Station	Maximum Mean	Minimum Mean	Annual Mean
Cold Bay	4.59 (October)	1.75 (March)	34.30
Sand Point	8.37 (August)	2.76 (March)	60.30
Chignik	14.61 (November)	4.54 (April)	127.15

At the village of Sand Point on Popof Island (fig. 41), the station situated closest to the center of the planning area and presumably the one that best reflects the weather conditions that could be expected on drilling rigs and supply vessels, the mean daily maximum and minimum temperatures for the months of January and July are 35.1 and 27.2, and 56.5 and 45.9 °F, respectively. At the village of Cold Bay on the Alaska Peninsula (fig. 41), a possible site for the shore-based facilities that would service future offshore production platforms, the mean daily maximum and minimum temperatures for the months of January and July are 32.6 and 22.9, and 54.3 and 45.0 °F, respectively. The small temperature range reflects the effect of the Gulf waters in both maintaining relatively warm temperatures year round and in damping the average monthly temperature range.

Precipitation measured at the same three stations is listed in table 5. Two patterns or trends can be discerned from this data set. The first is that the amount of precipitation, both in terms of the monthly mean and the annual mean, increases up the coast of the Alaska Peninsula from southwest to northeast. This pattern has been attributed primarily to differences in the terrain surrounding the stations and to their aspect (Arctic Environmental Information and Data Center

and Institute for Social, Economic, and Government Research, or AEIDC/ISER, 1974). The second pattern is that the minimum precipitation at all three stations occurs in late winter or early spring. This precipitation minimum is complemented by a precipitation maximum that occurs six to seven months later. This second pattern reflects the seasonal migration of the polar front, the boundary that separates the polar Hadley cell circulation to the north from the mid-latitude belt of prevailing westerly winds to the south, and the corresponding shift in the direction of the prevailing winds and storm tracks. In November, as a consequence of this shift, the main west-to-east storm track is across the southern Bering Sea (Wilson and Overland, 1987), rather than south of the Aleutian Islands, where it is situated for the remainder of the winter. This more northerly path brings moist air from the Bering Sea up over the Aleutian Range where it cools adiabatically, loses its ability to hold moisture, and releases heavy precipitation.

Offshore winds in the region of the planning area tend to be westerly but highly variable, with wind intensity greatest during the winter months of October through April (Wilson and Overland, 1987). The nearshore wind field tends to be highly variable because of the presence of mountains and volcanoes that form barriers to the onshore winds. Average wind speed and peak gust speed at Sand Point range from 12.9 and 64 knots, respectively, in February, to 7.1 and 35 knots, respectively, in July (unpublished data from the U.S. Army Corps of Engineers cited in AEIDC/ISER, 1974). The peak gusts recorded at Sand Point and Cold Bay are 64 and 83 knots, respectively (unpublished data from the U.S. Army Corps of Engineers and from the U.S. Air Force Air Weather Service cited in AEIDC/ISER, 1974), which reflects the influence of the differences in terrain at the two stations. Wind speed over water tends to be greater than over land because of the reduction in surface friction, and Thom (1968) reported that sustained extreme wind speeds may attain maximum gusts of up to 100 knots. Thom (1968) predicted a recurrence interval for 100-knot winds along the Alaska Peninsula of once every 25 years, and for 80-knot winds of once every two years. In the event that a major storm is slow moving or stationary, a persistent wind direction of several days duration would create substantial wave action along the coast and at offshore installations.

The meteorology of the Gulf of Alaska region is influenced by four seasonal atmospheric features: the Honolulu, Arctic, and Siberian high-pressure systems

and the Aleutian low-pressure system. The Aleutian low is present 25 percent of the time, making it the dominant influence on the weather in the Gulf of Alaska throughout the year (Overland and Heister, 1980). The Aleutian low-pressure system is a seasonal feature generated by the passage of intense storms (low-pressure systems) through this quadrant of the North Pacific (Wilson and Overland, 1987). The weather in the Gulf of Alaska is characterized by the passage of such storms, which typically have low sea-level barometric pressure and associated cold fronts. Most of these storms form in the western Pacific, next to the coast of Asia, where warm ocean currents flow adjacent to cold land masses. As these storms move across the North Pacific, they gain in intensity as they gather heat and moisture from the ocean surface. During the winter, from October through April, an average of one storm every 4 to 5 days crosses the Gulf, generally from west to east (Hartmann, 1974). These storms often have winds up to 80 knots and create waves up to 50 feet in height. The relatively warm, moist air associated with these storms typically creates cloudy weather, particularly in winter, and drops up to 300 inches of precipitation on the high coastal mountains.

During the summer, the air over the Gulf is cooler than over the adjacent land masses and a large high-pressure system, the Honolulu high, forms over the ocean. Part of this high-pressure system is present intermittently year round off the coast of California and Baja California, its presence in part related to the upwelling of cold, abyssal water. During the summer, this high-pressure system expands northward and reaches its maximum intensity in June through August.

From October through March, the weather in the Gulf of Alaska is influenced by the Siberian and Arctic high-pressure systems. These highs, which attain their maximum intensities in January, form as a result of the presence of very cold winter air over eastern Asia and northern Alaska. The presence of these high-pressure systems results in a southward shift in the location of the Aleutian storm track (Wilson and Overland, 1987).

Cloud cover and fog are persistent features of the Gulf of Alaska almost year round. Fog occurs in the Gulf of Alaska during every month of the year, but is most prevalent during the summer and early winter (Grubbs and McCollum, 1968; Guttman, 1975). During the summer, moist air is trapped near the sea surface by a low-level temperature inversion associated with the seasonal high-pressure system (Wilson and Overland,

1987). This relationship results in persistent fog and low stratus clouds. Cloud cover is least during the winter and reaches a maximum in July. Winter cloudiness is related either to the passage of storms or to the flow of cold, relatively dry continental air from the Alaskan continent or the seasonal Bering Sea ice shelf across the relatively warm waters of the Gulf (Wilson and Overland, 1987). The average number of "clear" days (those with less than one-eighth cloud cover) along the Gulf coast is four to seven per month (Grubbs and McCollum, 1968).

Superstructure icing can be a serious hazard to vessels operating in the Gulf. The development of icing is a function of several variables, the most critical being an air temperature colder than the freezing point of seawater (28.9 °F at a salinity of 35 parts per thousand)(Wilson and Overland, 1987). Under these conditions, any moisture in the air (fog, rain, sea spray)

will freeze to the superstructures of vessels. Other variables include sea temperature, wind speed, wave direction relative to the vessel, and configuration of the vessel or structure accumulating the ice. Brower and others (1988) compiled data on the locations of icing events in the North Pacific and Bering Sea, 64 of which occurred within the Shumagin Planning Area. Wilson and Overland (1987) categorized this region as having a very heavy to extreme potential for icing.

The weather in the Gulf of Alaska plays a major role in any endeavor there. The design and construction of any offshore or shore-based facility should take into consideration the likelihood of high winds, heavy precipitation, low visibility due to fog or clouds, and superstructure icing. Planning should also consider that for many days out of the year, the region is inaccessible by air because of the weather conditions.

Summary

This report, part of the support documentation related to Federal OCS Lease Sale 129, presents observations and preliminary conclusions on the regional geology, environmental geology, and petroleum potential of the Shumagin Planning Area.

The low hydrocarbon potential of the Shumagin margin, its complex and problematic geology, and the remote and hostile nature of the subarctic offshore environment have inhibited serious petroleum exploration efforts in the area. No wells have been drilled and only regional seismic data over the continental shelf has been collected. Because of this, the geology in this report is based on extrapolation from six DST wells drilled on the nearby Kodiak shelf, a limited number of dredge samples, and the extrapolation of applicable onshore geology. Seismic interpretations of the complicated forearc geology below the regional Miocene unconformity are often speculative.

The Shumagin forearc margin shares many characteristics with the adjacent Kodiak margin, both of which have grown since the Late Cretaceous by tectonic and sedimentary accretion, the emplacement of granitic intrusions, and conventional sedimentary processes. The basement complex (sequence A) that underlies much of the Shumagin margin is represented by the Late Cretaceous Shumagin Formation, which is intruded by Paleocene granodiorites. A thick section (25,000 feet) of Tertiary sediments accumulated in portions of the six forearc basins that occur along the Shumagin margin.

The geothermal gradient of the Shumagin margin is low (1.03 °F/100 ft), although higher paleogeothermal gradients may have been generated by accretionary processes at the trench, subduction of the Kula-Pacific spreading ridge, and emplacement of Paleocene intrusives on the shelf. During the initial late Paleogene rifting of the basins, some or all of these forearc basins may have been sites of anoxic sedimentation, which may have enhanced kerogen preservation. Quartz-rich sandstone deposited during the late Paleogene and Neogene represent potential reservoirs that are now involved in numerous and diverse structural and

stratigraphic configurations that might serve as petroleum traps.

The Shumagin forearc basin appears to have the greatest petroleum potential in the planning area. This basin contains over 6,000 feet of Eocene clastic sediments (sequence B) in which appropriate kerogen might have been preserved. An equal thickness of Oligocene(?), Neogene, and Pleistocene clastic sediments (sequence C), partially sourced from exhumed intrusives, was deposited in a basin formed by strike-slip motion. Continuous Neogene strike-slip motion generated folded structures that represent potential hydrocarbon traps.

The East Sanak basin formed as a margin-parallel accretionary basin at the same time as the West Sanak and Shumagin basins. This basin and the East Sanak slope ridge were translated into a shelf setting as the continental margin grew seaward. Steeply dipping sequence A and B strata were uplifted and truncated, and sequence C sediments were deposited above them in angular contact. The potential reservoirs are associated with tilted fault blocks and rollover anticlines formed by Neogene uplift along the Shumagin ridge. Sequence B strata may be a secondary reservoir objective in rollover anticlines along the Shumagin ridge and in stratigraphic traps along the eastern margin of the Central Sanak high.

The East Sanak slope basin, bounded by the East Sanak slope ridge and the Shumagin ridge, formed as a Paleogene accretionary basin. Landward-dipping normal faults that cut existing detachment surfaces within the basement complex define these fault-bounded ridges. Nearly 15,000 feet of sequence C sediments have accumulated in this basin. Adjacent ridges, the Alaska Peninsula, and the Outer Shumagin Islands were the source of the basin fill. Potential reservoir rocks are most likely in sequence C. The ridges may have restricted circulation and led to anoxic conditions during initial basin growth, thus increasing the opportunity for kerogen preservation and enrichment. Fault and stratigraphic traps are likely along the southern flank of the Shumagin ridge.

The West Sanak basin is a structurally complex, margin-oblique accretionary basin that formed in the Cretaceous parallel to the northwest-trending

Beringian transform margin. The basin and its bounding ridge translated upslope to shelf depths as the accretionary complex (sequence B) grew during the Paleogene. The basin is now bounded on the southwest by the Sanak Island Transverse High, which was uplifted as the Aleutian Ridge docked in its present position. Uplift of the transverse high continued by the process of underplating while the West Sanak basin was downdropped during the Neogene. The deposition of over 25,000 feet of sequence C sediments partially derived from granitic intrusives bodes well for the presence of reservoir rocks.

There are numerous, diverse structures in the West Sanak basin related to tectonism in the Sanak Island Wrench Zone, some of which are too young and active to be good traps. Small fault traps, faulted anticlines, anticlines "cored" by thrust faults, and stratigraphic traps have been generated by accretionary processes and associated strike-slip motion. Strike-slip tectonics inverted the West Sanak basin and generated small antiformal structures that contain Neogene clastic sediments with good reservoir potential.

The Sanak Island Transverse High, a margin-oblique structure located on the shelf between the West Sanak and Unimak basins, consists of a preserved section of the accretionary and underplated section of the Cretaceous and Paleogene Shumagin margin. The late Paleogene and Neogene uplift of the Sanak Island Transverse High may be related to underplating or strike-slip tectonics. Sequence C rests unconformably on sequence B. Source and reservoir rock may be present within the highly folded strata of sequence B. The early formation of structures related to sequence B accretion may have trapped hydrocarbons generated since the Paleogene. Normal-fault traps and stratigraphic pinchouts of sequence C strata overlie the Sanak Island Transverse High.

The Unimak basin is a 20,000-foot-thick progradational wedge of mostly marine sequence C sediments that accumulated over a sequence B basement complex. The accretionary basement complex began to grow in the early Eocene as the Aleutian Arc formed. The Unimak ridge, a major positive structural element composed of accretionary material (sequence B), served as a barrier landward of which the progradational wedge of sequence C accumulated.

Deformation associated with Pliocene strike-slip motion along the Sanak Island Wrench Zone and the Unimak wrench zone generated anticlines, thrust anticlines, and fault traps. As in the other forearc basins, reservoir rocks are more likely to be present in sequence C.

Potential geologic hazards in the Shumagin Planning Area can be grouped into three categories: hazards associated with seismicity, with volcanic activity, and those associated with sediment erosion and deposition. The susceptibility of the planning area to hazards associated with seismicity and volcanic activity is a consequence of its proximity to the Alaska-Aleutian arc-trench system. This region is a likely site for a great earthquake (M_s 7.8) sometime during the next few decades because of the continuing subduction of the Pacific lithospheric plate beneath the North American plate. This is particularly likely considering the absence of recent large, stress-relieving earthquakes in the area. Hazards associated with seismicity include regional tectonic uplift or subsidence, ground shaking, fault displacement, surface tilt, ground failure, and tsunami inundation. Hazards associated with volcanic activity include lava flows, nuée ardente, mud slides, pyroclastic bombs, floods, ash deposits, noxious fumes, poisonous gases, lightning strikes, earthquake swarms, radio interference, and acid rain. Sediment erosion and deposition pose hazards to bottom-founded structures by modification of seafloor topography, loading due to burial, and the undermining of structural supports.

The weather in the Shumagin margin plays a major role in any endeavor there. The design and construction of any offshore or shore-based facility should take into consideration the likelihood of high winds, heavy precipitation, low visibility due to fog or clouds, and superstructure icing.

The petroleum potential of the Shumagin Planning Area is low if the drilling results in the adjacent Kodiak shelf are indicative. Conditions traditionally thought to be conducive to the production and entrapment of hydrocarbons are absent or limited in the deep-water portions of the Shumagin Planning Area (trench lower slope, Aleutian Trench, Aleutian Abyssal Plain), and the hydrocarbon potential of these areas is considered to be very low.

References

- Allison, R. C., 1978, Late Oligocene through Pleistocene molluscan faunas in the Gulf of Alaska: *The Veliger*, v. 21, p. 171-188.
- Allison, R. C., and Marinovich, L., Jr., 1981, A late Oligocene or earliest Miocene molluscan fauna from Sitkinak Island, Alaska: U.S. Geological Survey Professional Paper 1233, 10 p.
- Anderson, R. N., DeLong, S. E., and Schwarz, W. M., 1978, Thermal model for subduction with dehydration in the downgoing slab: *Journal of Geology*, v. 86, p. 731-739.
- Anstey, N. A., 1977, *Seismic interpretation: the physical aspects*: Boston, International Human Resources Development Corporation, 625 p.
- Aoki, Y., Tamano, T., and Susumu, K., 1982, Detailed structure of the Nankai Trough from migrated seismic sections, in Watkins, J. S., and Drake, C. L., eds., *Studies in continental margin geology*: American Association of Petroleum Geologists Memoir 34, p. 309-322.
- Arctic Environmental Information and Data Center and Institute for Social, Economic, and Government Research, University of Alaska, 1974, *The western Gulf of Alaska, a summary of available knowledge*: Marine Minerals Division, Bureau of Land Management, U.S. Department of Interior, Washington, D.C., 559 p.
- Armentrout, J. M., 1979, Cenozoic stratigraphy, Kodiak Island Archipelago, Alaska [abs.]: *Geological Society of America Abstracts with Programs*, v. 11, no. 3, p. 66.
- Bally, A. W., and Oldow, J. S., 1984, *Plate tectonics, structural styles, and the evolution of sedimentary basins* (3d ed.): American Association of Petroleum Geologists Short Course Notes, p. 238.
- Baxendale, R. W., and Hemler, T., 1984, Palynological analysis of Tenneco Middleton Island No. 1, 59°24'33.15"N - 146°15'37.59"W, Gulf of Alaska: Amoco report on file with the State of Alaska, Department of Natural Resources, Oil and Gas Conservation Division, 3 p.
- Beavan, J., Bilham, R., and Hurst, K., 1984, Coherent tilt signals observed in the Shumagin seismic gap: detection of time-dependent subduction at depth?: *Journal of Geophysical Research*, v. 89, no. B6, p. 4478-4492.
- Beavan, J., Hauksson, E., McNutt, S. R., Bilham, R., and Jacob, K. H., 1983, Tilt and seismicity changes in the Shumagin seismic gap: *Science*, v. 222, 21 October, p. 322-325.
- Beikman, H. M., 1980, *Geologic map of Alaska*: U.S. Geological Survey, scale 1:2,500,000, 1 sheet.
- Biju-Duval, B., Le Quellec, P., Mascle, A., Renard, V., and Valery, P., 1982, Multibeam bathymetric survey and high-resolution seismic investigations on the Barbados Ridge complex (eastern Caribbean): a key to the knowledge and interpretation of an accretionary wedge: *Tectonophysics*, v. 86, p. 275-304.
- Black, R. F., 1974, Late Quaternary sea level changes, Unmak Island, Aleutians - their effects on ancient Aleuts and their causes: *Quaternary Research*, v. 4, p. 264-281.
- Boyd, M. T., Taber, J. J., Lerner-Lam, A. L., and Beavan, J., 1988, Seismic rupture and arc segmentation within the Shumagin Islands seismic gap, Alaska: *Geophysical Research Letters*, v. 15, no. 3, p. 201-204.

- Boyer, S. E., and Elliott, D., 1982, Thrust systems: *American Association of Petroleum Geologists Bulletin*, v. 99, no. 9, p. 1196-1230.
- Brockway, R., Alexander, B., Day, P., Lyle, W. M., Hiles, R., Decker, W., Polski, W., and Reed, B. L., 1975, Bristol Bay region, stratigraphic correlation section, southwest Alaska: *Alaska Geological Society*, P.O. Box 101288, Anchorage, Alaska, 99510, 1 oversized sheet.
- Brower, W. A., Baldwin, R. G., Williams, C. N., Jr., Wise, J. L., and Leslie, L. D., 1988, Climatic atlas of the Outer Continental Shelf waters and coastal regions of Alaska, volume I, Gulf of Alaska: Anchorage, University of Alaska, Arctic Environmental Information and Data Center, 550 p.
- Brown, K. M., and Westbrook, G. K., 1987, The tectonic fabric of the Barbados Ridge accretionary complex: *Marine and Petroleum Geology*, v. 4, p. 71-81.
- Bruhn, R. L., and Pavlis, T. L., 1981, Late Cenozoic deformation in the Matanuska Valley, Alaska: three-dimensional strain in a forearc region: *Geological Society of America Bulletin*, Part I, v. 92, no. 5, p. 282-293.
- Bruns, T. R., and Bayer, K. C., 1977, Multichannel seismic reflection data acquired on the M/V Cecil H. Green in the Gulf of Alaska, June-August 1975: *U.S. Geological Survey Open-File Report 77-352*.
- Bruns, T. R., Fisher, M. A., Carlson, P. R., and Parson, L. M., 1986, The Yakutat terrane and Aleutian convergent margin, northern Gulf of Alaska - GLORIA images obtained in the TACT corridor [abs.]: *EOS, Transactions, American Geophysical Union*, v. 67, no. 44, p. 1197.
- Bruns, T. R., Vallier, T. L., Pickthorn, L. B., and von Huene, R., 1987, Volcanic-arc dacite and early Miocene basalt dredged from the Shumagin margin, Alaska: *U.S. Geological Survey Circular 998*, p. 143-146.
- Bruns, T. R., and von Huene, R., 1977, Sedimentary basins on the Shumagin shelf, Western Gulf of Alaska: *Offshore Technology Conference, 9th, Houston, Texas, 1977, Proceedings*, v. 1, p. 41-50, OTC 2732.
- Bruns, T. R., von Huene, R., and Childs, J. R., in press, The Shumagin margin - record section 104, in von Huene, R., ed., *Seismic images of modern convergent margin tectonic structure: American Association of Petroleum Geologists Studies in Geology*.
- Bruns, T. R., von Huene, R., Culotta, R. C., and Lewis, S. D., 1985, Summary geologic report for the Shumagin Outer Continental Shelf (OCS) planning area, Alaska: *U.S. Geological Survey Open-File Report 85-32*, 58 p.
- Bruns, T. R., von Huene, R., Culotta, R. C., Lewis, S. D., and Ladd, J. W., 1987, Geology and petroleum potential of the Shumagin margin, Alaska, in Scholl, D. W., Grantz, A., and Vedder, J. G., eds., *Geology and resource potential of the continental margin of western North America and adjacent ocean basins: Circum-Pacific Council for Energy and Mineral Resources, Earth Science Series*, v. 6, p. 157-189 [distributed by AAPG Bookstore, Tulsa].
- Burk, C. A., 1965, Geology of the Alaska Peninsula - island arc and continental margin: *Geological Society of America Memoir 99*, 250 p. and maps 1:250,000 and 1:500,000.
- Burns, L. E., 1982, Gravity and aeromagnetic modeling of a large gabbroic body near the Border Ranges fault, southern Alaska: *U.S. Geological Survey Open-File Report 82-460*, 72 p.
- Butler, R. W. H., 1982, The terminology of structures in thrust belts: *Journal of Structural Geology*, v. 4, no. 3, p.239-245.
- Byrne, T., 1979, Late Paleocene demise of the Kula-Pacific spreading center: *Geology*, v. 7, p. 341-344.

- Byrne, T., 1982, Structural geology of coherent terranes in the Ghost Rocks Formation, Kodiak Island, Alaska, *in* Leggett, J. K., ed., Trench and forearc sedimentation and tectonics: Special Paper of Geological Society of London, p. 229-242.
- Byrne, T., 1984, Early deformation in melange terranes of the Ghost Rocks Formation, Kodiak Islands, Alaska: Geological Society of America Special Paper 1984, p. 21-51.
- Byrne, T., 1986, Eocene underplating along the Kodiak shelf, Alaska: implications and regional correlations: *Tectonics*, v. 5, p. 403-421.
- Byrne, T., and Hibbard, J., 1987, Landward vergence in accretionary prisms: the role of the backstop and thermal history: *Geology*, v. 15, p. 1163-1167.
- Carden, J. R., Connelly, W., Forbes, R. B., and Turner, D. L., 1977, Blueschists of the Kodiak Islands, Alaska: an extension of the Seldovia schist terrane: *Geology*, v. 5, p. 529-533.
- Carlson, P. F., Bruns, T. R., Molnia, B. F., and Schwab, W. C., 1982, Submarine valleys in the northeastern Gulf of Alaska - characteristics and probable origin: *Marine Geology*, v. 47, p. 217-242.
- Castano, J. R., and Sparks, D. M., 1974, Interpretation of vitrinite reflectance measurements in sedimentary rocks and determination of burial history using vitrinite reflectance and authigenic minerals, *in* Dutcher, R. R., Hacquebard, P. A., Schopf, J. M., and Simon, J. A., eds., Carbonaceous materials as indicators of metamorphism: Geological Society of America Special Paper 153, p. 31-52.
- Chase, C. G., 1978, Plate kinematics: the Americas, east Africa, and the rest of the world: *Earth and Planetary Science Letters*, v. 37, p. 355-368.
- Christie-Blick, N., and Biddle, K. T., 1985, Deformation and basin formation along strike-slip faults, *in* Biddle, K. T., and Christie-Blick, N., eds., Strike-slip deformation, basin formation, and sedimentation: Society of Economic Paleontologists and Mineralogists Special Publication No. 37, p. 1-34.
- Clark, S. H. B., 1972, Reconnaissance bedrock geologic map of the Chugach Mountains near Anchorage, Alaska: U.S. Geological Survey Miscellaneous Field Studies Map MF-350, scale 1:250,000.
- Clendenen, W. S., Byrne, T., Fisher, D., and Heine, B., 1987, Mid-Tertiary uplift and unroofing of the Kodiak accretionary prism, Alaska [abs.]: EOS, Transactions, American Geophysical Union, v. 68, no. 44, p. 1467.
- Cloos, M., 1984, Landward-dipping reflectors in accretionary wedges: active dewatering conduits?: *Geology*, v. 12, p. 519-522.
- Coe, R. S., Globerman, B. R., Plumley, P. W., and Thrupp, G. A., 1985, Paleomagnetic results from Alaska and their tectonic implications, *in* Howell, D. G., ed., Tectonostratigraphic terranes of the Circum-Pacific region: Circum-Pacific Council for Energy and Mineral Resources, Earth Science Series No. 1, p. 85-108.
- Collot, J. Y., and Fisher, M. A., 1989, Formation of forearc basins by collision between seamounts and accretionary wedges: an example from the New Hebrides subduction zone: *Geology*, v. 17, no. 10, p. 930-933.¹
- Comer, C. D., 1984, Map showing shallow faults and acoustic anomalies, St. George basin, Alaska: U.S. Minerals Management Service OCS Map MMS 84-0012, scale 1:250,000, 1 oversized sheet.
- Comer, C. D., Herman, B. M., and Zerwick, S. A., 1987, Geological report for the St. George Basin Planning Area, Bering Sea, Alaska: U.S. Minerals Management Service OCS Report MMS 87-0030, 84 p.

¹ This study was received too late to be incorporated into the report, but its contents are relevant to the evolution of the Shumagin forearc margin.

- Connelly, W., 1976, Mesozoic geology of the Kodiak Islands and its bearing on the tectonics of southern Alaska: Santa Cruz, Calif., University of California, Ph.D. dissertation, 197 p.
- Connelly, W., 1978, Uyak complex, Kodiak Islands, Alaska: a Cretaceous subduction complex: *Geological Society of America Bulletin*, v. 89, p. 755-769.
- Connelly, W., Hill, M., Hill, B., and Moore, J. C., 1977, The Uyak complex, Kodiak Islands, Alaska: a subduction complex of early Mesozoic age, *in* Talwani, M., and Pitman, W. C., III, eds., *Island arcs, deep sea trenches, and back-arc basins*: American Geophysical Union, Maurice Ewing Series, v. 1, 465 p.
- Cooper, A. K., and House, L., 1979, Aleutian subduction zone seismicity, volcano-trench separation, and their relation to great thrust-type earthquakes: *Journal of Geophysical Research*, v. 84, p. 4583-4591.
- Cooper, A. K., Marlow, M. S., and Vallier, T. L., 1984, Summary geologic report for the St. George OCS Planning Area, Bering Sea, Alaska: U.S. Geological Survey Open-File Report 84-418, 81 p.
- Cooper, A. K., Scholl, D. W., and Marlow, M. S., 1976, Plate tectonic model for the evolution of the Bering Sea basin: *Geological Society of America Bulletin*, v. 87, p. 1119-1126.
- Coulter, H. W., Hopkins, D. M., Karlstrom, T. N. V., Pewe, T. L., Wahrhaftig, C., and Williams, J. R., 1965, Map showing extent of glaciation in Alaska: U.S. Geological Survey Miscellaneous Geologic Investigations Map I-415, scale 1:2,500,000, 1 oversized map.
- Cowan, D. S., and Boss, R. F., 1978, Tectonic framework of the southwestern Kenai Peninsula, Alaska: *Geological Society of America Bulletin*, v. 89, no. 1, p. 155-158.
- Creager, J. S., Scholl, D. W., and others, 1973, Initial reports of the Deep Sea Drilling Project, v. 19: National Science Foundation, 913 p.
- Davenport, A. G., Novak, M., and Atkinson, G. M., 1981, Evaluation of seismic risk to pipelines in northern Canada [abs.]: AISPIT 21st General Assembly, Department of Geophysics, The University of Western Ontario, London, Canada, p.A3-40.
- Davies, D. L., and Moore, J. C., 1984, 60 m.y. intrusive rocks from the Kodiak Islands link the Peninsular, Chugach, and Prince William terranes [abs.]: 1984 Cordilleran Geological Society of America Meeting, Anchorage, May, Abstracts with program, p. 277.
- Davies, J., Sykes, L., House, L., and Jacob, K., 1981, Shumagin seismic gap, Alaska Peninsula: history of great earthquakes, tectonic setting, and evidence for high seismic potential: *Journal of Geophysical Research*, v. 86, no. B5, p. 3821-3855.
- Davis, D. M., and Hussong, D. M., 1984, Geothermal observations during Deep Sea Drilling Project Leg 78A, Leg 78, *in* Initial Reports of the Deep Sea Drilling Project, v. 78: National Science Foundation, p. 593-598.
- Deal, C. S., 1982, Oil and gas developments in South America, Central America, Caribbean area, and Mexico in 1981: *American Association of Petroleum Geologists Bulletin*, v. 66, p. 2114.
- Decker, J., and Johnson, B. R., 1981, The nature and position of the Border Ranges fault on Chichagof Island: U.S. Geological Survey Circular 823-B, p. B102-104.
- Delong, S. E., Fox, P. J., and McDowell, F. W., 1978, Subduction of the Kula Ridge at the Aleutian Trench: *Geological Society of America Bulletin*, v. 89, p. 83-95.

- Delong, S. E., Schwartz, W. M., and Anderson, R. N., 1979, Thermal effects of ridge subduction: *Earth and Planetary Science Letters*, v. 44, p. 239-246.
- Detterman, R. L., 1986, Glaciation of the Alaska Peninsula, *in* Hamilton, T. D., Reed, K. M., and Thorson, R. M., eds., *Glaciation in Alaska - the geologic record*: Alaska Geological Society, P.O. Box 101288, Anchorage, Alaska, 99510, p. 151-170.
- Detterman, R. L., Case, J. C., Wilson, F. H., and Yount, M. E., 1987, Geologic map of the Ugashik, Bristol Bay, and western part of Karluk quadrangle, Alaska: U.S. Geological Survey Map I-1685, scale 1:250,000.
- Detterman, R. L., and Miller, J. W., 1985, Kaguyak Formation--an Upper Cretaceous flysch deposit, *in* Bartsch-Winkler, Susan and Reed, K. M., eds., *The United States Geological Survey in Alaska: Accomplishments during 1985*: U.S. Geological Survey Circular 945, p. 49-51.
- Detterman, R. L., Miller, T. P., Case, J. C., Wilson, F. H., and Yount, E. M., in press, Mesozoic and Cenozoic stratigraphy, Alaska Peninsula, Alaska: U.S. Geological Survey Bulletin.
- Detterman, R. L., Miller, T. P., Yount, M. E., and Wilson, F. H., 1981, Quaternary geologic map of the Chignik and Sutwick Island quadrangles, Alaska: U.S. Geological Survey Miscellaneous Investigation Series Map I-1292, scale 1:250,000, 1 oversized sheet.
- Dickinson, W. R., and Seely, D. R., 1979, Structure and stratigraphy of forearc regions: *American Association of Petroleum Geologists Bulletin*, v. 63, p. 2-31.
- Dix, C. H., 1955, Seismic velocities from surface measurements: *Geophysics*, v. 20, no. 1, p. 68-86.
- Dow, W. G., 1981, Petroleum source beds on continental slopes and rises, *in* *Geology of continental margins: a 1977 short course*: American Association of Petroleum Geologists Educational Course Note Series No. 5, p. D1-D37.
- Dumoulin, J. A., 1988, Sandstone petrographic evidence and the Chugach-Prince William terrane boundary in southern Alaska: *Geology*, v. 16, p. 456-460.
- Eaton, G. P., 1963, Windborne ash as a guide to atmospheric circulation in the geologic past: *Journal of Geophysical Research*, v. 68, p. 521-528.
- Embley, R. W., and Jacobi, R. D., 1977, Distribution and morphology of large submarine sediment slides and slumps on Atlantic continental margins: *Marine Geotechnology, Volume 2, Marine Slope Stability*, p. 205-228.
- Engdahl, E. R., and Scholz, C. H., 1977, A double Benioff zone beneath the central Aleutians: an unbending of the lithosphere: *Geophysical Research Letters*, v. 4, no. 10, p. 473-476.
- Engebretsen, D. C., Cox, A., and Gordon, R. G., 1985, Relative motions between oceanic and continental plates in the Pacific Basin: *Geological Society of America Special Paper 206*, 59 p.
- Evitt, W. R., 1973, Dinoflagellates from Leg 19, sites 183 and 192, Deep Sea Drilling Project, *in* Creager, J. S., Scholl, D. W., and others, eds., *Initial reports of the Deep Sea Drilling Project*, v. 19: National Science Foundation, p. 737-738.
- Fisher, D., and Byrne, T., 1987, Structural evolution of underthrusting sediments, Kodiak Island, Alaska: *Tectonics*, v. 6, no. 6, p. 775-793.
- Fisher, M. A., 1979, Structure and tectonic setting of continental shelf southwest of Kodiak Island, Alaska: *American Association of Petroleum Geologists Bulletin*, v. 63, p. 373.

- Fisher, M. A., 1980, Petroleum geology of Kodiak shelf, Alaska: American Association of Petroleum Geologists Bulletin, v. 64, no. 1, p. 1140-1157.
- Fisher, M. A., 1981, Location of the Border Ranges fault southwest of Kodiak Island, Alaska: Geological Society of America Bulletin, v. 92, p. 19-30.
- Fisher, M. A., Bruns, T. R., and von Huene, R., 1981, Transverse tectonic boundaries near Kodiak Island, Alaska: Geological Society of America Bulletin, v. 92, no. 1, p. 10-18.
- Fisher, M. A., and Holmes, M. L., 1980, Large-scale structure of deep strata beneath Kodiak shelf, Alaska: Geological Society of America Bulletin, Part I, v. 91, p. 218-224.
- Fisher, M. A., and von Huene, R., 1984, Geophysical investigation of a suture zone: the Border Ranges fault of southern Alaska: Journal of Geophysical Research, v. 89, no. B12, p. 11333-11351.
- Fisher, M. A., and von Huene, R., 1980, Structure of upper Cenozoic strata beneath Kodiak Island, Alaska: American Association of Petroleum Geologists Bulletin, v. 64, p. 1014-1033.
- Fisher, M. A., von Huene, R., and Hampton, M. A., 1984, Summary geologic report for petroleum lease sale No. 100, Kodiak shelf, Alaska: U.S. Geological Survey Open-File Report 83-24, 46 p.
- Fisher, M. A., von Huene, R., and Smith, G. L., 1987, Reflections from midcrustal rocks within the Mesozoic subduction complex near the eastern Aleutian trench: Journal of Geophysical Research, v. 92, no. B8, p. 7907-7915.
- Forbes, R. B., Lanphere, M. A., 1973, Tectonic significance of mineral ages of blueschists near Seldovia, Alaska: Journal of Geophysical Research, v. 78, no. 8, p. 1383-1386.
- Funk, J. M., 1973, Late Quaternary geology of Cold Bay, Alaska, and vicinity: Storrs, Conn., University of Connecticut, unpublished Masters thesis, 45 p.
- Galloway, W., 1979, Diagenetic control of reservoir quality in arc-derived sandstones: implications for petroleum exploration: Society of Economic Paleontologists and Mineralogists Special Publication No. 26, p. 251-262.
- Gedney, L., and Davies, J. N., 1986, Additional evidence for down-dip tension in the Pacific plate beneath central Alaska: Bulletin of the Seismological Society of America, v. 76, no. 5, p. 1207-1214.
- Gordon, J. M., and Barker, L. H., 1986, Barbados, in Wiman, W. D., 1986, Oil and gas developments in South America, Central America, Caribbean area, and Mexico in 1985: American Association of Petroleum Geologists Bulletin, v. 70, no. 10, p. 1372.
- Gromme, C. S., and Hillhouse, S. W., 1981, Paleomagnetic evidence for northward movement of the Chugach terrane, southern and southeastern Alaska: U.S. Geological Survey Circular 823-B, p. B70-B72.
- Grow, J. A., and Atwater, T., 1970, Mid-Tertiary tectonic transition in the Aleutian Arc: Geological Society of America Bulletin, v. 81, p. 3715-3722.
- Grubbs, B. E., and McCollum, R. D., Jr., 1968, A climatological guide to Alaskan weather. An unpublished report, Scientific Services Section, 11th Weather Squadron, Elmendorf Air Force Base, Alaska.
- Guttman, N. B., 1975, Study of fog and stratus for selected cold regions: Asheville, North Carolina, U.S. Naval Weather Service Command, National Climate Center, 85 p.
- Hamilton, E. L., 1973, Marine geology of the Aleutian abyssal plain: Marine Geology, v. 14, p. 295-325.

- Delong, S. E., Schwartz, W. M., and Anderson, R. N., 1979, Thermal effects of ridge subduction: *Earth and Planetary Science Letters*, v. 44, p. 239-246.
- Detterman, R. L., 1986, Glaciation of the Alaska Peninsula, *in* Hamilton, T. D., Reed, K. M., and Thorson, R. M., eds., *Glaciation in Alaska - the geologic record*: Alaska Geological Society, P.O. Box 101288, Anchorage, Alaska, 99510, p. 151-170.
- Detterman, R. L., Case, J. C., Wilson, F. H., and Yount, M. E., 1987, Geologic map of the Ugashik, Bristol Bay, and western part of Karluk quadrangle, Alaska: U.S. Geological Survey Map I-1685, scale 1:250,000.
- Detterman, R. L., and Miller, J. W., 1985, Kaguyak Formation--an Upper Cretaceous flysch deposit, *in* Bartsch-Winkler, Susan and Reed, K. M., eds., *The United States Geological Survey in Alaska: Accomplishments during 1985*: U.S. Geological Survey Circular 945, p. 49-51.
- Detterman, R. L., Miller, T. P., Case, J. C., Wilson, F. H., and Yount, E. M., in press, Mesozoic and Cenozoic stratigraphy, Alaska Peninsula, Alaska: U.S. Geological Survey Bulletin.
- Detterman, R. L., Miller, T. P., Yount, M. E., and Wilson, F. H., 1981, Quaternary geologic map of the Chignik and Sutwick Island quadrangles, Alaska: U.S. Geological Survey Miscellaneous Investigation Series Map I-1292, scale 1:250,000, 1 oversized sheet.
- Dickinson, W. R., and Seely, D. R., 1979, Structure and stratigraphy of forearc regions: *American Association of Petroleum Geologists Bulletin*, v. 63, p. 2-31.
- Dix, C. H., 1955, Seismic velocities from surface measurements: *Geophysics*, v. 20, no. 1, p. 68-86.
- Dow, W. G., 1981, Petroleum source beds on continental slopes and rises, *in* *Geology of continental margins: a 1977 short course*: American Association of Petroleum Geologists Educational Course Note Series No. 5, p. D1-D37.
- Dumoulin, J. A., 1988, Sandstone petrographic evidence and the Chugach-Prince William terrane boundary in southern Alaska: *Geology*, v. 16, p. 456-460.
- Eaton, G. P., 1963, Windborne ash as a guide to atmospheric circulation in the geologic past: *Journal of Geophysical Research*, v. 68, p. 521-528.
- Embley, R. W., and Jacobi, R. D., 1977, Distribution and morphology of large submarine sediment slides and slumps on Atlantic continental margins: *Marine Geotechnology, Volume 2, Marine Slope Stability*, p. 205-228.
- Engdahl, E. R., and Scholz, C. H., 1977, A double Benioff zone beneath the central Aleutians: an unbending of the lithosphere: *Geophysical Research Letters*, v. 4, no. 10, p. 473-476.
- Engelbreetsen, D. C., Cox, A., and Gordon, R. G., 1985, Relative motions between oceanic and continental plates in the Pacific Basin: *Geological Society of America Special Paper 206*, 59 p.
- Evitt, W. R., 1973, Dinoflagellates from Leg 19, sites 183 and 192, Deep Sea Drilling Project, *in* Creager, J. S., Scholl, D. W., and others, eds., *Initial reports of the Deep Sea Drilling Project*, v. 19: National Science Foundation, p. 737-738.
- Fisher, D., and Byrne, T., 1987, Structural evolution of underthrusting sediments, Kodiak Island, Alaska: *Tectonics*, v. 6, no. 6, p. 775-793.
- Fisher, M. A., 1979, Structure and tectonic setting of continental shelf southwest of Kodiak Island, Alaska: *American Association of Petroleum Geologists Bulletin*, v. 63, p. 373.

- Fisher, M. A., 1980, Petroleum geology of Kodiak shelf, Alaska: *American Association of Petroleum Geologists Bulletin*, v. 64, no. 1, p. 1140-1157.
- Fisher, M. A., 1981, Location of the Border Ranges fault southwest of Kodiak Island, Alaska: *Geological Society of America Bulletin*, v. 92, p. 19-30.
- Fisher, M. A., Bruns, T. R., and von Huene, R., 1981, Transverse tectonic boundaries near Kodiak Island, Alaska: *Geological Society of America Bulletin*, v. 92, no. 1, p. 10-18.
- Fisher, M. A., and Holmes, M. L., 1980, Large-scale structure of deep strata beneath Kodiak shelf, Alaska: *Geological Society of America Bulletin, Part I*, v. 91, p. 218-224.
- Fisher, M. A., and von Huene, R., 1984, Geophysical investigation of a suture zone: the Border Ranges fault of southern Alaska: *Journal of Geophysical Research*, v. 89, no. B12, p. 11333-11351.
- Fisher, M. A., and von Huene, R., 1980, Structure of upper Cenozoic strata beneath Kodiak Island, Alaska: *American Association of Petroleum Geologists Bulletin*, v. 64, p. 1014-1033.
- Fisher, M. A., von Huene, R., and Hampton, M. A., 1984, Summary geologic report for petroleum lease sale No. 100, Kodiak shelf, Alaska: U.S. Geological Survey Open-File Report 83-24, 46 p.
- Fisher, M. A., von Huene, R., and Smith, G. L., 1987, Reflections from midcrustal rocks within the Mesozoic subduction complex near the eastern Aleutian trench: *Journal of Geophysical Research*, v. 92, no. B8, p. 7907-7915.
- Forbes, R. B., Lanphere, M. A., 1973, Tectonic significance of mineral ages of blueschists near Seldovia, Alaska: *Journal of Geophysical Research*, v. 78, no. 8, p. 1383-1386.
- Funk, J. M., 1973, Late Quaternary geology of Cold Bay, Alaska, and vicinity: Storrs, Conn., University of Connecticut, unpublished Masters thesis, 45 p.
- Galloway, W., 1979, Diagenetic control of reservoir quality in arc-derived sandstones: implications for petroleum exploration: *Society of Economic Paleontologists and Mineralogists Special Publication No. 26*, p. 251-262.
- Gedney, L., and Davies, J. N., 1986, Additional evidence for down-dip tension in the Pacific plate beneath central Alaska: *Bulletin of the Seismological Society of America*, v. 76, no. 5, p. 1207-1214.
- Gordon, J. M., and Barker, L. H., 1986, Barbados, in Wiman, W. D., 1986, Oil and gas developments in South America, Central America, Caribbean area, and Mexico in 1985: *American Association of Petroleum Geologists Bulletin*, v. 70, no. 10, p. 1372.
- Gromme, C. S., and Hillhouse, S. W., 1981, Paleomagnetic evidence for northward movement of the Chugach terrane, southern and southeastern Alaska: U.S. Geological Survey Circular 823-B, p. B70-B72.
- Grow, J. A., and Atwater, T., 1970, Mid-Tertiary tectonic transition in the Aleutian Arc: *Geological Society of America Bulletin*, v. 81, p. 3715-3722.
- Grubbs, B. E., and McCollum, R. D., Jr., 1968, A climatological guide to Alaskan weather. An unpublished report, Scientific Services Section, 11th Weather Squadron, Elmendorf Air Force Base, Alaska.
- Guttman, N. B., 1975, Study of fog and stratus for selected cold regions: Asheville, North Carolina, U.S. Naval Weather Service Command, National Climate Center, 85 p.
- Hamilton, E. L., 1973, Marine geology of the Aleutian abyssal plain: *Marine Geology*, v. 14, p. 295-325.

- Hamilton, T. D., and Thorson, R. M., 1983, The Cordilleran ice sheet in Alaska, *in* Porter, S. C., ed., Late Quaternary environments of the United States, v. 1, The Late Pleistocene: Minneapolis, University of Minnesota Press, p. 38-52.
- Hampton, M. A., and Kvenvolden, K. A., 1981, Geology and geochemistry of gas-charged sediment on Kodiak shelf, Alaska: *Geo-Marine Letters*, v. 1, p. 141-147.
- Harbert, W., 1987, New paleomagnetic data from the Aleutian Islands: implications for terrane migration and deposition of the Zodiac fan: *Tectonics*, v. 6, p. 585-602.
- Harbert, W., Scholl, D. W., Vallier, T. L., Stevenson, A. J., and Mann, D. M., 1986, Major evolutionary phases of a forearc basin of the Aleutian terrace: relation to North Pacific tectonic events and the formation of the Aleutian subduction complex: *Geology*, v. 14, p. 757-761.
- Harding, T. P., Vierbuchen, R. C., and Christie-Blick, N., 1984, Structural styles, plate-tectonic settings, and hydrocarbon traps of divergent wrench faults, *in* Strike-slip deformation, basin formation, and sedimentation, Society of Economic Paleontologists and Mineralogists, Special Publication No. 37.
- Hartmann, D. L., 1974, Time spectral analysis of mid-latitude disturbances: *Monthly Weather Review*, v. 102, p. 348-362.
- Hasebe, K., Fujii, N., and Uyeda, S., 1970, Thermal processes under island arcs: *Tectonophysics*, v. 10, p. 335-355.
- Hauksson, E., Armbruster, J., and Dobbs, S., 1984, Seismicity patterns (1963-1983) as stress indicators in the Shumagin seismic gap, Alaska: *Bulletin of the Seismological Society of America*, v. 74, no. 6, p. 2541-2558.
- Hayes, D. E., and Pitman, W. C., III, 1970, Magnetic lineations in the north Pacific, *in* Hays, J. D., ed., Geological investigations of the North Pacific: Geological Society of America Memoir 126, p. 291-314.
- Hays, J. D., and Ninkovich, D., 1970, North Pacific deep-sea ash chronology and age of present Aleutian underthrusting, *in* Hays, J. D., ed., Geological investigations of the North Pacific: Geological Society of America Memoir 126, p. 263-290.
- Herman, B. M., Comer, D. C., Hoose, P. J., Steffy, D. A., and Zerwick, S. A., 1987, Tertiary wrench faulting on the Bering Sea shelf [abs.]: *EOS, Transactions, American Geophysical Union*, v. 68, no. 16, April 21, p. 423-424.
- Heusser, C. J., 1983, Pollen diagrams from the Shumagin Islands and adjacent Alaska Peninsula, southwestern Alaska: *Boreas*, v. 12, no. 4, p. 279-295.
- Hill, M. D., 1978, Volcanic and plutonic rocks of the Kodiak-Shumagin shelf, Alaska: subduction deposits and near-trench magmatism: Santa Cruz, Calif., University of California, Ph.D. dissertation.
- Hillhouse, J. W., 1987, Accretion of southern Alaska: *Tectonophysics*, v. 139, p. 107-122.
- Holmes, M. L., 1979, Distribution of gas-charged sediment in Norton Sound and Chirikov basin, *in* Environmental assessment of the Alaskan continental shelf, annual reports of principal investigators for the year ending March 1979, v. 10: U.S. National Oceanic and Atmospheric Administration, Outer Continental Shelf Environmental Assessment Program, p. 75-94.
- Holmes, M. L., Cline, J. D., and Johnson, J. L., 1978, Geological setting of the Norton basin gas seep: Offshore Technology Conference, 10th, Houston, Texas, 1978, Proceedings, v. 1, p. 73-80, OTC 3056.
- Holmes, M. L., Meader, C. A., and Creager, K. C., 1978, Sonobuoy refraction data near Kodiak, Alaska: U.S. Geological Survey Open-File Report 78-368, 9 p.

- Hoose, P. J., 1987, Wrench-fault tectonics: S.E. Bering Sea shelf [abs.]: EOS, Transactions, American Geophysical Union, v. 68, no. 16, p. 423.
- Hoose, P. J., Ashenfelter, K. H., Lybeck, L. D., and House, M. J., 1984, Prelease investigation maps of the North Aleutian shelf, Outer Continental Shelf, Bering Sea, Alaska: U.S. Minerals Management Service, MMS Map Series 84-0002, 5 maps.
- Horowitz, W. L., and Steffy, D. A., 1988, Oblique strike-slip fault movement within Shumagin basin, Alaska [abs.]: 1988 Cordilleran Geological Society of America Meeting, Las Vegas, Nevada, March, Abstracts with program, p. 170.
- House, L. S., and Jacob, K. H., 1983, Earthquakes, plate subduction, and stress reversals in the eastern Aleutian Arc: *Journal of Geophysical Research*, v. 88, no. B11, p. 9347-9373.
- House, L. S., Sykes, L. R., Davies, J. N., and Jacob, K. H., 1981, Evidence for a possible seismic gap near Unalaska Island in the eastern Aleutians, Alaska, *in* Simpson, D. W., and Richards, P. G., eds., Earthquake prediction, An international review: American Geophysical Union, Maurice Ewing Series, v. 4, p. 81-92.
- Hubbert, M. K., and Rubey, W. W., 1960, Role of fluid pressure in the mechanics of overthrust faulting: *Geological Society of America Bulletin*, v. 71, p. 617-628.
- Hudnut, K. W., and Taber, J. J., 1987, Transition from double to single Wadati-Benioff zone in the Shumagin Islands, Alaska: *Geophysical Research Letters*, v. 14, no. 2, p. 143-146.
- Hudson, T., Plafker, G., and Pcterman, Z. E., 1979, Paleogene anatexis along the Gulf of Alaska margin: *Geology*, v. 7, p. 573-577.
- Hunt, J. M., 1979, Petroleum geochemistry and geology: San Francisco, W. H. Freeman and Company, 617 p.
- Isacks, B. L., and Barazangi, M., 1977, Geometry of Benioff zones: lateral segmentation and downwards bending of the subducted lithosphere, *in* Talwani, M., and Pitman, W. C., III, eds., Island arcs, deep sea trenches, and back-arc basins: American Geophysical Union, Maurice Ewing Series, v. 1, p. 99-114.
- Jackson, D., and others, 1978, Drilling confirms hot-spot origins: *Geotimes*, v. 23, no. 2, p. 23-26.
- Jacob, K. H., 1983, Aleutian seismic gaps quantified: high probability for great Shumagin earthquake in next 10 years [abs.]: EOS, Transactions, American Geophysical Union, v. 64, no. 18, p. 258.
- Jacob, K. H., 1984, Estimates of long-term probabilities for future great earthquakes in the Aleutians: *Geophysical Research Letters*, v. 11, no. 4, p. 295-298.
- Jacob, K. H., and Hauksson, E., 1986, A seismotectonic analysis of the seismic and volcanic hazards in the Pribilof Islands-eastern Aleutian Islands region of the Bering Sea, *in* Outer Continental Shelf Environmental Assessment Program, final reports of principal investigators, v. 49: U.S. National Oceanic and Atmospheric Administration, p. 135-367.
- Jones, D. L., and Clark, S. H. P., 1973, Upper Cretaceous (Macstrichtian) fossils from the Kenai-Chugach Mountains, Kodiak and Shumagin Islands, southern Alaska: U.S. Geological Survey *Journal of Research*, v. 1, p. 125-136.
- Jones, D. L., Silberling, N. J., Berg, H. C., and Plafker, G., 1981, Map showing tectonostratigraphic terranes of Alaska, columnar sections, and summary description of terranes: U.S. Geological Survey Open-File Report 81-792, 20 p., 2 sheets.

- Kanamori, H., 1977, The energy release in great earthquakes: *Journal of Geophysical Research*, v. 82, no. 20, p. 2981-2987.
- Karig, D. E., and Sharman, G. F., III, 1975, Subduction and accretion in trenches: *Geological Society of America Bulletin*, v. 86, p. 377-389.
- Karlstrom, T. N. V., and others, 1964, Surficial geology of Alaska: U.S. Geological Survey Miscellaneous Geologic Investigations Map I-357, scale 1:1,584,000, two oversized sheets.
- Kawakatsu, H., 1986, Double seismic zones: kinematics: *Journal of Geophysical Research*, v. 91, no. B5, p. 4811-4825.
- Kehle, R. O., 1973, Geothermal gradient of North and South America (portfolio map area no. 26): *American Association of Petroleum Geologists*, scale 1:1,000,000, 1 oversized sheet.
- Kelleher, J. A., 1970, Space-time seismicity of the Alaska-Aleutian seismic zone: *Journal of Geophysical Research*, v. 75, no. 29, p. 5745-5756.
- Kelleher, J. A., Sykes, L., and Oliver, J., 1973, Possible criteria for predicting earthquake locations and their application to major plate boundaries of the Pacific and the Caribbean: *Journal of Geophysical Research*, v. 78, no. 14, p. 2547-2585.
- Keller, G., von Huene, R. E., McDougall, K., and Bruns, T. R., 1984, Paleoclimatic evidence for Cenozoic migration of Alaskan terranes: *Tectonics*, v. 3, p. 473-495.
- Kowalik, Z., and Murty, T. S., 1987, Influence of the size, shape, and orientation of the earthquake source area in the Shumagin seismic gap on the resulting tsunami: *Journal of Physical Oceanography*, v. 17, p. 1057-1062.
- Kulm, L. D., von Huene, R., and others, 1973, Initial reports of the Deep Sea Drilling Project, v. 18: *National Science Foundation*, v. 18, 1077 p.
- Kvenvolden, K. A., and McMennamin, M. A., 1980, Hydrates of natural gas: a review of their geologic occurrence: *U.S. Geological Survey Circular* 825, 11 p.
- Kvenvolden, K. A., and von Huene, R., 1985, Natural gas generation in sediments of the convergent margin of the eastern Aleutian Trench area, in Howell, D. G., ed., *Tectonostratigraphic terranes of the Circum-Pacific region*: *Circum-Pacific Council for Energy and Mineral Resources, Earth Science Series No. 1*, p. 31-49.
- Larson, J., Calderwood, K., Crandall, R., Rogers, J., and Sisson, A., 1985, Offshore to onshore stratigraphic correlation section Middleton Island #1 to Chaix Hills #1, Eastern Gulf of Alaska: *Alaska Geological Society*, P.O. Box 101288, Anchorage, AK 99510, scale 1:6000, 1 oversized sheet.
- Larue, D. K., 1985, Quartzose turbidites of the accretionary complex of Barbados, II: variations in bedding styles, facies, and sequences: *Sedimentary Geology*, v. 42, p. 217-253.
- Larue, D. K., Schoonmaker, J., Torrini, R., Clark, J. L., Clark, M., and Schneider, R., 1985, Barbados: maturation, source rock potential, and burial history within a Cenozoic accretionary complex: *Marine and Petroleum Geology*, v. 2, p. 96-110.
- Larue, D. K., and Speed, R. C., 1983, Quartzose turbidites of the accretionary complex of Barbados, I: Chalky Mount succession: *Journal of Sedimentary Petrology*, v. 53, no. 4, p. 1337-1352.
- Levin, F. K., 1978, The reflection, refraction, and diffraction of waves in media with an elliptical velocity dependence: *Geophysics*, v. 43, no. 3, p. 528-532.

- Lewis, K. B., 1971, Slumping on a continental slope inclined at 1-4 degrees: *Sedimentology*, v. 16, no. 1, p. 97-110.
- Lewis, K. B., Ladd, J. W., Bruns, T. R., 1988, Structural development of an accretionary prism by thrust and strike-slip faulting: Shumagin region, Aleutian Trench: *Geological Society of America Bulletin*, v. 100, p. 767-782.
- Lewis, K. B., Ladd, J. W., Bruns, T. R., and von Huene, R., 1986, Structural development of the accretionary prism, Shumagin region of the Aleutian Trench, from SEABEAM and seismic reflection surveys [abs.]: *EOS, Transactions, American Geophysical Union*, v. 67, p. 1197.
- Little, T., Blome, C. D., and Wolfe, J. A., 1986, Paleocene-Eocene sedimentation and wrench tectonics along the Border Ranges Fault system, northcentral Chugach Mountains, Alaska [abs.]: 82nd annual meeting of Geological Society of America Cordilleran Section, Abstracts with programs, p. 127.
- Lonsdale, P., 1988, Paleogene history of the Kula plate: offshore evidence and onshore implications: *Geological Society of America Bulletin*, v. 100, p. 733-754.
- Lowell, J. D., 1985, *Structural styles in petroleum exploration*: Oil & Gas Consultants International, Inc., Publications, Tulsa, 460 p.
- Lyle, W., Morehouse, J., Palmer, I. F., Bolm, J. G., Moore, G. W., and Nilsen, T. H., 1978, Tertiary formations in the Kodiak Island area, Alaska, and their petroleum reservoir and source-rock potential: State of Alaska Department of Natural Resources Open-File Report 114, 56 p.
- MacKevett, E.M., Jr., and Plafker, G., 1974, The Border Ranges fault in south-central Alaska: *U.S. Geological Survey Journal of Research*, v. 2, p. 323-329.
- MacLeod, M. K., 1982, Gas hydrates in ocean bottom sediments: *American Association of Petroleum Geologists Bulletin*, v. 66, p. 2649-2662.
- Magoon, L. B., 1986, Present-day geothermal gradient, *in* Magoon, L. B., ed., *Geologic studies of the Lower Cook Inlet COST No. 1 well, Alaska Outer Continental Shelf*: U.S. Geological Survey Bulletin 1596, p. 41-46.
- Magoon, L. B., and Egbert, R. M., 1986, Framework geology and sandstone composition, *in* Magoon, L. B., ed., *Geologic studies of the Lower Cook Inlet COST No. 1 well, Alaska Outer Continental Shelf*: U.S. Geological Survey Bulletin No. 1596, p. 65-90.
- Mancini, E. A., Deeter, T. M., and Wingate, F. H., 1978, Upper Cretaceous arc trench gap sedimentation on the Alaska Peninsula: *Geology*, v. 6, p. 437-439.
- Marincovich, L., Jr., 1983, Molluscan paleontology, paleoecology, and north Pacific correlations of Miocene Tachilni Formation, Alaska Peninsula, Alaska: *Bulletin of American Paleontology*, v. 84, no. 317, p. 59-155.
- Marincovich Jr., L., 1988, Recognition of an earliest middle Micoene warm-water event in a southwestern Alaskan molluscan fauna: *Saito Ho-on Kai Special Publication, Professor T. Kotaka Commemorative Volume*, August 25, p. 1-24.
- Marlow, M. S., and Cooper, A. K., 1980, Mesozoic and Cenozoic structural trends under southern Bering Sea shelf: *American Association of Petroleum Geologists Bulletin*, v. 64, no. 12, p. 2139-2155.
- Marlow, M. S., Gardiner, J. V., Vallier, T. L., McLean, H., Scott, E. W., and Lynch, M. B., 1979, Resource report on the proposed OCS Lease Sale No. 70, St. George basin shelf area, Alaska: *U.S. Geological Survey Open-File Report 79-1650*, 79 p.

- Marlow, M. S., Scholl, D. W., Buffington, E. C., and Alpha, T. R., 1973, Tectonic history of the central Aleutian Arc: *Geologic Society of America Bulletin*, v. 84, p. 1555-1574.
- Marlow, M. S., Scholl, D. W., Cooper, A. K., and Buffington, E. C., 1976, Structure and evolution of Bering Sea shelf south of St. Lawrence Island: *American Association of Petroleum Geologists Bulletin*, v. 60, p. 161-83.
- Masclé, A., and others, 1988, *Proceedings of the Ocean Drilling Program*, v. 110, Part A, Initial Report, Barbados Ridge: Ocean Drilling Program, Texas A & M University, in cooperation with the National Science Foundation and Joint Oceanographic Institution, Inc., 603 p.
- Matsuda, T., and Uyeda, S., 1971, On the Pacific-type orogeny and its model: extension of the paired belts concept and possible origin of marginal seas: *Tectonophysics*, v. 5, p. 5-217.
- McCann, W. R., Nishenko, S. P., Sykes, L. R., and Krause, J., 1979, Seismic gaps and plate tectonics: seismic potential of major boundaries: *Pure and Applied Geophysics*, v. 117, p. 1082-1147.
- McCarthy, J., and Scholl, D. W., 1985, Mechanisms of subduction-accretion along the central Aleutian Trench: *Geological Society of America Bulletin*, v. 96, p. 691-701.
- McClellan, P. H., Arnal, R. E., Barron, J. A., von Huene, R. E., Fisher, M. A., and Moore, G. W., 1980, Biostratigraphic results of dart-coring in the western Gulf of Alaska, and their tectonic implications: U.S. Geological Survey Open-File Report 80-63.
- McKenzie, D. P., and Sclater, J. G., 1968, Heat flow inside the island arcs of the northwest Pacific: *Journal of Geophysical Research*, v. 73, p. 3172-3179.
- McLean, H., 1977, Organic geochemistry, lithology, and paleontology of Tertiary and Mesozoic rocks from wells on the Alaska Peninsula: U.S. Geological Survey Open-File Report 77-813, 63 p.
- McLean, H., 1979, Observations on the geology and the petroleum potential of the Cold Bay-False Pass area, Alaska Peninsula: U.S. Geological Survey Open-File Report 79-1605, 34 p.
- McLean, Hugh, Engelhardt, C. L., and Howell, D. C., 1978, Reconnaissance geologic map of the Cold Bay and False pass quadrangle, Alaska: U.S. Geological Survey Open-File Report 78-323, scale 1:250,000.
- McLeod, M. K., 1982, Gas hydrates in ocean bottom sediments: *American Association of Petroleum Geologists Bulletin*, v. 66, no. 12, p. 2649-2662.
- Miller, T. P., and Smith, R. L., 1977, Spectacular mobility of ash flows around Aniakchak and Fisher calderas, Alaska: *Geology*, v. 5, p. 173-176.
- Minster, J. B., and Jordan, T. H., 1978, Present-day plate motions: *Journal of Geophysical Research*, v. 83, p. 5331-5354.
- Mitra, S., 1986, Duplex structures and imbricate thrust systems: geometry, structural position, and hydrocarbon potential: *American Association of Petroleum Geologists Bulletin*, v. 70, p. 1087-1112.
- Molnia, B. F., 1986, Glacial history of the northeastern Gulf of Alaska - a synthesis, *in* Hamilton, T. D., Reed, K. M., and Thorsen, R. M., eds., *Glaciation in Alaska - the geologic record*: Alaska Geological Society, P.O. Box 101288, Anchorage, Alaska, 99510, p. 219-235.
- Molnia, B. F., and Sangrey, D. A., 1979, Glacially derived sediments in the northern Gulf of Alaska - geology and engineering characteristics: *Offshore Technology Conference*, 11th, Proceedings, Houston, Texas, v. 1, p. 647-655, OTC 3433.

- Moore, G. W., 1969, New formations on Kodiak and the adjacent islands, Alaska: U.S. Geological Survey Bulletin 1247-A, p. A28-A35.
- Moore, J. C., 1971, Geologic studies of the Cretaceous(?) flysch southwestern Alaska: Princeton, New Jersey, Princeton University, Ph.D. dissertation.
- Moore, J. C., 1973, Complex deformation of Cretaceous trench deposits, southwestern Alaska: Geological Society of America Bulletin, v. 84, p. 2005-2020.
- Moore, J. C., 1974a, Geologic and structural map of part of the outer Shumagin Islands, southwestern Alaska: U.S. Geological Survey Miscellaneous Investigations Series Map I-815, scale 1:63,360, 1 oversized sheet.
- Moore, J. C., 1974b, Geologic and structural map of the Sanak Islands, southwestern Alaska: U.S. Geological Survey Miscellaneous Investigations Series Map I-817, scale 1:63,360, 1 oversized sheet.
- Moore, J. C., 1978, Orientation of underthrusting during latest Cretaceous and earliest Tertiary time, Kodiak Islands, Alaska: *Geology*, v. 6, p. 209-213.
- Moore, J. C., and Allwardt, A., 1980, Progressive deformation of a Tertiary trench slope, Kodiak Islands, Alaska: *Journal of Geophysical Research*, v. 85, p. 4741-4756.
- Moore, J. C., and Byrne, T., 1987, Thickening of fault zones: a mechanism of melange formation in accreting sediments: *Geology*, v. 15, p. 1040-1043.
- Moore, J. C., Byrne, T., Plumley, P. W., Reid, M., Gibbons, H., and Coe, R. S., 1983, Paleogene evolution of the Kodiak Islands, Alaska: consequences of ridge-trench interactions in a more southerly latitude: *Tectonics*, v. 2, no. 3, p. 265-293.
- Morley, C. K., 1986, A classification of thrust fronts: *American Association of Petroleum Geologists Bulletin*, v. 70, no. 1, p. 12-25.
- Muench, R. D., and Schumacher, J. D., 1980, Physical oceanographic and meteorological conditions in the northwest Gulf of Alaska: U.S. National Oceanic and Atmospheric Administration Technical Memorandum ERL PMEL-22, Pacific Marine Environmental Laboratory, Seattle, 147 p.
- Muller, E. H., 1953, Northern Alaska Peninsula and eastern Kilbuck Mountains, Alaska, *in* Pewe, T. L., and others, eds., *Multiple glaciation in Alaska*: U.S. Geological Survey Circular 289, p. 2-3.
- Nelson, C. H., Kvenvolden, K. A., and Clukey, E. C., 1978, Thermogenic gases in near-surface sediments of Norton Sound, Alaska: *Offshore Technology Conference*, 10th, Houston, Texas, 1978, *Proceedings*, v. IV, p. 2623-2633, OTC 3354.
- Nelson, C. H., Thor, D. R., Sandstrom, M. W., and Kvenvolden, K. A., 1979, Modern biogenic gas-generated craters (sea-floor "pockmarks") on the Bering shelf, Alaska: *Geological Society of America Bulletin*, Part I, v. 90, no. 12, p. 1144-1152.
- Nilsen, T. H., and Moore, G. W., 1979, Reconnaissance study of Upper Cretaceous to Miocene stratigraphic units and sedimentary facies, Kodiak and adjacent islands, Alaska: U.S. Geological Survey Professional Paper 1093, 33 p.
- Overland, J. E., and Heister, T. R., 1980, Development of a synoptic climatology for the northeast Gulf of Alaska: *Journal of Applied Meteorology*, v. 19, p. 1-14.

- Pavlis, T. L., and Bruhn, R. L., 1983, Deep-seated flow as a mechanism for the uplift of broad forearc ridges and its role in the exposure of high P/T metamorphic terranes: *Tectonics*, v. 2, no. 5, p. 473-497.
- Peter, G., Erickson, B. H., and Grim, P. U., 1971, Magnetic structure of the Aleutian Trench and northeast Pacific basin, *in* Maxwell, A. E., ed., *The Sea*: New York, Wiley-Interscience, p. 191-222.
- Pettijohn, F. J., Potter, P. E., and Siever, R., 1972, *Sand and sandstone*: New York, Springer-Verlag, 618 p.
- Pitman, W. C., III, and Andrews, J. A., 1985, Subsidence and thermal history of small pull-apart basins: strike-slip deformation, basin formation, and sedimentation: *Society of Economic Paleontologists and Mineralogists Special Publication 37*, p. 45-49.
- Pitman, W. C., III, and Hayes, D. E., 1968, Sea-floor spreading in the Gulf of Alaska: *Journal of Geophysical Research*, v. 73, p. 6571-6580.
- Plafker, G., 1965, Tectonic deformation associated with the 1964 Alaska earthquake: *Science*, v. 148, p. 1675-1687.
- Plafker, G., 1971, Pacific margin Tertiary basin, *in* *Petroleum provinces of North America*: American Association of Petroleum Geologists Memoir 15, p. 120-135.
- Plafker, G., 1987, Regional geology and petroleum potential of the northern Gulf of Alaska continental margin, *in* Scholl, D. W., Grantz, A., and Vedder, J. G., eds., *Geology and resource potential of the continental margin of western North America and adjacent ocean basins*: Circum-Pacific Council for Energy and Mineral Resources, Earth Science Series, v. 6, p. 229-268 [distributed by AAPG Bookstore, Tulsa].
- Plafker, G., and Campbell, R. B., 1979, The Border Ranges fault in the Saint Elias Mountains: U.S. Geological Survey Circular 804B, p. B102-B104.
- Plafker, G., Jones, D. L., and Pessagno, E. A., 1977, A Cretaceous accretionary flysch and melange terrane along the Gulf of Alaska margin, *in* Blean, K. M., ed., *The United States Geological Survey in Alaska: accomplishments during 1976*: U.S. Geological Survey Circular 751-B, p. 41-43.
- Plafker, G., Keller, G., Barron, J. A., and Blueford, J. R., 1985, Paleontological data on the age of the Orca Group, Alaska: U.S. Geological Survey Open-File Report 85-429, 23 p.
- Plafker, G., and Rubin, M., 1967, Vertical tectonic displacements in southcentral Alaska during and prior to the great 1964 earthquake: *Journal of Geoscience*, Osaka City University, p. 50-52.
- Platt, J. P., Young, J., Leggett, J. K., Alam, S., and Raza, H., 1985, Large-scale sediment underplating in the Makran accretionary prism, southwest Pakistan: *Geology*, v. 13, p. 507-511.
- Plumley, P. W., Coe, R. S., and Byrne, T., 1983, Paleomagnetism of the Paleocene Ghost Rocks Formation, Prince William terrane, Alaska: *Tectonics*, v. 2, p. 295-314.
- Pulpan, H., and Frohlich, C., 1985, Geometry of the subducted plate near Kodiak Island and Lower Cook Inlet, Alaska, determined from relocated earthquake hypocenters: *Bulletin of the Seismological Society of America*, v. 75, no. 3, p. 791-810.
- Rau, W. W., Plafker, G., and Winkler, G. R., 1983, Foraminiferal biostratigraphy and correlations in the Gulf of Alaska Tertiary province: U.S. Geological Survey Oil and Gas Investigations Chart OC-120, 11 p., 3 oversized plates.
- Rea, D. K., and Duncan, R. A., 1986, North Pacific plate convergence: a quantitative record of the past 140 m.y.: *Geology*, v. 14, p. 373-376.

- Reed, B. L., and Lanphere, M. A., 1973, Alaska-Aleutian Range batholith: geochronology, chemistry, and relation to the circum-Pacific plutonism: *Geological Society of America Bulletin*, v. 84, no. 8, p. 2583-2610.
- Reed, R. K., and Schumacher, J. D., 1987, Physical oceanography, *in* Hood, D. W., and Zimmerman, S. T., eds., *The Gulf of Alaska - physical environment and biological resources*: U.S. National Oceanic and Atmospheric Administration; and U.S. Minerals Management Service, OCS Study, MMS 86-0095, p. 57-75.
- Reid, M. R., and Gill, J. B., 1980, Near-trench volcanism, Kodiak Island, Alaska, implication for ridge-trench encounter [abs.]: *Geological Society of America Abstracts with Programs*, v. 12, p. 148.
- Reyners, M., and Coles, K. S., 1982, Fine structure of the dipping seismic zone and subduction mechanics in the Shumagin Islands, Alaska: *Journal of Geophysical Research*, v. 87, no. B1, p. 356-366.
- Sample, J. C., and Fisher, D. M., 1986, Duplex accretion and underplating in an ancient accretionary complex, Kodiak Islands, Alaska: *Geology*, v. 14, p. 160-163.
- Sample, J. C., and Moore, J. C., 1987, Structural style and kinematics of an underplated slate belt, Kodiak and adjacent islands, Alaska: *Geological Society of America Bulletin*, v. 99, p. 7-20.
- Savage, J. C., and Lisowski, M., 1986, Strain accumulation in the Shumagin seismic gap, Alaska: *Journal of Geophysical Research*, v. 91, no. B7, p. 7447-7454.
- Savage, J. C., Lisowski, M., and Prescott, W. H., 1986, Strain accumulation in the Shumagin and Yakataga seismic gaps, Alaska: *Science*, v. 231, p. 585-587.
- Scholl, D. W., 1974, Sedimentary sequences in the north Pacific trenches, *in* Burk, C. A., and Drake, C. L., eds., *The Geology of continental margins*: New York, Springer-Verlag, p. 493-504.
- Scholl, D. W., Buffington, E. C., and Marlow, M. S., 1975, Plate tectonics and the structural evolution of the Aleutian-Bering Sea region, *in* Forbes, R. B., ed., *Contributions to the geology of the Bering Sea basin and adjacent regions*: Geological Society of America Special Paper 151, p. 1-32.
- Scholl, D. W., and Creager, J. S., 1973, Geologic synthesis of Leg 19 (DSDP) results: far North Pacific, Aleutian Ridge, and Bering Sea, *in* Creager, J. S., Scholl, D. W., and others, eds., *Initial reports of the Deep Sea Drilling Project*, v. 19: National Science Foundation, p. 897-913.
- Scholl, D. W., Hein, J. R., Marlow, M. S., and Buffington, E. C., 1977, Meiji sediment tongue: North Pacific evidence for limited movement between the Pacific and North American plates: *Geological Society of America Bulletin*, v. 88, p. 1567-1576.
- Scholl, D. W., and Marlow, M. S., 1974, Sedimentary sequence in modern Pacific trenches and the deformed circum-Pacific eugeosyncline, *in* Dott, R. H., Jr., and Shaver, R. H., eds., *Modern and ancient geosynclinal sedimentation*: Society of Economic Paleontologists and Mineralogists Special Publication No. 19, p. 193-211.
- Seely, D. R., and Dickinson, W. R., 1977, Stratigraphy and structure of compressional margins, *in* *Geology of continental margins - a 1977 short course*: American Association of Petroleum Geologists, Education Course Note Series #5, p. C1-C23.
- Sherwood, K. W., 1987, Abnormal formation pressure, *in* Turner, R. F., ed., *Geological and operational summary, Kodiak shelf stratigraphic test wells, western Gulf of Alaska*: U.S. Minerals Management Service, OCS Report, MMS 87-0109, p. 229-252.
- Shi, Y., 1986, Pore pressure, temperature, and deformation in accretionary complexes: a coupled study on the Barbados Ridge complex: Berkley, California, University of California, Ph.D. dissertation, 393 p.

- Simkin, T., Siebert, L., McClelland, L., Bridge, D., Newhall, C., and Latter, J. H., 1981, *Volcanoes of the world*: Stroudsburg, Penn., Hutchinson Ross Publishing Co., 232 p.
- Soloviev, S. L., 1968, Sanak-Kodiak tsunami 1788: *in Problema Tsunami*, Nauka, Moscow, p. 232-237.
- Spence, W., 1977, The Aleutian Arc: tectonic blocks, episodic subduction, strain diffusion, and magma generation: *Journal of Geophysical Research*, v. 82, p. 213-230.
- Steffy, D. A., and Hoose, P. J., 1981, Map showing acoustic anomalies and near-surface faulting, Norton Sound, Alaska: U.S. Geological Survey Open-File Report 81-722, scale 1:250,000, 1 oversized sheet.
- Steffy, D. A., and Horowitz, W. L., 1987, Sanak Island Transverse High of the Shumagin continental margin, Alaska [abs.]: 1987 Cordilleran Section Meeting, Geological Society of America, Hilo, Hawaii, Abstracts with Program, p. 454.
- Steffy, D. A., and Horowitz, W. L., 1988, Inversion of the West Sanak basin, Shumagin forearc margin, Alaska [abs.]: EOS, Transactions, American Geophysical Union, v. 69, no. 16, p. 407.
- Steffy, D. A., Turner, R. F., Martin, G. C., and Flett, T. O., 1985, Evolution and petroleum geology of the Navarin basin, Bering Sea, Alaska: *Oil & Gas Journal*, Aug. 5, 1986.
- Stevenson, A. J., Scholl, D. W., and Vallier, T. L., 1983, Tectonic and geologic implications of the Zodiac Fan, Aleutian abyssal plain, northeast Pacific: *Geological Society of America Bulletin*, v. 94, p. 259-273.
- Stewart, R. J., 1976, Turbidites of the Aleutian abyssal plain - mineralogy, provenance, and constraints for Cenozoic motion of the Pacific plate: *Geological Society of America Bulletin*, v. 87, p. 793-808.
- Stone, D. B., and Packer, D. R., 1977, Tectonic implications of Alaskan Peninsula paleomagnetic data: *Tectonophysics*, v. 37, p. 183-201.
- Stone, D. B., Panuska, B. C., and Packer, D. R., 1982, Paleolatitudes versus time for southern Alaska: *Journal of Geophysical Research*, v. 87, p. 3697-3707.
- Sykes, L. R., 1971, Aftershock zones of great earthquakes, seismicity gaps, and earthquake prediction for Alaska and the Aleutians: *Journal of Geophysical Research*, v. 76, p. 8021-8041.
- Sykes, L. R., Kisslinger, J. B., House, L., Davies, J. N., and Jacob, K. H., 1980, Rupture zones of great earthquakes in the Alaska-Aleutian Arc, 1784 to 1980: *Science*, v. 210, p. 1343-1345.
- Sykes, L. R., Kisslinger, J. B., House, L., Davies, J. N., and Jacob, K. H., 1981, Rupture zones and repeat times of great earthquakes along the Alaska-Aleutian Arc, *in* Simpson, D. W., and Richards, P. G., eds., *Earthquake prediction, an international review*: American Geophysical Union, Maurice Ewing Series, v. 4, p. 1784-1980.
- Taber, J. J., Boyd, T. M., Lerner-Lam, A. L., and Beavan, J., 1987, Seismic moment release and arc segmentation within the Shumagin seismic gap, Alaska [abs.]: EOS, Transactions, American Geophysical Union, v. 68, no. 44, p. 1351.
- Thom, H. C. S., 1968, New distributions of extreme winds in the United States: *Proceedings of the American Society of Structural Engineers*, v. 68, St. 7, p. 1787. (Article also appears in the *Proceedings of the American Society of Civil Engineers*, p. 6038.)
- Thorson, R. M., and Hamilton, T. D., 1986, Glacial geology of the Aleutian Islands based on the contributions of Robert F. Black, *in* Hamilton, T. D., Reed, K. M., and Thorson, R. M., eds., *Glaciations in Alaska - the geologic record*: Alaska Geological Society, P.O. Box 101288, Anchorage, Alaska, 99510, p. 171-191.

- Thrasher, G. P., 1979, Geologic map of the Kodiak outer continental shelf, western Gulf of Alaska: U.S. Geological Survey Open-File Report 79-1267, scale 1:250,000, 2 oversized sheets.
- Thrasher, G. P., and Turner, B. W., 1980, Bathymetric map of the outer continental shelf between Yakutat Bay and Dry Bay, eastern Gulf of Alaska: U.S. Geological Survey Open-File Report 80-649, scale 1:250,000, 1 oversized sheet.
- Thrupp, G. A., and Coe, R. S., 1986, Early Tertiary paleomagnetic evidence and the displacement of southern Alaska: *Geology*, v. 14, p. 213-217.
- Tissot, B. P., and Welte, D. H., 1984, *Petroleum formation and occurrence*: New York, Springer-Verlag, 699 p.
- Tobin, D. G., and Sykes, L. R., 1968, Seismicity and tectonics of the northeast Pacific: *Journal of Geophysical Research*, v. 73, p. 3821-3843.
- Tucker, B. E., King, J. L., and Shpilker, G. L., 1981, Experimental measurements of the response of sediment-filled valleys to earthquake motion [abs.]: Abstracts IASPEI 21st General Assembly, Department of Geophysics, The University of Western Ontario, London, Canada, p. A3.31.
- Turner, B. W., Thrasher, G. P., Shearer, G. B., and Holden, K. D., 1979, Bathymetric maps of the Kodiak outer continental shelf, western Gulf of Alaska: U.S. Geological Survey Open-File Report 79-263, scale 1:250,000, 13 sheets.
- Turner, R. F., Lynch, M. B., Conner, T. A., Hallin, P. J., Hoose, P. J., Martin, G. C., Olson, D. L., Larson, J. A., Flett, T. O., Sherwood, K. W., and Adams, A. J., 1987, Geological and operational summary, Kodiak shelf stratigraphic test wells, western Gulf of Alaska: U. S. Minerals Management Service OCS Report MMS 87-0109, 341 p.
- Uyeda, S., 1977, Some basic problems in the trench-arc-back arc system, *in* Talwani, M., and Pitman, W. C., III, eds., *Island arcs, deep sea trenches, and back-arc basins*: American Geophysical Union, Maurice Ewing Series, v. 1, p. 1-14.
- Vail, P. R., Mitchum, R. M., Thompson, S., 1977, Global cycles of relative changes of sea level, *in* Payton, C. E., ed., *Seismic stratigraphy - applications to hydrocarbon exploration*: American Association of Petroleum Geologists Memoir 26, p. 49-212.
- von Huene, R., 1972, Structure of the continental margin and tectonism of the eastern Aleutian Trench: *Geological Society of America Bulletin*, v. 83, p. 3613-3636.
- von Huene, R., 1984, Tectonic processes along the front of modern convergent margins- research of the past decade: *Annual Review of Earth and Planetary Science*, v. 12, p. 359-381.
- von Huene, R., Bruns, T. R., and Childs, J. R., *in press*, Aleutian Trench, Shumagin segment, seismic section 104, part I, *in* von Huene, R., ed., *Seismic images of modern convergent margin tectonic structure*: American Association of Petroleum Geologists Studies in Geology Series.
- von Huene, R., Fisher, M. A., Bruns, T. R., and Shor, Jr., G. G., 1977, Continental margins of the Gulf of Alaska and late Cenozoic tectonic plate boundaries, *in* Sisson, A., ed., *The relationship of plate tectonics to Alaskan geology and resources*: Proceedings of the 6th Alaska Geological Society Symposium, April 4-6, Anchorage, AK, p. J1-J33.
- von Huene, R., Fisher, M. A., Hampton, M. A., and Lynch, M., 1980, Petroleum potential, environmental geology, and the technology for exploration and development of the Kodiak Lease Sale Area No. 61: U.S. Geological Survey Open-File Report 80-592, 70 p.

- von Huene, R., and Shor, G. G., Jr., 1969, The structure and tectonic history of the eastern Aleutian Trench: *Geological Society of America Bulletin*, v. 80, p. 1889-1902.
- Wallace, W. K., and Engebretson, D. C., 1984, Relationships between plate motions and Late Cretaceous to Paleogene magnetism in southwestern Alaska: *Tectonics*, v. 3, no. 2, April, p. 295-315.
- Watanabe, T., Langseth, M. G., and Anderson, R. N., 1977, Heat flow in back-arc basins of the western Pacific, *in* Talwani, M., and Pitman, W. C., III, eds., *Island arcs, deep sea trenches and back-arc basins: American Geophysical Union, Maurice Ewing Series*, v. 1, p. 137-161.
- Weber, F. R., 1985, Late Quaternary glaciation of the Pavlof Bay and Port Moller areas, Alaska Peninsula, *in* Bartsch-Winkler, S., ed., *U.S. Geological Survey in Alaska - accomplishments during 1984: U.S. Geological Survey Circular 967*, p. 42-44.
- Westbrook, G. K., Ladd, J. W., Buhl, P., Bangs, N., Tiley, G. J., 1988, Cross section of an accretionary wedge: Barbados Ridge complex: *Geology*, v. 16, p. 631-635.
- Westbrook, G. K., and Smith, M. J., 1983, Long decollements and mud volcanoes: evidence from the Barbados Ridge complex for the role of high pore-fluid pressure in the development of an accretionary complex: *Geology*, v. 11, p. 279-283.
- Westbrook, G. K., Smith, M. J., Peacock, J. H., and Poulter, M. J., 1982, Extensive underthrusting of undeformed sediment beneath the accretionary complex of the Lesser Antilles subduction zone: *Nature*, v. 300, p. 625-628.
- Whelen, T., Coleman, J. M., Roberts, H. A., and Suhayda, J. N., 1976, The occurrence of methane in recent deltaic sediments and its effect on soil stability: *International Association of Engineering Geologists Bulletin*, v. 14, p. 55-64.
- Whitney, J. W., and Wallace, W. K., 1984, Oceanic plate motions and tectonic evolution of the Bering Sea shelf [abs.]: 80th annual meeting, Cordilleran Section, Geological Society of America, May 30-June 1, 1984, Anchorage, Alaska, Abstracts with programs, p. 340.
- Wilcox, R. E., 1959, Some effects of recent volcanic ash falls with special reference to Alaska: *U.S. Geological Survey Bulletin 1028-N*, p. 409-476.
- Wilcox, R. E., Harding, T. P., and Seely, D. R., 1973, Basic wrench tectonics: *American Association of Petroleum Geologists Bulletin*, v. 57, no. 1, p. 74-96.
- Wilson, F. H., 1985, The Meshik Arc - an Eocene to earliest Miocene magmatic arc on the Alaska Peninsula: *Alaska Division of Geological and Geophysical Surveys, Professional Report 88*, 14 p.
- Wilson, F. H., Case, J. E., and Detterman, R. L., 1985, Preliminary description of a Miocene zone of structural complexity, Port Moller and Stepovak Bay quadrangles: *U.S. Geological Survey Circular No. 945*, P. 55-56.
- Wilson, F. H., Detterman, R. L., and Case, J. E., 1985, The Alaska Peninsula Terrane; a definition: *U.S. Geological Survey Open-File Report 85-450*, 17 p.
- Wilson, F. H., Detterman, R. L., Miller, J. W., and Case, J. E., 1989, Geologic map of the Port Moller, Stepovak Bay, and Simeonof Island quadrangles, Alaska: *U.S. Geological Survey Miscellaneous field studies map*, in press, 1:250,000.

- Wilson, F. H., Guam, W. C., and Herzon, P. L., 1981, Map and tables showing geochronology and whole-rock geochemistry of the Chignik and Sutwik Island quadrangles, Alaska: U.S. Geological Survey Miscellaneous Field Studies Map MF-1053-M, scale 1:250,000.
- Wilson, J. G., and Overland, J. E., 1987, Meteorology, *in* Hood, D. W., and Zimmerman, S. T., eds., The Gulf of Alaska - physical environment and biological resources: U.S. National Oceanic and Atmospheric Administration; and U.S. Minerals Management Service, OCS Study, MMS 86-0095, p. 31-54.
- Winkler, G. R., Silberman, M. L., Grantz, A., Miller, R. J., and Mackevett, E. M., Jr., 1981, Geologic map and summary geochronology of the Valdez quadrangle, southern Alaska: U.S. Geological Survey Open-File Report 80-892-A, scale 1:250,000, 2 oversized sheets.
- Wisheart, R. M., 1979, Paleoenvironmental analysis of the Bear Lake Formation (upper and middle Miocene), Alaska Peninsula: Los Angeles, Calif., University of California, M.S. thesis, 112 p.
- Wolfe, J. A., 1973, Reconnaissance spore and pollen examination, early Tertiary turbidite beds, Aleutian Abyssal Plain, Site 183, *in* Creager, J. S., Scholl, D. W., and others, eds., Initial reports of the Deep Sea Drilling Project v. 19: National Science Foundation, v. 19, p. 739.
- Worzel, J. L., 1959, Extensive deep sea bottom reflections identified as white ash: Proceedings of the National Academy of Sciences, v. 45, p. 349-355.
- Yerkes, R. F., McCulloch, T. H., Schoellhamer, J. E., and Vedder, J. G., 1965, Geology of the Los Angeles basin, California - an introduction: U.S. Geological Survey Professional Paper 420-A, 57 p.

Authors	<i>Warren L. Horowitz David A. Steffy Peter J. Hoose</i>
Editor	<i>Ronald F. Turner</i>
Principal Illustrators	<i>Linda Stromquist Rich Rothley</i>
Additional Illustrators	<i>Dennis Tayman Shawna Hampton Virginia Hoffman Kristine Stoenner Bill Chambers</i>
Graphic Designer and Typist	<i>Virginia Hoffman</i>
Copyeditor	<i>Jody Lindemann</i>
Cover Artist	<i>Jean Thomas</i>
Technical Reviewers	<i>Dennis K. Thurston Bruce M. Herman Susan Zerwick David E. Risley Drew Comer Gary Martin Kirk W. Sherwood Donald L. Olson Tabé O. Flett Maurice B. Lynch John Larson James Craig John Parker</i>

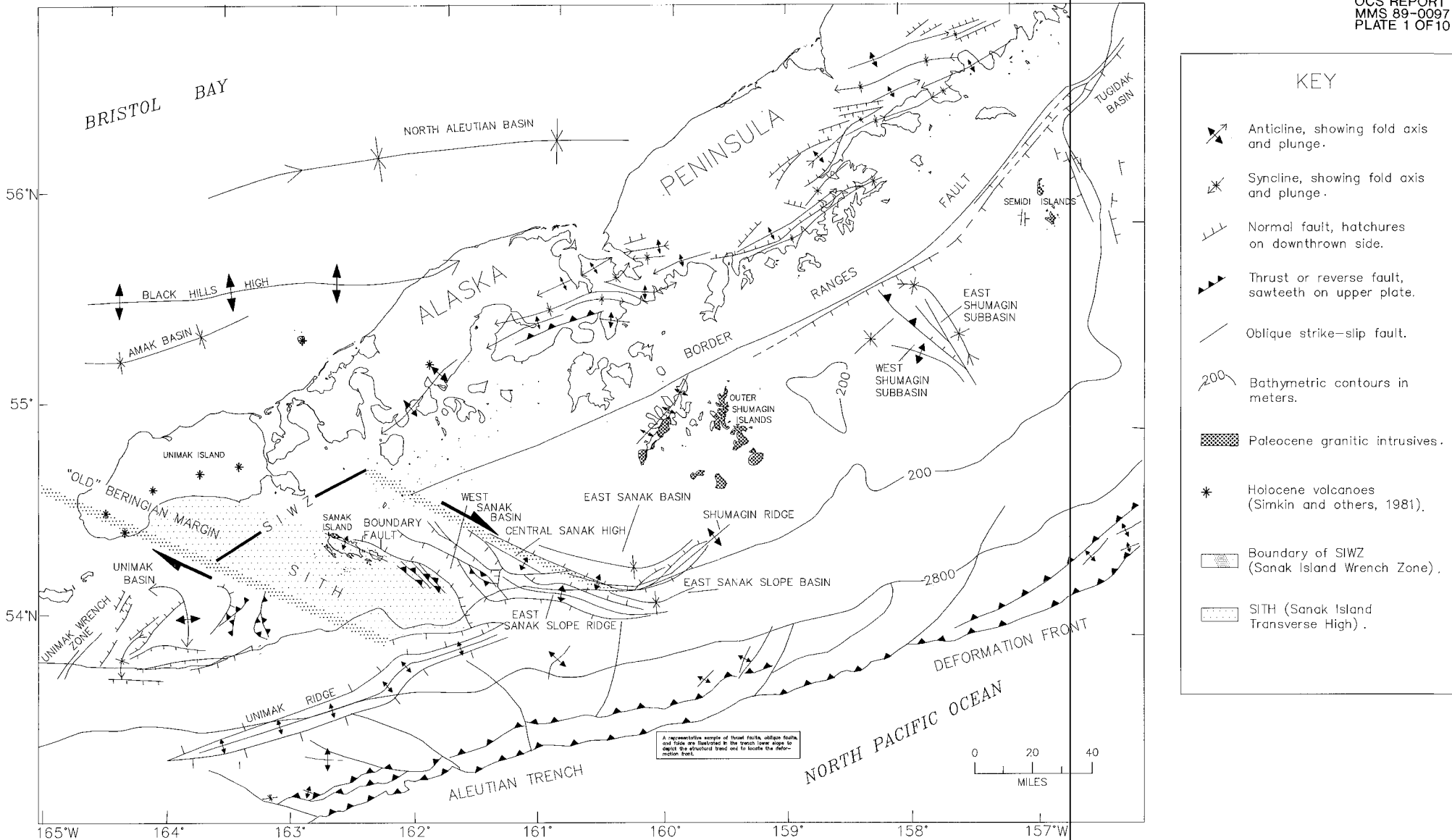


PLATE 1. Tectonic elements of the Shumagin margin and adjacent areas (adapted from McLean and others, 1978; Moore, 1974a and 1974b; Marlow and Cooper, 1980; Bruns, von Huene, and others, 1987).

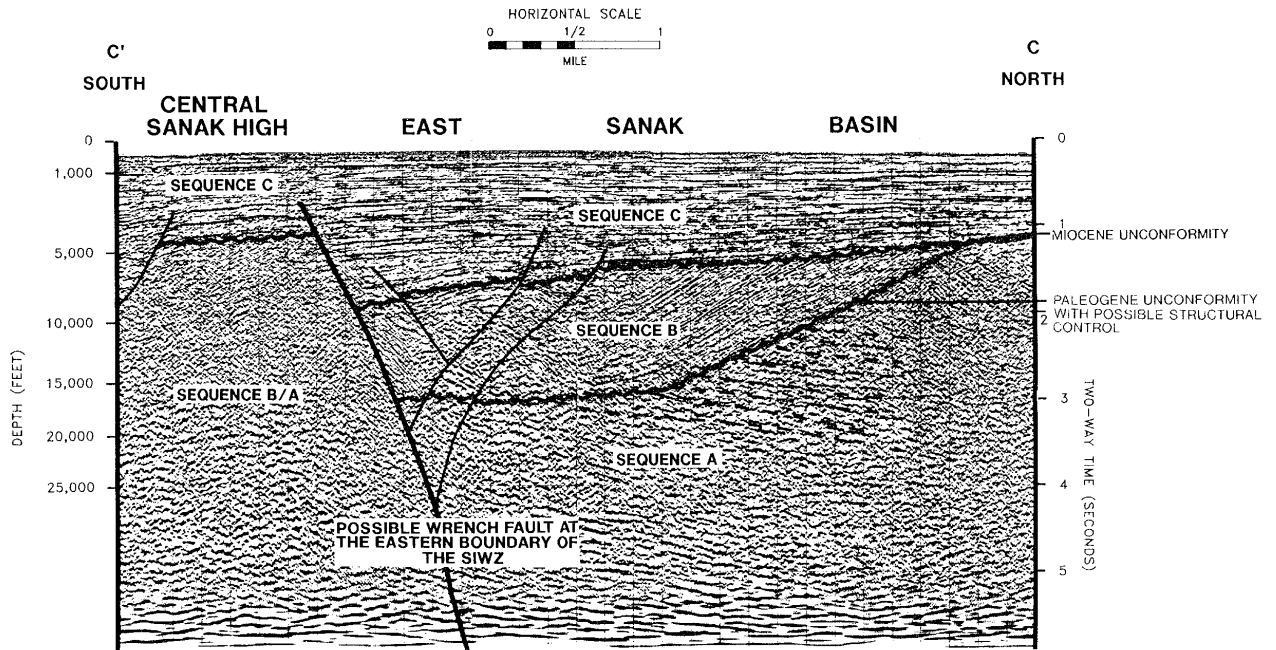
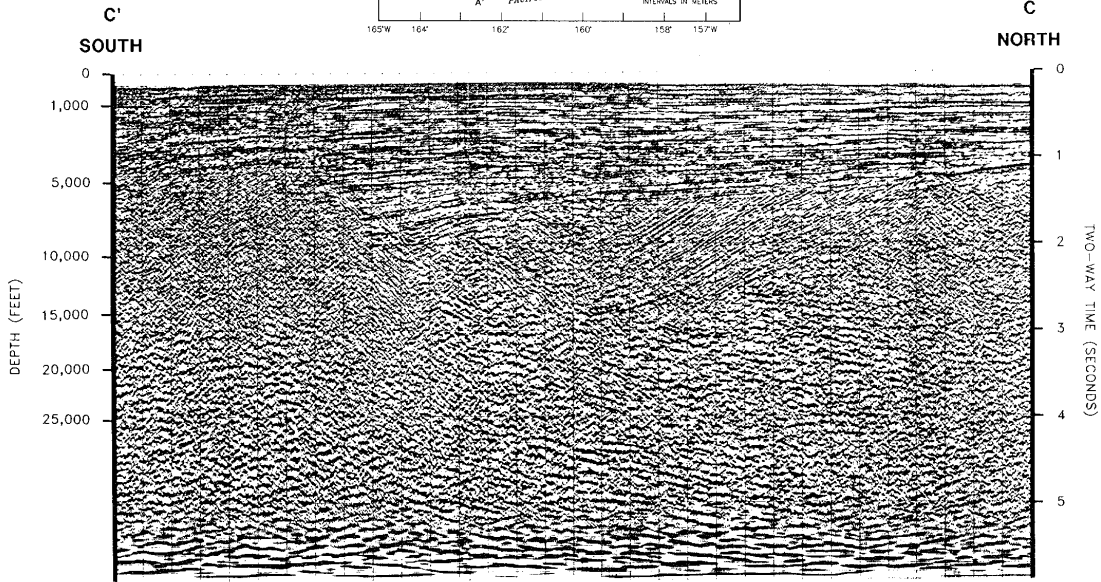
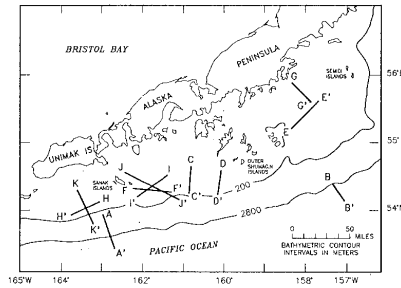


PLATE 2. Seismic-reflection profile showing the Central Sanak high and three major seismic sequences of the East Sanak basin.

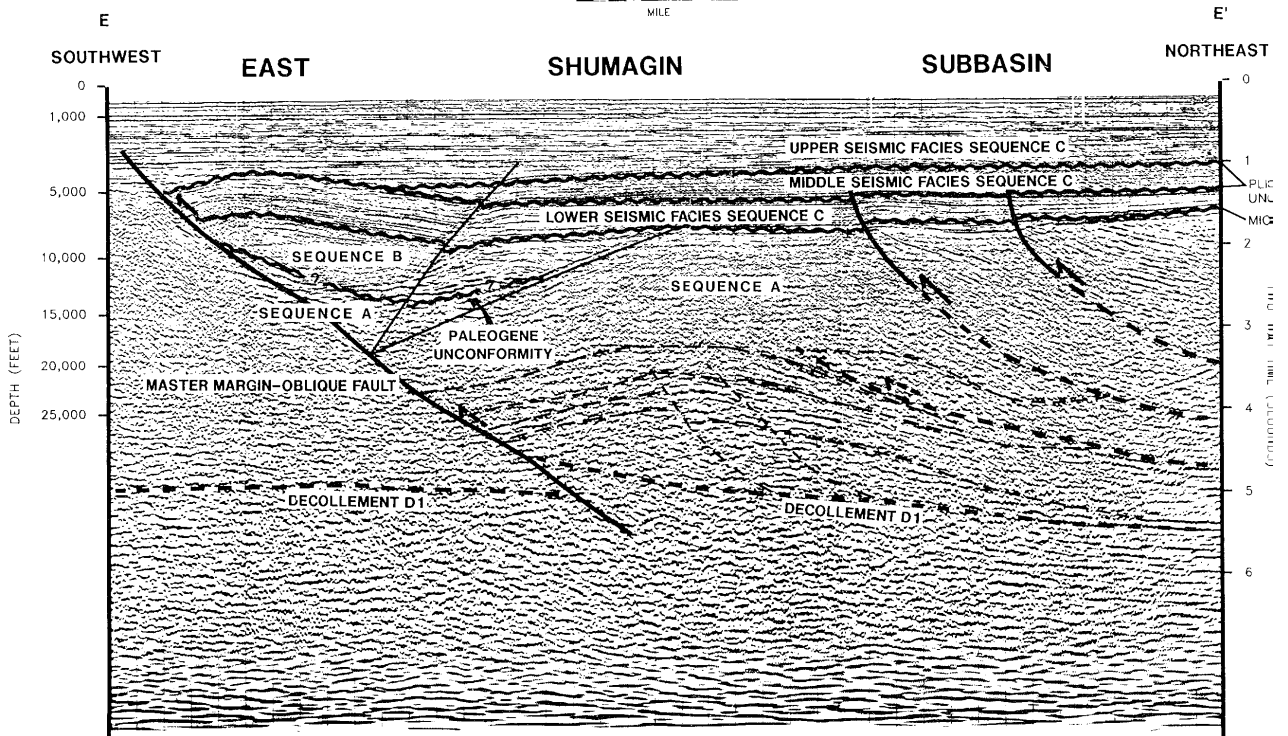
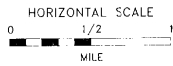
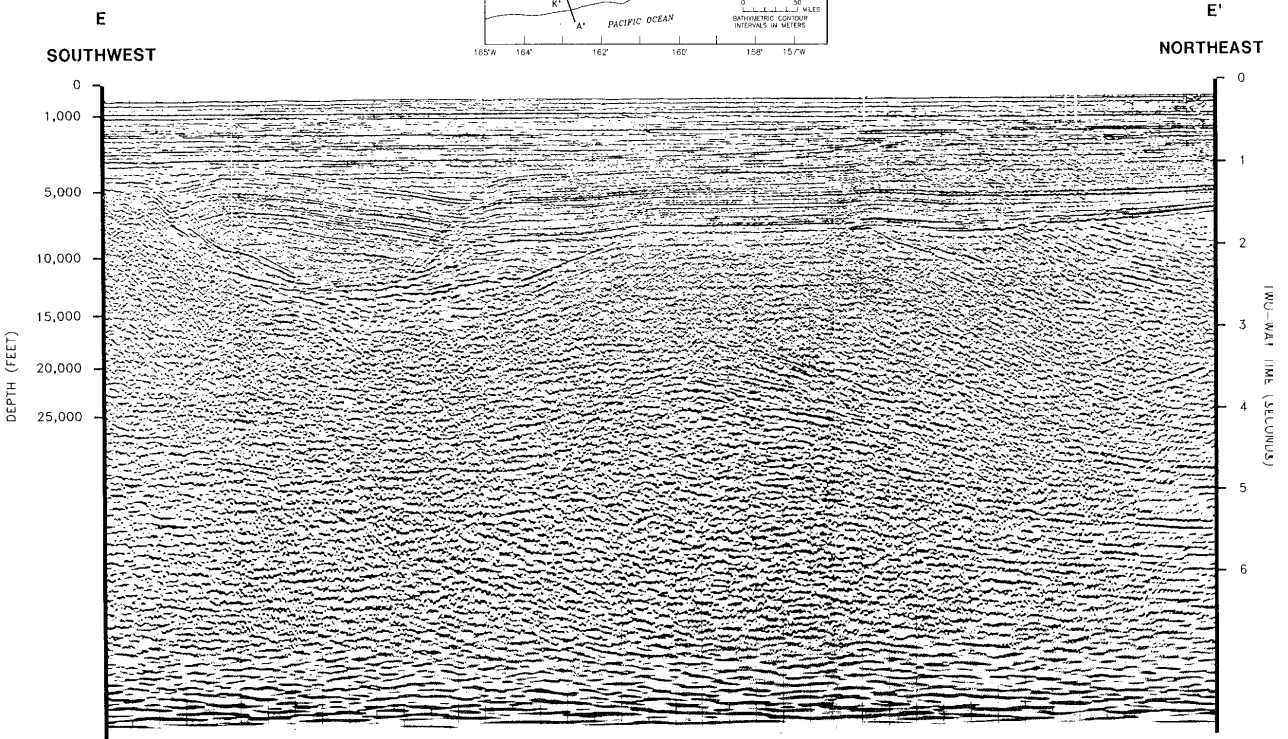
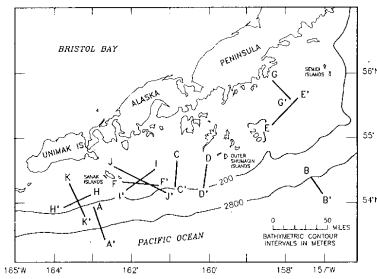


PLATE 3. Seismic-reflection profile of the East Shumagin subbasin showing the margin-oblique master fault and its splays, Neogene basement-involved thrusting, and decollement D1.

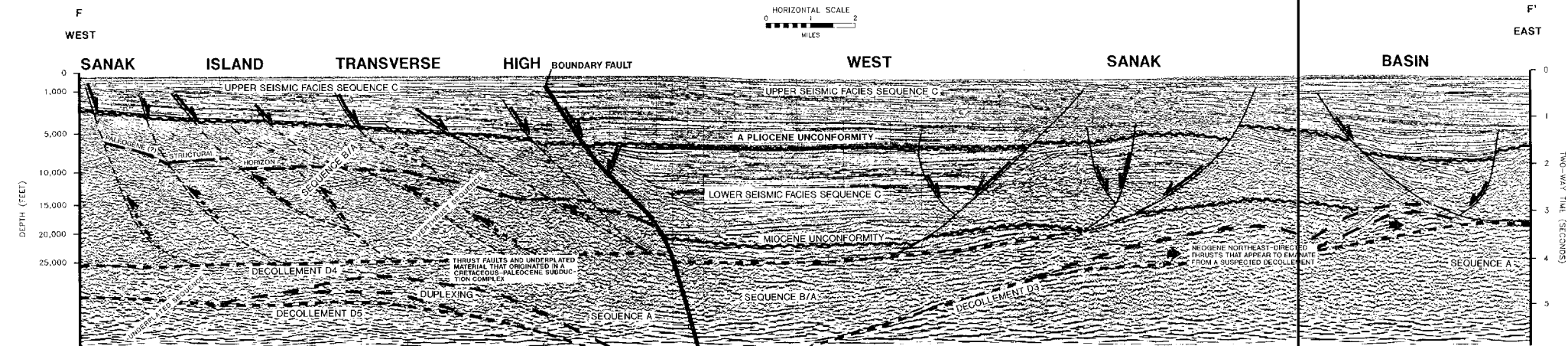
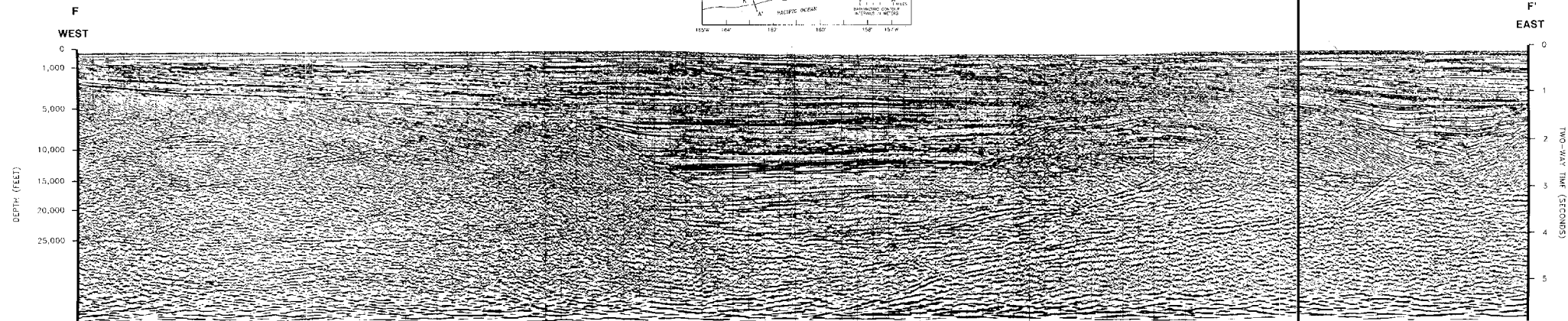
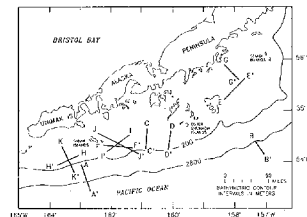


PLATE 4. Seismic-reflection profile showing the internal structure of the Sanak Island Transverse High and West Sanak basin. Decollement D4 in the Sanak Island Transverse High separates offscraped sequence B/A from underplated sequence A. The West Sanak basin displays Neogene thrusting and extensional faulting.

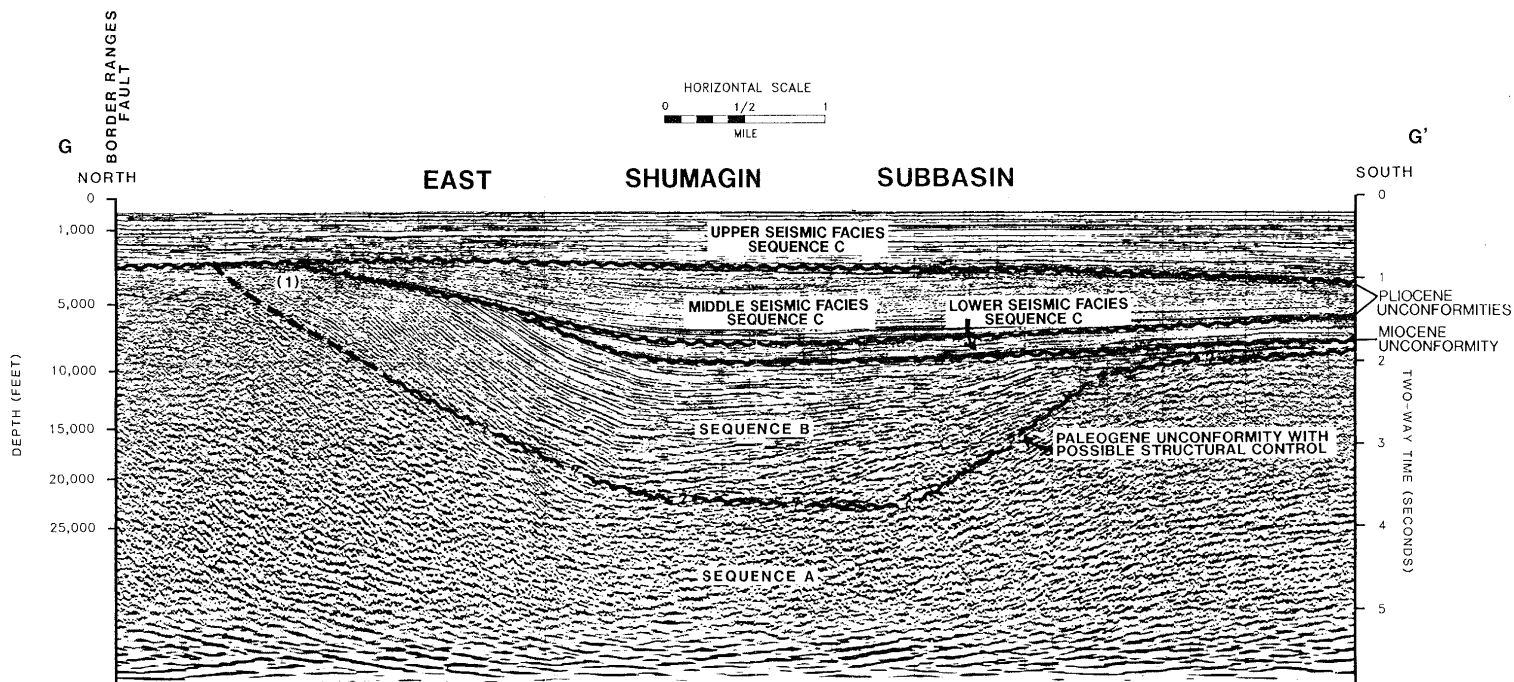
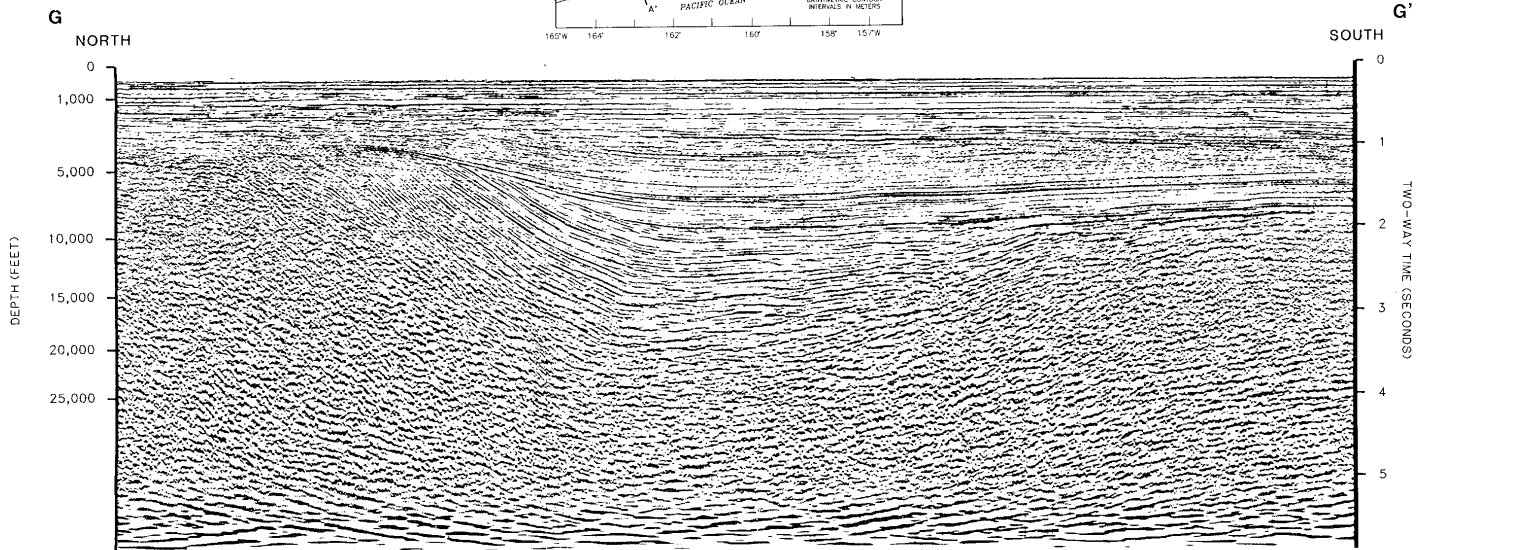
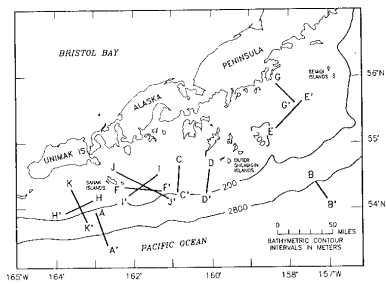


PLATE 5. Seismic-reflection profile showing the three seismic stratigraphic sequences of the East Shumagin subbasin. The truncation of seismic sequence B and the lower and middle facies of sequence C is shown at (1).

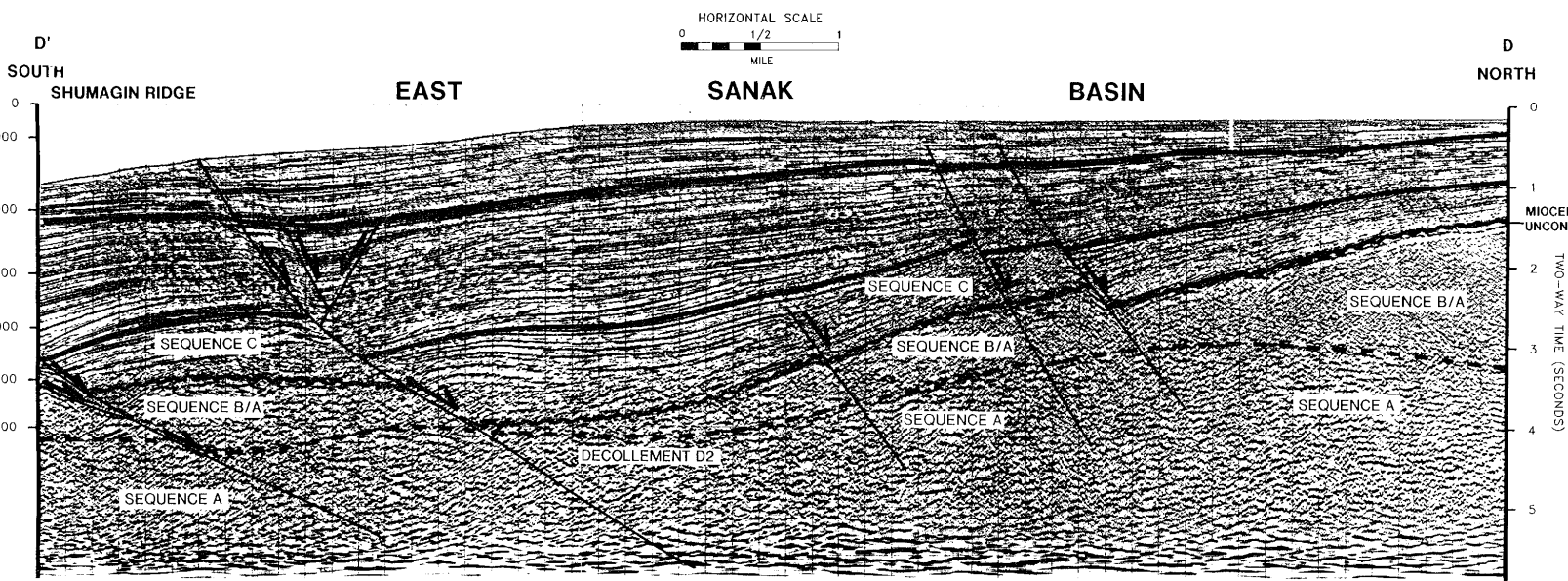
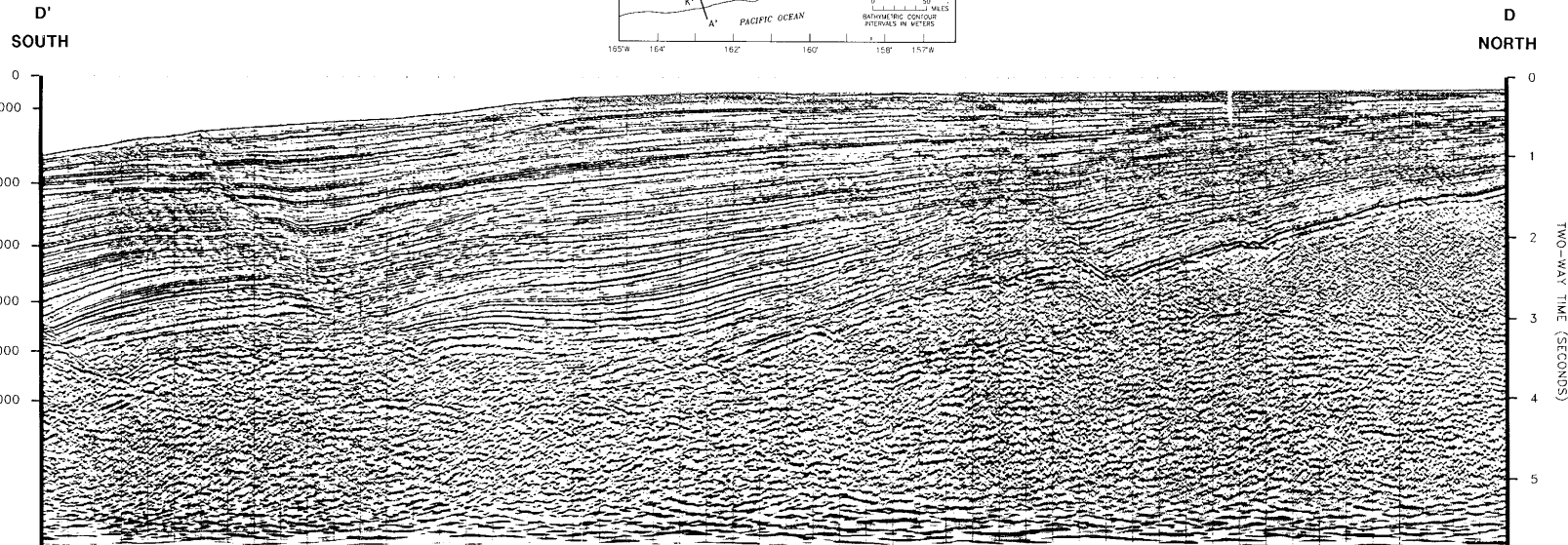


PLATE 6. Seismic-reflection profile showing decollement D2 and extensional faulting and uplift along the outer shelf margin of the East Sanak basin.

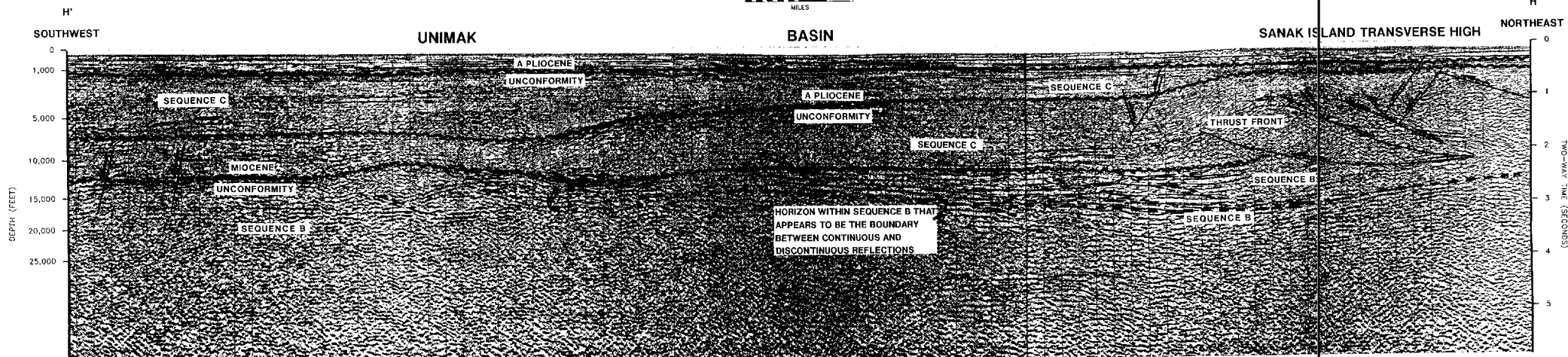
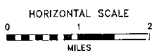
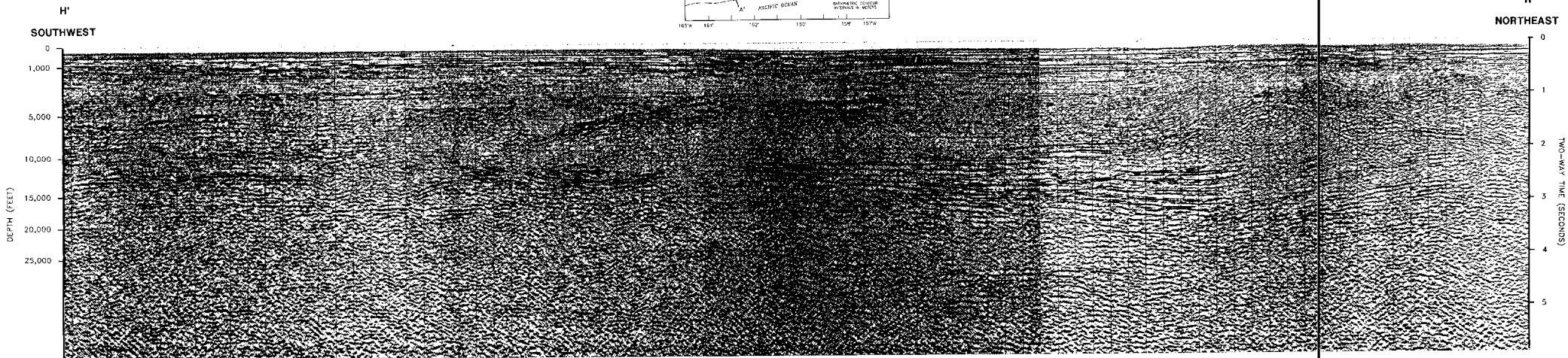
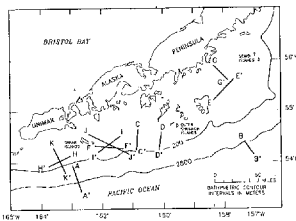


PLATE 7. Seismic-reflection profile showing a possible Pliocene thrust complex that originates in the Sanak Island Transverse High and extends into the Unimak basin.

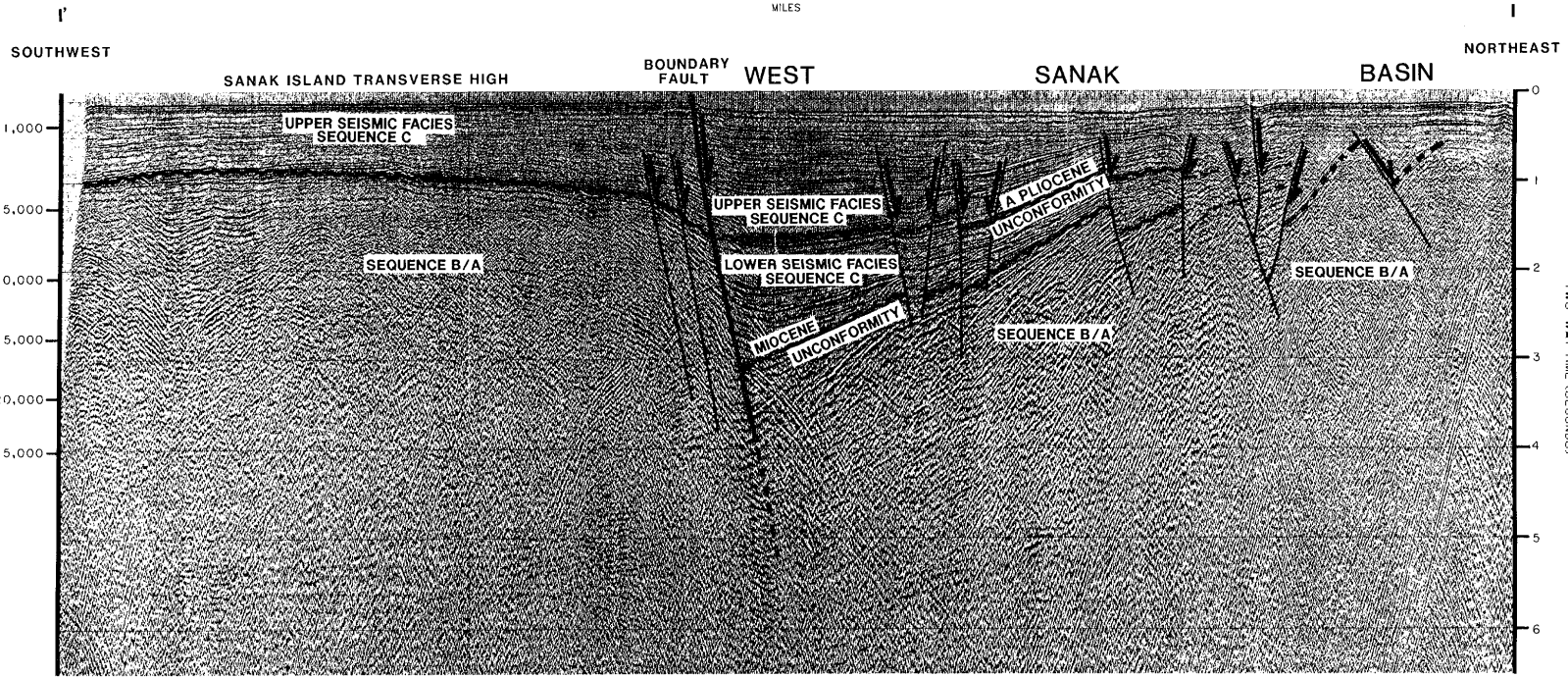
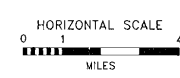
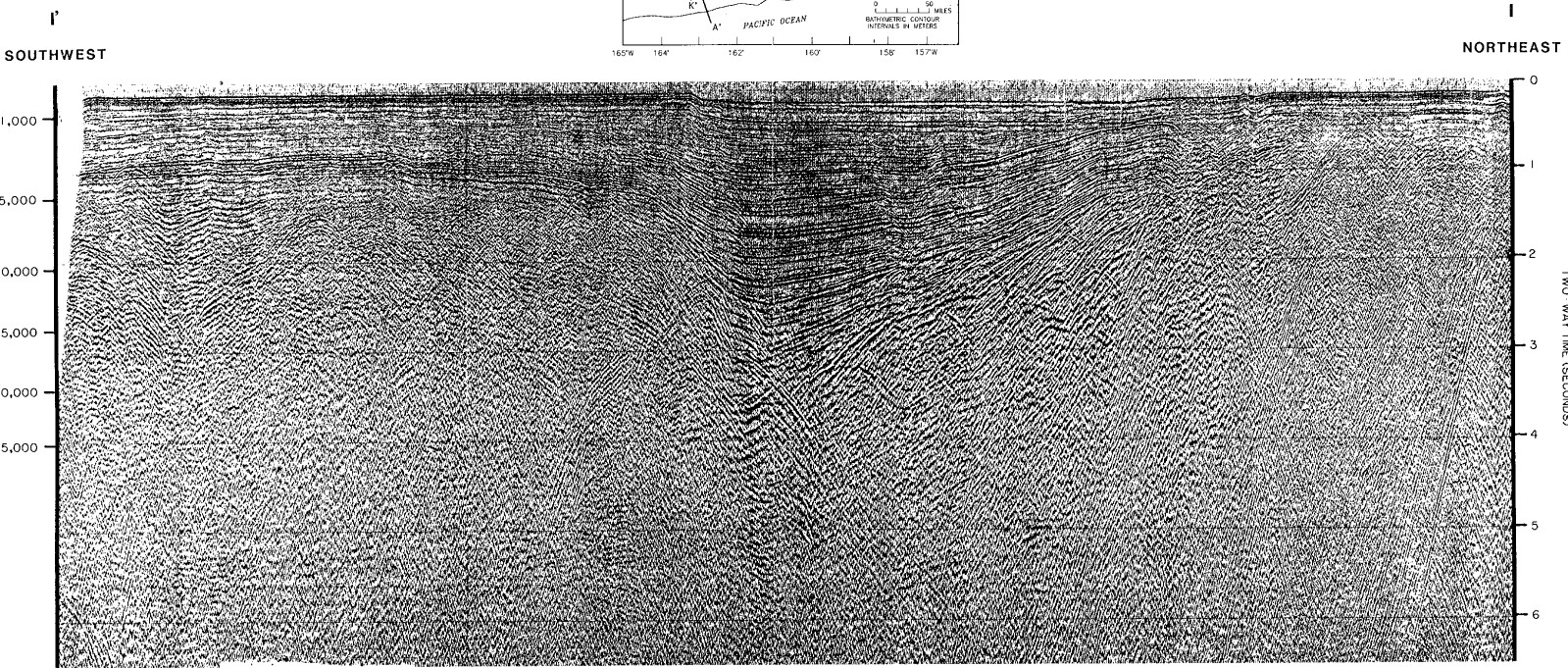
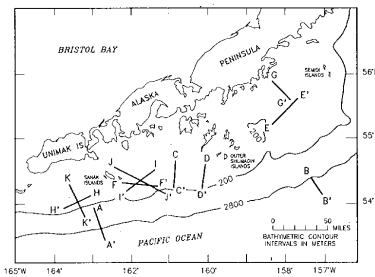
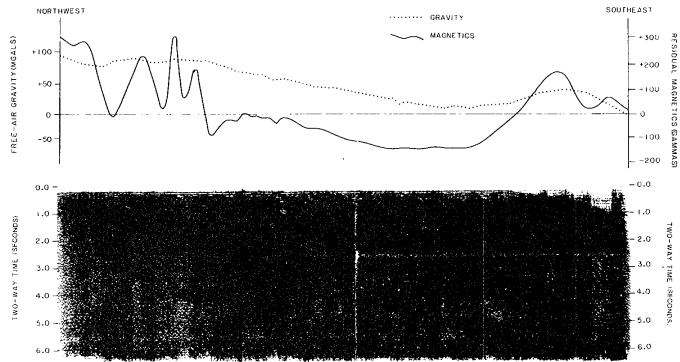
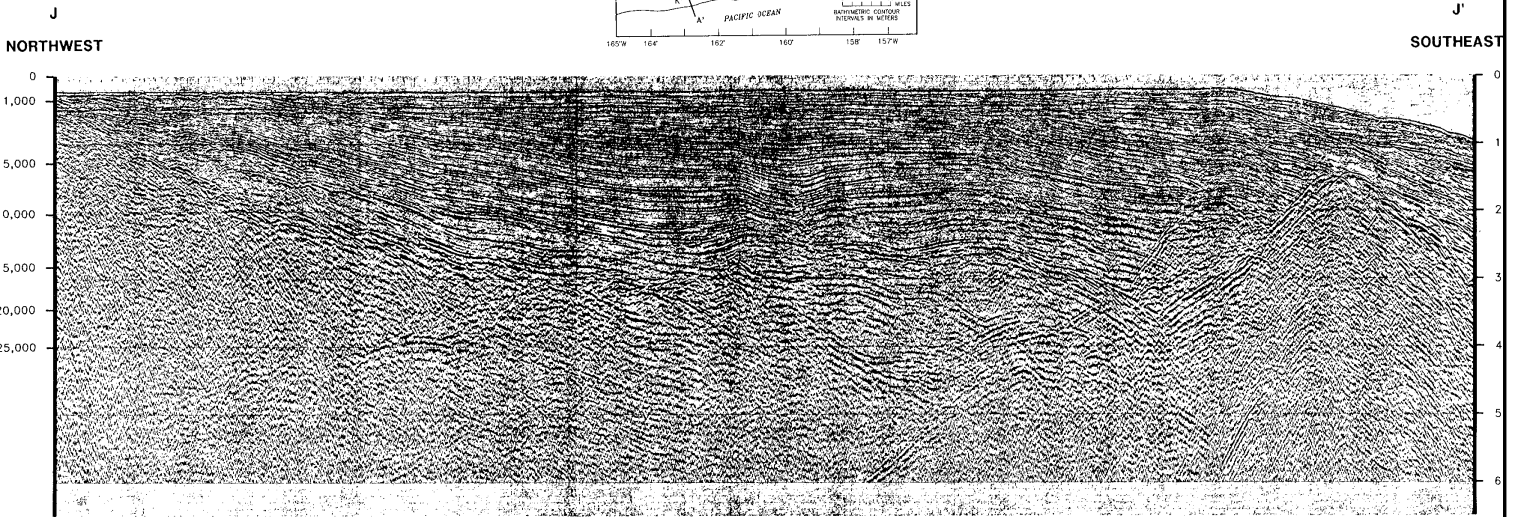
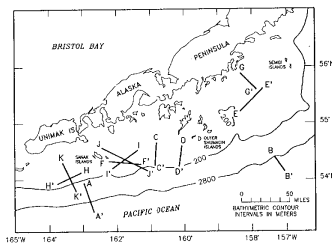


PLATE 8. USGS seismic-reflection profile showing the asymmetric graben of West Sanak basin and the thickening of seismic sequence C against the Boundary fault.



USGS gravity and magnetics profile of seismic profile J-J'. A magnetic high is shown over the East Sanak slope ridge. Data from Bruns and von Huene, 1977.

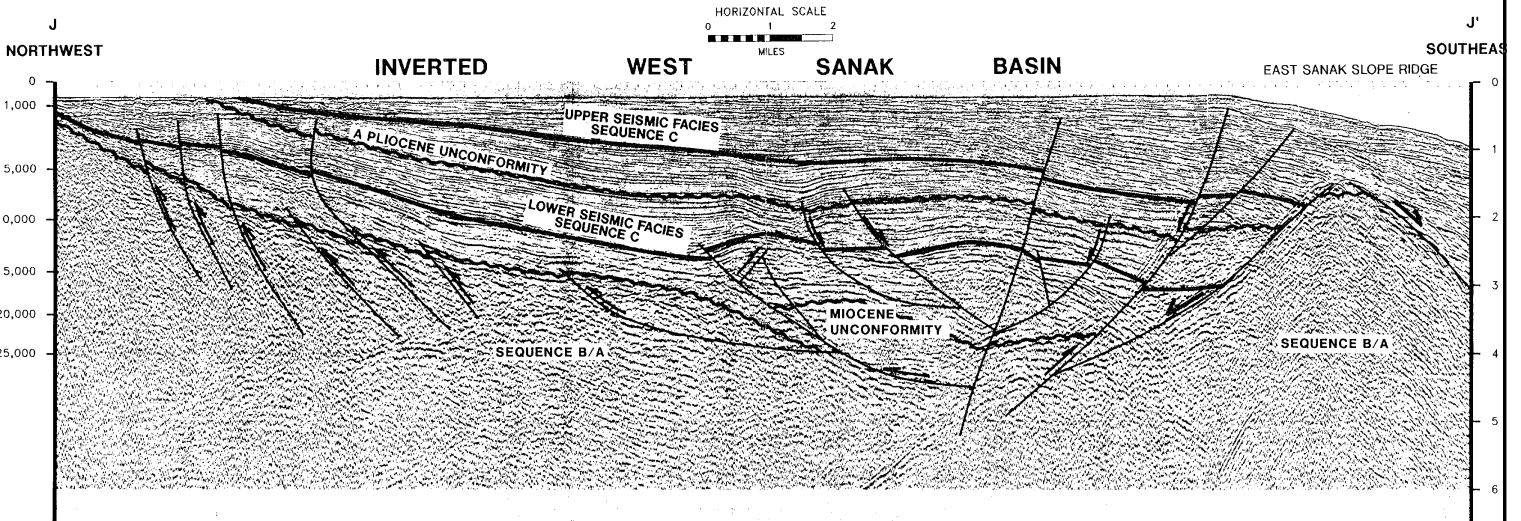


PLATE 9. USGS seismic-reflection profile across the inverted West Sanak basin.

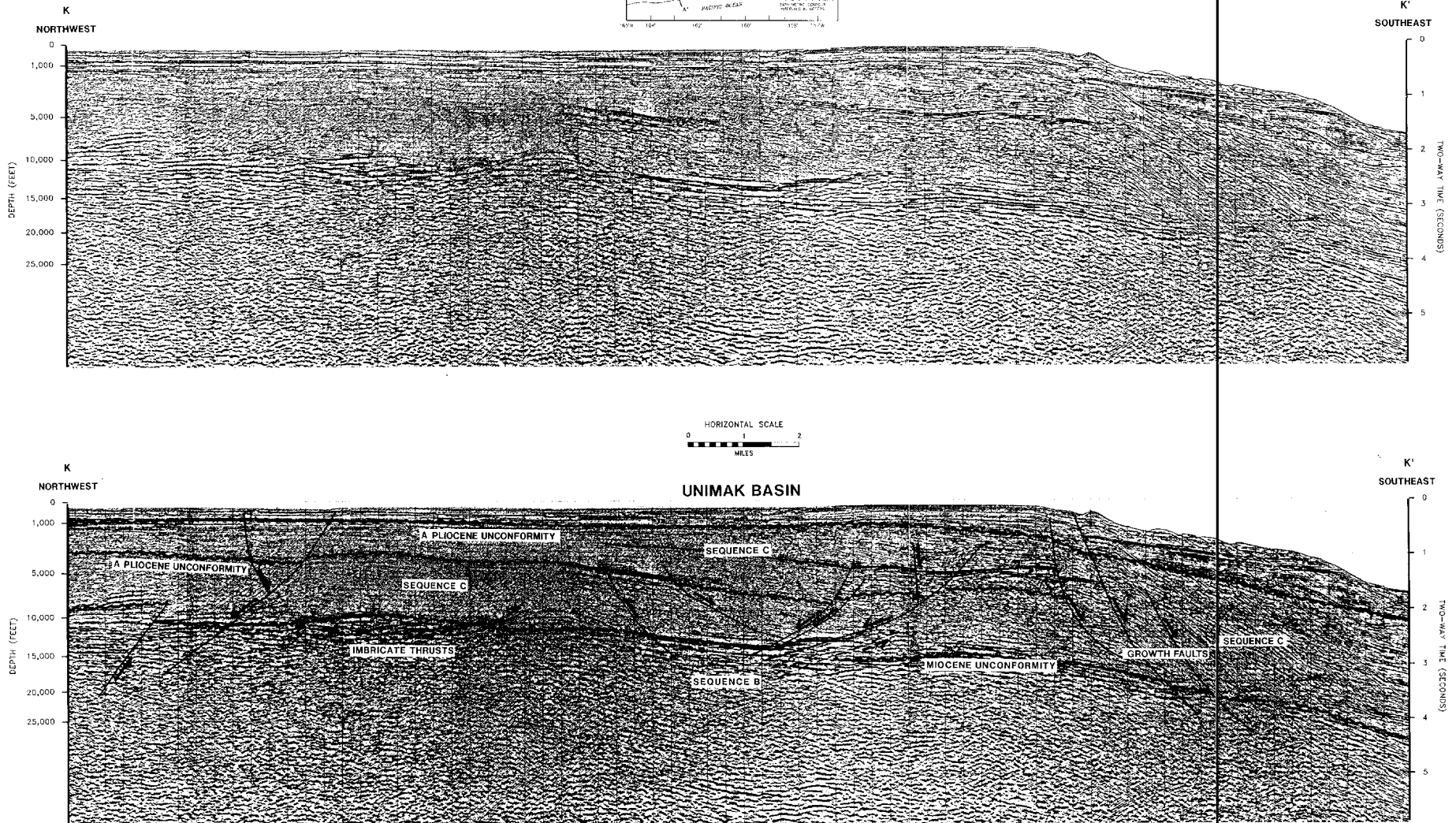
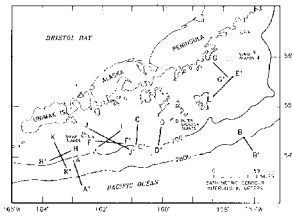


PLATE 10. Seismic-reflection profile showing imbricate thrusts and growth faults in the Unimak basin.

As the Nation's principal conservation agency, the Department of the Interior has responsibility for most of our nationally owned public lands and natural resources. This includes fostering the wisest use of our land and water resources, protecting our fish and wildlife, preserving the environmental and cultural values of our national parks and historical places, and providing for the enjoyment of life through outdoor recreation. The Department assesses our energy and mineral resources and works to assure that their development is in the best interest of all our people. The Department also has a major responsibility for American Indian reservation communities and for people who live in Island Territories under U.S. Administration.

